UNIVERSIDAD COMPLUTENSE DE MADRID
FACULTAD DE CIENCIAS QUÍMICAS

TESIS DOCTORAL

Mecanismos moleculares implicados en la capacidad del cannabinoide sintético WIN55,212-2 para inmunomodular células mieloides y epitelio bronquial en asma y otras enfermedades inflamatorias

Molecular mechanisms underlying the capacity of the synthetic cannabinoid WIN55,212-2 to immunomodulate myeloid and bronchial epithelial cells in asthma and other inflammatory diseases

MEMORIA PARA OPTAR AL GRADO DE DOCTOR

PRESENTADA POR

Mario Pérez Diego

DIRIGIDA POR

Óscar Palomares Gracia

Madrid

UNIVERSIDAD COMPLUTENSE DE MADRID

FACULTAD DE CIENCIAS QUÍMICAS

Programa de Doctorado en Bioquímica, Biología Molecular y Biomedicina

TESIS DOCTORAL

Mecanismos moleculares implicados en la capacidad del cannabinoide sintético WIN55,212-2 para inmunomodular células mieloides y epitelio bronquial en asma y otras enfermedades inflamatorias

Molecular mechanisms underlying the capacity of the synthetic cannabinoid WIN55,212-2 to immunomodulate myeloid and bronchial epithelial cells in asthma and other inflammatory diseases

MEMORIA PARA OPTAR AL GRADO DE DOCTOR

Presentada por

Mario Pérez Diego

Director

Óscar Palomares Gracia

Madrid, 2025

A mis padres,

Aurora y Esteban

AGRADECIMIENTOS

Escribiendo estos párrafos parece que llega a su fin una etapa de algo más de cinco años. Un tiempo que ha estado lleno de lecciones personales y profesionales que agradezco profundamente. No obstante, no podría definir esta tesis de otra manera que no sea como una montaña rusa emocional, ya que he vivido muchos momentos de alegría, pero también enfrentado frustraciones, desafíos y desconfianza. Por eso, quiero que estas líneas vayan dedicadas a esas personas que me han acompañado, ayudado, apoyado, motivado, abstraído y echo disfrutar de tantos momentos durante este tiempo.

En primer lugar, me gustaría agradecer a mi director de tesis, Dr. Óscar Palomares. Gracias Óscar por depositar tu confianza en mí y darme la oportunidad de dar rienda suelta a mi curiosidad. Valoro mucho tu cercanía y esa capacidad para compartir tu entusiasmo y pasión por la ciencia. También quiero agradecer a todo el departamento de Bioquímica y Biología Molecular de la UCM, por hacer posible y facilitar la realización de esta tesis. De igual forma, no podría pasar estas líneas sin dar gracias al personal de los centros de apoyo a la investigación UCM, cuyo soporte técnico en citometría de flujo, microscopía y genómica han ayudado a la consecución de este trabajo.

El laboratorio 19 de la Facultad de Ciencias Químicas ha cambiado mucho desde que llegué. Una pequeña familia que se ha hecho grande y a la que debo y agradezco gran parte de mi progreso y trabajo. Alba, Cris y Leti son sinónimo de eficiencia alemana y hacen de su alrededor un equipo enorme, que ese compañerismo y liderazgo os acompañen siempre. Gracias por enseñarme organización, gestión, dedicación y buenas prácticas dentro del labo, pero también por compartir tantos buenos momentos fuera. Especial mención a Alba, quien me ha guiado desde el principio en la tesis compartiendo las penas y glorias del proyecto, para mí (con permiso de Óscar) algo parecido a una supervisora de este trabajo. Gracias también a Carmen por ser compañera de inquietudes, quejas y alegrías durante estos años. Eres un ejemplo de perseverancia, paciencia y resiliencia, vales mucho. Quién sabe en cuantos universos paralelos seríamos millonarios gracias a nuestras locas ideas de negocio para huir de la tesis… Andrés, gracias por ser un compañero empático y comprensivo, me has ayudado a lidiar con los problemas del día a día y desconectar con datos curiosos y mucho humor. Ángel, gracias por tu proactividad y diligencia en el trabajo, así como tu colaboración en tantos apartados del proyecto, siempre con afán de ayudar. A las jóvenes talentos del labo, Natalia, Silvia, Isabel, Lucía, gracias por vuestro compañerismo y por generar esa atmósfera de buen rollo. Os auguro un futuro prometedor. Gracias también al insaciable carácter combativo de Sofía para no darme la razón, aunque parezca que no, voy aprendiendo… No me olvido de los que pasaron por el labo y tuve la suerte de disfrutar y aprender. Bego y Bea, qué bien haber podido contar con vuestra experiencia y diferentes perspectivas de afrontar la carrera científica/laboral. Jacobo, gracias por enseñarme que puede haber hueco para el humor en el trabajo sin dejar de ser profesional. ¡Muchísimas gracias a todos por vuestro apoyo y ayuda estos años!

I would also like to express my gratitude to Dr. Cezmi Akdis for hosting me in a six-month stay at the Swiss Institute of Allergy and Asthma Research (SIAF) in Davos, Switzerland. Thank you Cezmi

for your supervision and warm welcome to SIAF. I appreciate the scientific discussions and the Tuesday team sport routine we had. The isolated Swiss Alps in a post-pandemic era would have felt dramatic without the amazing people I met there: Nino, Rubén, Mengting, Juan, Jana, Ozan, Stephan, Debbie, Elena, Yi, Yasu, Beate, Ismail, and the rest of the SIAFians. Especially, I would like to thank Yağiz and Duygu for their support and friendship, who I have been so lucky to reconnect with at every congress. There is always something to learn from you, I hope we can spend more times together.

Thanks also to Dr. Jorge Domínguez-Andrés, Dr. Mihai Netea and their team in Radboud University Medical Centre, Netherlands, for their collaboration and support, and for allowing me to be involved in the fascinating projects they are carrying out.

Fuera de lo que es el trabajo en el laboratorio, no me puedo olvidar de tantas otras personas que me han apoyado y animado durante estos años, indirectamente, han hecho posible esta tesis.

Marcos e Isma me acogieron en el piso de Pablo Iglesias cuando llegué en 2019. Cuánto me alegra haber sido testigo de la autodenominada “espiral autodestructiva” de Isma ese año, me trajo muchos momentos para abstraerme y también para compartir nuestras preocupaciones por el doctorado, lo pasé genial. Marcos aka Bueu y yo nos hicimos fuertes en el piso durante la pandemia, luego todo ha ido rodado. Marcos, eres un tío genial, gracias estar siempre tan atento a mis preocupaciones y agobios, tienes ese don de ayudar a los demás a relativizar incluso cuando tú también estás con la soga al cuello. Más tarde llegó Guillaume, un golpe de aire fresco para esos días que volvía a casa cansado o desanimado. Gracias por ese espíritu libre que arrancaste a mostrar al mundo en nuestra casa cada tarde.

Durante este tiempo en Madrid también he tenido la suerte de conservar muchas de mis amistades de la Universidad de Alcalá, esto va también por ellos. En especial, quiero agradecer a mi amigo Javi, probablemente la persona más antagónica a mí que conozco en cuanto a cómo afrontar la vida, y al mismo tiempo con quién comparto muchos hobbies e inquietudes. Gracias por darme esa visión despreocupada de la vida siempre y acompañarme durante estos años. Me gustaría también agradecer a Sergio por haber estado ahí, sobre todo en los inicios, con cada risa en los entrenamientos se me iba cualquier preocupación, pocas lesiones nos han costado todas las tonterías que hacíamos.

Bea y Nacho me vieron entrar como un enano en el CIB durante mi TFG, y no contentos con dejarlo estar ahí, me siguen acompañando e incluso me llegaron a venir a visitar a Davos durante la estancia. Bea, tu experiencia y consejos me han ayudado mucho a ir llevando la tesis desde el inicio, muchas gracias por tu enorme sentido del humor y esa risa contagiosa que te caracteriza. Nacho, me fascina la visión optimista y positiva de la vida que tienes, gracias por irradiarla también a los demás, incluso desde California.

Óscar, Emilio y Bea son mi pandi del máster, y no me imagino estos años sin ellos ni todos los planes y apoyo mutuo que nos hemos dado. Óscar, valoro mucho esa capacidad resolutiva que tienes y la facilidad con que diriges tu vida hacia los objetivos que quieres cumplir. Ojalá más años de rutas, baloncesto y tardes de juegos que me sirvan para picarte y sacarte la vena más competitiva, me lo paso

muy bien. Bea, gracias por tu empatía, por comprender y compartir las frustraciones de nuestro trabajo, así como por esos ratos de desconexión también necesarios. Emilio, gracias por esos días de risas rememorando batallitas, porque tienes esa capacidad de poner en un pedestal a todos tus colegas y generas un círculo de confianza alrededor. Una de las cosas que más te debo es haberme presentado a Isma, Juanpa y Antonio. Todas esas tardes de viernes cuando nos juntábamos con el resto de la FDJ sabían a gloria, igual que todas las pachangas, excursiones y viajes con el grupito que juntamos. Especial mención a Isma, con el que comparto el sentido del humor y del ridículo, y tantos buenos momentos hemos tenido por ello. Muchas gracias chavales, ¡al final lo hemos conseguido todos!

De mayores nos solemos rodear de gente con intereses, trabajos, rutinas y personalidades afines. Lo bonito de las amistades de la infancia es que construimos nuestra personalidad con ellas, primero se forjan y luego se diversifican. No creo que sienta nunca la integración que tengo cuando estoy con mis amigos de siempre en Zamora, por muy distintos que seamos. Gracias por haber sido cortafuegos de mi trabajo y despejarme la cabeza tantos días, por sentir que nunca me he ido de casa cada vez que vuelvo, por los partidos de balonmano, por las excursiones, por las tardes de tomar algo, las barbacoas, los paseos... Hay más que agradecer de lo que corresponde a esta tesis doctoral.

Gracias a toda mi familia por su apoyo, por preguntar con curiosidad y por haber mostrado siempre interés en lo que hago. Especial dedicatoria a mis abuelos, quienes a pesar de no haber sido capaz de explicarles qué es esto del doctorado, si trabajo o estudio, o por qué narices no he curado ninguna enfermedad en tantos años, siguen orgullosos de su nieto y regalándome lecciones de vida. Por supuesto, a mis padres les debo ser la persona que soy hoy, y muchos días me arrepiento de no tenerlos más cerca. Mamá eres un ejemplo de constancia, esfuerzo y de cómo gestionar las responsabilidades, aunque nos cueste la cabeza por los nervios, porque siempre nos hemos parecido en ese sentido. Ojalá me pareciera más a ti en todo lo demás. Papá, tú también eres un ejemplo, gracias por no haberme puesto nunca la presión de tener que cumplir unos objetivos, sino de hacer lo que me haga feliz. Nunca os podré agradecer suficiente el apoyo constante e incondicional durante estos años y desde siempre. Os quiero mucho.

Por último, Claudia, eres el ejemplo perfecto de que en mitad de una pandemia mundial también se puede tener suerte. Me has sabido traer calma en los momentos de más angustia y felicidad cuando he estado de bajón, me ayudas a conocerme y a creer en mí mismo. Gracias por tu paciencia infinita, por ser la primera en disfrutar de mis éxitos y alegrarme en los malos momentos. Más allá de lo que respecta a esta tesis, me hace mucho bien tu alegría, tu risa fácil, tu fascinación por las cosas más simples… Acompáñame mucho tiempo más, te quiero.

En fin, como veis, esto ha sido un trabajo en equipo.

¡Muchas gracias a todos de corazón!

INDEX

ABREVIATIONS

2-AG: 2-arachidonoylglycerol.

2-DG: 2-deoxyglucose.

AA: antimycin A.

acetyl-CoA: acetyl coenzyme A.

AEA: anandamide.

AHR: Aryl hydrocarbon receptor.

AJs: adherence junctions.

ALI: air-liquid-interface.

AMPK: adenosine monophosphate-activated protein kinase.

AP-1: activation protein 1.

APC: antigen presenting cell.

ATP: adenosine triphosphate.

ATRA: all-*trans* retinoic acid.

BALF: bronchoalveolar lavage fluid.

BEBM: bronchial epithelial basal medium.

BEGM: bronchial epithelial growth medium.

BHR: bronchial hyperresponsiveness.

BSA: bovine serum albumin.

CASP1: caspase 1.

CB1: type 1 cannabinoid receptor.

CB2: type 2 cannabinoid receptor.

CBD: cannabidiol.

CBRs: cannabinoid receptors.

CCR7: C-C chemokine receptor 7.

CD40L: CD40 ligand.

cDC1s: type 1 conventional dendritic cells.

cDC2s: type 2 conventional dendritic cells.

cDCs / mDCs: conventional / myeloid dendritic cells.

CDP: common dendritic cell progenitor.

CLP: common lymphoid progenitor.

CLRs: C-type lectin receptors.

CNS: central nervous system.

CTLA4: cytotoxic T lymphocyte antigen 4

CTLs: $CD8^+$ cytotoxic T lymphocytes.

DAG: diacylglycerol.

DAGL: diacylglycerol lipase.

DAMPs: damage-associated molecular patterns.

DCs: dendritic cells.

Dex: dexametasone.

DMEM: Dulbecco´s modified Eagle medium.

DMSO: dimethyl sulfoxide.

ECAR: extracellular acidification rate.

ECS: endocannabinoid system.

EMT: endocannabinoid membrane transporter.

FA: fatty acid.

FAAH: fatty acid amide hydrolase.

FAD: flavin adenine dinucleotide.

FAO: fatty acid oxidation.

FAS: fatty acid synthesis.

FCCP: carbonyl cyanide 4-(trifluoromethoxy)phenylhydrazone.

FcεRI: high affinity IgE receptor.

FITC: fluorescein isothiocyanate.

FLT3: Fms-like tyrosine kinase 3.

FOXP3: transcription factor forkhead box 3.

GATA3: GATA binding protein 3.

GINA: global initiative for asthma.

GlycoPER: glycolytic proton efflux rate.

GM-CSF: granulocyte-macrophage colony-stimulating factor.

GM-MΦs: primary human monocyte-derived macrophages differentiated with GM-CSF.

GMP: granulocyte-monocyte progenitor.

GPCR: G protein-coupled receptor.

GSDMD: gasdemin D.

GSEA: gene set enrichment analysis.

HBECs: human bronchial epithelial cells.

HDM: house dust mite.

HIF1α: hypoxia-inducible factor 1 alpha.

HmoDCs: human monocyte-derived dendritic cells.

HRP: horseradish peroxidase.

ICOS: inducible T-cell costimulator

ICOSL: inducible costimulator ligand

ICS: inhaled corticosteroids.

iDC: immature dendritic cell.

IDO: indoleamine 2,3-dioxygenase

IFNs: interferons.

Ig: immunoglobulin.

IL: interleukin.

ILC2s: type 2 innate lymphoid cells.

ILCs: innate lymphoid cells.

iNOS: inducible nitric oxide synthase.

IRF: interferon response factor.

IRF8: interferon regulatory factor 8.

Kyn: kynurenine.

LABA: long-acting β_2 agonist.

LAG3: lymphocyte activation gene 3.

LAMA: long-acting muscarinic antagonist.

LDH: lactate dehydrogenase.

LPS: lipopolysaccharide.

MAGL: monoacylglycerol lipase.

MAPKs: mitogen activated protein kinases.

MAS: macrophage activation syndrome.

M-CSF: macrophage colony-stimulating factor.

MDP: monocyte-dendritic cell progenitor.

MHC: major histocompatibility complex.

mTOR: mammalian target of rapamycin.

NAD: nicotinamide adenine dinucleotide.

NADP: Nicotinamide adenine dinucleotide phosphate.

NAPE: N-acyl-phosphatidylethanolamine.

NAPE-PLD: NAPE-hydrolyzing phospholipase D.

NAT: N-acyltransferase.

NF-κB: nuclear factor-κB.

NKs: natural killer cells.

NLRP3: nucleotide-binding domain leucine-rich–containing family pyrin domain–containing-3.

NLRs: NOD-like receptors.

Noladin ether: O-arachidonoylglyceryl ether.

OCR: oxygen consumption rate.

OEA: N-oleoylethanolamine.

Oligo: oligomycin.

OVA: ovalbumin.

OX40L: OX40 ligand.

OXPHOS: oxidative phosphorylation.

PAMPs: pathogen-associated molecular patterns.

PAR: Protease activated receptor.

PBMCs: peripheral blood mononuclear cells.

PD-1: programmed cell death-1.

pDCs: plasmacytoid dendritic cells.

PD-L1: programmed death-ligand 1.

PD-L2: programmed death-ligand 2.

PEA: N-palmitoylethanolamide.

PFA: paraformaldehyde.

PMΦs: peritoneal macrophages.

PPAR: peroxisome proliferator activated receptor.

PPP: pentose phosphate pathway.

PRRs: pattern recognition receptors.

pTregs: peripherally derived regulatory T cells.

RA: retinoic acid.

RALDH: retinaldehyde dehydrogenase.

RLRs: RIG-I-like receptors.

RORγt: Retinoic acid-related orphan receptor γt.

ROS: reactive oxygen species.

ROT: Rotenone.

RV: rhinovirus.

RV-A16: human rhinovirus A 16.

RXR: retinoic X receptor.

SABA: short-acting β_2 agonist.

SEAP: secreted embryonic alkaline phosphatase.

STAT: signal transducer and activator of transcription.

STAT6: signal transducer and activator of transcription 6.

T-bet: T-box expressed in T cells.

TCA cycle: tricarboxylic acid cycle.

TCR: T cell receptor.

tDCs / ASDCs: transitional dendritic cells / $Axl^{+}Siglec\text{-}6^{+}$ dendritic cells.

TER: transepithelial electrical resistance.

TGF-β: transforming growth factor β.

Th: $CD4^{+}$ T helper lymphocyte.

THC: Δ^{9}-tetrahydrocannabinol.

TIGIT: T cell immunoreceptor with immunoglobulin and ITIM domains.

TJs: tight junctions.

TLRs: Toll-like receptors.

Tregs: regulatory T cells.

TRP: transient receptor potential.

TRPV1: transient receptor potential vanilloid 1.

tTregs: thymus-derived regulatory T cells.

UV-RV-A16: ultraviolet inactivated human rhinovirus A 16.

Virodhamine: O-arachidonoylethanolamide.

VitD3: vitamin D3.

RESUMEN / ABSTRACT

RESUMEN

El asma es la enfermedad inflamatoria crónica de las vías respiratorias más común, afectando a más de 300 millones de personas en todo el mundo, lo que supone una gran carga sanitaria y socioeconómica. Se caracteriza por una obstrucción del flujo aéreo, generalmente reversible, acompañada de inflamación de las vías respiratorias e hiperreactividad bronquial. Los síntomas clínicos son recurrentes e incluyen tos, sibilancias, presión en el pecho o dificultad respiratoria. Diversos estudios han demostrado que las infecciones recurrentes del tracto respiratorio, generalmente causadas por virus, y la sensibilización alérgica son dos factores de riesgo para el desarrollo y mal pronóstico del asma. La inflamación crónica de las vías respiratorias y los defectos en la barrera epitelial bronquial son dos de las principales características fisiopatológicas que subyacen a las señales y síntomas clínicos asociados al asma. Por tanto, la identificación y caracterización, a nivel celular y molecular, del modo de acción de nuevas terapias que combinen, de forma simultánea, propiedades antiinflamatorias con la capacidad de restaurar la función de la barrera epitelial bronquial representa un área de investigación crucial para el desarrollo de futuras estrategias para la prevención y tratamiento del asma.

El sistema endocannabinoide (ECS) es una red compleja de señalización involucrada en múltiples procesos fisiológicos. Alteraciones del ECS se han asociado a diversas patologías inflamatorias, entre ellas el asma. En este sentido, los cannabinoides se postulan como agentes terapéuticos prometedores con capacidad antiinflamatoria y función reguladora sobre las barreras epiteliales. Sin embargo, los mecanismos moleculares por los que los cannabinoides ejercen sus efectos son complejos y requieren ser estudiados en detalle. Nuestro grupo de investigación ha demostrado que WIN55,212-2, un cannabinoide sintético no selectivo, exhibe propiedades antiinflamatorias e inmunomoduladoras tanto *in vitro* como *in vivo*. WIN55,212-2 promueve la generación de células dendríticas (DCs) tolerogénicas capaces de inducir células T reguladoras (Tregs) funcionales en modelos preclínicos de enfermedades inflamatorias tales como sepsis y alergia a alimentos. Por otro lado, hemos demostrado previamente que la administración de WIN55,212-2 durante el inicio de infecciones causadas por rinovirus restaura significativamente la integridad de la barrera epitelial bronquial en los cultivos infectados. Teniendo en cuenta todos estos antecedentes, el objetivo principal de esta Tesis Doctoral es investigar la capacidad del cannabinoide sintético WIN55,212-2 para regular la función de otras células mieloides relevantes, tales como monocitos y macrófagos, y la barrera epitelial bronquial. Además, se pretenden dilucidar los mecanismos moleculares subyacentes a dichos efectos en modelos preclínicos de asma y otras enfermedades inflamatorias, tanto *in vitro* como *in vivo*.

En este trabajo, hemos demostrado que la presencia del cannabinoide sintético WIN55,212-2 durante la diferenciación de monocitos humanos a DCs confiere propiedades tolerogénicas, al generar DCs que responden con una menor producción de citocinas inflamatorias ante la estimulación con lipopolisacárido bacteriano (LPS) y que presentan una mayor capacidad para generar Tregs. Además, WIN55,212-2 inhibe la señalización mediada por NF-κB, la inducción del inflamasoma y la activación

proinflamatoria de macrófagos humanos mediante mecanismos asociados al bloqueo de la glucólisis aeróbica y de las adaptaciones metabólico-epigenéticas inducidas por LPS. Estos resultados se validaron en cultivos *ex vivo* de macrófagos peritoneales de origen múrido, así como en un modelo *in vivo* de sepsis inducida por LPS, confirmando que WIN55,212-2 presenta una gran capacidad antiinflamatoria en células inmunes innatas de origen mieloide. Por otro lado, las funciones protectoras del cannabinoide sintético WIN55,212-2 sobre la barrera epitelial bronquial se evaluaron en el contexto de infecciones causadas por rinovirus e inflamación de tipo 2, caracterizadas por contribuir a generar un ciclo vicioso de inflamación y daño epitelial muy perjudicial en la patogénesis del asma. La administración profiláctica de WIN55,212-2 no previene la infección por rinovirus en células epiteliales bronquiales humanas (HBECs), pero al igual que su administración terapéutica, acelera la recuperación del daño en la barrera epitelial después de la infección. Además, hemos demostrado que WIN55,212-2 impide la adquisición de características fisiopatológicas del asma tipo 2 inducidas por IL-13 en cultivos en interfase aire-líquido de HBECs, cultivos de esferoides epiteliales bronquiales 3D y en un modelo múrido de inflamación de las vías respiratorias mediado por IL-13. A nivel mecanístico, estos efectos se asociaron a la capacidad de WIN55,212-2 para inhibir el estrés oxidativo inducido por IL-13 en HBECs, lo que interfiere en la transducción de señales mediada por STAT6 al prevenir la inactivación inducida por especies reactivas de oxígeno de proteínas con actividad tirosina fosfatasa. Finalmente, la capacidad de WIN55,212-2 para interferir en la sensibilización y asma alérgica se evaluó en modelos *in vitro* e *in vivo* de asma alérgica eosinofílica inducida por ácaros del polvo doméstico (HDM, del inglés “House Dust Mite”). WIN55,2212-2 inhibe la maduración de DCs humanas *in vitro* y su capacidad para promover respuestas T efectoras tras la exposición a HDM. Del mismo modo, WIN55,212-2 también inhibe la sensibilización alérgica y reduce la inflamación local de las vías respiratorias y las respuestas inmunitarias sistémicas en un modelo múrido de asma alérgica eosinofílica inducida por HDM. En conjunto, nuestros hallazgos sugieren que el cannabinoide sintético WIN55,212-2 podría representar un candidato prometedor para el desarrollo de futuras estrategias basadas en cannabinoides para la prevención y tratamiento del asma y otras enfermedades inflamatorias.

Durante las últimas décadas, muchas sustancias dañinas para el epitelio se han introducido en nuestra vida cotidiana como consecuencia de la urbanización e industrialización. Estos agentes perjudiciales son conocidos por deteriorar las barreras epiteliales y se han asociado a un preocupante aumento de enfermedades crónicas no transmisibles, como el asma y otros trastornos inflamatorios de las vías respiratorias. En este sentido, la identificación de nuevas sustancias potencialmente dañinas es necesaria para desarrollar estrategias adecuadas de prevención. Las últimas perspectivas y avances en la carrera aeroespacial sugieren la posibilidad de futuros asentamientos humanos y la explotación de los recursos minerales presentes en el espacio exterior. Considerando que estos avances podrían ir acompañados de nuevas exposiciones a agentes potencialmente dañinos, en este estudio nos propusimos analizar los posibles efectos perniciosos en las vías respiratorias humanas de polvos presentes en las superficies de cuerpos celestes, denominados regolitos. A través del uso de modelos humanos *in vitro* de exposición del epitelio bronquial a simulantes de regolitos, hemos demostrado que las partículas lunares y marcianas pueden comprometer potencialmente la integridad de la barrera epitelial y desencadenar respuestas inflamatorias en las vías respiratorias. Además, ratones expuestos

por vía intranasal a simulantes de regolitos presentaron una barrera epitelial bronquial comprometida, daño en las vías respiratorias, reclutamiento de células inflamatorias e inducción de marcadores tempranos de fibrosis en sus pulmones. De manera conjunta, nuestros datos indican que los regolitos presentes en las superficies de la Luna y Marte podrían constituir agentes ambientales perjudiciales para la salud humana.

En resumen, esta Tesis Doctoral proporciona un estudio integral de las propiedades antiinflamatorias e inmunomoduladoras del cannabinoide sintético WIN55,212-2 y de sus funciones reguladoras sobre la barrera epitelial bronquial, así como la caracterización detallada de los mecanismos celulares y moleculares subyacentes a tales efectos. Además, hemos identificado los regolitos lunares y marcianos como posibles agentes perjudiciales para el epitelio de las vías respiratorias y para la salud humana en general. Nuestros hallazgos podrían contribuir al desarrollo de nuevas estrategias alternativas basadas en cannabinoides para la prevención y tratamiento del asma y otras enfermedades inflamatorias, así como a ampliar nuestro conocimiento sobre posibles agentes perjudiciales para las barreras epiteliales de las vías respiratorias.

ABSTRACT

Asthma is the most common chronic inflammatory disease of the airways affecting over 300 million people worldwide, with a significant health and socioeconomic burden. It is characterized by reversible airflow obstruction, airway inflammation and bronchial hyperresponsiveness. The main clinical symptoms are recurrent and encompass cough, wheezing, shortness of breath and chest tightness, along with difficulty breathing. Several studies have convincingly demonstrated that recurrent respiratory viral infections and allergic sensitization represent two main risk factors for asthma development and worsening. Airway inflammation and bronchial epithelial barrier defects are two major hallmarks of asthma pathophysiology underlying the main clinical signs and symptoms associated to the disease. Therefore, the identification and characterization at the cellular and molecular level of the mode of action of novel drugs combining anti-inflammatory properties with the ability to restore airway epithelial barrier function is crucial for the development of future strategies for the prevention and treatment of asthma.

The endocannabinoid system (ECS) is a complex signaling network involved in many physiological processes. Alterations in the ECS have been associated with several inflammatory diseases, including asthma. At this regard, cannabinoids are postulated as promising agents with anti-inflammatory and epithelial barrier regulatory properties. However, the molecular mechanisms by which cannabinoids exert their effects are complex and require further investigation. Previous studies from our research group have demonstrated that WIN55,212-2, a non-selective synthetic cannabinoid, displays potent anti-inflammatory and immunomodulatory functions both *in vitro* and *in vivo*. WIN55,212-2 promotes the generation of tolerogenic dendritic cells (DCs) able to induce functional regulatory T cells (Tregs) in preclinical models of inflammatory diseases such as sepsis and food allergy. Furthermore, administration of WIN55,212-2 during the onset of rhinoviral infections significantly restored airway epithelial barrier integrity in infected cultures. Considering all these aspects, the major aim of this Doctoral Thesis is to investigate the capacity of the synthetic cannabinoid WIN55,212-2 to regulate functional properties in relevant myeloid immune cells, such as monocytes and macrophages, and the airway epithelial barrier. We also sought to elucidate the underlying molecular mechanisms of such effects using preclinical *in vitro* and *in vivo* models of asthma and other inflammatory diseases.

In this Doctoral Thesis, we have demonstrated that the synthetic cannabinoid WIN55,212-2 imprints tolerogenic properties during the differentiation of human monocytes into DCs by rendering DCs with compromised inflammatory cytokine responses upon stimulation with lipopolysaccharide (LPS) and enhanced capacity to polarize Tregs. WIN55,212-2 also impaired NF-κB signaling, inflammasome induction and proinflammatory activation of human macrophages, which were associated with the inhibition of aerobic glycolysis and impairment of the metabolic-epigenetic adaptations induced by the proinflammatory stimulus of LPS. Of note, these findings were validated in *ex vivo* cultures of murine peritoneal macrophages as well as in an *in vivo* model of LPS-induced sepsis, confirming the potent anti-inflammatory capacity of WIN55,221-2 by acting on innate myeloid immune cells. The barrier protective functions of the synthetic cannabinoid WIN55,212-2 were evaluated in the context of rhinoviral infections and type 2 inflammation, which are known to create a deleterious vicious cycle that promotes

airway inflammation and bronchial epithelial barrier damage in asthma pathogenesis. Prophylactic administration of WIN55,212-2 does not prevent rhinovirus infection of human bronchial epithelial cells (HBECs), but similar to its therapeutic administration, accelerates the recovery of epithelial barrier damage after infection. In addition, we have demonstrated that WIN55,212-2 impairs the acquisition of major type 2 asthmatic features induced by IL-13 in air-liquid-interface (ALI) cultures of HBECs, in cultures of 3D bronchial epithelial spheroids and in a murine model of IL-13-driven airway inflammation. Mechanistically, these effects were dependent on the capacity of WIN55,212-2 to inhibit IL-13-induced oxidative stress in HBECs, which impairs STAT6 signal transduction through preventing oxidative inactivation of protein tyrosine phosphatases. Finally, the therapeutic potential of WIN55,212-2 was assessed in *in vitro* and *in vivo* models of allergic eosinophilic asthma induced by the common indoor allergen, house dust mite (HDM). The synthetic cannabinoid inhibited *in vitro* human DCs maturation and suppressed their capacity to promote effector T cell responses upon HDM exposure. Supporting these data, WIN55,212-2 treatment impaired allergic sensitization, local airway inflammation and systemic effector immune responses in a murine model of HDM-driven allergic eosinophilic asthma. Together, our findings indicate that the synthetic cannabinoid WIN55,212-2 might well represent a promising candidate for the development of future cannabinoid-based strategies for the prevention and treatment of asthma and other inflammatory diseases.

Over the last decades, many epithelial-damaging substances have been introduced into our daily lives as a consequence of urbanization and industrialization. These deleterious agents are known to impair epithelial barriers and have been associated with an alarming rise in chronic non-communicable diseases including asthma and other airway inflammatory disorders. In this sense, the identification of new potentially harmful substances is required to develop proper avoidance and prevention strategies. The latest perspectives and advances in the aerospace field suggest the possibility of future human settlements and the exploitation of mineral resources in outer space. Considering that these events may be accompanied by new exposures to potential deleterious agents, herein, we aimed to study the potential harmful effects of particulate materials found in the surfaces of celestial bodies, termed as regoliths, in the human airways. Through the use of human *in vitro* models of repetitive airway exposure to regolith simulants, we have demonstrated that Lunar and Martian particles can potentially compromise the epithelial barrier integrity and trigger inflammatory responses in the airways. Additionally, mice intranasally exposed to regolith simulants displayed impaired bronchial epithelial integrity, airway damage, recruitment of inflammatory cells and induction of early fibrosis markers in the lungs. Collectively, our data indicate that regoliths found on the surfaces of the Moon and Mars might constitute harmful environmental agents to human health.

In summary, this Doctoral Thesis provides a comprehensive study of the anti-inflammatory, immunomodulatory and bronchial epithelial barrier regulatory properties of the synthetic cannabinoid WIN55,212-2, along with the detailed characterization of the molecular mechanisms underlying such effects. Moreover, we have identified Lunar and Martian regoliths as potential deleterious agents to the airway epithelium and overall health. Our findings might well contribute to pave the way for the development of novel alternative cannabinoid-based strategies for the prevention and treatment of

asthma and other inflammatory diseases as well as to enhance our knowledge on potential deleterious agents for airway epithelial barriers.

INTRODUCTION

1. The immune system

1.1. Overview of the immune response

The immune system is a complex network of organs, cells and molecules that cooperate to elicit defensive responses against exogenous (e.g. pathogens) or endogenous (e.g. tumors) threats, while keeping tolerance to self (e.g. host cells) and non-self- (e.g. commensal microbes, allergens) innocuous antigens (1, 2). The orchestration of proper immune responses is a tightly regulated process that depends on the capacity of immune components to sense multiple antigenic input variables and surrounding signals (antigen origin, chemical nature, pathogenicity, viability, abundance, etc.), which ultimately shape the robustness and type of reaction (1, 3). Dysregulation of this finely tuned process leads to the development of immune-mediated pathologies such as cancer, susceptibility to infections, autoimmune disorders or allergic diseases (**Figure I.1**) (1-3).

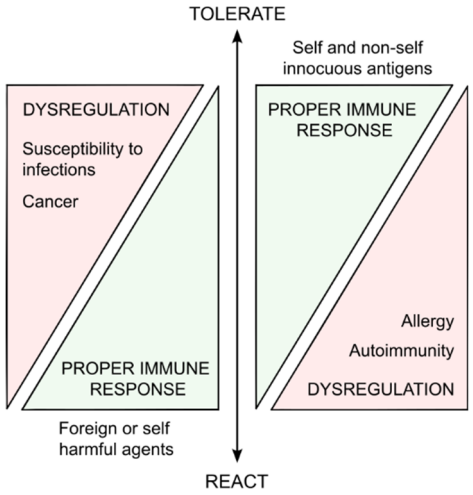

Figure I.1. Major functions of the immune system. The immune system preserves tolerance to innocuous antigens while defends the host from threats by mounting proper immune responses. Dysregulation of this process favors the development of immune-mediated pathologies. Inadequate response to pathogens or host malignant cells results in susceptibility to infections or cancer; while excessive reactions to innocuous self or environmental antigens leads to autoimmunity or allergies, respectively.

Traditionally, the host immune response has been divided into two major branches: innate and adaptive. Innate immunity provides a first line of defense against threats in a broad and non-specific manner. It is composed by structural barriers, either physical (epithelial cells), chemical (antimicrobial secretions) or microbial (commensal microbiota); innate leukocytes, including dendritic cells (DCs), mononuclear phagocytes, granulocytes, natural killer cells (NKs) and other innate lymphoid cells; as well as humoral elements such as the complement system and a wide range of soluble mediators . In contrast, the adaptive arm of immunity includes T and B lymphocytes, together with immunoglobulins (Ig) or antibodies. Adaptive immune responses take longer to develop and support the innate immune mechanisms through providing antigen specificity, amplification of the response, and memory development (1-4).

For decades, immunological memory has been thought to be exclusively stored in the form of expanded numbers of antigen-specific memory lymphocytes, as a hallmark feature of adaptive immune responses (1). However, recent findings outline the capacity of innate immune cells to acquire memory, leading to a novel concept defined as trained immunity (5). Trained immunity is the process by which innate immune cells undergo long-lasting functional, metabolic, epigenetic and transcriptional

reprogramming after exposure to a first stimulus, which favors the development of enhanced immune responses against secondary related- or unrelated challenges. While conventional adaptive immunity relies on clonal selection and expansion of antigen-specific lymphocytes together with the generation of memory T and B cells, innate memory depends on metabolic and epigenetic rewiring of innate immune cells and their progenitors, resulting in functional changes that confer a broader and long-lasting protection against heterologous insults (**Figure I.2**) (5-8). Remarkably, immunology is an evolving field of research and other new forms of immunological memory including neuro-immune crosstalk are already been explored (1).

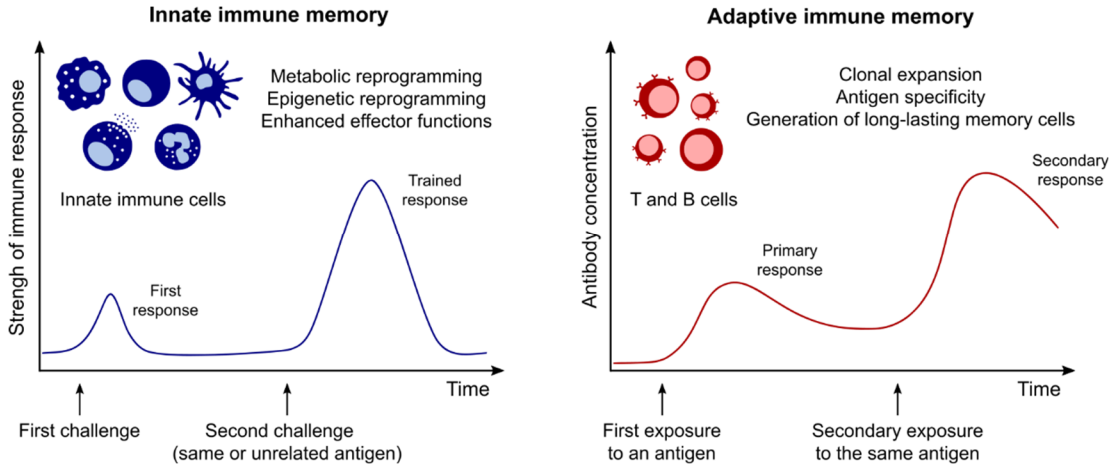

Figure I.2. Immunological memory in innate and adaptive immune response. Adapted from *Induction of innate immune memory: the role of cellular metabolism. Curr. Opin. Immunol.*, 2019; 56:10-16.

1.2. Antigen presenting cells as link of innate and adaptive immune responses

1.2.1. Dendritic cells

In 1973, Steinman and Cohn identified a new cellular population in peripheral lymphoid organs of mice, which they named as dendritic cells (DCs), from the Greek dendron (tree), due to their tree-shaped morphology (9). More than 50 years later, those stellate and elongated cells are widely recognized as the main and most potent professional antigen presenting cell (APC), with crucial roles connecting innate and adaptive immune responses (2, 10-13). DCs are present in peripheral tissues, lymphoid organs and blood, working as sentinels for threats and initiators of immune responses (2, 13, 14). To perform this key immune surveillance function, they are equipped with a series of pattern recognition receptors (PRRs) such as Toll-like receptors (TLRs), NOD-like receptors (NLRs), RIG-I-like receptors (RLRs) and C-type lectin receptors (CLRs), that allow them to sense foreign or self-antigens in the context of danger or homeostasis through the detection of pathogen- and damage-associated molecular patterns (PAMPs and DAMPs, respectively) (15-17). Additionally, other signals coming from different cell types such as cell-to-cell interactions and other released soluble mediators might shape the activation of DCs (18).

A major feature of DCs is their dual capacity to induce effector or tolerogenic responses depending on the local environmental signals in which they encounter antigens. In steady state, DCs display an immature phenotype and continuously screen the tissues, sampling and internalizing

antigens. Immature DCs (iDCs) are characterized by a high phagocytic capacity, reduced expression of maturation makers and costimulatory molecules (CD40, CD80, CD83 and CD86), low cytokine secretion, and limited ability to activate T cells. In contrast, upon stimulation DCs undergo maturation by increasing the expression of the above-mentioned molecules and upregulating chemokine receptors, such as C-C chemokine receptor 7 (CCR7), which allow them to migrate to the lymph nodes where they present antigens to T cells (16, 19, 20). Depending on their source, two classes of major histocompatibility complex (MHC) molecules direct the presentation of processed antigens on the surface of DCs. Endogenous antigens are loaded in class I MHCs and are recognized by $CD8^+$ T cells (cytotoxic T lymphocytes, CTL). Conversely, exogenous antigens are presented in class II MHC to $CD4^+$ T cells (T helper, Th). Nonetheless, under certain conditions, DCs can present extracellular antigens to CTLs by class I MHCs, a process called cross-presentation (16, 21). During maturation, MHC expression levels in DC surface significantly increase while their antigen uptake machinery shuts down after an early transient induction, resulting in an enhanced antigen presenting capacity and reduced phagocytic activity (16, 20, 22). Classically, it has long been thought that DCs preserving an immature phenotype lead to the promotion of tolerance through the induction of T cell anergy and generation of regulatory T cells (Tregs), while mature DCs are immunogenic and promote the activation of effector T cell responses. However, recent studies have demonstrated that there are specific conditions in which mature DCs are also capable of inducing tolerance (22-25). Therefore, tolerogenic DCs can be considered as a DC population consisting of immature-like and mature DC phenotypes induced by many different pathways and stimuli that lead to a shared hallmark feature: their immunosuppressive capacity (22-28) (**Figure I.3**).

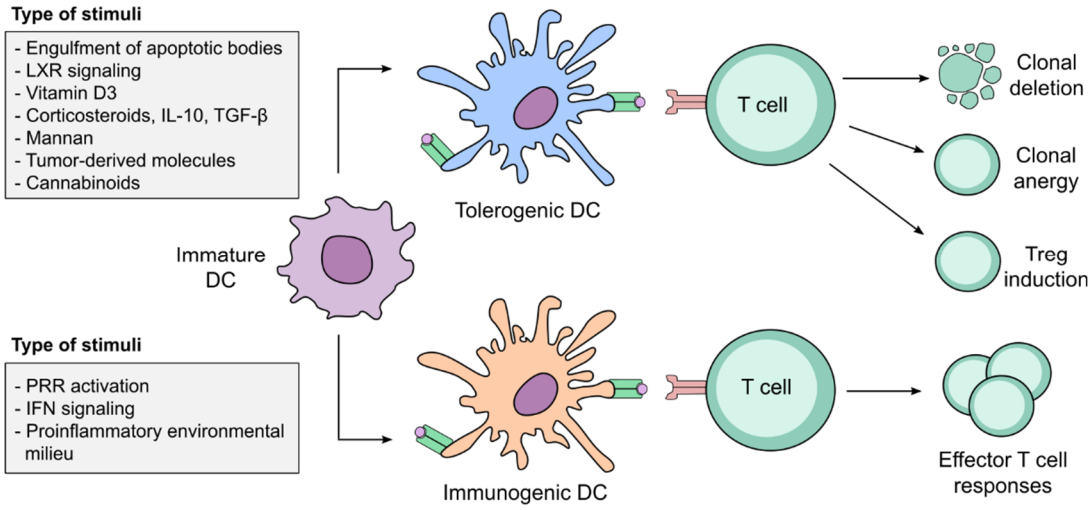

Figure I.3. Generation of tolerogenic vs. immunogenic DCs. Adapted from I*nduction of tolerance and immunity by dendritic cells: mechanisms and clinical applications. Front. Immunol*. 2019;10:2393.

The classification of DCs is quite challenging as the term “dendritic cell” encompasses a wide range of heterogeneous subpopulations with different developmental trajectories, expression of surface markers, PRRs, morphologies, migratory patterns and stimulatory capabilities on T cells. In humans, DCs develop from $CD34^+$ bone marrow precursors, mainly depending on interferon regulatory factor 8 (IRF8) and FMS-like tyrosine kinase 3 (FLT3) signaling, with the contribution of granulocyte-macrophage

colony-stimulating factor (GM-CSF) and macrophage colony-stimulating factor (M-CSF) in specific cell subsets (29, 30). According to ontogeny, DCs have been traditionally separated into conventional DCs, also known as myeloid DCs (cDCs or mDCs, respectively); plasmacytoid DCs (pDCs) and human monocyte-derived DCs (hmoDCs). Additionally, cDCs can be further divided into $CD141^+$ type 1 cDC (cDC1s) and $CD1c^+$ type 2 cDCs (cDC2s) (31-33). However, recent advances in high-dimensional technologies revealed novel DCs subpopulations such as DC3s and transitional DCs (tDCs) (34, 35) (**Figure I.4**).

cDC1s. Type 1 conventional DCs originate in the bone marrow from the common dendritic cell progenitor (CDP) and are characterized by the expression of surface markers like CD11c, CD141 and Clec9A. They are specialized in the activation of CTLs due to their efficiency in cross-presenting antigens and ability to produce interleukin (IL)-12 and type III interferons (IFNs), which allow them to also prime and stimulate potent Th1 responses. In this context, mice models lacking cDC1s show reduced control of tumor growth as well as impaired immunity against viruses and intracellular pathogens (14, 31, 32, 36, 37).

cDC2s. Similar to cDC1s, type 2 conventional DCs develop from the CDP and express CD11c. However, they can be differentially identified by their surface expression of CD1c. Together with cDC1s, they can be found in peripheral tissues, blood and lymphoid organs, where they are the primary subsets involved in T cell priming and the induction of potent adaptive immune responses. In particular, cDC2s are more specialized in the presentation of antigens in MHC II molecules to $CD4^+$ T cells and, although they may play certain roles during viral infections, cDC2s are widely recognized as inducers of immune responses against extracellular pathogens by promoting Th2, Th17 and Tfh polarizations (14, 31, 32, 36, 37).

tDCs. Originally termed as $AXL^+Siglec6^+$ DCs (ASDCs) by their expression markers, transitional DCs display spanning features from both cDC2s and pDCs. Their ontogeny is still unclear but closely related to pDCs. They have been proposed to be a transitional population between pDCs and cDC2s due to their *in vitro* capacity to differentiate into cDC2. tDCs lack the expression of type I IFNs but are good responders to viral stimuli and inducers of T cell responses (31, 32, 35, 38).

pDCs. Plasmacytoid DCs are characterized by the specific expression of the surface makers CD123, CD303 and CD304, as well as their specialized capacity to sense viral threats and mount antiviral immune responses through the production of type I and III IFNs. The ontogeny of pDCs is still a matter of debate with no current consensus on their lymphoid or myeloid origin (39-41). At the steady state, pDCs are mainly located in lymphoid organs and their capacity to prime T cell responses is limited compared to other DC subsets. However, several studies demonstrated that they are able to promote Th1 and regulatory T cell responses (32, 36, 42).

DC3s. The human DC3 subset was initially identified by single-cell technology as a subpopulation of cDC2s mainly characterized by the surface expression of CD1c, lack of CD5 and varying levels of CD14 and CD163 (34). Further studies showed independent developmental pathways compared to cDC2s which determined their characterization as a different DC lineage. DC3s display an

intermediate phenotype between monocytes and cDC2s and originate from a Ly6C$^+$ monocyte-dendritic cell progenitor (MDP) (43). DC3s are efficient in naïve T cell priming, driving polarization towards Th17 and Th1 phenotypes (32, 34, 44).

hmoDCs. In the steady state and specially under inflammatory conditions, blood monocytes are recruited into tissues and differentiated into monocyte-derived DCs. Ontogeny studies in mice show that both granulocyte-monocyte progenitors (GMP) and MDP give rise to monocytes, however, only monocytes derived from MDPs can be differentiated into monocyte-derived DCs (45). *In vivo*, hmoDCs are potent producers of cytokines and have demonstrated capacity to activate CD4$^+$ T cells and cross-present antigens to CD8$^+$T lymphocytes (46). *In vitro*, human monocytes can be differentiated into DCs in the presence of GM-CSF and IL-4 (47). These extensively used protocols allow the generation of hmoDCs with an immature phenotype, which can be later on activated to achieve immunogenic or tolerogenic phenotypes (23, 48, 49).

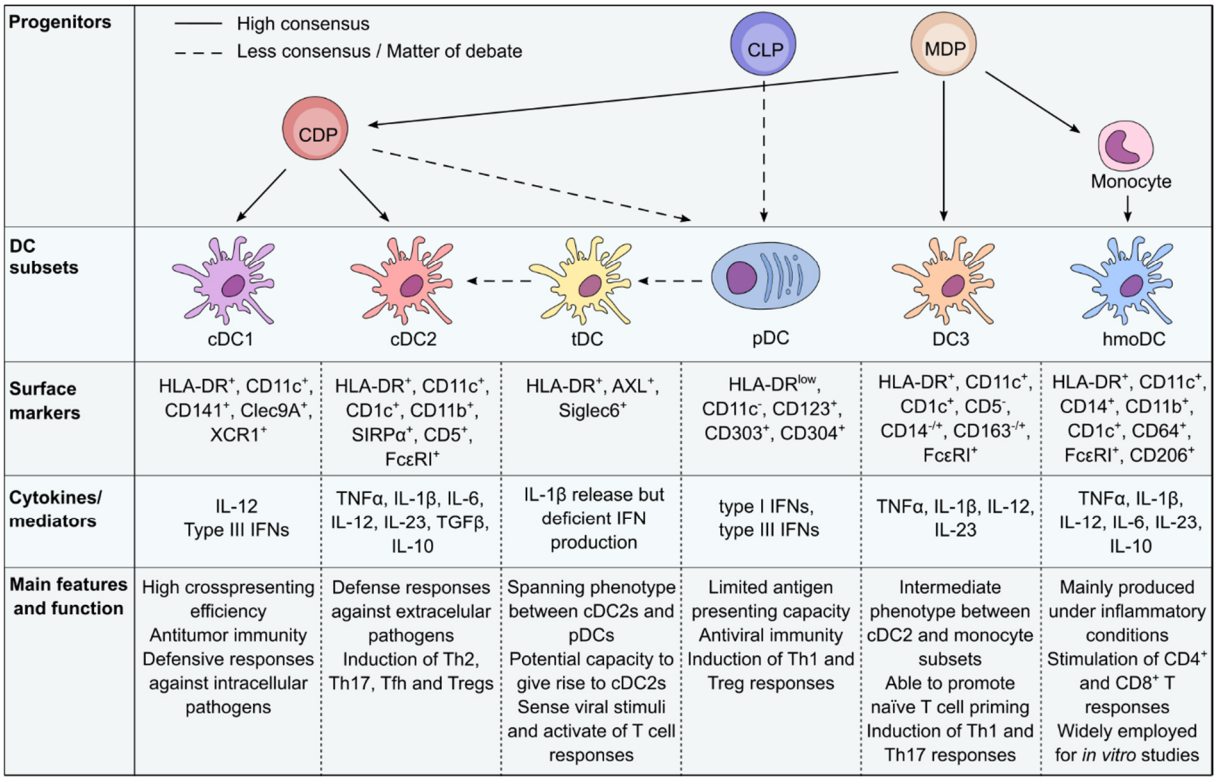

Figure I.4. Classification and major molecular and functional features of DC subsets (14, 31-33, 36-38, 46, 50). CLP, common lymphoid progenitor; MDP, monocyte-dendritic cell progenitor; CDP, common dendritic cell progenitor; cDC1, type 1 conventional DC; cDC2, type 2 conventional DC; tDC, transitional DC; pDC, plasmacytoid DC; hmoDC, human monocyte-derived DC.

1.2.2. CD4$^+$ T cell priming and polarization of adaptive responses by dendritic cells

T cell priming is the crucial process by which professional APCs promote the activation of naïve T cells and provide the information that allows them to develop specialized effector functions in an antigen-specific manner. Although it is not exclusively limited to them (51, 52), the priming of T cell responses is the quintessential specialization of DCs, being far superior to other APCs in performing this key function (10-12, 37).

Three major signals are required for successful activation of naïve CD4⁺ T cells by DCs: antigen recognition (signal 1), detection of costimulatory molecules in the surface of DCs by T lymphocytes (signal 2) and the soluble factors released during this process (signal 3). The first signal provides the specificity of the interaction through engagement of peptide-MHC II complexes with the T cell receptor (TCR). Meanwhile, signals 2 and 3 complete the activation and shape the differentiation of T cells towards different phenotypes (17, 18, 37). A wide range of costimulatory molecules are involved in this process, with different outcomes in T cell stimulation. The best-characterized ones are the costimulatory molecules from the B7 family (CD80 and CD86) which interact with CD28 expressed by T cells to promote their activation. Nonetheless, some other stimulatory and inhibitory molecules influencing the activation of T cells have been described. For example, OX40 ligand (OX40L) and CD40 expressed in the surface of DC are recognized by OX40 and CD40 ligand (CD40L) molecules, respectively, in activated T cells resulting in a potent stimulatory capacity. In contrast, programmed death-1 (PD-1) and cytotoxic T lymphocyte antigen 4 (CTLA4) molecules present in T lymphocytes interact with programmed death-ligand 1 and 2 (PD-L1 and PD-L2, respectively), or CD80 and CD86, respectively, on the surface of DCs to promote the limitation and control of T cell effector activity (53). Together with cytokines and other soluble molecules, all these signals complete T cell activation (**Figure I.5**) (17, 18, 37). In this context, the capacity of DCs to polarize T lymphocytes into different phenotypes is influenced by several factors, which can be broadly classified into intrinsic or environmental. Intrinsic factors include the type of PRRs expressed that may have been stimulated during the encounter with the antigen as well as the DC cell subset involved in its presentation. In contrast, environmental factors encompass the signals received from other cellular population sources in the tissue context such as epithelial cells or ILCs (**Figure I.5**). The comprehensive integration of this information allows DCs to promote the differentiation of diverse and relatively plastic Th phenotypes that adapt their functions depending on the environmental circumstances (17, 18, 54). The different phenotypes involved in T helper cell specialized effector functions include: Th1, Th2, Th9, Th17, Th22, Tfh and Treg (**Figure I.6**).

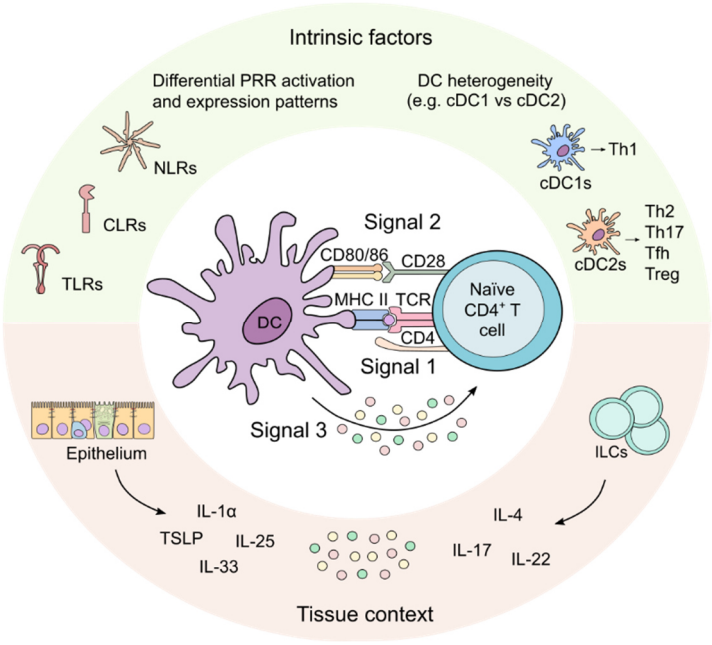

Figure I.5. Signals required for T cell priming and factors influencing DC polarization of T cell responses. Adapted from *Control of adaptive immunity by pattern recognition receptors. Immunity*. 2024;57(4):632-648.

Th1. T helper 1 cells are major contributors to immune defense against intracellular pathogens. The differentiation towards this phenotype is driven by IL-12 and IFN signaling, which determine the expression of its master transcription factor T-box expressed in T cells (T-bet). Activated Th1 cells

produce large amounts of IFNγ, activating macrophages, NK cells and CTLs to fight microbes and kill infected cells (18, 37, 55).

Th2. T helper 2 polarization is mainly driven by exogenous or autocrine sources of IL-4 that activate the master transcription factor GATA binding protein 3 (GATA3). Th2 cells produce IL-4, IL-5 and IL-13 contributing to immunological defense against extracellular parasites and venoms as well as drive wound healing responses. However, dysregulated functions are associated to pathologies, mainly allergic diseases (18, 37, 55).

Th9. T helper 9 cells are defined by their production of large amounts of IL-9, but not of IL-4, IL-5 or IL-13, which differentiate them from Th2 cells. IL-4 and TGF-β are the main drivers of Th9 polarization, which is involved in anti-helminth responses as well as cancer, allergies and autoimmune diseases (56).

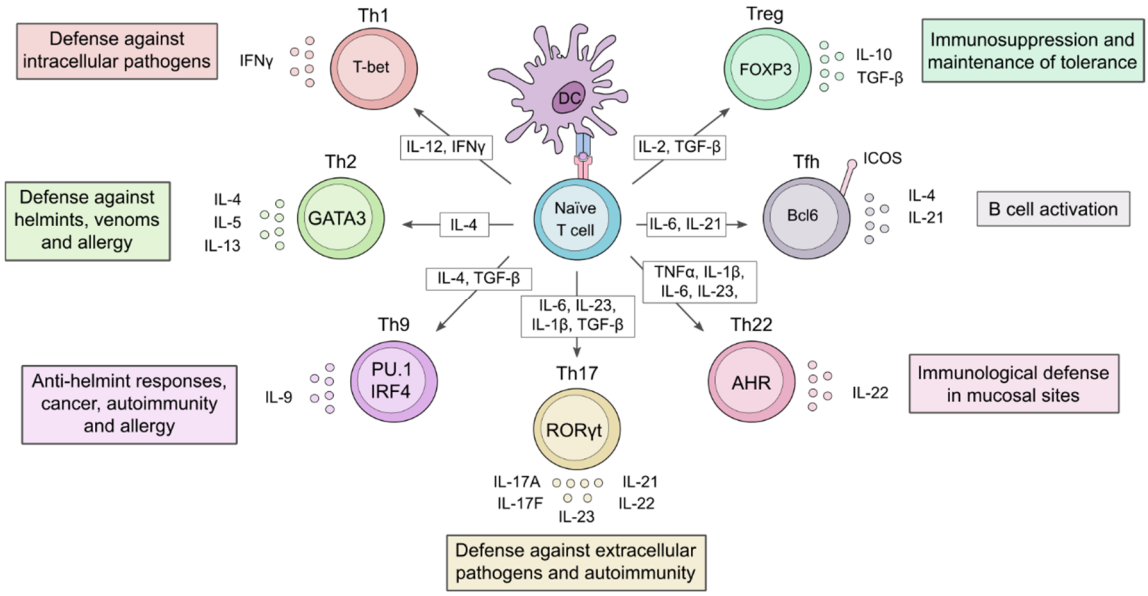

Figure I.6. Differentiation signals and functions of $CD4^+$ T cell subsets. Adapted from *T cells in health and disease*. *Signal Transduct Target Ther*. 2023;8(1):235.

Th17. T helper 17 subset is characterized by the production of IL-17A-F, IL-21, IL-22 and IL-23 as well as the expression of the master transcription factor retinoic acid-related orphan receptor γt (RORγt). Th17 cells are differentiated by IL-6, IL-1β, IL-23 and TGF-β and contribute to the immunological defense against extracellular pathogens, especially in mucosal tissues. Remarkably, they also play important roles in autoimmune disorders (18, 37, 55).

Th22. T helper 22 cells are generated in response to various cytokines, including IL-6, IL-23, IL-1β, and TNF-α. They are characterized by the expression of the transcription factor aryl hydrocarbon receptor (AHR) and secrete high levels of IL-22 without IL-17 or IFNγ production. Th22 cells mainly contribute to the reinforcement of epithelial cell linings through increasing the secretion of antimicrobial peptides and enhancing barrier integrity (57, 58).

Tfh. T follicular helper cells are a heterogeneous population specialized in supporting humoral responses. Their development is promoted by IL-6 and IL-21 cytokines, which induce the expression of Bcl6, their master transcription factor. Tfh cells express IL-21 and IL-4 cytokines together with surface molecules such as CD40 and inducible T cell costimulator (ICOS) that promote the proliferation of B cells and their differentiation into antibody-secreting plasma cells (55, 59).

Tregs. Regulatory T cells play essential roles in the control of excessive immune responses and the maintenance of tolerance to self- and non-self- innocuous antigens. According to their origin, there are two major subsets of Tregs: thymus-derived Tregs (tTregs), generated upon self-antigen recognition during T cell development, and peripherally derived Tregs (pTregs), which are differentiated from naïve T cells in peripheral tissues. In addition, the latter ones can be further classified into peripherally induced $FOXP3^+$ Tregs, IL-10-producing Tregs (Tr1), and transforming growth factor β (TGF-β)-producing Th3 cells (60, 61).

As previously described, tolerogenic DC can promote the generation of Tregs in the periphery. The mechanisms involved in this process include (**Figure I.7**) (26, 27, 61, 62):

- The secretion of soluble mediators such as IL-10 or TGF-β.
- Production of specific enzymes like indoleamine 2,3-dioxygenase (IDO) or retinaldehyde dehydrogenase (RALDH), which participate in the generation of tolerogenic metabolites such as kynurenine or retinoic acid, respectively.
- Expression of co-stimulatory molecules such as PD-L1 or inducible costimulator ligand (ICOSL).
- Other forms of cell-to-cell communication such as the release of extracellular vesicles.

Currently, the most widely used markers to identify or isolate Tregs consist of the expression of IL-2 receptor ($CD25^+$), lack of IL-7 receptor ($CD127^-$) and the expression of the transcription factor forkhead box P3 ($FOXP3^+$). In fact, FOXP3 constitutes the master regulator of Treg development, maintenance and immunomodulatory function. To perform their immunosuppressive properties, Tregs target many different cellular populations through four major mechanisms (**Figure I.7**) (60, 61, 63, 64):

- Secretion of anti-inflammatory cytokines: IL-10, TGF-β or IL-35.
- Metabolic disruption of target cells such as the constitutive expression of CD25 which depletes IL-2 availability for effector T cells, or the expression of the enzymes CD39 and CD74, that act in tandem to generate the immunosuppressive nucleoside, adenosine, from adenosine triphosphate (ATP).
- Cell-to-cell interactions through the expression of co-inhibitory receptors including PD-1, cytotoxic T lymphocyte antigen 4 (CTLA4), T cell immunoreceptor with Ig and ITIM domains (TIGIT), lymphocyte activation gene 3 (LAG3) or inducible T-cell costimulator (ICOS), among others.
- Cytolysis of target effector cells through the release of granzymes and perforins.

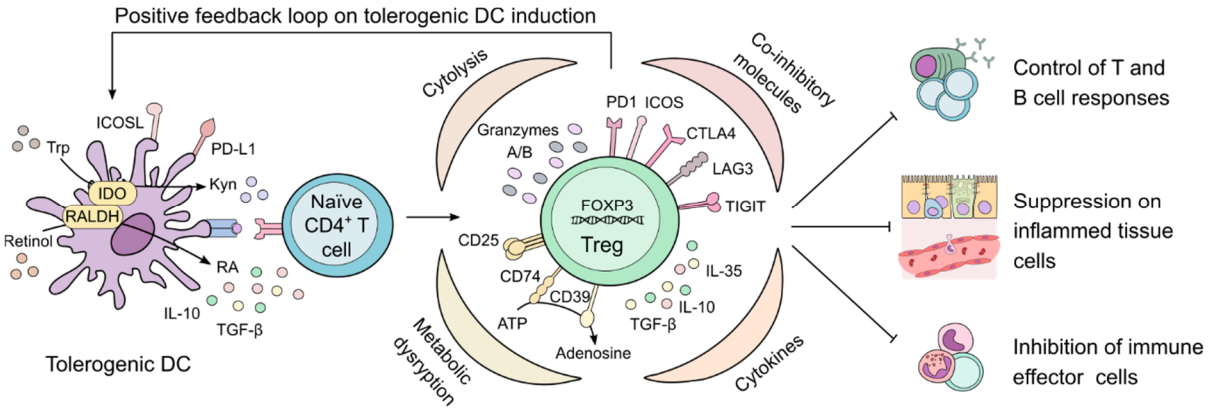

Figure I.7. Induction of Tregs by DCs and their immunosuppressive mechanisms. IDO, indoleamine 2,3-dioxygenase; RALDH, retinaldehyde dehydrogenase; ICOSL, inducible costimulator ligand; PD-L1, programmed death-ligand 1; RA, retinoic acid; Kyn, kynurenine; FOXP3, forkhead box P3; PD-1, programmed cell death-1; ICOS, inducible T-cell costimulator; CTLA4, cytotoxic T lymphocyte antigen 4; LAG3, Lymphocyte Activation Gene-3; TIGIT, T cell immunoreceptor with Ig and ITIM domains; ATP, adenosine triphosphate. Adapted from *Regulatory T cells and immunoglobulin E: A new therapeutic link for autoimmunity?. Allergy*. 2022;77(11):3293-3308.

1.2.3. Macrophages

Macrophages were originally described by Metchnikoff in 1891 who named them from the Greek makro- (big) and -phagos (eater), based on their large size and ability to engulf foreign materials (65). Similar to DCs, macrophages are professional APCs able to mount and amplify innate and adaptive immune responses. They are equipped with a wide range of PRRs to sense harmful or foreign antigens as well as complement and Fc receptors for IgG to carry out the clearance of opsonized material and pathogenic threats (66, 67). This phagocytic function is key for host defense against microbes but also for other housekeeping tasks such as clearance of apoptotic cells and remodeling of extracellular matrix (ECM). In recent decades, it has become apparent that considering macrophages as immune cells solely characterized for their phagocytic activities is too reductive, as compelling evidence demonstrates their involvement in many other homeostatic functions (68). Apart from detecting phagocytable material, macrophages sense physiological parameters (pH, temperature, osmolarity, hypoxia, pressure, metabolites, ECM components, metal ions) and act as biochemical transducers integrating these inputs to direct tissue growth, remodeling and preserving its proper function (66, 67). In this sense, macrophages are regarded as homeostasis gatekeepers distributed across all body tissues and performing both systemic and tissue-specific functions, including organogenesis, tissue remodeling and regeneration, clearance of apoptotic and senescent cells, recycling of nutrients, control of neuronal activity, regulation of systemic metabolism, defense against pathogens and malignant cells and the re-establishment of homeostasis after inflammation, among many other (66, 67, 69, 70).

The capacity of macrophages to carry out this wide variety of functions relies on two major features: their heterogeneity and plasticity. The heterogenicity of macrophage populations is extremely complex due to the fact that ontogeny and tissue-specific location shape macrophage phenotypical and functional properties. For a long time, macrophages were thought to be continuously replenished in tissues from blood monocytes originated in the bone marrow. However, current evidence supports that

tissue-resident macrophages comprise cells coming from either embryonic progenitors with self-renewal capacity or adult blood monocytes, with the relative contributions of one source or the other varying by tissue and through lifetime. Notably, during disease, monocytes are recruited to inflamed tissues and differentiate into monocyte-derived macrophages, providing another step of complexity (69, 70). Both tissue resident and monocyte-derived macrophages are quite plastic and share the capacity to timely adapt to their microenvironment through the acquisition of several functional profiles, also known as polarization states. Under inflammatory conditions, macrophages increase their antigen presenting capacity and secrete large amounts of cytokines. Traditionally, this proinflammatory state was termed as classical or M1 activation. In contrast, a pro-resolving anti-inflammatory phenotype was termed as M2 or alternative activation, in a parallel dichotomy to Th1 vs Th2 adaptive responses (71). Nowadays, this concept of two extremes of macrophage polarization is currently obsolete and has been replaced by the consideration of macrophage activation as a continuum of different functional adaptations that macrophages acquire after the sensing environmental cues together with the influence of their ontogeny and tissue specific context (68, 72). However, the M1/M2 dichotomy is still useful in certain experimental situations *in vitro*, where environmental signals are finely controlled. In this sense, GM-CSF, TLR agonists such as LPS, IFNs and inflammatory cytokines are commonly used to achieve proinflammatory M1-like polarizations *in vitro*, which are characterized by the expression of markers like CD80, CD86, CCR7, enhanced levels of MHC-II molecules as well as high production inflammatory cytokines (TNFα, IL-1β, IL-6, IL-12). Conversely, M-CSF, IL-4, IL-13, IL-10, TGF-β, glucocorticoids and other stimuli are employed to generate M2-like states characterized by their low inflammatory cytokine production and the expression of CD163, CD206 and CD209 markers. Moreover, M2 polarizations can be further divided into M2a, M2b, M2c or M2d depending on the stimulation employed (71, 73, 74) (**Figure I. 8**).

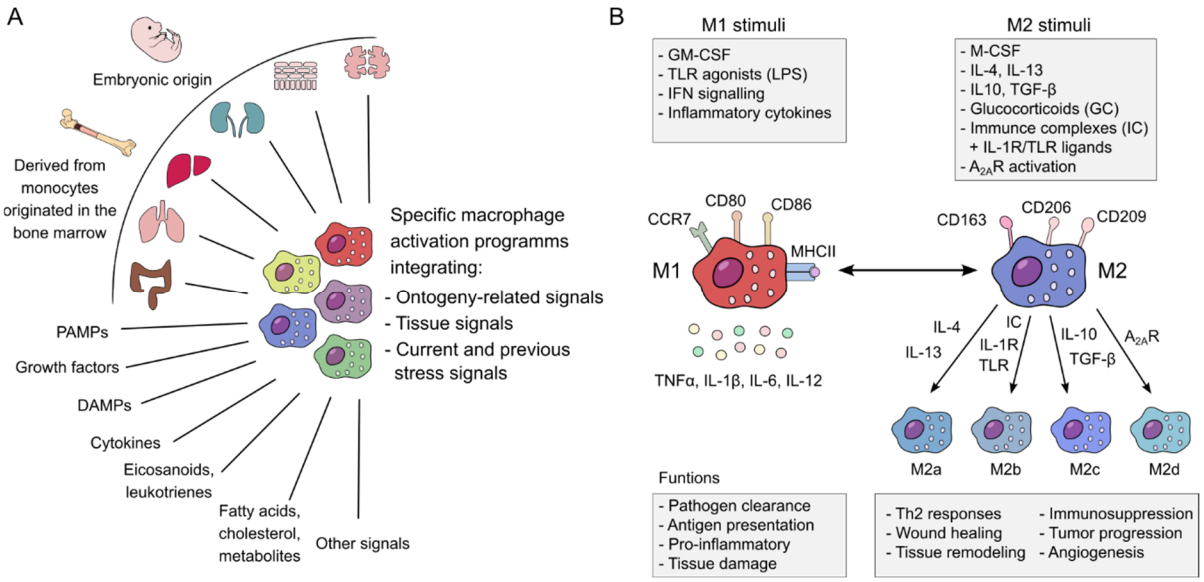

Figure I.8. Multidimensional (**A**) and conventional (**B**) models of macrophage polarization. PAMPs, pathogen associated pattern recognition receptors; DAMPs, damage associated pattern recognition receptors; GM-CSF, granulocyte-macrophage colony-stimulating factor; TLR, Toll-like receptor; IFN, interferon; M-CSF, macrophage colony-stimulating factor; IL-1R, interleukin 1 receptor; $A_{2A}R$, Adenosine A2 receptor. Adapted from (71-73).

1.3. Immunometabolism: metabolic regulation of immune function

1.3.1. An overview of the main metabolic pathways

Immunometabolism is an emerging field of research that explores how immune cells rely on diverse metabolic pathways to achieve specific responses and how modulation of this cellular metabolism alters immune cell activation, differentiation, survival and growth. There are six main metabolic pathways playing crucial roles in immunometabolism: glycolysis, tricarboxylic acid (TCA) cycle, pentose phosphate pathway, fatty acid synthesis, fatty acid oxidation, and amino acid metabolism (75-77) (**Figure I.9**).

Glycolysis. The glycolytic pathway begins with the uptake of extracellular glucose, which is processed in the cytosol to generate pyruvate along with other products. During this process, glycolysis allows the reduction of nicotinamide adenine dinucleotide (NAD^+) to NADH and provides biosynthetic intermediates for cellular anabolism. The pyruvate derived from glucose may take two different routes depending on oxygen availability. In normoxia, pyruvate enters the mitochondria where it is converted to acetyl coenzyme A (acetyl-CoA) and fuels the TCA cycle, while under hypoxic conditions, pyruvate is reduced to lactate (lactic acid fermentation) and exits the cell. Lactic fermentation is a relatively low efficient process as only obtains 2 ATP molecules from one glucose, compared to the generation of up to 32 ATP molecules when pyruvate fuels the TCA cycle. However, in certain situations, cells rely on glycolysis and lactic fermentation to rapidly obtain ATP. This may occur even under aerobic conditions, in a process described by Otto Warburg in tumoral cells and termed as aerobic glycolysis or Warburg metabolism (75-77).

TCA cycle and oxidative phosphorylation (OXPHOS). Also known as Krebs cycle or citric acid cycle, the TCA cycle takes place in the mitochondrial matrix and represents a highly efficient process of ATP generation when coupled to OXPHOS. Many different metabolic inputs can fuel the TCA cycle, such as the acetyl-CoA obtained from fatty acids or glucose-derived pyruvate, as well as the products coming from amino acid metabolism. This metabolic path generates NADH and reduced flavin adenine dinucleotide ($FADH_2$) which can feed the electron transport chain of the inner mitochondrial membrane and allow the production of ATP through OXPHOS in a process that requires oxygen consumption (75, 76).

Pentose phosphate pathway (PPP). PPP occurs in the cytosol and allows the diversion of glycolysis intermediates towards the production of nucleotide and amino acid precursors necessary for cell growth and proliferation. Additionally, it is also involved in the generation of equivalents of reduced NAD phosphate (NADPH) which play important roles in redox balance and production of reactive oxygen species (ROS) (75, 76).

Fatty acid synthesis (FAS). The synthesis of fatty acids (FA) occurs in the cytosol and allows the production of lipids necessary for cellular growth and proliferation from the precursors obtained from other metabolic pathways including glycolysis, TCA cycle and PPP (75).

Fatty acid oxidation (FAO). FAO begins in the cytosol were FA are activated by conjugation with ATP, generating FA acyl-CoA that enters the mitochondria. Once there, β-oxidation of FA acyl-CoA takes place yielding large numbers of acetyl-CoA, NADH and FADH2, which can be further used in the TCA cycle and the electron transport chain to produce huge amounts of energy through OXPHOS (75).

Amino acid metabolism. Amino acids are involved in multiple metabolic pathways due to their structural diversity. They are the major substrates for protein synthesis and consequently are closely related to cellular anabolism. However, some amino acids are employed as precursors for other molecules such as branched-chain fatty acids, and others like glutamine can serve to fuel TCA cycle in proliferative cells (75, 76).

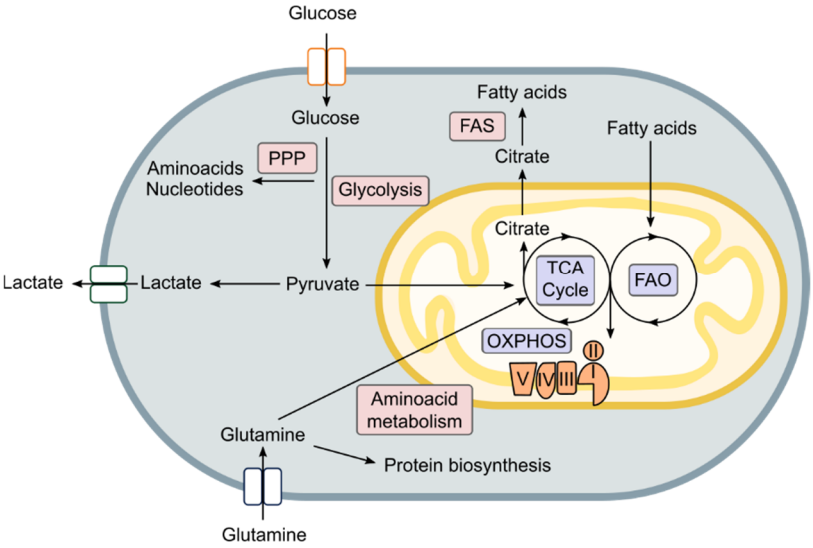

Figure I.9. Metabolic pathways governing immune function. Glycolysis, TCA cycle, oxidative phosphorylation (OXPHOS), pentose phosphate pathway (PPP), fatty acid oxidation (FAO) , fatty acid synthesis (FAS) and amino acid metabolism. Oxygen-dependent pathways are represented in blue and pathways that do not require oxygen are represented in red. Adapted from *A guide to immunometabolism for immunologists. Nat Rev Immunol*, 2016; 16(9):553-65.

Apart from this broad perspective, other specific metabolic routes can also shape immune performance in different cell subsets. For instance, the mevalonate pathway involved in the synthesis of cholesterol plays a key role in the generation of innate immune memory (78). A better understanding of the metabolic pathways that specific immune cells commit to during the acquisition of different functional profiles may well provide the basis for the development of novel immunomodulatory drugs.

1.3.2. Metabolic control of macrophage activation

As previously mentioned, macrophages are characterized by their plasticity to adapt their functional features to environmental inputs though the acquisition of different activation or polarization states. This process is associated with a series of metabolic changes, also known as metabolic reprogramming, that modulate transcriptional and posttranscriptional events ultimately controlling the activation profile (77). The metabolic reprogramming of macrophages in response to different stimuli has been extensively investigated, specially between the two extremes of the M1/M2 dichotomy, which display completely different metabolic profiles (**Figure I.10**) (77, 79-81).

In response to M1 stimuli such as LPS or LPS+IFNγ, macrophages initiate signal transduction pathways that activate nuclear factor-κB (NF-κB), activation protein 1 (AP-1), interferon response factors (IRFs) and/or signal transducers and activators of transcription (STATs), leading to the expression of

multiple inflammatory genes (80). These macrophages are characterized by an enhanced glucose uptake, commitment to Warburg metabolism and a compromised OXPHOS, which results in the generation of large amounts of lactate (77, 79-81). Upregulation of glycolytic metabolism also feeds the PPP to support the high demand for amino acids and nucleotides, but also for NADPH needed for the production of ROS (77, 79). Moreover, the TCA cycle of proinflammatory macrophages is broken at two stages: after citrate and after succinate, leading to the accumulation of both metabolites. Citrate exits the mitochondria and gives rise to acetyl-CoA in the cytosol through the enzyme ATP citrate lyase. This acetyl-CoA can serve as precursor for FA and prostaglandin synthesis, but it may also provide acetyl groups for histone acetylation, fueling a metabolic-epigenetic axis to induce the expression of inflammatory mediators. Additionally at this step, the parallel induction of aconitate decarboxylase 1 allows the mitochondrial production of the metabolite itaconate from isocitrate. Itaconate is an inflammatory product with antimicrobial and immunoregulatory properties which in turn can inhibit succinate dehydrogenase promoting the second break in the TCA cycle. Increased intracellular levels of succinate contribute to the stabilization of hypoxia-inducible factor 1 alpha (HIF1α), a key transcription factor for the induction of IL-1β and the upregulation of glycolytic-related enzymes. Therefore, the metabolic reprogramming of M1 macrophages coordinates the acquisition of inflammatory properties at different levels (79-82).

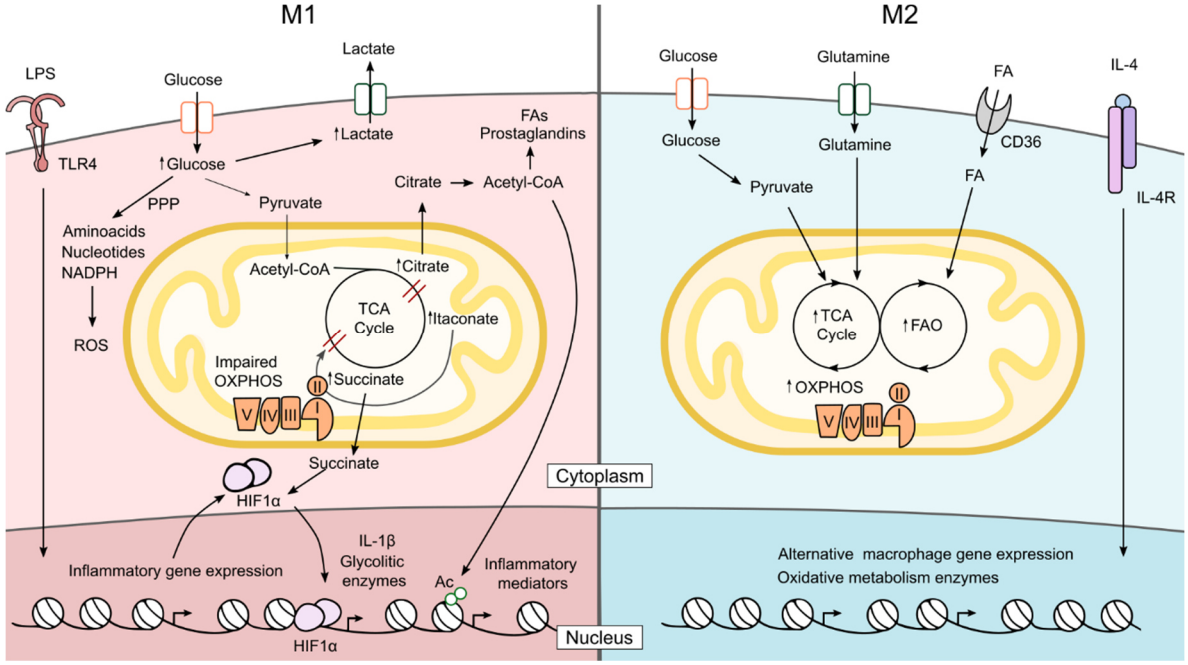

Figure I.10. Metabolic reprogramming of macrophage activation. Adapted from *Integration of transcriptional and metabolic control in macrophage activation. EMBO Rep*. 2021;22(9):e53251.

In contrast, M2 stimuli such as IL-4 or IL-4+IL-13 promotes an alternative activation characterized by a strong commitment to OXPHOS and an intact TCA cycle. IL-4 signaling enhances the uptake of FA via CD36 and upregulates the expression of several genes involved in oxidative metabolism. These changes potentiate FAO, that together with glutaminolysis, are the main fuel of TCA cycle and OXPHOS in alternatively activated macrophages. Additionally, glycolysis has been suggested

to also play a role in M2 macrophages, either directly fueling TCA cycle or contributing to *de novo* FAS to sustain FAO (77, 79, 80).

2. The epithelial barrier theory

2.1. Epithelial barriers as gatekeepers of immune tolerance and body homeostasis

In the last decades we have witnessed a steep rise in the prevalence of chronic non-communicable diseases including allergic, autoimmune and other inflammatory disorders that have reached pandemic proportions affecting up to one fourth of the world's population (83). The epithelial barrier theory proposed by Dr. Akdis attributes the increase in non-communicable diseases to a deleterious impact on epithelial barrier function of environmental agents introduced in our daily lives during industrialization and modernization (84, 85).

Epithelial tissues form a continuous layer covering the inner and outer surfaces of our body and protecting us from physical, chemical or biological environmental stressors. The structure of epithelial tissues differs depending on their location to meet specific functional needs, ranging from the stratified squamous epithelium of the skin, the pseudostratified epithelium of the conducting airways, or the columnar epithelium of the intestine, among others (86, 87). However, all of them share common elements. They are bound to the underlying extracellular matrix by a fibrous basement membrane and are equipped with a series of intercellular junctions that provide their integrity: tight junctions (TJs), adherence junctions (AJs) and desmosomes. TJs are protein complexes in the apicolateral borders of cells that regulate cell polarity and paracellular molecule traffic. AJs are located underneath TJs and, together with them, link to the actin cytoskeleton of the cell. Desmosomes are present in the lateral surface of cells connecting neighboring epithelial cells (86) (**Figure I.11**). Of note, on top of this mechanical function, epithelial cells display defensive features such as mucociliary clearance, secretion of antimicrobial peptides, proteases or antioxidants, as well as the ability to sense pathogens through PRRs and activate inflammatory signaling pathways. Collectively, all these features allow epithelial tissues to perform their key homeostatic functions, however, when disrupted, organ damage, inflammation, and diseases take place (87).

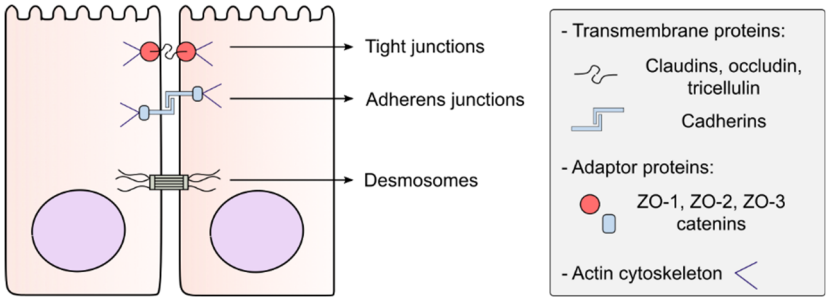

Figure I.11. Epithelial cell to cell junctional complexes. Adapted from *Environmental factors in epithelial barrier dysfunction. J Allergy Clin Immunol.* 2020;145(6):1517-1528.

The human exposome is the sum of all the environmental exposures such as diet, microbiome, and pollutants during the lifetime of an individual. Since the 1960s many potentially harmful substances

have been introduced into our exposome as a consequence of industrialization, urbanization and modernized lifestyle. Genetic factors, together with the exposure to epithelial-damaging agents including pollutants, microbes, allergens, micro- and nano-plastics, certain hygiene products and food additives, compromise the protective functions of epithelial cells (86-88). During this process, epithelial injury impairs cell to cell junctions, the epithelium becomes leaky and secretes inflammatory mediators, mainly alarmins (IL-25, IL-33 and TSLP), promoting epithelitis. In parallel, the opening of the epithelium allows the translocation of microbes to sub-epithelial locations as well as the colonization of opportunistic pathogens and loss of commensal diversity, resulting in microbial dysbiosis. An inflammatory response, usually type 2 mediated, is then generated to facilitate the expulsion of leaked microbiota, in a similar mechanism to the expulsion response orchestrated during the immune defense against some parasite larvae and hookworms. The expulsion phase creates a vicious cycle in which unresolving inflammation increases epithelial permeability, impedes barrier healing and perpetuates microbial dysbiosis and barrier defects. In this context, local inflammation and impaired epithelial barrier function facilitate the induction of aberrant immune responses to allergens, commensals and opportunistic pathogens as well as contribute to circulating microinflammation that reach distal organs. Altogether, this cascade of events links epithelial dysfunction with allergic, autoimmune and other chronic non-communicable diseases (**Figure I.12**) (83-85, 87-89).

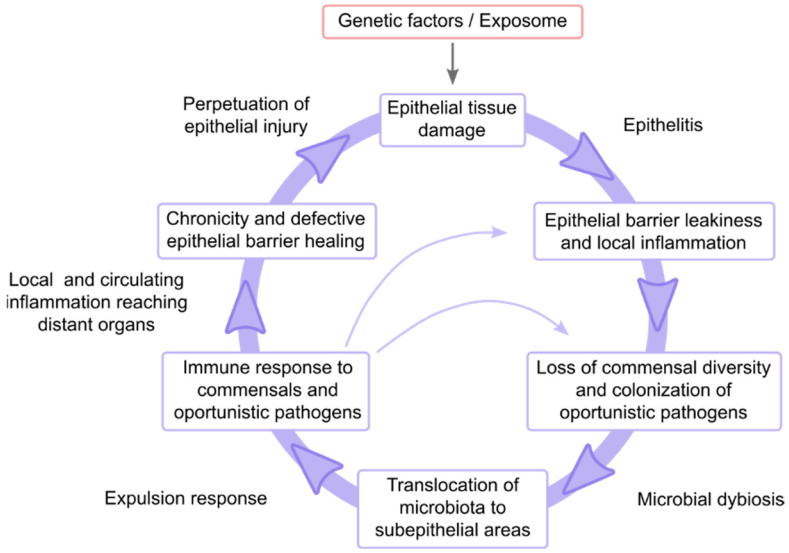

Figure I.12. The vicious cycle of epithelial barrier damage. Adapted from *Does the epithelial barrier hypothesis explain the increase in allergy, autoimmunity and other chronic conditions?. Nat Rev Immunol*. 2021;21(11):739-751.

2.2. Diseases associated with epithelial barrier defects

Several criteria have been proposed to identify diseases fitting within the concept of the epithelial barrier theory: increasing prevalence in the last decades (not influenced by the improvement in diagnosis methods), detection of epithelial barrier defects in biopsies, evidence of microbial dysbiosis, and the presence of inflammatory biomarkers in circulation (microinflammation) (87). According to these criteria, pathologies classified as epithelial barrier associated diseases include:

- Diseases with a local barrier defect, which is a hallmark of allergic inflammatory diseases such as asthma, allergic rhinitis, atopic dermatitis, food allergy or eosinophilic esophagitis (83-85).
- Systemic diseases with gut or lung barrier defect and dysbiosis, which include autoimmune and metabolic disorders affecting organs distant from the site of barrier impairment like rheumatoid arthritis, systemic lupus erythematosus, multiple sclerosis or diabetes (83-85).
- Neuropsychiatric diseases with gut barrier defect and dysbiosis such as autism spectrum disorder, Parkinson disease or Alzheimer disease (83-85).

These evidence highlights that epithelial barriers are gaining insight into the pathogenesis of multiple non-communicable diseases affecting many different organs and tissue locations. The identification of novel preventive and therapeutic strategies targeting epithelial barrier impairment and its subsequent pathological consequences are required to face the increased development of allergic, autoimmune and other inflammatory disorders (83, 84, 87).

3. Asthma

Asthma is the most prevalent chronic inflammatory disease of the airways, affecting more than 300 million people worldwide. It is defined by the history of variable respiratory symptoms including cough, wheezing, shortness of breath and chest tightness, along with expiratory airflow limitation; both of them fluctuating over time and varying in intensity (90-92). The symptomatology of asthma is closely associated with airway inflammation, which, through the interplay between immune cells with structural cells (e.g. bronchial epithelium), drives the main pathophysiological features of the disease: tendency of the smooth muscle to react to unspecific stimuli (bronchial hyperresponsiveness, BHR), mucus overproduction and airway remodeling (91, 93) (**Figure I.13**). Additionally, a common feature of asthmatic patients is their susceptibility exacerbations. Under certain situations or when exposed to trigger factors such as exercise, drugs, allergens or respiratory viruses, patients suffer flare-up episodes (asthma attacks) resulting in the aggravation of the disease and accounting for the major causes of morbidity, mortality and health care costs (90, 91, 94).

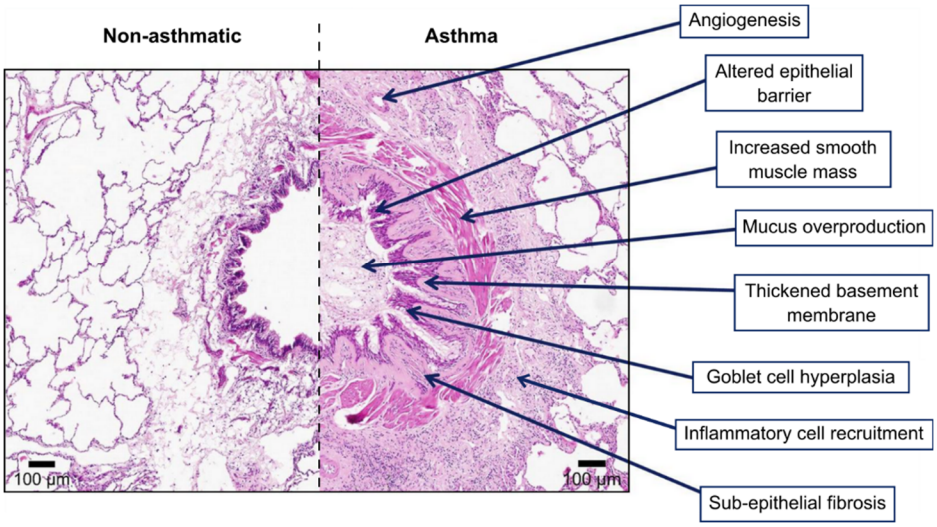

Figure I.13. Pathophysiological events observed in the asthmatic airways. Adapted from *Airway remodeling heterogeneity in asthma and its relationship to disease outcomes*. *Front Physiol*. 2023;14:1113100.

3.1. Asthma phenotypes and endotypes

In recent years, asthma has been widely recognized as a complex and heterogeneous syndrome, as it displays many different clinical presentations (phenotypes) with specific pathophysiological mechanisms (endotypes) (95, 96). According to the underlying inflammatory profile, asthma can be broadly classified into two main endotypes: type 2 (T2) high and T2 low. Patients are categorized as T2 high when display at least one of the following biomarkers: elevated serum and/or sputum eosinophil levels (≥150 cells/μL or ≥ 2%, respectively), high fractional exhaled nitric oxide (FeNO, ≥ 20 ppb), enhanced serum IgE levels (>114 kU/L) and/or clinical evidence of allergen sensitization. In addition, the requirement of sustained maintenance of oral corticosteroids (OCS) may also be considered as potential biomarker of underlying type 2 inflammation (90, 97). The T2-high endotype is characterized by eosinophilic airway inflammation orchestrated by T2-associated cytokines such as IL-4, IL-5, and IL-13, and includes atopic and non-atopic patients with different phenotypes including allergic asthma, late onset eosinophilic asthma or aspirin-exacerbated respiratory disease. In contrast, the T2 low endotype includes all asthmatic patients lacking or displaying low levels T2 biomarkers and presents with either neutrophilic or paucigranulocytic inflammation and involves various asthma phenotypes related to obesity, smoking, late onset or occupational exposures (92, 95, 98, 99). Remarkably, both T2 high and low endotypes comprise patients with different degrees of severity and responsiveness to treatment. Therefore, the correct identification of their pathophysiological mechanisms may be critical for patients to benefit from molecular-tailored therapies, such as biologicals (95, 99, 100).

3.2. Pathophysiological mechanisms of T2 asthma

3.2.1. The airway epithelium as central player of asthma pathogenesis

In the conducting airways, epithelial cells form a pseudostratified epithelium that makes the first line defensive barrier against airborne threats (101). It consists of different cell types with specific functional properties (**Figure I.14**):

- Ciliated cells are the most abundant cell population, and, equipped with large numbers of cilia, contribute to the clearance of debris and pathogenic threats out of the airways (101, 102).
- Goblet cells are specialized mucus-producing cells that secrete mucins onto the luminal surface of the airways. They collaborate with ciliated cells by trapping environmental agents and facilitating their removal, a process known as mucociliary clearance (101, 102).
- Club cells are secretory cells characterized by the production of antimicrobial peptides and anti-inflammatory mediators contributing to tissue homeostasis and possessing the ability to differentiate into ciliated and mucus-secreting goblet cells (101, 102).
- Basal epithelial cells are multipotent stem cells attached to the epithelial basement membrane primarily involved in tissue regeneration and replenishment by giving raise to the other major subsets of airway epithelial cells. (101, 102).
- Other rare airway epithelial cell populations include chemosensory cells (Tuft cells), pulmonary neuroendocrine cells (PNECs), Hillock cells, airway Microfold cells (M cells) and ionocytes. These cell subsets are less abundant and participate in many diverse of processes, ranging

from the crosstalk with the nervous and immune systems through the secretion of neurotransmitters and inflammatory mediators, to regulating mucus viscosity and the transport of antigens to subepithelial areas (102).

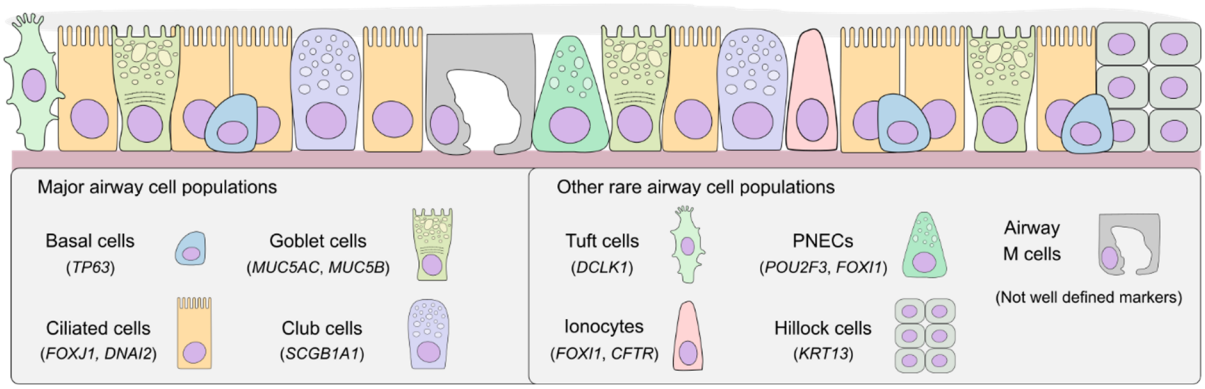

Figure I.14. Cellular components of the airway epithelium. Figure shows major airway cell populations as well as other rare cell subsets found in the airways. Specific gene markers for each cell type are included in parentheses. Adapted from *Cellular and functional heterogeneity of the airway epithelium. Mucosal immunology.* 2021; 14(5), 978–990.

The collective cooperation of these epithelial cell subsets, effectively sealed by intercellular tight junction complexes, provides the three major functions of the airway epithelium: acting as a mechanical barrier against airborne insults, providing mucociliary clearance of debris and environmental agents, and serving as first line immunological defense against pathogens. Notably, in asthmatic patients, these critical features are altered and contribute to disease development and progression (101, 103-106).

In asthma, the integrity of the airway epithelial barrier is compromised and directly correlates with disease severity (107). The expression of tight junction molecules between adjacent epithelial cells is impaired and there is enhanced permeability to environmental substances, potentially increasing the susceptibility to exacerbations or allergen sensitization (101, 105, 107). This epithelial barrier disruption can be caused by diverse factors including the inhalation of allergens with protease activity like house dust mite (HDM), respiratory tract infections, or the exposure to other epithelial-damaging substances in the environment (e.g. pollutants, particulate matter, etc.) (88, 101, 104). Moreover, several studies highlight that the underlying inflammatory process in the airways of asthmatics contributes to the perpetuation of barrier alterations. Cytokines such as IL-4 and IL-13 are known to disrupt tight junction expression and increase the permeability of the epithelium (108, 109). Similarly, the underlying inflammation also reshapes the cellular composition of the airway epithelium. Th2 cytokines, mainly IL-13, promote the hyperplasia of mucus-secretory goblet cells, while reducing the proportions of Club cells and ciliated cells (110, 111). This imbalance, along with decreased ciliary beating activity (111), compromises mucociliary clearance and contributes to airflow obstruction. Besides, when airway epithelial injury and inflammation persist, it may further result in epithelial-mesenchymal transition, contributing to airway wall remodeling and fibrosis (112) (**Figure I.15**).

The immunomodulatory properties of the airway epithelium are also integral to the pathogenesis of asthma. Airway epithelial cells are equipped with a wide variety of PRRs to detect pathogenic and injury signals including TLRs, NLRs and RLRs. Additionally, they also express protease activated

receptors (PARs) that allow them to sense the protease activity of certain allergens (93, 102, 113). Therefore, during epithelial damage or exposure to environmental triggers, airway epithelial cells have the ability to elicit immune responses by producing chemokines and cytokines. In the context of asthma, epithelial-derived alarmins IL-25, IL-33, and TSLP have the most well-defined roles due to their involvement in the orchestration of type 2 inflammatory responses. Upon allergen challenge, microbial infections or other airborne triggers (e.g. pollutants, particulate matter, etc.), epithelial cells secrete large amounts of those alarmins, whose major functions include: shaping DC maturation towards a Th2 polarizing profile and promoting the activation of type 2 ILCs (ILC2s) and other innate immune effector cells such as basophils, eosinophils or mast cells (103, 113, 114). Moreover, other mediators secreted by epithelial cells include TNFα, IL-1β, IL-6, IL-8, GM-CSF, CCL20 as well as eotaxins (CCL11, CCL24, CCL26); which may support the inflammatory process and facilitate the recruitment of monocytes, DCs, T cells, B cells, eosinophils or neutrophils (106). Consequently, the airway epithelium is the first line mucosal defense against infections, but it can also contribute to the initiation and maintenance of innate and adaptive T2 responses involved in the onset and progression of asthma (**Figure I.15**).

Given the outstanding contribution of the airway epithelium to the pathophysiology of asthma, several *in vitro* and *in vivo* models have been developed to assess the airway epithelial barrier function in different contexts. One of the most significant contributions in this field was the development of air-liquid-interface (ALI) culture systems (115), which allow the differentiation of polarized epithelia using cells from different airway sources. In the context of asthma, human epithelial cells from tracheobronchial origin are the most commonly used. Cell lines such as 16-HBE or Calu3 differentiate at ALI conditions and achieve tight junction formation, allowing the study of epithelial barrier integrity (116). Nonetheless, the use of human bronchial epithelial cells (HBECs) isolated from biopsies of healthy or asthmatic individuals provides more physiologically relevant cultures, reproducing the pseudostratified morphology and major epithelial cell populations found in human tissue (107, 116, 117). Recently, cultures of airway epithelial spheroids were developed and allowed the evaluation of epithelial barrier functions in self-assembling structures that mimic the formation of an airway lumen (110). The latest studies also include airway-on-a-chip systems, in which epithelial cells are able to differentiate at ALI conditions while receiving a dynamic nutrient delivery through a chamber that mimics tissue vasculature (118, 119). On top of this, the airway epithelial barrier function can also be assessed *in vivo*. Conventional models of allergen-induced asthma allow the evaluation of barrier integrity through the assessment of lung expression of tight junctions, translocation of serum proteins in bronchoalveolar lavage fluid (BALF) or by monitoring fluorescent compounds administered to the animals (120). Moreover, murine models involving the intranasal administration of IL-33 or IL-13 have demonstrated the capacity to recapitulate major epithelial barrier alterations of the disease (121).

3.2.2. Type 2 cytokines in asthma pathophysiology

The pathophysiological features of T2 asthma primarily rely on the pleiotropic effects of type 2 effector cytokines: IL-4, IL-5 and IL-13. Two cell subsets are the major producers of these mediators in the lungs, Th2 cells and ILC2s, constituting a paradigm of the collaborative interplay between innate and adaptive immunity in the development of pathology (122-124) (**Figure I.15**).

In allergic asthma, the initiation of adaptive Th2 responses in the lungs has been attributed to cDC2s. This subset of DCs captures the allergen in the airways and migrates to tissue draining lymph nodes where promotes the differentiation of allergen-specific Th2 cells. As described previously, the exposure to epithelial-derived alarmins is key in conditioning the capacity of cDC2s to polarize type 2 responses by promoting the upregulation of Th2-polarizing factors such as OX40L and suppressing the production of IL-12 (93, 123, 125). Subsequently, in the lymph node, T-B cell collaboration in the presence of Th2-derived cytokines, mainly IL-4 but also IL-13, induces B cell isotype class switching and the generation of IgE-producing plasma cells. The secretion of large amounts of allergen-specific IgE sensitizes effector cells expressing the high affinity IgE receptor (FcεRI) such as mast cells and basophils. Upon new encounters with the causative allergen, the crosslinking of membrane-bound IgE-receptor complexes in these cells causes the release of preformed bioactive mediators (histamine) and proteases (tryptase and chymase) accompanied by the production of eicosanoids and cytokines (93, 122, 126). Beyond their role in allergen sensitization, DCs also express FcεRI and contribute to adaptive effector responses by increasing T cell activation via FcεRI-mediated allergen presentation (127). Another cellular population expressing the FcεRI is the airway epithelium, which upon crosslinking, upregulates the production of mediators, decreases tight junction integrity and enhances its permeability to environmental agents (128). Of note, airway epithelial cells also express the low affinity IgE receptor (CD23), which mediates the transport of IgE-allergen complexes across the epithelium (129). Together, these mechanisms contribute to the acute and late-phase hypersensitivity reactions observed in allergic asthmatic patients (126) (**Figure I.15**).

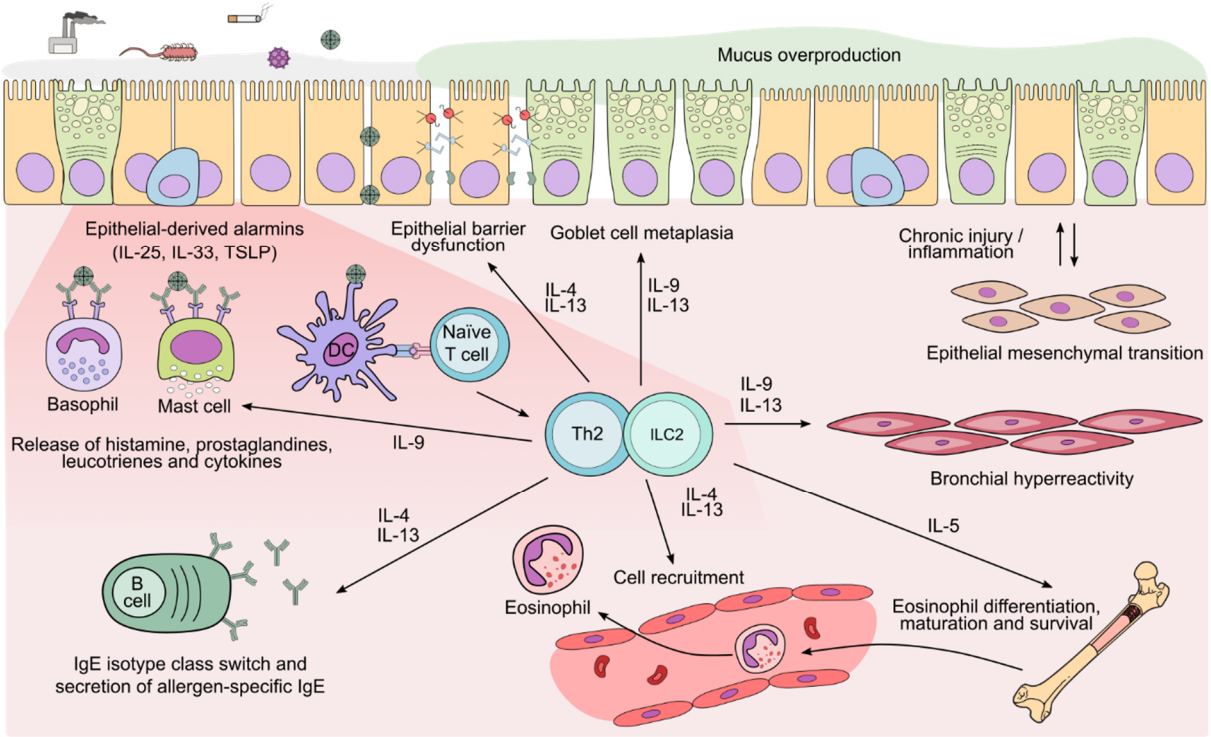

Figure I.15. Overview of the main pathophysiological mechanisms of T2 asthma, focusing on type 2 effector cytokines. Adapted from *The immunology of asthma. Nat Immunol.* 2015;16(1):45-56.

In parallel to the generation of Th2 responses, ILC2s have become important players in asthma pathophysiology. Epithelial-derived alarmins secreted in response to harmful airborne agents promote ILC2 activation and proliferation (113, 125). Activated ILC2s can participate in the sensitization to allergens by facilitating the migration of DCs to the lymph nodes via the production of IL-13. Moreover, they can act as APCs and collaborate in the re-stimulation of memory T cells in mucosal tissue (93, 123). However, their major function consists of the production of type 2 cytokines, playing complementary roles with Th2 cells at different levels (93, 122-124). The release of IL-5 promotes eosinophil differentiation, maturation and survival, while IL-4 and IL-13 regulate eosinophil migration into tissues (130). IL-4 and IL-13 signaling also target other immune and structural cells such as endothelial cells or airway epithelial cells, enhancing vascular permeability and cell recruitment, or impairing epithelial barrier integrity, respectively (93, 122-124). Remarkably, both cytokines display similar roles in asthma, as they share the capacity to act via the IL-4Rα and activate signal transducer and activator of transcription 6 (STAT6) in target cells (123). Nonetheless, mice models have demonstrated the predominant involvement of IL-13 over IL-4 in driving mucus overproduction, goblet cell hyperplasia and BHR (131, 132), whereas IL-4 plays a unique role in memory maintenance at the T cell level (122). Finally, another mediator produced mainly by Th9 cells but also by both Th2 cells and ILC2s is IL-9, which can cooperate with the rest of type 2 effector cytokines in asthma through promoting mast cell survival, BHR and mucus overproduction (93, 122, 123) (**Figure I.15**).

3.2.3. Viral infections in asthma development and exacerbation

Compelling experimental and epidemiological evidence demonstrate that viral infections together with allergen sensitization represent two major risk factors for asthma development and progression to difficult-to-treat and severe asthma (94, 133). Human rhinoviruses (RVs), the etiologic agents of common colds, are the most common respiratory viruses causing asthma attacks, and their infection during early childhood constitutes a major risk factor for the development of asthma later in life. In recent years, a bidirectional relationship between rhinoviral infections and T2 inflammation has been reported in asthma (133). On one hand, allergic sensitization and T2 inflammation predispose individuals to RV-induced wheeze by impairing antiviral immunity at different stages. For instance, airway epithelial cells exposed to type 2 cytokines display defective IFN responses to viruses (134). Similarly, atopic patients present higher expression of FcεRI in pDCs, and the crosslinking of IgE-receptor complexes by allergens impairs the production of IFNs by this DC subset specialized in antiviral immunity (94, 133, 135). On the other hand, RVs damage the airway epithelium and disrupt epithelial barrier integrity, thus increasing the penetration of allergens and other environmental substances to subepithelial areas (105, 136). In addition, RV infection stimulates the release of epithelial-derived alarmins that shape immune responses towards a T2 profile and favors allergen sensitization (137, 138). Collectively, this complex crosstalk between viral infections and T2 inflammation creates a vicious cycle that ultimately enhances susceptibility to infections and sensitization to allergens, which together contribute to asthma onset and worsening (**Figure I.16**).

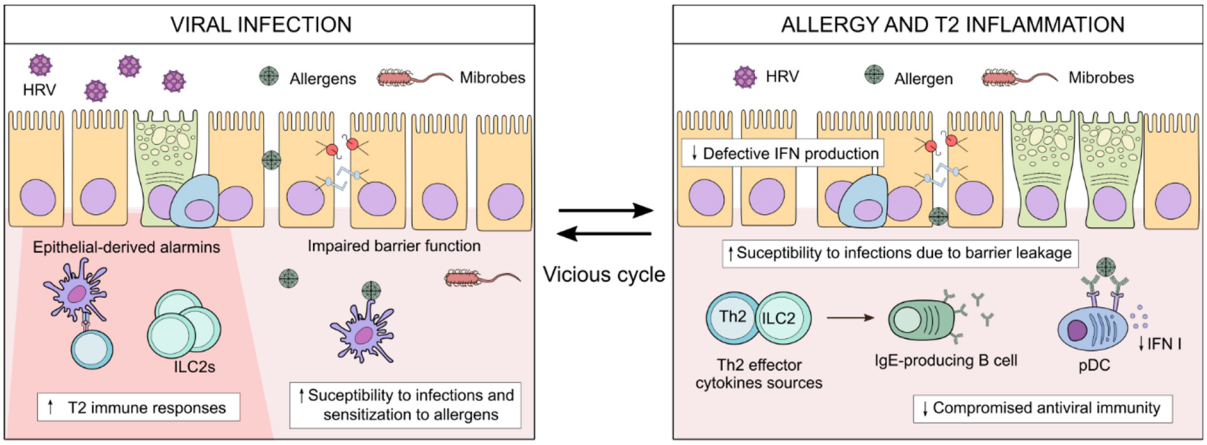

Figure I.16. Bidirectional relationship between viral infections and type 2 inflammation in asthma (94, 105, 133).

3.3. Current treatments and challenges in asthma therapy

The major goal of asthma management is to achieve long-term control of symptoms and reduce the risk of exacerbation, disease-related mortality and airflow limitation, while minimizing the side effects of treatment (90). Two main categories of pharmacological options are employed in asthma treatment:

- Controller medications: include treatments usually prescribed in a regular regime that target airway inflammation, alleviate symptoms and prevent exacerbations.
- Reliever medications: consist of rapidly acting treatments that mitigate bronchoconstriction during worsening of asthma symptoms and exacerbations.

The 2024 global initiative for asthma (GINA) report on asthma management and prevention proposes two different tracks for asthma treatment depending on the reliever medication of choice. Track 1 is based on a combination of inhaled corticosteroids (ICS) and formoterol as a reliever, while track 2 consists of a short acting β_2 agonist (SABA) as reliever along with intermittent or regular ICS. The controller medications of both tracks are mainly relying in ICS, either combined with formoterol (track 1) or with SABA or long acting β_2 agonist (LABA) (track 2). In this context, most international guidelines are based on a stepwise approach of increasing the dose of ICS as patients are less well controlled by treatment. This may be supported by other add-on therapies which include long-acting muscarinic antagonists (LAMAs) or leukotriene receptor antagonists (LTRAs) (90, 91).

Despite the efforts made in achieving the best management of the disease, approximately 5-10% of patients are considered as severe asthmatics, meaning that they remain uncontrolled with maximal use of ICS and additional controller medications in spite of proper treatment adherence, or that they require high-dose treatment to maintain symptom control and reduce exacerbations (91). In recent years, several biologicals have been approved for asthma treatment including anti-IgE (Omalizumab), anti-IL-5 (Mepolizumab, Reslizumab), anti-IL-5Rα (Benralizumab), anti-IL-4Rα (Dupilumab) and anti-TSLP (Tezepelumab). The introduction of biologicals has provided a novel personalized medicine approach that has significantly improved asthma control and quality of life for many severe asthma patients. However, the therapeutic efficacy of severe asthma remains suboptimal due to the challenges in proper phenotyping and endotyping of the disease, and novel therapeutic strategies are still

demanded for non-responder patients (97, 100, 139, 140). Moreover, the generation of anti-drug antibodies raises some concerns about the safety and long-term efficacy of biologicals (141). Currently, new therapeutics are under development, targeting different inflammatory pathways: epithelial-derived alarmins, costimulatory ligands or JAK-STAT signaling, among others (97, 142). A better understanding of the pathophysiological mechanisms of asthma is of utmost importance to improve efficacy and safety of current, developing and newly designed drugs (97, 100, 139, 140, 142).

In summary, the current mainstay treatments for asthma primarily target airway inflammation and smooth muscle constriction through the use of corticosteroids and bronchodilators (90, 91). The recent development of biologicals has provided an opportunity for certain severe patients to benefit from tailored therapies. Nonetheless, a better understanding of asthma phenotypes and endotypes is still needed to exploit the potential of biologicals and promote the development of many other therapeutic strategies (97, 100, 139, 142). Advances in multiomic integration technologies may contribute to overcome these challenges (99, 140). Additionally, the involvement of epithelial barrier alterations in the development of chronic inflammatory diseases like asthma has been reviewed in several studies during last years (83-85, 87-89). However, the potential therapeutic capacity of epithelial targeting treatments is still limited. Novel therapies not only targeting the inflammatory process but also directly improving the airway epithelial barrier function may be a promising field for future research in asthma management (97, 103).

4. The endocannabinoid system (ECS)

The human endocannabinoid system (ECS) is a complex signaling network comprising cell receptors (CBRs), endogenous ligands (endocannabinoids), and the enzymes responsible for their synthesis, transport, and degradation. It participates in a wide plethora of physiological functions including neuronal development, brain plasticity, learning and memory, regulation of appetite, stress, pain and emotions, cell proliferation, differentiation, cell survival, metabolism and immunity. Alterations of the ECS are associated with diseases such as cancer, autoimmunity, allergies or neurological disorders. Therefore, the pharmacological manipulation of the ECS is emerging as a promising strategy for the management of many different pathologies (143-146).

4.1. The ECS components

4.1.1. Endocannabinoids, phytocannabinoids and synthetic cannabinoids.

The signaling of the ECS is triggered by multiple ligands able to bind and act through CBRs. These cannabinoid ligands can be broadly classified into three groups depending on their origin: endocannabinoids, phytocannabinoids and synthetic cannabinoids (**Figure I.17**).

Endocannabinoids are endogenously synthesized lipid-derived mediators. The most well-characterized ones are arachidonoylethanolamide, also known as anandamide (AEA), and 2-arachidonoylglycerol (2-AG). AEA acts as a partial agonist showing higher affinity for type 1 cannabinoid receptors (CB1) than type 2 cannabinoid receptors (CB2), while 2-AG is a full agonist of both CB1 and

CB2 (147, 148). Other endocannabinoids interacting with CBRs include 2-arachidonoylglyceryl ether (noladin ether) or O-arachidonoylethanolamine (virodhamine). In addition, structurally similar molecules with low affinity for CB1 and CB2 such as N-oleoylethanolamine (OEA) and N-palmitoylethanolamine (PEA) are considered as endocannabinoid-like compounds due to their capacity to modulate endocannabinoid signaling indirectly via substrate competition and their ability to act on other non-canonical CBRs (147-149).

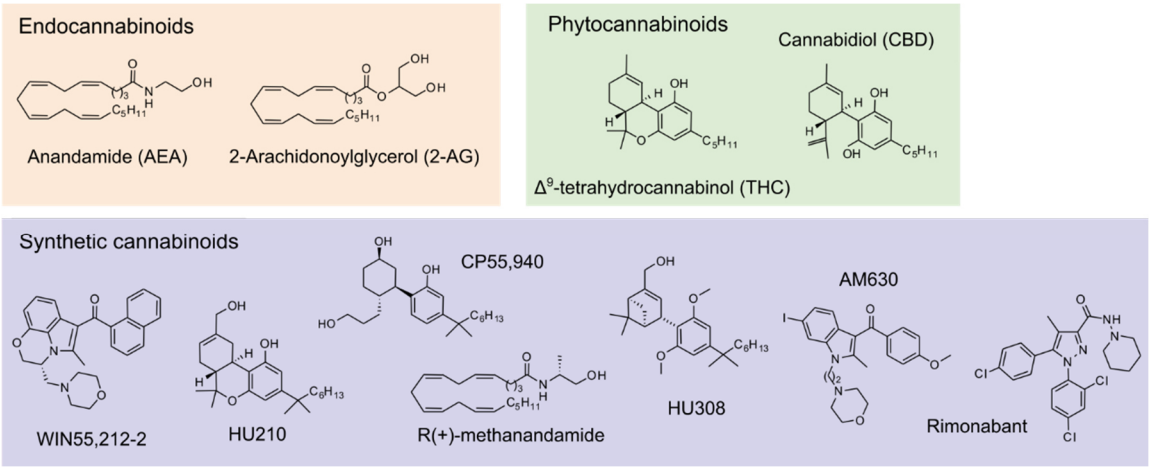

Figure I.17. Most relevant cannabinoid ligands classified according to their origin. Adapted from *The Role of Cannabinoids in Allergic Diseases: Collegium Internationale Allergologicum (CIA) Update 2020. Int Arch Allergy Immunol.* 2020;181(8):565-584.

Phytocannabinoids are the cannabinoid ligands derived from the extracts of *Cannabis sativa*, the plant of marijuana. To date, more than 100 compounds have been classified as phytocannabinoids, among them, the most abundant and best studied are Δ^9-tetrahydrocannabinol (THC) and cannabidiol (CBD). THC is partial agonist for both CB1 and CB2 receptors and the major contributor to the psychoactive effects of cannabis. In contrast, CBD does not have psychoactive effects and is a negative allosteric modulator of CB1 and a partial agonist of CB2 receptors. The therapeutic effects of these phytocannabinoids have been extensively studied in different preclinical models of multiple diseases such as Parkinson disease, Alzheimer's disease, cancer or multiple sclerosis, among many others. Nowadays, botanical CBD is approved and commercialized as Epidiolex for the treatment of pediatric epilepsies. In addition, Sativex, a mixture of THC and CBD is marketed for the treatment of spasticity in patients with multiple sclerosis (148-150).

Synthetic cannabinoids are man-made cannabinoid ligands whose development over the last decades has provided great insights into the field through the generation of potential therapeutic agents but also by serving as research tools to study the ECS. THC analogues such as Nabilone and Dronabinol are approved by the FDA for the treatment of chemotherapy-induced nausea and vomiting, chronic pain conditions, multiple sclerosis, palliative care, glaucoma and appetite stimulant for AIDS patients (148, 149, 151). Other synthetic cannabinoids used in basic research and preclinical studies include agonists with similar affinity for CB1 and CB2 such as WIN55,212-2, HU-210 and CP55,940; agonists with specific selectivity like R(+)-methanandamide (CB1-selective) and HU-308 (CB2-selective); and

selective antagonists such as Rimonabant (CB1-selective) and AM630 (CB2-selective) (**Figure I.17**) (144, 146).

4.1.2. Synthesis, degradation and trafficking of endocannabinoids

The biological activities of endocannabinoids are strictly regulated by the synthetic, catabolic and transport pathways that control their intracellular and extracellular concentrations. In this context, major efforts have been focused on the elucidation of the synthesis and degradation routes of the main endocannabinoids: AEA and 2-AG. The most classical pathway for the synthesis of anandamide consists of its generation from membrane phospholipid precursors by the combined activities of N-acyltransferase (NAT) generating N-acyl-phosphatidylethanolamines (NAPEs) and their consecutive hydrolysis by NAPE-hydrolyzing phospholipase D (NAPE-PLD). Regarding 2-AG, its biosynthesis consists of the hydrolysis of arachidonoyl-containing phosphatidylinositols from the plasma membrane by phospholipase C to generate 1, 2- DAGs and their sequential hydrolysis by DAG-lipase (DAGL) (147, 149) (**Figure I.18A**).

Endocannabinoids can be taken up, released, degraded or accumulated in organelles of the cell (149). In this context, as lipophilic molecules, the transport of endocannabinoids within the aqueous cytosol is supported by carrier proteins. Additionally, their traffic across cell membranes consists of either passive diffusion, microvesicle-mediated exocytosis or facilitated diffusion by a putative endocannabinoid membrane transporter (EMT). However, the existence of this latter one is still a matter of debate in the field, as it is only based on indirect evidence (147, 149). The catabolic pathways of the main endocannabinoids are mediated by the enzymes fatty acid amide hydrolase (FAAH) and monoacylglycerol lipase (MAGL), which catalyze the degradation of AEA and 2-AG, respectively. Arachidonic acid is the major catabolic product of both substrates, together with ethanolamine in the case of AEA degradation and glycerol in the case of 2-AG (**Figure I.18A**). Besides, other alternative catabolic pathways include the oxidative degradation of AEA and 2-AG by cyclooxygenase and lipoxygenase enzymes. Therefore, the degradation of endocannabinoids is closely associated with eicosanoid metabolism, by serving as a source of arachidonic acid for eicosanoid production, or by direct oxygenation of endocannabinoids, generating eicosanoid-related bioactive metabolites (147, 149).

4.1.3. Canonical and non-canonical cannabinoid receptors (CBRs)

The multiple and diverse effects of cannabinoid ligands depend on their capacity to activate CBRs in target cells. Canonical CBRs include CB1 and CB2, which belong to the family of G protein-coupled receptors (GPCRs) and consist of seven transmembrane protein domains inserted in the plasma membrane, displaying an extracellular N-terminus and an intracellular C-terminus domains. CB1 is predominantly expressed in the central nervous system (CNS) and attributed to the psychotropic effects of cannabis, while CB2 is abundant in immune system cells. Nonetheless, the expression of CB1 has also been confirmed in peripheral tissues including immune cells (144, 152). Signaling of CB1 and CB2 receptors depends on the coupling to heterotrimeric G-proteins, composed of α, β, and γ subunits. Both CBRs are generally coupled to inhibitory Gαi/o proteins, thus inhibiting adenylate cyclase and protein

kinase A activation. However, in certain circumstances, CB1 can couple with G_s to promote adenylate cyclase activity. Other pathways described for CBR signal transduction include stimulation of mitogen-activated protein kinases (MAPKs), recruitment β-arrestins, modulation of ion channels and the activation of phospholipase C, PI3K signaling, or ceramide biosynthesis (144, 152-155). Importantly, CBRs display biased signaling, meaning that the preference for a signal transduction pathway depends on the ligand that activates the receptor (152, 155). Besides, pharmacological evidence demonstrated that cannabinoid ligands can interact with other non-CB1 and non-CB2 receptors, adding another degree of complexity to the ECS signaling. These non-canonical CBRs include other GPCRs such as GPR55, GPR119, and GPR18; transient receptor potential (TRP) channels like TRP vanilloid 1 (TRPV1); and nuclear receptors such as peroxisome proliferator-activated receptors (PPARs) α, β and γ, which heterodimerize with retinoic X receptor (RXR) in the cell nuclei to bind to their DNA response elements (144, 149, 151, 156) (**Figure I.18B**).

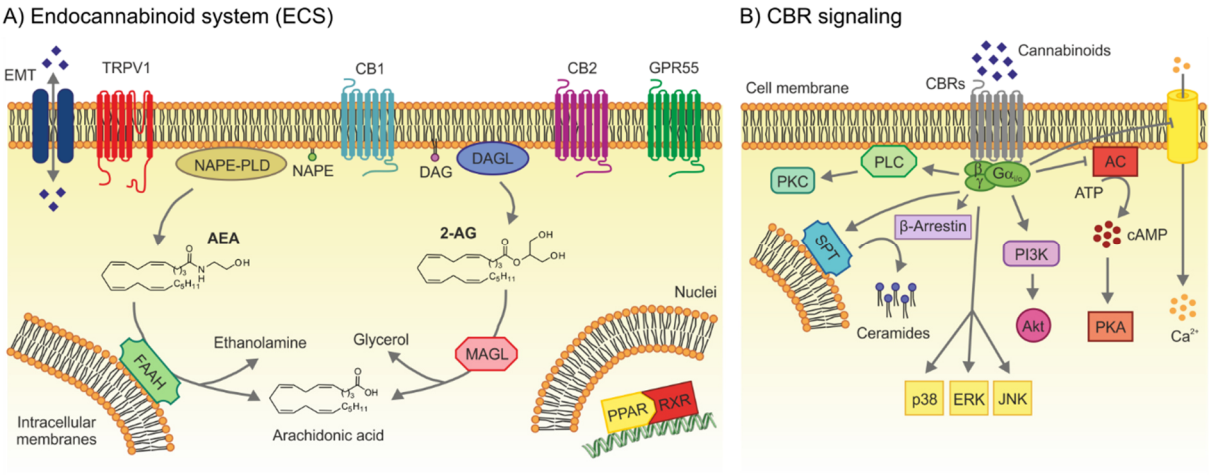

Figure I.18. (**A**) ECS components and (**B**) CBR signaling pathways. Adapted from *The Role of Cannabinoids in Allergic Diseases: Collegium Internationale Allergologicum (CIA) Update 2020. Int Arch Allergy Immunol*. 2020;181(8):565-584.

4.2. Modulation of inflammatory responses by cannabinoids

The immunosuppressive capacity of cannabinoids is well-known and widely recognized by multiple studies. Cannabinoids display specific ability to regulate functional properties in a wide variety of immune cell populations including the modulation of cytokine production, cell migration, polarization of T cell responses, cell proliferation, and apoptosis (144, 145, 157, 158). However, the molecular mechanisms by which cannabinoids exert their immunosuppressive effects are complex and need further clarification.

The activation of PRRs such as TLRs and NLRs, and their corresponding signaling transduction pathways is key in the development of innate and adaptive immune responses (17). Upon stimulation of TLRs, MYD88 and/or TRIF- dependent signaling pathways are initiated, leading to the activation of MAPKs and proinflammatory transcription factors like IRF3, IRF7, NF-κB and AP-1. The crosstalk between cannabinoids and TLR signal transduction pathways has long been accredited. Special attention has been paid to the effects of cannabinoids in the production of inflammatory mediators by

several immune cell types after TLR activation, displaying immunosuppressive effects in most cases (159, 160).

In addition, the potential inhibitory effects of cannabinoids have been studied in other inflammatory signaling pathways such as the assembly of the cytosolic signal transduction complexes known as inflammasomes. Inflammasomes are made of three major components: (i) sensor proteins (NLRs, AIM2-like receptors), (ii) adaptor proteins (ASC) and (iii) effector enzymes (caspase-1). Stimulation of sensor proteins promotes their oligomerization and the assembly of the inflammasome complex, which ultimately induces the self-proteolysis of pro-caspase 1 into its active form, caspase 1. Active caspase 1 cleaves pro-IL-1β, pro-IL-18 and pore-forming molecules (gasdermin D) into their active forms, ultimately promoting the release of these mediators and the inflammatory cell death, in a mechanism termed as pyroptosis (161). In this context, the inhibitory effects of cannabinoids have been observed in terms of compromising the expression of the inflammasome complex components, reducing secretion of IL-1β and IL-18, or diminishing the activity of caspase 1 (162).

Finally, novel findings associate the immunomodulatory effects of cannabinoids to their ability to shape immune cell metabolism. Cannabinoids induce the activation of adenosine monophosphate-activated protein kinase (AMPK), a key molecular player that represses the anabolic cell metabolism governed by mammalian target of rapamycin (mTOR) and promotes the induction of autophagy. This shift shuts down cell anabolism predominantly associated to the glycolytic pathway and promotes OXPHOS, which is a hallmark of the acquisition of anti-inflammatory phenotypes in innate immune cells (163).

Collectively, these evidence indicate a clear anti-inflammatory and immunosuppressive role of cannabinoids in immune cells, which is supported by multiple *in vivo* therapeutic models of inflammatory diseases such as sepsis, rheumatoid disease, multiple sclerosis, atopic dermatitis, food allergies or asthma, among many other (144, 145). However, exacerbation of the inflammatory responses may occur with the use of certain cannabinoid compounds and doses (159, 162, 164). A better understanding of the heterogenicity of cannabinoid ligands, doses and effects in different cell types as well as the intricated molecular mechanisms of such effects is needed for the responsible and sensible design of cannabinoid-based drugs for inflammatory disorders.

4.3. Regulation of the epithelial barrier function by cannabinoids

As above mentioned, the epithelial barriers exert protective and homeostatic functions that, when dysregulated, may contribute to the development of chronic non-communicable diseases (84, 85). Evidence of the modulation of epithelial barrier function by cannabinoids suggests potential protective capabilities.

In the gut, CB1 receptors seem to have a role in the preservation of barrier function. CB1 KO mice display increased intestinal permeability in response to stress and the specific deletion of CB1 in intestinal epithelial cells aggravates diet-induced gut barrier dysfunction (165, 166). Moreover, agonism of CB1 prevented the onset of arthritis by preserving gut barrier integrity (167). *In vitro*, exposure of gut

epithelial cells to THC or CBD increased the recovery from EDTA- and cytokine-induced epithelial permeability, while opposite effects were observed after the administration of AEA or 2-AG. Interestingly, both opposing effects were sensitive to CB1 antagonism, suggesting complex regulatory mechanisms (168, 169).

In the skin, the involvement of CB1 in the regulation of barrier integrity is also evident. The topical use of a CB1 agonist promoted an accelerated recovery of epidermal barrier function in an atopic dermatitis model (170). Mice lacking CB1 receptors completely or exclusively in the keratinocyte compartment displayed enhanced Th2 responses and delayed epithelial barrier repair compared to WT mice in a murine model of atopic-like dermatitis (171). Furthermore, CB1 and CB2 may play opposing roles, as mice lacking CB1 display delayed recovery of barrier permeability after tape stripping-induced skin damage, while it was found to be accelerated in CB2 null mice (172). Remarkably, the phytocannabinoid CBD and the endocannabinoid analogue N-palmitoyl serinol improved skin barrier function by the activation of antioxidant pathways and the synthesis of ceramides, respectively (173, 174).

In the lung, bibliography on the effects of cannabinoids is scarce. *In vitro* studies point out that AEA increases the permeability of airway epithelial cell cultures, but this effect was attributed to its conversion into other bioactive metabolites (175). In contrast, THC displayed a barrier protective effect by reversing TNFα-induced bronchial epithelial permeability (176). Similarly, WIN55,212-2, a non-selective synthetic cannabinoid with immunomodulatory functions, restored the airway epithelial barrier disruption induced by RV infection (177).

4.4. The ECS as a therapeutic target for asthma therapy

As previously described, asthma is the most prevalent chronic inflammatory disease of the lungs, and its management still faces challenges in terms of disease control of severe patients, side-effects of conventional treatments, and the high costs, safety concerns and phenotyping difficulties associated to the recently developed biological therapies. In this context, multiple studies addressing the potential therapeutic efficacy of cannabinoids in asthma have been conducted over the past decades (144, 178, 179). The first evidence of the therapeutical exploitation of the ECS for asthma therapy dates back to the 1970s with the observation of the potential bronchodilator effects of marijuana smoke and oral THC administration in asthmatics (180). However, its potential therapeutic use was dampened after the report of psychotropic effects and paradoxical bronchoconstriction observed in some patients (181, 182).

Nowadays, a better knowledge of the involvement of the ECS in asthma reflects very complex interactions. Alterations of the ECS have been observed in patients and animal models of airway disease, such as the increased AEA levels in BALF of allergic asthmatics after allergen challenge, or the reduced amounts PEA in the bronchi of allergen-sensitized mice (183, 184). Changes in the expression pattern of CBRs have also been described. Increased mRNA expression levels of CB1 were reported in the tonsils and peripheral blood mononuclear cells (PBMCs) from atopic and asthmatic patients (185). Likewise, the expression of CB2 is upregulated in eosinophils from allergic patients with seasonal respiratory symptoms (186), and enhanced CB2 and CPR55 levels are found in the airways

of OVA-sensitized mice (183). Interestingly, CB1 and CB2 receptors seem to display opposing roles in the pathogenesis of asthma. CB1 displays a potent inhibitory role on human mast cell activation in the airway mucosa (187) and its stimulation exerts protective effects on BHR in both mice and humans (188, 189). Moreover, the inhibition CB1 exacerbated the airway damage and eosinophilia in a mice model of helminth infection, suggesting potential regulatory functions on type 2 immune responses in the lung (190). In contrast, the engagement of CB2 receptors has been associated with the recruitment and stimulation of eosinophils (186, 191) as well as the direct and indirect activation of ILC2s (192, 193), leading to the aggravation of airway disease. Nonetheless, CB2 activation may also play a protective role in asthma due to studies reporting the inhibition of antigen-induced plasma extravasation and the impairment of bronchial smooth cell contraction in a CB2-dependent manner in the airways of guinea pigs (194, 195) (**Figure I.19**).

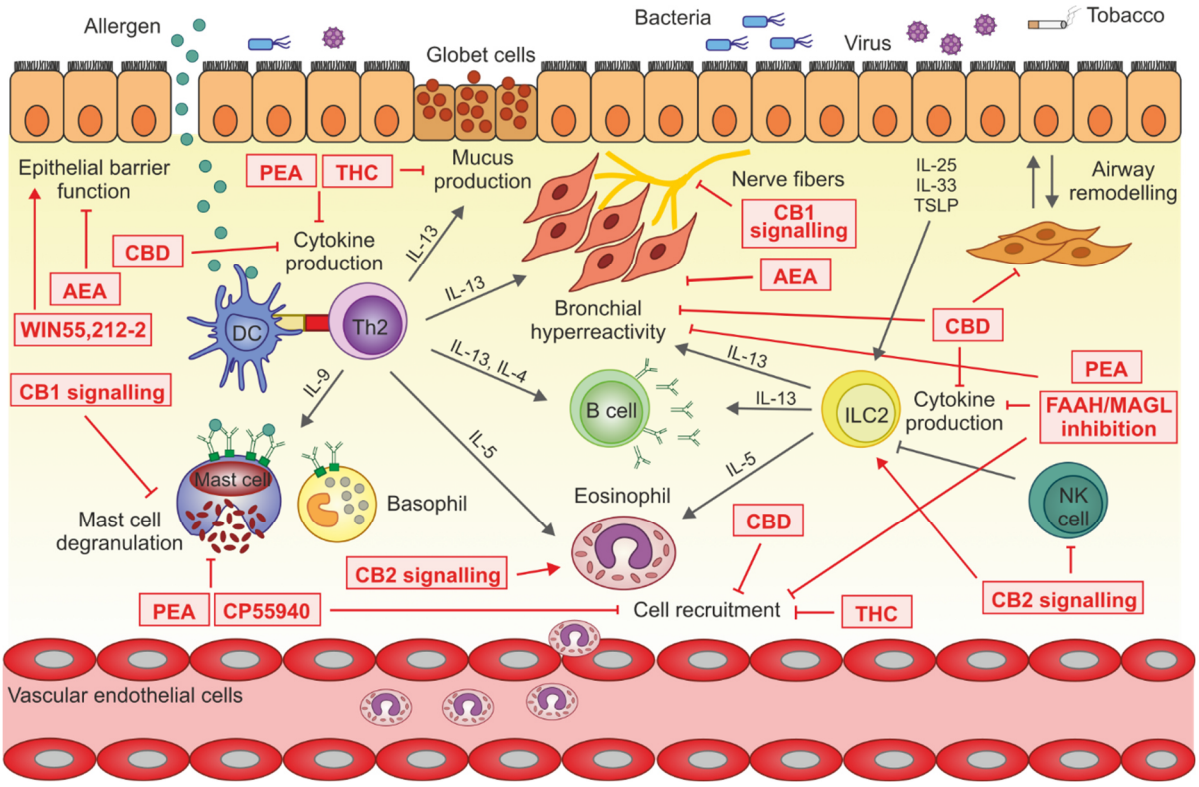

Figure I.19. Pathophysiological pathways regulated by the ECS in T2 asthma. Adapted from *The Role of Cannabinoids in Allergic Diseases: Collegium Internationale Allergologicum (CIA) Update 2020. Int Arch Allergy Immunol*. 2020;181(8):565-584.

Most preclinical *in vivo* studies showing the potential therapeutic capacity of cannabinoids for asthma treatment focus on their role as bronchodilators or immunosuppressors. In animal models of allergic asthma, CBD decreased BHR, cytokine production and airway remodeling (196); THC compromised cell recruitment, mucus and cytokine production, and decreased total IgE levels (197, 198); CP55940 decreased respiratory abnormalities, leukocyte infiltration and mast cell degranulation (199); and PEA inhibited BHR, cell recruitment and mast cell activation (183). Similarly, the FAAH inhibitor URB597 decreased inflammatory markers in a model of OVA-induced allergic airway inflammation, while the MAGL inhibitor, JZL184, and the dual inhibitor of FAAH/MAGL, JZL195, ameliorated both pulmonary inflammation and airway hyperreactivity (200). Recent studies also report

the airway relaxant effects of the endocannabinoid AEA both in healthy and asthma conditions (201) (**Figure I.19**).

Despite these promising findings, our knowledge of how cannabinoids influence airway epithelial function and barrier integrity remains limited. The better understanding of the capacity of cannabinoids to regulate airway epithelial barrier functions may provide new insights in the development of cannabinoid-based therapeutic alternatives combining immunomodulatory properties with the ability to preserve the homeostatic functions of the airway epithelium.

OBJECTIVES

Airway inflammation and bronchial epithelial barrier dysfunction are two major hallmark features of asthma pathophysiology. The development of anti-inflammatory drugs with concomitant ability to improve epithelial barrier function might well represent novel suitable strategies for the prevention and treatment of asthma and other airway inflammatory diseases. At this regard, cannabinoids are postulated as promising agents with immunosuppressive and epithelial barrier regulatory potential. However, the mechanisms by which cannabinoids exert their effects are complex and require further elucidation, particularly in the context of airway diseases. Previous studies from our research group have demonstrated that the synthetic cannabinoid WIN55,212-2 displays potent anti-inflammatory functions by suppressing effector T cell responses in human tonsils and promoting the generation of tolerogenic DCs able to induce Tregs in both *in vitro* and *in vivo* models of Th1- and Th2- mediated inflammatory diseases (49, 202, 203). Of note, the administration of WIN55,212-2 during the onset of RV infection restore RV-induced bronchial epithelial barrier alterations *in vitro* (177). However, the immunomodulatory effects of WIN55,212-2 on other immune cell types and in different contexts of airway epithelial barrier disruption, as well as the underlying molecular mechanisms involved in such effects are still elusive and require further investigations.

We hypothesize that WIN55,212-2 could exert immunosuppressive and immunomodulatory effects on additional myeloid immune cells, such as monocytes or macrophages. We also hypothesize that the epithelial barrier protective features described for WIN55,212-2 may be taking place in other situations of epithelial barrier impairment, including those caused by type 2 inflammatory processes. The better understanding of these potential therapeutic benefits as well as their underlying molecular mechanisms may provide the basis for the development of novel cannabinoid-based therapies for asthma and other immune-mediated inflammatory diseases.

Considering all these aspects, the main objective of this thesis is to investigate the capacity of the synthetic cannabinoid WIN55,212-2 to modulate the functional properties of myeloid cells and bronchial epithelial cells, to uncover the underlying molecular mechanisms of such effects, and to assess their potential therapeutic implications in preclinical *in vitro* and *in vivo* models of asthma and other inflammatory diseases.

To achieve our goal, we pursued the following specific aims:

1. **Study of the capacity of the synthetic cannabinoid WIN55,212-2 to reprogram monocyte differentiation and macrophage activation under inflammatory conditions.**

   1.1. Evaluation of the phenotypic and functional characteristics of human monocyte-derived dendritic cells differentiated in the presence of WIN55,212-2.

   1.2. Assessment of the immunomodulatory capacity of WIN55,212-2 in the activation of proinflammatory M1 macrophages.

   1.3. Elucidation of the molecular mechanisms by which WIN55,212-2 impairs inflammatory responses in human macrophages.

   1.4. Assessment of the e*x vivo* and *in vivo* anti-inflammatory properties of WIN55,212-2.

2. **Assessment of the capacity of WIN55,212-2 to regulate human bronchial epithelial integrity and function.**

   2.1. Study of the potential preventive and/or therapeutic capacity of WIN55,212-2 to restore epithelial barrier function in ALI cultures of human bronchial epithelial cells during RV-A16 infection.

   2.2. Evaluation of the potential efficacy of WIN55,212-2 to improve epithelial barrier function in ALI cultures and epithelial spheroid cultures of human bronchial epithelial cells during type 2 inflammation.

   2.3. Investigation of the molecular mechanisms involved in the ability of WIN55,212-2 to regulate epithelial barrier integrity and function in human bronchial epithelial cells.

3. **Evaluation of the potential therapeutic efficacy of the synthetic cannabinoid WIN55,212-2 in preclinical *in vivo* models of asthma.**

   3.1. Study of the potential capacity of WIN55,212-2 to restore epithelial barrier function *in vivo* in murine models of IL-13-induced type 2 asthma.

   3.2. Investigate the potential immunomodulatory properties of WIN55,212-2 in *in vitro* and *in vivo* models of HDM-induced asthma.

Over the last decades, lifestyle changes associated with modernization, industrialization and urbanization have been accompanied by a step rise in chronic non-communicable diseases. This phenomenon has been attributed to the introduction into our daily lives of harmful substances which compromise epithelial barrier homeostatic functions (83-85). The identification of those deleterious agents potentially disrupting our epithelial barriers is of utmost importance for the development of proper avoidance recommendations and prevention strategies. In this context, future advances in aerospace technologies and perspectives on plausible human settlements in outer space raise concerns about the potential new exposomes that humanity will face. Particulate materials found in the surfaces of celestial bodies, known as regoliths, may be one of the first potential exposures encountered by astronauts in future space missions. Considering these facts and taking advantage of our established models to study airway epithelial barrier function, we sought to investigate the potential consequences of the exposition to regoliths in the human respiratory tract. To fulfill this goal, we proposed the following additional aims:

4. **Identification of new potentially harmful agents for the airway epithelium and lung function.**

   4.1. Study the potential deleterious effects of Lunar and Martian regolith exposure on the integrity and function of the human bronchial epithelium.

   4.2. Assessment of the potential capacity of Lunar and Martian regoliths to induce *in vivo* acute lung inflammation in mice.

MATERIALS AND METHODS

1. Materials, reagents and media

We used RPMI 1640 medium (Corning) supplemented (complete RPMI, cRPMI) with 10% heat-inactivated fetal bovine serum (FBS, Hyclone), 100 mg/mL normocin (InvivoGen), 50 mg/mL penicillin, 50 mg/mL streptomycin, 1% non-essential amino acids, 1% MEM vitamins and 1 mmol/L sodium pyruvate (all from Life Technologies) for monocyte, hmoDC, macrophage, T cell and splenocyte cultures.

Airway epithelial cell cultures required several media depending on the differentiation stage: bronchial epithelial basal medium (BEBM, Lonza), Dulbecco´s modified Eagle medium (DMEM, Gibco) and Opti-MEM (Gibco) medium were used. Supplementations with bronchial epithelial growth medium (BEGM) SingleQuots (Lonza) and all-*trans*-retinoic acid (ATRA, Sigma-Aldrich) were also employed depending on the differentiation stage. In addition, cultures of human bronchial epithelial spheroids required the use of growth factor reduced extracellular matrix gel (GFR-ECM, Sigma-Aldrich).

In vitro immune cell activation was performed with lipopolysaccharide (LPS) from *Escherichia coli* (O127:B8, Sigma-Aldrich) and/or human recombinant IFNγ (PeproTech). In *ex vivo* and *in vivo* experiments, LPS from *E. coli* (O155:B5, Sigma-Aldrich) was employed. House dust mite (HDM, *Dermatophagoides pteronyssinus*) extracts for *in vitro* hmoDC activation and generation of murine models allergic asthma model were provided by Inmunotek S.L.

For the infection of airway epithelial cells, human rhinovirus A16 (RV-A16, Virapur) was employed. UV-light inactivated RV-A16 (UV-RV-A16) was used as a control after 60 min exposure to 254 nm UV-light. Moreover, human recombinant IL-13 and mouse recombinant IL-13 (both from PeproTech) were used for *in vitro* and *in vivo* experiments targeting the airway epithelium, respectively.

The effects of ECS intervention in human monocytes, macrophages, hmoDCs, bronchial epithelial cells (HBECs) and *in vivo* mice models were evaluated using the synthetic cannabinoid agonist WIN55,212-2 (Sigma-Aldrich). In all cases, comparative doses of dimethyl sulfoxide (DMSO, Sigma-Aldrich) were included as vehicle treatment in control conditions.

Particulate reagents (maximum particle size of 20 μm) including Earth silica quartz, Lunar regolith simulant, LMS-1, and Martian regolith simulants, MGS-1 and MGS-1S, were kindly provided by our collaborators Dr. Jorge Domínguez-Andrés and Dr. Mihai Netea at Radboud University Medical Centre, Netherlands. Before use, silica and regolith simulants were autoclaved for sterilization.

2. Cell culture procedures

2.1. Differentiation and activation of human monocyte-derived-DCs

Peripheral blood mononuclear cells (PBMCs) were isolated from buffy coats of healthy anonymous donors (Transfusion Centre of Comunidad de Madrid) by Ficoll Paque density-gradient. Subsequently, monocytes were purified by positive magnetic isolation using anti-human CD14 microbeads and AutoMACS technology (Miltenyi Biotec).

To generate hmoDCs, monocytes were seeded at $1x10^6$ cells/mL concentration and differentiated in the presence of 100 ng/mL of granulocyte macrophage colony-stimulating factor (GM-CSF) and 100 ng/mL IL-4 (PeproTech) for 6 days at 37 ºC in a humidified 5% CO_2 incubator. To generate WIN-hmoDCs, WIN55,212-2 (Sigma-Aldrich) at a final concentration of 50 nM was added at days 0 and 4 of the hmoDCs differentiation (**Figure M.1**).

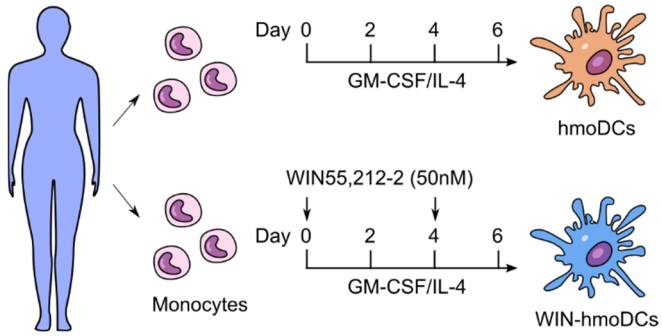

Figure M.1. Schematic representation of the differentiation protocol of hmoDCs and WIN-hmoDCs from human peripheral blood monocytes.

For the stimulation of hmoDCs, cells were treated with LPS (100 ng/mL), HDM (100 µg/mL) and/or WIN55,212-2 (10 µM) for 18 h at 37 ºC in a humidified 5% CO_2 incubator. Subsequently, cells were harvested and centrifuged at 300*g*. Then, cell pellets were employed for flow cytometric analysis and cell-free supernatants were collected to quantify cytokine production by ELISA.

2.2. Coculture experiments

Human peripheral blood naïve $CD4^+$ T cells were purified from PBMCs obtained from buffy coats of healthy donors using the "Naïve $CD4^+$ T Cell Isolation Kit" (Miltenyi Biotec) in a two-step protocol consisting of the negative selection of unlabeled cells. To assure the purity of isolated cells, the kit was supplemented with anti- human CD45RO and anti- human CD14 microbeads (both from Miltenyi Biotec).

After the treatment and/or stimulations of hmoDCs, cells were harvested, washed and cocultured with allogeneic naïve $CD4^+$ T cells (hmoDC:T cell ratio of 1:5) during 5 days at 37 ºC in a humidified 5% CO_2 incubator (**Figure M.2**).

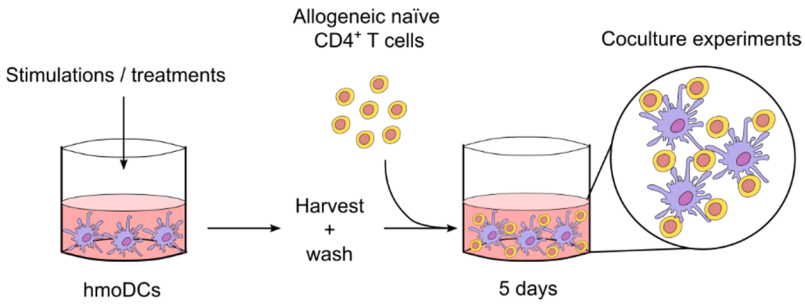

Figure M.2. Illustrative protocol of allogeneic coculture experiments combining hmoDCs with naïve $CD4^+$ T cells.

2.3. Differentiation and culture of THP-1 MΦs

THP-1 and THP-1 XBlue cell lines (InvivoGen) were seeded at 0,25x10^6 cells/mL and stimulated with 10 ng/mL phorbol 12- myristate 13-acetate (PMA, Sigma-Aldrich) for 24 h. Next, culture media was removed, and fresh media was added. After resting for 24 h, cells acquire macrophage-like features and are considered THP-1 MΦs (**Figure M.3**).

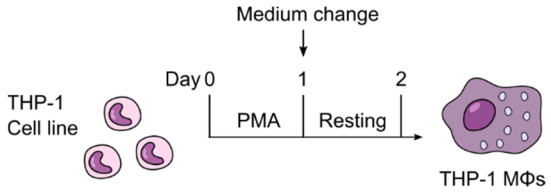

Figure M.3. Schematic representation of the differentiation protocol of THP-1 MΦs.

For the stimulation of THP-1 MΦs, cells were treated with LPS (100 ng/mL) and IFNγ (50 ng/mL) in the presence or absence of WIN55,212-2 (specific doses in figure legends) for 18 h at 37 ºC in a humidified 5% CO_2 incubator. Subsequently, cells were harvested and centrifuged at 300*g*. Then, cell pellets were employed for RNA isolation followed by gene expression assessment or flow cytometric analysis, and cell-free supernatants were collected to quantify cytokine production by ELISA and NF-kB/AP-1 activation.

2.3.1. NF-kB/AP-1 activation assay

The evaluation of NF-kB/AP-1 activation in human macrophages was performed specifically using the THP-1 XBlue™ cell line, which is stably integrated with a NF-kB/AP-1 inducible secreted embryonic alkaline phosphatase (SEAP) reporter construct. THP-1™ XBlue monocytes were differentiated into human THP-1 MΦs as described above. Then, after incubation with the indicated stimuli, the activation of NF-kB/AP-1 was determined in cell-free supernatants using a SEAP colorimetric detection reagent called QUANTIBlue™. Briefly, 20 µL of the supernatants were added to 180 µL of QUANTI-Blue™, the mixture was incubated at 37 ºC and the optical density was measured at 655 nm using a MultiskanFC microplate reader (Thermo Scientific).

2.4. Generation and stimulation of human monocyte-derived macrophages

To generate primary human macrophages, monocytes were purified from PBMCs as described previously. Then, they were seeded at 0,5x10^6 cells/mL and cultured in the presence of 100 ng/mL of GM-CSF (Peprotech) for 7 days at 37 ºC in a humidified 5% CO_2 incubator. Cultures were supplemented with GM-CSF every second day. According to the nomenclature guidelines proposed by Murray et al. (74), we termed this primary macrophages differentiated from monocytes in the presence of GM-CSF as GM-MΦs (**Figure M.4**).

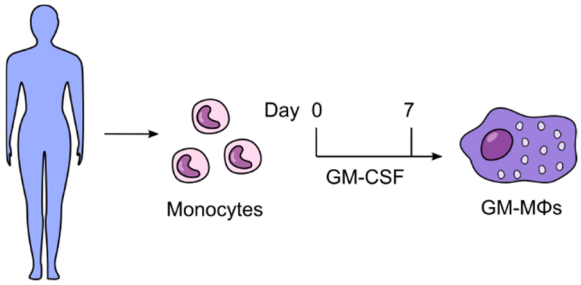

Figure M.4. Schematic differentiation protocol of primary human monocyte-derived macrophages (GM-MΦs).

For the stimulation of GM-MΦs, cells were treated with LPS alone (10 ng/mL) or LPS (100 ng/mL) in combination with IFNγ (50 ng/mL), in the absence or presence of WIN55,212-2 (specific doses in figure legends) for 18 h at 37 ºC in a humidified 5% CO_2 incubator. Subsequently, cells were harvested and centrifuged at 300*g*. Then, cell pellets were employed for RNA isolation followed by gene expression assessment or flow cytometric analysis, and cell-free supernatants were collected to quantify cytokine production by ELISA.

2.4. Differentiation and stimulation of air-liquid interphase cultures of HBECs

Primary human bronchial epithelial cells (HBECs) of healthy donors were purchased from commercial distributors (Epithelix and Lonza). HBECs in passage 1 or 2 were expanded in monolayer cultures with BEBM supplemented with all BEGM SingleQuots in 150 cm^2 T-flask at 37 ºC and 5% CO_2. Once cultures reach 80-90% confluency, HBECs were harvested with 0.05% trypsin-EDTA and seeded onto 6.4-mm-diameter 0.4 µm-pore size polyester membrane transwells (Corning) at a density of $1.5x10^5$ cells per well. From this point, growth medium was replaced by BEBM supplemented with BEGM SingleQuots, except for retinoic acid and triiodothyronine, and mixed 1:1 with DMEM. ATRA was freshly supplemented to the differentiation medium at a concentration of 15 ng/mL and the medium was changed every second day. First, cells were grown submerged for 3-5 days until they reach confluency. Then, the apical compartment medium was removed to allow differentiation in air-liquid-interface (ALI) of a pseudostratified epithelium during the next 21 days (**Figure M.5**).

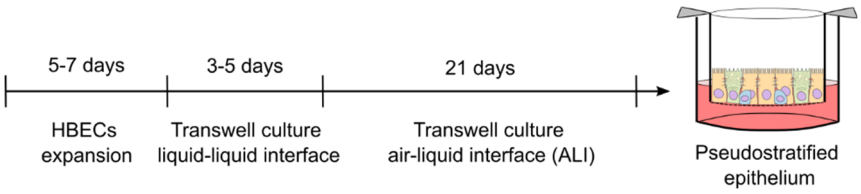

Figure M.5. Schematic representation of the differentiation protocol of ALI cultures of HBECs.

Stimulation of fully differentiated ALI cultures was performed in Opti-MEM medium. For RV-A16 infection experiments, RV-A16 or UV-RV-A16 were apically added to ALI cultures at a multiplicity of infection (MOI) of 2. Alternatively, IL-13 (50 ng/mL) and WIN55,212-2 (2.5 µM) treatments were performed in the basolateral compartment.

For mechanistic studies, ALI cultures of HBECs were preincubated for 1 h with the inhibitor of ROS, N-acetyl-L-cysteine (NAC, 5 mM) (Sigma-Aldrich), or the inhibitor of protein tyrosine phosphatases H_3VO_4 (10 µM) (Sigma- Aldrich). Both stimuli were administered in the basolateral compartment.

For experiments assessing the effects of particulate materials in ALI cultures, silica or regolith simulants were daily administered into the apical compartment in a model of repetitive exposure for three consecutive days. Briefly, fully differentiated cultures were apically exposed to the regolith simulants for 24 h. Then, the apical compartment was emptied and re-filled with fresh regolith-containing medium for additional 24 h. The following day, this same process was repeated to complete the protocol. Of note, to neutralize possible LPS contamination, medium-containing regolith simulants and medium-only controls were incubated with 5 µg/ml Polymyxin B sulfate (Sigma-Aldrich) for 1 hour at 37 ºC before experiments.

All experiments were performed at 37 ºC in a 5 % CO_2 humidified incubator, except for infection experiments, which were carried out at 34.5 ºC.

2.5. Generation and stimulation of human bronchial epithelial spheroids

Primary HBECs of healthy or asthma donors were purchased from commercial distributors (Epithelix and Lonza). HBECs in passage 2 were seeded at a density of 2000 cells per well in 96-well plates pre-coated with 25% GFR-ECM. Bronchospheroid differentiation medium was composed of BEBM mixed 1:1 with DMEM supplemented with 5% GFR-ECM, 15 ng/mL ATRA and all BEGM SingleQuots, except for retinoic acid and triiodothyronine. Cultures were maintained at humidified conditions 37°C, 5% CO_2 and medium was refreshed every second day.

Stimulation of fully differentiated bronchospheroids with IL-13 (50 ng/mL) and/or WIN55,212-2 (2,5 µM) was performed after 13-16 days of culture, depending on the donor, once lumen development in the majority of the bronchospheroids was confirmed by light microscopy imaging.

Treatment during the differentiation of bronchospheroids with IL-13 (2 ng/mL) and/or WIN55,212-2 (specific doses indicated in figure legends) was performed every second day starting from day two until the end of the culture.

3. Metabolic studies

3.1. Glucose and lactate quantification

The determination of glucose concentration in cell-free culture supernatants was assessed by using the Glucose (GO) Assay Kit (Sigma-Aldrich). The metabolic rate was derived mathematically as the percentage of glucose consumed relative to its concentration in medium without cells (2 mg/mL).

Lactate concentration was measured in perchloric acid deproteinized culture supernatants by means of a two-step coupled lactate oxidase (Sigma-Aldrich) and horseradish peroxidase (HRP, Thermo

Scientific) enzymatic reactions. Briefly, lactate was oxidized producing H_2O_2 which was coupled to the conversion of Amplex Red reagent (Invitrogen) to fluorescent resorufin by HRP. The fluorescence intensity of resorufin was analyzed using FLUOstar OPTIMA fluorescence reader (BMG LabTech).

3.2. Seahorse experiments

Real-time metabolic profiling of macrophages and airway epithelial cells was performed using a Seahorse XF HS Mini Analyzer (Agilent) following conventional protocols for adherent cells, with minor modifications.

Primary human macrophages were harvested on day 5 of differentiation and seeded at a density of $50x10^3$ cells per well in XFp Cell Culture Miniplates (Agilent) with cRPMI supplemented with 100 ng/mL GM-CSF. Cells were incubated 24 h and then activated for 18 h with LPS or LPS+WIN55,212-2 (LPS+WIN), 10 ng/mL and 10 mM respectively. For peritoneal macrophage experiments, mice peritoneal cells were seeded ($400x10^3$ cells per well) in XFp Cell Culture Miniplates with cRPMI supplemented with 20 ng/mL mouse M-CSF (PeproTech) and incubated for 3 h. Peritoneal macrophages were purified by adherence through three consecutive washing steps and stimulated for 18 h with LPS or LPS+WIN55,212-2 (LPS+WIN), 10 ng/mL and 10 mM, respectively. After stimulation, cRPMI medium was removed and cells were cultured with XF DMEM medium (Agilent) supplemented with 10 mM glucose (Sigma-Aldrich), 1 mM pyruvate (Life Technologies) and 2 mM glutamine (Sigma-Aldrich) in a CO_2- free incubator for at least 1 h at 37 °C before the assay. To accurately monitor glycolysis, we analyzed the glycolytic proton efflux rate (glycoPER) at three consecutive stages: basal conditions (no drugs administrated), inhibition of the electron transport chain (0,5 µM Rotenone, ROT, and 0,5 µM Antimycin A, AA) and inhibition of glycolysis (50 mM 2-deoxy-D-glucose, 2-DG) (Sigma-Aldrich).

For real-time metabolic profiling of airway epithelial cells, HBECs in passage 2 or 3 were seeded into XFp Cell Culture Miniplates at a density of $3x10^4$ cells per well and incubated overnight. Next, cells were stimulated with medium (control) or IL-13 (50 ng/mL) in the absence or presence of WIN55,212-2 (2.5 µM) for 24 h. Then, HBEC culture medium was removed, cells were washed and cultured with XF DMEM medium supplemented with 10 mM glucose, 1 mM pyruvate and 2 mM glutamine in a CO_2-free incubator at 37 °C for at least 1 h before the assay. To specifically assess mitochondrial function, the oxygen consumption rate (OCR) and extracellular acidification rate (ECAR) were monitored basally or after the consecutive inhibition of mitochondrial complex V (1.5 µM oligomycin, Oligo), uncoupling of mitochondrial membrane proton gradient (1 µM carbonyl cyanide 4-(trifluoromethoxy)phenylhydrazone, FCCP), and inhibition of the electron transport chain (0.5 µM ROT + 0.5 µM AA).

3.3. Quantification of reactive oxygen species

HBECs in passage 2 or 3 were seeded into dark 96-well plates at a density of $5x10^4$ cells per well. Cells were allowed to adhere during 24 h incubation and stimulated with the indicated treatments for additional 24 h. Then, the reactive oxygen species (ROS) detection probe, Cell Rox Green (5 µM, Invitrogen), was directly added to the culture medium and incubated at 37 ºC for 30 min in the dark. After incubation,

cells were washed three times with PBS and fluorescence intensity was analysed using a FLUOstar OPTIMA fluorescence reader (BMG LabTech).

4. Epithelial barrier studies

4.1. Transepithelial electrical resistance (TER) measurements

Monitorization of TER values was performed in fully differentiated ALI cultures using Millicell-ERS Volt Ohm Meter (Millipore). The electrode was washed with PBS, sterilized for 15 min in 70 % ethanol and washed again with PBS before use. Once prepared, TER values were measured by placing the long arm of the electrode into the basolateral compartment while the short arm was carefully positioned into the liquid in the apical compartment of the transwells.

4.2. Paracellular flux assays

The paracellular flux of ALI cultures of HBECs was assessed after 72 h of treatment with the indicated stimuli. Fluorescein isothiocyanate (FITC)-labelled 4-kDa dextran (FITC-dextran, 2 mg/mL) (Sigma-Aldrich) was apically administered to the cultures and the fluorescence intensity in the basolateral compartment was analyzed after 24 h using a fluorescence plate reader (BMG LabTech).

For the evaluation of paracellular flux in airway bronchospheroids, 0.5 mg/mL of FITC-dextran was added into the culture medium 24 h after the incubation with the indicated treatments. After additional 24 h of incubation in the presence of FITC-dextran, images of at least 20 spheroids per donor were taken with confocal microscopy (Zeiss LSM780) and analyzed with ImageJ/Fiji software. Briefly, the mean fluorescence intensity of each luminal area was relativized to the medium background intensity and represented as lumen-to-background fluorescence intensity ratio.

4.3. Analysis of spheroid count, size and lumen-to-total spheroid area ratios

The average spheroid count and size were calculated with ImageJ/Fiji software using the analyse particles tool after subtracting background and setting the threshold. The lumen-to-total spheroid area ratios were mathematically calculated from the separate measurements of the spheroid lumen and total spheroid areas in Image J software.

4.4. Immunofluorescence staining of ALI cultures and bronchospheroids.

After incubation with the indicated stimuli, ALI cultures of HBECs were washed with PBS and fixed with 4% paraformaldehyde (PFA). Samples were then washed with PBS and incubated for 10 min with 0.1 M Glycine. Permeabilization was performed using 0.1% Triton X-100, 0.02% SDS in PBS for 5 min and it was immediately followed by a blocking step with 1% BSA, 10% goat serum in PBS for 15 min. Anti-human ZO-1 primary antibodies were incubated for 45 min at room temperature. Samples were then washed with 0.01% Tween-20 in PBS and incubated with the combination of anti-rabbit IgG Alexa Fluor 647 secondary antibody, anti-human occludin Alexa Fluor 488 and the nuclei dye, Hoechst, for 45 min

at room temperature. Finally, after a last washing step, samples were mounted with ProLong-Gold containing antifade reagent (Invitrogen) and examined under an Olympus FluoView-1200 confocal microscope (Olympus). For tight junction staining, 6-7 Z-focal plane images were taken from each region at 6 µm intervals. Later analysis and quantification were performed by combining images with maximum intensity projection using ImageJ/Fiji software.

Bronchospheroids were harvested with ice-cold PBS and fixed with 4% paraformaldehyde (Sigma-Aldrich) for 45 min. Fixed spheroids were washed with ice-cold PBS. Subsequently, the permeabilization and blocking of spheroids was performed in a single step using 1% DMSO, 1% goat serum, 1% bovine serum albumin (BSA), 0.5% Triton X-100 in PBS for 60 min. After perm-block, spheroids were washed with 0.1% BSA in PBS and incubated with anti-acetylated α-tubulin and anti-human MUC5AC primary antibodies overnight at 4 °C. Then, they were washed with 0.1% BSA and 0.1% Triton X-100 in PBS, and incubated with the corresponding goat anti-rabbit IgG Alexa Fluor 488 and goat anti-mouse IgG Alexa Fluor 546 secondary antibodies, as well as the nuclei dye, DAPI, overnight at 4°C. Finally, after washing with 0.1% BSA, 0.1% Triton X-100 in PBS, bronchospheroid samples were kept in 0.1% BSA in PBS until confocal microscopy analysis (Zeiss LSM780). For cellular composition analysis (staining of human MUC5AC and acetylated α-tubulin) a minimum of 15 spheroids were evaluated per condition and donor. Three images were taken from each spheroid at 10 µm intervals. Finally, images were combined with maximum intensity projection in ImageJ/Fiji software to analyze the mean fluorescence intensity of MUC5AC.

All the information about the antibodies employed in these procedures is listed in **Table M.1**.

Antigen target	Target species	Host species	Conjugate	Clone	Dilution	Supplier
MUC5AC	Human	Rabbit	None	EPR16904	1:200	Abcam
Acetylated α-tubulin	Human	Mouse	None	6-11B-1	1:500	Abcam
ZO-1	Human	Rabbit	None	Polyclonal	1:250	ThermoFisher
Occludin	Human/Mouse	Mouse	A488	OC-3F10	1:250	Invitrogen
IgG	Rabbit	Goat	A488	Polyclonal	1:500	Life technologies
IgG	Mouse	Goat	A546	Polyclonal	1:500	Life technologies
IgG	Rabbit	Goat	A647	Polyclonal	1:500	Life technologies

Table M.1. List of antibodies employed for immunofluorescence staining.

5. Cytokine quantification

Concentrations of human TNF-α, IL-1β, IL-6, IL-8, IL-10, IL-5, and IFN-ɣ, as well as murine IL-6 in cell-free supernatants were quantified by ELISA kits from BD Biosciences. Human TSLP and CCL26 were quantified using commercial kits from R&D Systems and murine TNF-α, IL-1β, IL-10, IL-5, and IFN-ɣ levels were assessed using specific ELISA kits from Invitrogen. In all cases, the manufacturer protocols were followed with minor modifications.

6. Flow cytometry

6.1. Surface staining

For surface staining, cells were harvested, washed with 2 mM ethylenediaminetetraacetic acid (EDTA), 0.5% BSA in PBS with and stained in darkness for 15 min at room temperature with the corresponding fluorescence-labelled or isotype control antibodies. Then, cells were washed with 2 mM EDTA, 0.5% BSA in PBS and centrifuged at 300*g* for 5 min at room temperature. Lastly, cells were suspended in 2 mM EDTA, 0.5% BSA in PBS for immediate acquisition or 0.1 % PFA in PBS when samples were acquired at later timepoints.

6.2. Intranuclear staining of FOXP3

For the analysis of FOXP3 expression, conventional surface staining was followed by subsequent fixation and permeabilization with FOXP3 Fix/Perm buffer (Biolegend) for 20 min in darkness at room temperature. A second permeabilization was carried out with FOXP3 Perm buffer (Biolegend) for 15 min in darkness at room temperature. Then, cells were stained with Alexa Fluor 488 anti-human FOXP3 for 30 minutes in darkness at room temperature. Finally, cells were washed and suspended in 1 % PFA in PBS for flow cytometry analysis.

6.3. CB1 and CB2 staining

For the evaluation of the expression of CB1 in different cell subsets, single cell suspensions were incubated for 30 min in darkness with HU210-AlexaFluor488 fluorescent probe, a validated for the identification of CB1 in biological systems (204), at a final concentration of 1 μM in PBS at room temperature and with shaking. Alexa Fluor 488 alone was used as control. Subsequently, cells were washed with PBS and fixed with 0.1 % PFA in PBS before flow cytometry analysis.

For the detection of CB2, cells were first incubated with the primary CB2 polyclonal antibody (PA1744, Invitrogen) in darkness for 30 min in 10% FBS in PBS at room temperature and with shaking. After washing with PBS, samples were incubated for 30 min in darkness with a goat anti-rabbit Alexa Fluor 488 secondary antibody (Invitrogen) in 3% BSA in PBS at room temperature and with shaking. Finally, samples were washed again and fixed with 0.1 % PFA in PBS prior to flow cytometry analysis.

6.4. Sample acquisition, analysis and reagents

Sample acquisition was carried out in the Flow Cytometry and Fluorescence Microscopy Unit at Complutense University of Madrid, using FACS Calibur or FACS Aria III cytometers (Beckton Dickinson, BD). Data analysis was performed by using Flow-Jo software.

Cell viability was analyzed using propidium iodide (PI, Life technologies), eFluor660 (eBioscience) or eFluor780 (Invitrogen) staining. All antibodies and probes used for flow cytometry determinations are listed in **Table M. 2**.

Antigen target / Reagent	Target species	Host species	Conjugate	Clone	Dilution	Supplier
FcR Blocking	Human	-	-	-	1:100	Miltenyi
HLA-DR	Human	Mouse	FITC	L243	1:50	Biolegend
CD83	Human	Mouse	APC	HB15e	1:50	Biolegend
CD83	Human	Mouse	PE	HB15e	1:50	Biolegend
CD86	Human	Mouse	PE	IT2.2	1:50	Biolegend
OX40L	Human	Mouse	PE	ik-1	1:20	BD
CD4	Human	Mouse	PerCP	OKT4	1:50	Biolegend
CD25	Human	Mouse	APC	BC96	1:100	Biolegend
CD127	Human	Mouse	PE	A019D5	1:100	Biolegend
FOXP3	Human	Mouse	A488	259D	1.5:50	Biolegend
CB2	Human	Rabbit	None	Polyclonal	1:50	Invitrogen
CD16/ CD32	Mouse	Rat	-	2.4G2	1:100	BD
CD3	Mouse	Armenian Hamster	FITC	145-2C11	7:100	Biolegend
Siglec F	Mouse	Rat	PE	S17007L	1:50	Biolegend
CD11b	Mouse	Rat	PerCP-Cy5.5	M1/70	1:50	Biolegend
MHCII	Mouse	Rat	PE-Cy7	M5/114.15.2	1:100	Biolegend
CD11c	Mouse	Armenian Hamster	APC	N418	1:50	Biolegend
Ly6G	Mouse	Rat	BV405	1A8	1:25	Biolegend
ST1/ST2	Mouse	Rat	BV605	DIH9	1:25	Biolegend
HU210-A488 (CB1)	-	-	A488	-	-	* Not commercially available
IgG	Rabbit	Goat	A488	Polyclonal	1:500	Life technologies
Propidium iodine	-	-	-	-	1:2000	Life technologies
eFluor660	-	-	-	-	1:2000	eBioscience
eFluor780	-	-	-	-	1:2000	Invitrogen

Table M.2. List of antibodies and reagents employed in cell staining for flow cytometry. * The HU210-A488 fluorescent probe was kindly provided by our collaborator Dr. Martín-Fontecha at Medicinal Chemistry Lab in Complutense University of Madrid, Spain.

7. Western blot

After the indicated treatments, cells were washed with PBS and lysed in RIPA buffer (Thermo Scientific) supplemented with Protease/Phosphatase Inhibitor Cocktail (Cell Signaling) and 1 mM phenylmethylsulfonyl fluoride (PMSF, Sigma-Aldrich) for 30 min at 4 °C. Sample protein content was quantified using Micro BCA Kit (Thermo Scientific) following the manufacturer's protocols. 10 µg of total protein from cell lysates were separated in SDS-polyacrylamide gel electrophoresis (SDS-PAGE) and transferred onto a nitrocellulose or polyvinylidene difluoride (PVDF) membrane (Bio-Rad Laboratories). The membrane was blocked with 5% BSA, 0.1% Tween-20 in Tris buffered saline for 1 h and incubated with the indicated primary antibodies: phospho-Akt, phospho-p70 S6 Kinase (p70S6K), inducible Nitric

Oxide Synthase (iNOS), phospho-STAT6, STAT6 (all from Cell signaling). All primary antibodies and dilutions employed are listed in **Table M.3**. Then, the membrane was washed and incubated with goat anti-rabbit (1:4000; Bio-Rad Laboratories) or goat anti-mouse (1:2500, Pierce) conjugated with HRP as a secondary antibody. The signal was developed with Clarity Western ECL Substrate (Bio-Rad), detected in a Fujifilm LAS-3000 developer and analyzed with Fujifilm Multi Gauge software. The quantification of the images was obtained displaying same-size regions of interest (ROIs) over the different bands and the intensity/mm^2 of each ROI was quantified. After removal of the background value, the quantification of each band was then relativized to the one of its corresponding loading controls (β-actin).

Antigen	Target species	Host species	Clone	Dilution	Supplier
Phospho-Akt (Ser473)	Human	Rabbit	D9E	1:1000	Cell signaling
Phospho-p70S6K (Thr389)	Human	Rabbit	Polyclonal	1:750	Cell signaling
iNOS	Human	Rabbit	E3W6B	1:1000	Cell signaling
Phospho-STAT6	Human	Rabbit	Polyclonal	1:1000	Cell signaling
STAT6	Human	Rabbit	Polyclonal	1:1000	Cell signaling
β-Actin	Human	Mouse	AC15	1:30000	Sigma-Aldrich

Table M.3. List of primary antibodies employed in western blotting.

8. RNA isolation and cDNA synthesis

The RNA from collected samples was isolated with RNeasy Mini Kit (Qiagen) according to the manufacturer's protocol. Next, complementary DNA was generated with a PrimeScript RT Reagent Kit (Takara Bio).

9. Quantitative PCR (qPCR)

Quantitative PCR was performed on cDNA by using FastStart Universal SYBR Green Master (Roche). The sequences of all primer pairs employed are shown in **Table M.4**. Samples were run on a real-time PCR system (ABI Prism 7900 HT; Applied Biosystems). Human data were normalized to elongation factor 1A (*EF1A*) housekeeping gene, while eukaryotic translation elongation factor 1 alpha 1 (*Eef1a1)* was used as housekeeping for mice samples. All the results are displayed as $2^{-\Delta CT}$ arbitrary values, with Δ cycle threshold (ΔCT) defined as the difference between the CT value for the gene of interest and the housekeeping control.

Gene target	Species	Forward primer sequence	Reverse primer sequence
EF1A	Human	CTGAACCATCCAGGCCAAAT	GCCGTGTGCAATCCAAT
CD80	Human	GATAACCTGCTCCCATCCTGG	CTTGGGGCAAAGCAGTAGGT
CCR7	Human	CATGGACCTGGGGAAACCAA	AAAGTTCCGCACGTCCTTCT
IL1B	Human	TTCGACACATGGGATAACGAGG	TTTTTGCTGTGAGTCCCGGAG
IL6	Human	GGTACATCCTCGACGGCATCT	GTGCCTCTTTGCTGCTTTCAC
IL8	Human	GCAGCTCTGTGTGAAGGTGCAGTT	TTCTGTGTTGGCGCAGTGTGGTC
NLRP3	Human	TTGAGAACTGTCATCGGGTGG	CGCCCCAACCCATGAGAAC
CASP1	Human	AGGATATGGAAACAAAAGTCGGC	AGATAATGAGAGCAAGACGTGTG
GSDMD	Human	ACAACTTCCTGACAGATGGGG	GGCACAGCTCTCTGTCCAA
HK2	Human	TTCGCACTGAGTTTGACCAG	TCACCAGGATAAGCCTCACC
PFKB3	Human	AGCCCGGATTACAAAGACTGC	GGTAGCTGGCTTCATAGCAAC
LDHA	Human	ATGGCAACTCTAAAGGATCAGC	CCAACCCCAACAACTGTAATCT
HIF1A	Human	TCGCATCTTGATAAGGCCTCT	ACAAAACCATCCAAGGCTTTCA
TNF (ChIP)	Human	ACCACGCTCTTCTGCCTGCT	TCCATCCCTCCCTATCAGCGCA
IL1B (ChIP)	Human	GGCCACCACCACCAACGTTA	AAGGGAGTTCTGGGCCACTTTG
IL6 (ChIP)	Human	ACGCCTTGAAGTAACTGCACGA	TTCCTCTGACTCCATCGCAGCC
MUC5AC	Human	CAGAAGATGGACGACCCCAC	TCCTCACAGATGCCAAAGCC
MUC5B	Human	GTGGAGCAGAGCAGCGTCTAC	GCTCCAGCAGGGCACTGT
CCL26	Human	CCACACGTGGGAGTGACATA	CCTCTTTTGGTAGTGAATATCACAG
POSTN	Human	GACCGTGTGCTTACACAAATTG	AAGTGACCGTCTCTTCCAAGG
UBE2Z	Human	ACTCCGGATCAAGCGGATA	AGGAGTGTCAAATGGGCCTG
OCLN	Human	GACCTGAATGGGTACATGTGTGTAA	GGAATTCTCACAACACCAACTGAAG
ZO1	Human	ACAGTGCCTAAAGCTATTCCTGTGA	TCGGGAATGGCTCCTTGAG
ITGA6	Human	TTTGAAGATGGGCCTTATGAA	CCCTGAGTCCAAAGAAAAACC
P63	Human	CAGGAAGACAGAGTGTGCTGGT	AATTGGACGGCGGTTCATCCCT
FOXJ1	Human	TTCAATCCGCCACAACCTGT	CTCCCGAGGCACTTTGATGA
DNAI2	Human	CCGCATTTGGTCTGAAGACAGC	GTTCCGTCCATCCTGGTGGTAA
Eef1a1	Mouse	CGGCAGTCGCCTTGGACGTT	CGGTGGTTTTCACAACACCTGCGT
Muc5ac	Mouse	TGCACAGGCCAGGCTCAACA	CCCGCCTGGTATGTCCTGGGT
Clca1 (gob5)	Mouse	AACGGAGCAGGTGCCGATGC	AGTGACTCCTCCCAGAGCCCA
Scgb1a1	Mouse	TGCTGCAGCTCAGCTTCTTCGG	GCCAGGGTTGAAAGGCTTCAGGG
Zo1	Mouse	GGAGATGTTTATGCGGACGG	CCATTGCTGTGCTCTTAGCG
Ocln	Mouse	ACAAGAGAAATTTTGATGCAGGTCT	CATCAGCAGCAGCCATGTACTC
Il5	Mouse	GTTGACAAGCAATGAGACGATGAG	CCCACGGACCGTTTGATTCTTC
Tnf	Mouse	CCACCACGCTCTTCTGTCTA	TGATGAGAGGGAGGCCATTTG
Il6	Mouse	GAAACCGCTATGAAGTTCCTCTCTG	GTATCCTCTGTGAAGTCTCCTCTCC
Nlrp3	Mouse	ACCAGCCAGAGTGGAATGAC	ACAAATGGAGATGCGGGAGAG
Il1b	Mouse	GCTGAAAGCTCTCCACCTCA	CTTGGGATCCACACTCTCCAG
Col1a1	Mouse	GAACTGGACTGTCCCAACCC	TTGGGTCCCTCGACTCCTAC
Tgfb1	Mouse	CTTCAATACGTCAGACATTCGGG	GTAACGCCAGGAATTGTTGCTA

Table M.4. List of oligonucleotides employed for qPCR analysis.

10. Chromatin immunoprecipitation

For chromatin immunoprecipitation (ChIP), cells were harvested after stimulation and fixed in 1% methanol-free formaldehyde. Then, samples were lysed and sonicated for 10 minutes (30 seconds on; 30 seconds off) using a Branson 1200 Ultrasonic Cleaner to obtain chromatin fragments of optimal size (300-800 bp). Sheared chromatin was incubated using 2 µL of anti-H3K27ac antibody (Abcam, ab4729)

or 2 µL of anti-IgG antibody (Millipore, 12-370), and immunoprecipitated with Dynabeads A (Invitrogen, 10001D) and Dynabeads G (Invitrogen, 10003D) magnetic beads. ChIP samples were de-cross-linked with proteinase K (Fisher Scientific) at 65°C for 4 h. Then, DNA was purified with the DNA Clean Kit & Concentrator TM-5 (Zymo Research), following the manufacturer's protocol. Quantitative analysis of the purified ChIP and Input DNAs was performed by using FastStart Universal SYBR Green Master (Roche) by real time qPCR.

11. Gene set enrichment analysis

Data from next generation RNA sequencing of differentiated HBECs from healthy controls and asthma patients, unstimulated or stimulated with 50 ng/mL IL-13 for 24 h was obtained from the publicly available Gene Expression Omnibus platform (accession number: GSE206510) (205). Gene set enrichment analysis (GSEA) was performed using the GSEA software version 4.3.3 (http://software.broadinstitute.org/gsea/index.jsp). GSEA was employed to identify HALLMARK and Kyoto Encyclopaedia of Genes and Genomes (KEGG) gene sets from the Molecular Signatures database (MSigDB) that were enriched after IL-13 stimulation in HBECs from either control subjects or asthmatics. Graphical representations (bar plots) of normalized enrichment score (NES) were produced with GraphPad Prism software, 8.0 version using the data obtained in the GSEA. Statistical significance was considered when FDR q value < 0.25.

12. Transmission electron microscopy

Sample preparation and visualization was performed with the support of the Electron Microscopy Unit at the Complutense University of Madrid. Briefly, after complete differentiation of ALI cultured HBECs, cells were washed in PBS and fixed in 4% paraformaldehyde + 2.5% glutaraldehyde for 4-5 h at 4ºC. Samples were then washed four times in PBS and kept overnight at 4ºC. Next, samples were washed in doubly distilled water and a post fixation step with 1% osmium tetroxide was performed at room temperature for 1 h. After additional washing, samples were dehydrated in increasing concentrations of acetone and progressively infiltrated in Spurr resin. Finally, sample blocks were made, cut (ultramicrotome Leica Reichert Ultracut S) and visualized under the electron microscope (JEM1010, JEOL).

13. Animal models

All mice procedures included in this Doctoral Thesis were reviewed and ethically approved by Universidad Complutense de Madrid (UCM) and Comunidad Autónoma de Madrid (CAM) within the context of project SAF-2017-84978-R and PID2020-114396RB-I00 to Dr. Óscar Palomares under PROEX 152/18, PROEX 322.1/21, and PROEX 227.3/24 from CAM.

13.1. LPS-induced sepsis model

BALB/c mice (female, 6-week-old, Charles River) were randomly assigned into 4 groups. Then, mice were intraperitoneally injected with vehicle (PBS+DMSO), WIN55,212-2 (5 mg/kg), LPS (20 mg/kg), or LPS plus WIN55,212-2, respectively. Serum samples were collected 12 h after LPS administration. Then, the presence of bilirubin in mice sera was determined by its absorbance at 450 nm, lactate dehydrogenase (LDH) activity was analyzed using CyQUANT LDH Cytotoxicity Assay Kit (Invitrogen) and the concentration of IL-1β was measured by ELISA (Invitrogen).

13.2. Purification and *ex vivo* culture of murine peritoneal macrophages (PMΦs)

BALB/c mice were anesthetized using isoflurane and subjected to intraperitoneal lavage with 3 mL of 10 mM EDTA in PBS. The peritoneal cells were then washed, seeded in medium at $0{,}5x10^6$ cells/mL and allowed to rest for 3 h. Then, PMΦs were purified by adherence after three consecutive washing steps and treated with the indicated stimuli.

13.3. IL-13-induced airway inflammation model

C57BL/6J mice (female, 6-week-old, Charles River) were randomly assigned into 5 groups. Then, mice were intranasally instilled for three consecutive days with PBS (control), IL-13 (50 µg/kg), IL-13+WIN55,212-2 (0.2 mg/kg) or IL-13+WIN55,212-2 (1 mg/kg). Comparative doses of the vehicle (DMSO) were administered to control and IL-13-stimulated mice. Alternatively, to address the effects of different administration routes, one group of mice received intranasal IL-13 (50 µg/kg) and intraperitoneal WIN55,212-2 treatment (5 mg/kg). All mice were sacrificed 24 h after the last IL-13 administration and bronchoalveolar lavage fluid (BALF), right (mRNA expression) and left (histological assessment) lung samples were collected.

13.4. HDM-driven allergic airway inflammation model

BALB/c mice (female, 6-week-old, Charles River) were randomly assigned into 3 groups. An acute HDM-induced asthma model was developed following conventional protocols in one group of mice (HDM group). Briefly, animals were intranasally sensitized with 1 µg HDM (Inmunotek S.L.), and 7 days later, challenged with 10 µg HDM for 5 consecutive days (days 8-12). Alternatively, a second group of mice were intranasally sensitized with 1 µg HDM in the presence of WIN55,212-2 (0.5 mg/kg) and challenged with 10 µg HDM on days 8-12 (Therapeutic group). Finally, a group receiving PBS during sensitization and challenge was also included (Control group). Importantly, both control and HDM groups received the corresponding vehicle (DMSO) intranasally during sensitization. All mice were sacrificed 72 hours after the last challenge and BALF, spleen and serum samples were collected.

13.5. Murine model of acute regolith exposure

C57BL/6J mice (female, 6-week-old, Charles River) were randomly assigned into 4 groups. Then, mice were intranasally instilled for three consecutive days with 50 µL containing PBS (Control), SiO_2 (50

mg/kg), LMS-1 (50 mg/kg) or MGS-1 (50 mg/kg). To achieve homogeneous particle suspensions, PBS-containing silica or regolith simulants was vigorously vortexed before each intranasal treatment. All mice were sacrificed 24 hours after the last particulate exposure and BALF, right (mRNA expression) and left (histological assessment) lung samples were collected.

13.6. Histology

Mice left lungs were collected and immediately fixed in 4% paraformaldehyde for 48 h. Afterwards, the lungs were washed 5 times with PBS and embedded in paraffin. Then, paraffin-embedded tissues were cut into 5 µm-thick sections and stained with Hematoxylin & Eosin (H&E) or Periodic acid-Schiff (PAS), to evaluate airway inflammation and mucus production, respectively.

For quantitative analysis of H&E- and PAS-stained tissue samples, 10 equal-sized perivascular and/or peribronchial areas per mice were analyzed combining Zen Blue and ImageJ software.

13.7. Lung RNA isolation and retrotranscription

A portion of 20-30 mg from the right lung was collected, snap-frozen in liquid nitrogen and stored at -80 ºC. Afterwards, samples were disrupted in liquid nitrogen with a pestle and immediately homogenized in lysis buffer before continuing with the RNA isolation, cDNA synthesis and qPCR protocols as described above.

13.8. Spleen processing and splenocyte culture

Spleens were isolated aseptically, minced, and filtered through a 40 µm nylon cell strainers to obtain a single-cell suspensions. Subsequently, red blood cells were lysed with ACK lysis buffer and splenocytes were resuspended in cRPMI. Triplicates of $0.8x10^6$ splenocytes of each group of mice were cultured with HDM (100 µg/mL) in 96-well flat-bottom plates (Corning). After 3 days of culture at 37ºC and 5% CO_2, triplicates were pooled, and cell-free supernatants were used to quantify cytokine production by ELISA.

13.9. BALF collection

BALF samples were collected from each mouse by infusion and extraction of 0,7 mL of ice-cold 10 mM EDTA in PBS. The procedure was repeated twice using 1 mL of 10 mM EDTA in PBS for optimal collection of BAL cellular infiltration. BALF obtained from first lavage was centrifuged 300*g* for 10 min. Subsequently, cell-free BALF supernatants were collected and stored at -80 ºC for further analysis. Cell pellets from all lavages of each mouse were pooled and analyzed to assess cell recruitment and composition by flow cytometry (see gating strategy of major BALF cell populations in **Figure M.6**).

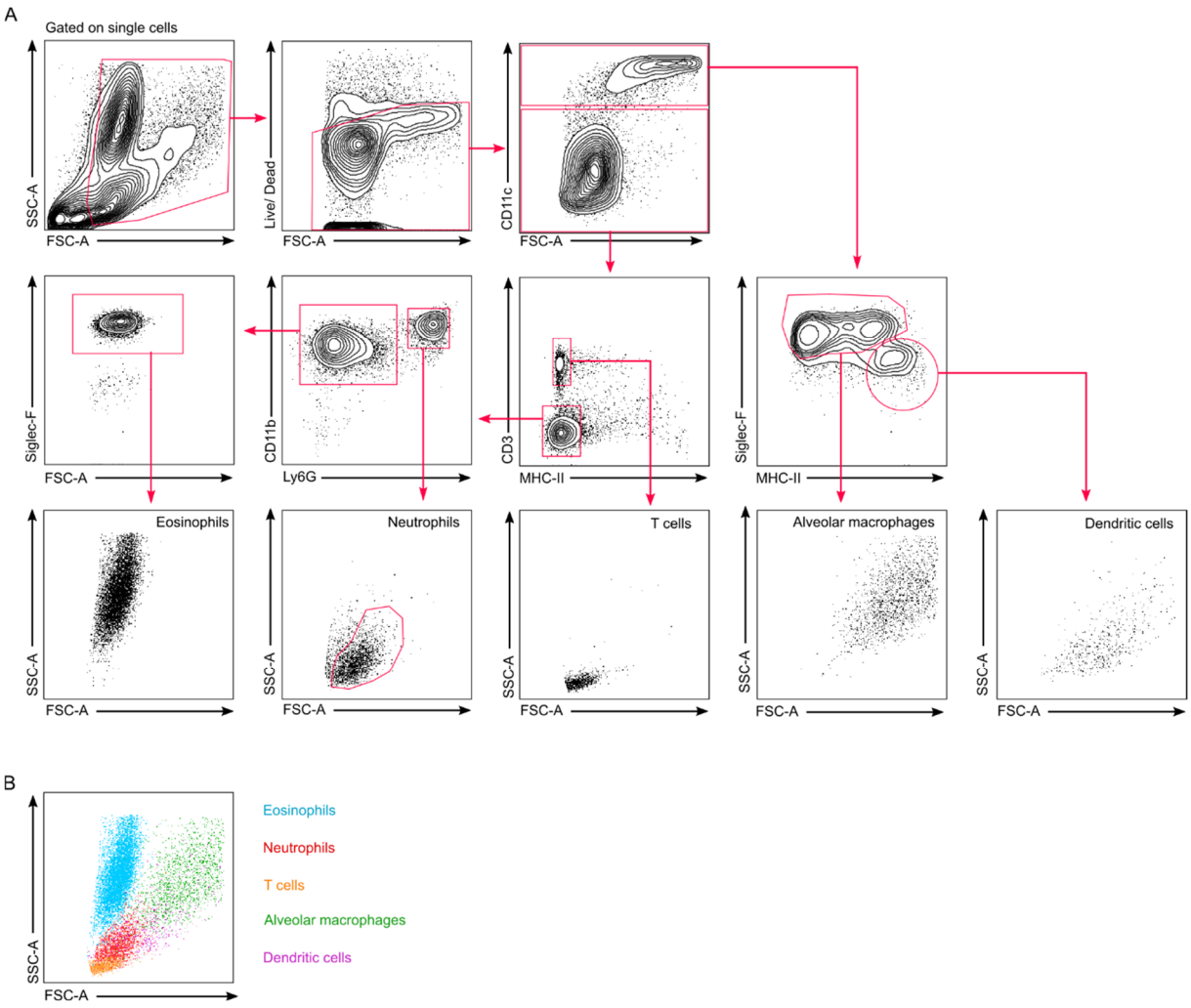

Figure M.6. Flow cytometry analysis and gating strategy of major cell populations contained in BALF. (**A**) Gating strategy for CD11c^{low} CD3^{-} MHC-II^{-} CD11b^{high} Ly6G^{-} Siglec-F^{high} eosinophils, CD11c^{low} CD3^{-} MHC-II^{-} CD11b^{high} Ly6G^{+} neutrophils, CD11c^{low} CD3^{+} MHC-II^{-} T cells, CD11c^{high} Siglec-F^{high} MHC-IIi^{nt} alveolar macrophages, and CD11c^{high} Siglec-F^{int} MHC-II^{high} dendritic cells in BALF. (**B**) Distribution of the main BALF cell populations according to size and complexity. The representative data displayed belongs to the analysis of BAL from an IL-13-treated mouse.

13.10. Quantification of markers of epithelial barrier status in BALF

Epithelial barrier leakage to the airway lumen was assessed by the analysis of total protein and serum albumin content in BALF. Measurement of total protein concentration in cell-free BALF supernatants was performed using the Micro BCA Kit (Thermo Scientific). For the analysis of mouse albumin content in BALF, samples were quantified using a competitive ELISA kit (Abcam). All procedures were carried out following the manufacturer's protocols.

Epithelial damage was assessed by determining LDH activity in BALF using CyQUANT LDH Cytotoxicity Assay Kit (Invitrogen), following the manufacturer's protocol.

13.11. Serum sample collection

Blood samples were collected via retroorbital bleeding using lime grass Pasteur pipettes and microtainer tubes (Beckton Dickinson). To obtain serum, samples were centrifuged at 10,000 rpm for 10 min at room temperature.

13.12. IgE measurement

Mouse total IgE was measured in serum samples using a commercial ELISA kit (BD Biosciences) following the manufacturer's protocol with minor modifications.

14. Statistical analysis

Statistical analyses were performed using GraphPad Prism software, 6.0 and 8.0 versions. All data were expressed as mean ± SEM of the corresponding parameter. The tests employed are specifically detailed in the corresponding figure legend. Significance was defined as: * $p < 0.05$, ** $p < 0.01$, *** $p < 0.001$ and **** $p < 0.0001$.

RESULTS AND DISCUSSION

Objective 1: Study of the capacity of the synthetic cannabinoid WIN55,212-2 to reprogram monocyte differentiation and macrophage activation under inflammatory conditions

Inflammation can be defined as a vital defensive response initiated by the immune system after detecting invading pathogens and/or cellular damage, with the main aim of eliminating the cause of injury and restoring tissue homeostasis. Myeloid cells including DCs, monocytes and macrophages, are central to the development and regulation of inflammatory responses. They possess the ability to sense threats through the expression of PRRs, which enables them to orchestrate and amplify inflammatory responses effectively (206, 207). Under certain pathological conditions, the chronic or uncontrolled activation of myeloid cells significantly contributes to perpetuate inflammation and tissue damage, which leads to the main clinical manifestations associated with diseases such as autoimmune and allergic disorders, autoinflammatory syndromes or sepsis (207, 208).

Compelling experimental evidence validates the immunosuppressive potential of cannabinoids on myeloid cells (144, 145). However, further clarification of the molecular mechanisms underlying the multiple and heterogenous effects of the diverse family of cannabinoid ligands is still needed to advance the development of novel cannabinoid-based therapies (159, 162). Recent findings from our research group showed that the non-selective cannabinoid agonist WIN55,212-2 promotes anti-inflammatory immune responses by inducing metabolic reprogramming in fully differentiated DCs. WIN55,212-2 triggers functional autophagy while represses NF-κB, MAPK and mTOR signaling pathways in human DCs, resulting in a decreased glycolytic metabolism and enhanced OXPHOS, which is linked to the acquisition of tolerogenic properties such as the ability to prime functional $FOXP3^+$ Tregs both *in vitro* and *in vivo* (49). Additional potential therapeutic features of WIN55,212-2 on DCs also include the capacity to impair epicutaneous allergic sensitization in a preclinical model of peanut allergy (203). However, the potential capacity of WIN55,212-2 to modulate the differentiation of monocytes into hmoDCs or its anti-inflammatory properties on other myeloid cell subsets such as macrophages remains poorly understood. To fill this knowledge gap, in the first objective of this thesis, we sought to investigate the immunomodulatory properties of WIN55,212-2 during monocyte to DC differentiation and macrophage activation in different inflammatory settings.

1.1. Evaluation of the phenotypic and functional characteristics of human monocyte-derived dendritic cells differentiated in the presence of WIN55,212-2

A major feature of monocytes consists of their immune versatility due to the capacity to differentiate into DCs or macrophages (209, 210). Notably, the environmental signals that monocytes encounter during this process are closely linked to the immunogenicity of the resulting differentiated cells. For instance, stimuli such as dexamethasone (Dex), vitamin D3 (VitD3), rapamycin, allergoid-mannan conjugates or tumor-derived molecules shape monocyte differentiation towards the generation of tolerogenic DCs or

immunosuppressive macrophages (23, 25, 211-213). In contrast, exposure to whole heat-inactivated *Candida albicans* or β-glucans from its cell wall give raise to trained monocyte-derived macrophages (48, 214).

In order to explore the capacity of WIN55,212-2 to modulate the differentiation of monocytes, we first corroborated the expression of canonical CBRs in this leukocyte subset by qPCR and flow cytometry. As shown in **Figure R.1A**, human monocytes purified from peripheral blood of healthy donors showed detectable levels of CBRs at the mRNA level. Moreover, the protein expression of both CB1 and CB2 was confirmed by using the HU210-A488 fluorescent probe specifically validated to detect CB1 in biological systems (204) or an anti-CB2 antibody, respectively (**Figure R.1B**).

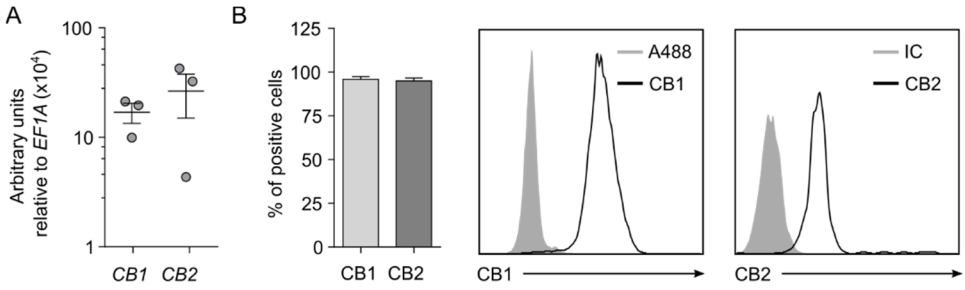

Figure R.1. Expression of CBRs in human monocytes. (**A**) Quantitative mRNA levels and (**B**) percentage of cells expressing protein levels of CB1 and CB2 (n=3). A488, Alexa Fluor 488; IC, isotype control. Values are shown as mean ± SEM.

Based on the protocols employed for the study of other immunomodulatory compounds (25, 213), we developed an experimental design in which human monocytes were differentiated into DCs following conventional protocols (hmoDCs) or in the presence WIN55,212-2 (WIN-hmoDCs) (see **Figure M. 1** in Materials and Methods section). After complete differentiation, cells were harvested and stimulated with the TLR4-ligand LPS for 18 h to evaluate their potential anti-inflammatory properties. A first screening of different doses of the cannabinoid was conducted to determine cytotoxicity and optimal dosing. The dose of 50 nM of WIN55,212-2 was selected to continue with further experiments as showed the most effective reduction of the LPS-induced proinflammatory cytokine TNFα, while preserved cell viability and anti-inflammatory IL-10 production (**Figure R.2**).

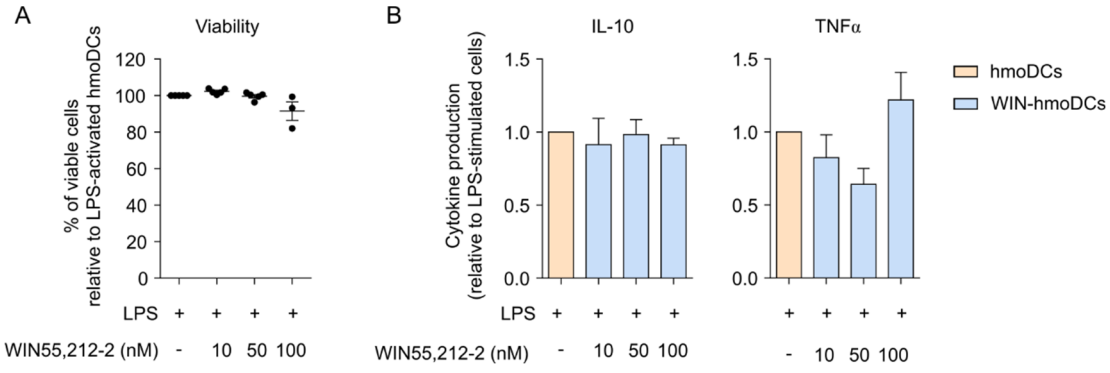

Figure R.2. Viability (**A**) and relative cytokine production (**B**) of LPS-activated conventional hmoDCs or hmoDCs differentiated from monocytes in the presence of the indicated doses of WIN55,212-2 (n=2-5). Values are shown as mean ± SEM.

A detailed analysis of the cytokine response to LPS between hmoDCs and WIN-hmoDCs showed that WIN-hmoDCs produced significantly reduced amounts of the inflammatory cytokines TNFα, IL-1β and IL-6 compared to conventionally differentiated hmoDCs, without changes in the levels of the paradigmatic anti-inflammatory cytokine IL-10 (**Figure R.3A**). Consequently, higher IL-10/TNFα, IL-10/IL-1β and IL-10/IL-6 ratios were found in WIN-hmoDCs, suggesting a potential anti-inflammatory profile (**Figure R.3B**). In fact, these changes resemble the cytokine responses of other tolerogenic hmoDCs generated by differentiation in the presence of immunomodulatory compounds such as allergoid mannan conjugates or tumor-derived molecules (23, 25). In addition, studies involving the use of phytocannabinoids during the differentiation of monocytes to DCs consistently support our findings, as hmoDCs differentiated in the presence of THC displayed reduced proinflammatory IL-12 production while intact IL-10 secretion (215).

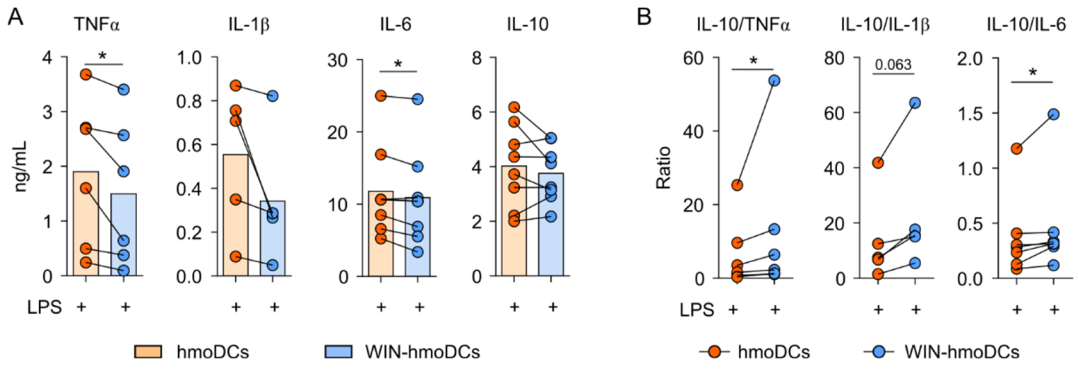

Figure R.3. Cytokine response of hmoDCs and WIN-hmoDCs to LPS. Cytokine concentrations (**A**) and ratios (**B**) of conventional hmoDCs and WIN-hmoDCs after 18 h of LPS stimulation (100 ng/mL) (n=5-8). Values are shown as mean ± SEM. Statistical significance was determined by Paired t test (A) or Wilcoxon test (B): * $p < 0.05$.

We also assessed the phenotype and maturation status of hmoDCs and WIN-hmoDCs by monitoring the expression of MHC-II molecules, costimulatory ligands and maturation markers using flow cytometry. No changes were observed in either HLA-DR expression or CD86 and CD83 presence in the surface of WIN-hmoDCs compared to conventional hmoDCs after the stimulation with LPS (**Figure R.4**). Our findings indicate that the differentiation in the presence of WIN55,212-2 does not alter LPS-induced phenotypic maturation of WIN-hmoDCs, which may preserve their capacity for antigen presentation and T cell activation.

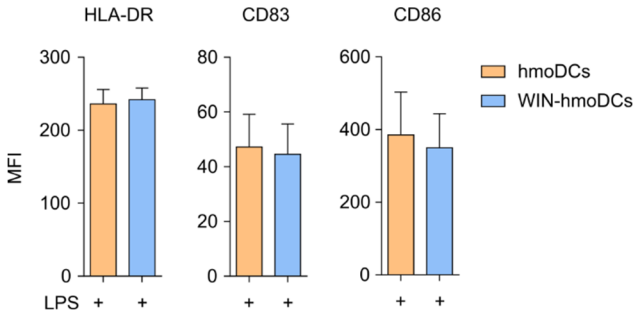

Figure R.4. Phenotypic analysis of LPS-activated hmoDCs and WIN-hmoDCs. Mean fluorescence intensity (MFI) of the indicated surface molecules expressed by LPS-activated conventional hmoDCs or WIN-hmoDCs (n=7). Values are shown as mean ± SEM.

Next, to investigate the capacity of WIN-hmoDCs to polarize T cell responses after exposure to the proinflammatory stimuli of LPS, allogeneic coculture experiments with naïve $CD4^+$ T cells were

performed (see **Figure M. 2** in Materials and Methods section). After 5 days of coculture, the cytokines released by hmoDC- or WIN-hmoDC- primed T cells were measured in cell-free supernatants by ELISA. Interestingly, LPS-stimulated WIN-hmoDCs generated T cells producing significantly lower amounts of IFNγ and IL-5 than LPS-activated hmoDCs, without significant differences observed in the production of IL-10 (**Figure R. 5A**). Accordingly, the IL-10/IL-5 and IL-10/IFNγ ratios were significantly higher in T cells generated by WIN-hmoDCs than conventional hmoDCs (**Figure R. 5B**). These changes in cytokine production indicate that WIN-hmoDCs can suppress Th1 and Th2 effector cells while preserving IL-10-producing T cells, which suggests the induction of Tregs (55, 61). In line with our findings, it has been previously shown that hmoDCs differentiated in the presence of the phytocannabinoid THC displayed reduced capacity to activate effector T cell responses and the production of IFNγ during coculture experiments. However, the potential contribution of the generation of Tregs during those experiments was not addressed (215).

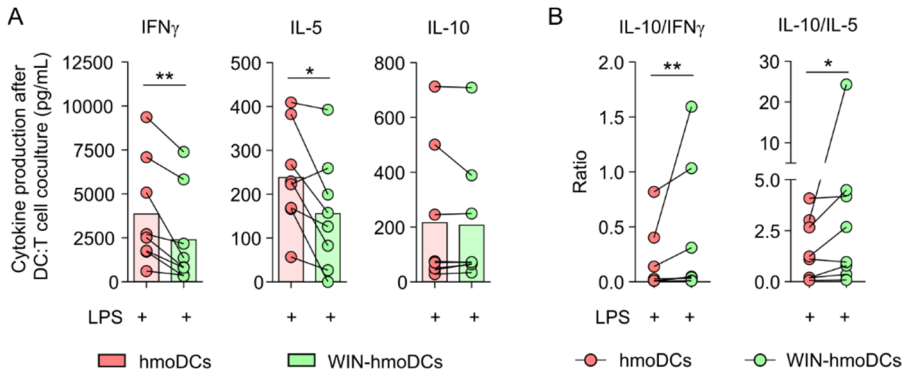

Figure R.5. Polarization of T cell responses by hmoDCs and WIN-hmoDCs. Cytokines (**A**) and ratios (**B**) produced by allogeneic naïve CD4⁺ T cells primed by LPS-stimulated hmoDCs or WIN-hmoDCs after 5 days of coculture (n=8). Statistical significance was determined by Paired t test (A) or Wilcoxon test (B). * $p < 0.05$, ** $p < 0.01$.

The induction and/or expansion of Tregs is crucial to preserve homeostasis in the context of immune-mediated and inflammatory diseases (60, 61). In order to corroborate the potential generation of Tregs in our coculture system, flow cytometric analysis was carried out after the 5 days cocultivation of hmoDCs or WIN-hmoDCs with naïve T cells. We observed that the proportion of FOXP3⁺ Tregs, identified as $CD4^+CD127^-CD25^{high}FOXP3^{high}$ cells, was significantly enhanced in cocultures primed by WIN-hmoDCs compared to the ones consisting of conventional hmoDCs (**Figure R.6**).

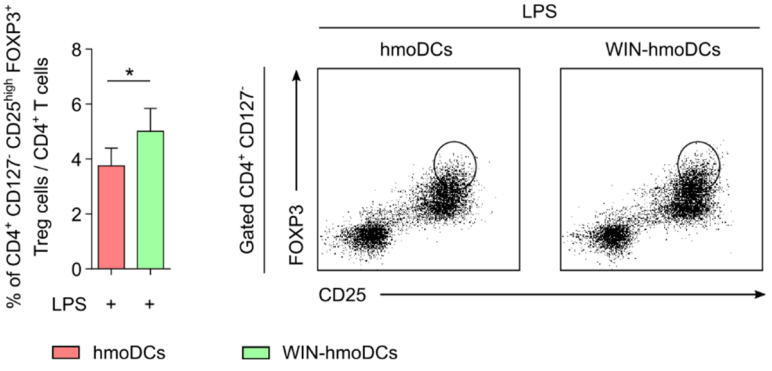

Figure R.6. Treg induction by hmoDCs and WIN-hmoDCs. Percentage (left), and representative dot plots (right) of induced $CD4^+CD25^{high}CD127^-FOXP3^{high}$ Tregs by allogeneic LPS-stimulated hmoDCs or WIN-hmoDCs (n=7). Values are shown as mean ± SEM. Statistical significance was determined by Paired t test: * $p < 0.05$.

In summary, our findings confirm that WIN-hmoDCs display tolerogenic features in response to LPS, characterized by a reduced proinflammatory cytokine production, sustained IL-10 secretion and enhanced ability to polarize regulatory T cell responses. Previous reports have already described the anti-inflammatory mechanisms of WIN55,212-2 in human DCs through the ability to induce Tregs (49, 203). However, our current work expands the knowledge on how WIN55,212-2 could promote Tregs not only by directly acting on fully differentiated DCs, but also by imprinting tolerogenic properties during monocyte differentiation.

1.2. Assessment of the immunomodulatory capacity of WIN55,212-2 in the activation of proinflammatory M1 macrophages

Macrophages are major contributors to inflammation due to their capacity to secrete large amounts of cytokines and chemokines that amplify innate immune responses. The phenotypical and functional properties that macrophages acquire during inflammatory conditions are termed as classical M1 activation, which is usually reproduced *in vitro* by the combined stimulation of macrophages with LPS and IFNγ (71, 73). Therefore, we sought to evaluate the potential anti-inflammatory effects of WIN55,212-2 in the M1 macrophage activation profile. For that, we differentiated human macrophages from the THP-1 monocytic cell line (THP-1 MΦs, see **Figure M.3** in Materials and Methods section) and stimulated them with the combination of LPS and IFNγ for 18h in the absence or presence of WIN55,212-2. First, we evaluated the potential cytotoxicity of different doses of the synthetic cannabinoid as well as their capacity to impair inflammatory signaling pathways. The analysis of cell death by flow cytometry showed that the viability of THP-1 MΦs was not altered even at the highest assayed dose of WIN55,212-2 (**Figure R.7A**). Additionally, by using THP-1 XBlue cell lines, which are modified to stably integrate a NF-kB/AP-1 reporter construct, we were able to demonstrate a dose-dependent inhibition of NF-kB/AP-1 activity in THP-1 MΦs treated with LPS/ IFNγ in the presence increasing doses of the cannabinoid (**Figure R.7B**).

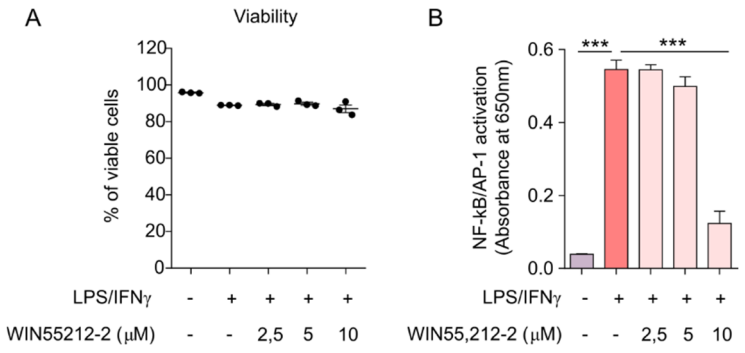

Figure R.7. Effects of WIN55,212-2 on THP-1 MΦs viability and inflammatory signaling. Cell viability (**A**) and NF-kB/AP-1 activation (**B**) in THP-1 MΦs after 18h of stimulation with medium, LPS/IFNγ (100 ng/mL and 50 ng/mL, respectively) or LPS/IFNγ plus the indicated doses of WIN55,212-2 (n=3-6). Values are shown as mean ± SEM. Statistical significance was determined One-way ANOVA followed by Dunnett's multiple comparisons correction: ** $p < 0.01$, *** $p < 0.001$.

To further explore the immunosuppressive potential of WIN55,212-2, we evaluated the expression of M1 markers and proinflammatory cytokines by THP-1 MΦs stimulated with LPS/ IFNγ in the presence or absence of the cannabinoid. As shown in **Figure R.8**, stimulated THP-1 MΦs in the presence of WIN55,212-2 displayed a clear impairment of the expression of M1 activation markers such as *CCR7*, *TNF* and *CD80*, which was associated with a dose-dependent inhibition of TNFα and IL-6 production. These findings, together with the capacity of WIN55,212-2 to impair NF-kB/AP-1 activation, indicated a potent anti-inflammatory effect, which was consistent with previous studies investigating the therapeutic efficacy of this cannabinoid in hmoDCs, TLR3/4-transfected HEK293 cells stimulated with LPS, and murine macrophages activated with oxidized-LDL (49, 216, 217).

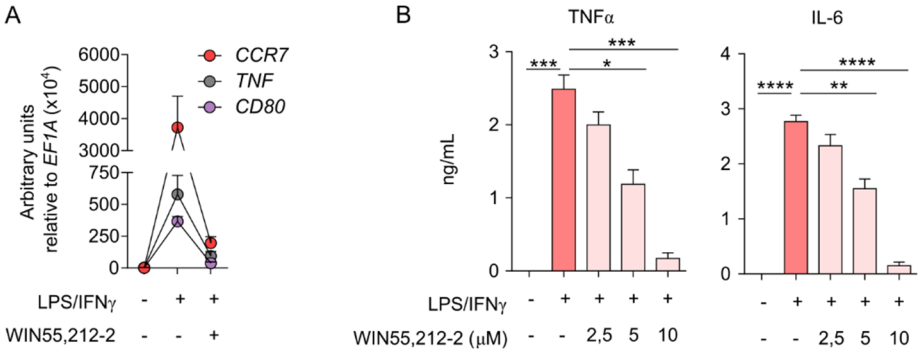

Figure R.8. Modulation of M1 expression markers and cytokine production by WIN55,212-2 in THP-1 MΦs. (**A**) Gene expression levels of the indicated inflammatory markers and (**B**) cytokine production after 18h of stimulation with medium, LPS/IFNγ (100 ng/mL and 50 ng/mL, respectively) or LPS/IFNγ plus the indicated doses of WIN55,212-2 (n=5-6). Values are shown as mean ± SEM. Statistical significance was determined One-way ANOVA followed by Dunnett's multiple comparisons correction: * $p < 0.05$, ** $p < 0.01$, *** $p < 0.001$ and **** $p < 0.001$.

To validate our findings, we differentiated human monocytes purified from peripheral blood with GM-CSF to generate primary human monocyte-derived macrophages (see **Figure M.4** in Materials and Methods section). We termed these macrophages as GM-MΦs according to Murray et al. (74) and evaluated their expression of CBRs at the mRNA and protein level. RT-PCR and flow cytometric analysis validated the expression of both CB1 and CB2 receptors in GM-MΦs (**Figure R.9**), consistently to previous reports in other subsets of human macrophages (218).

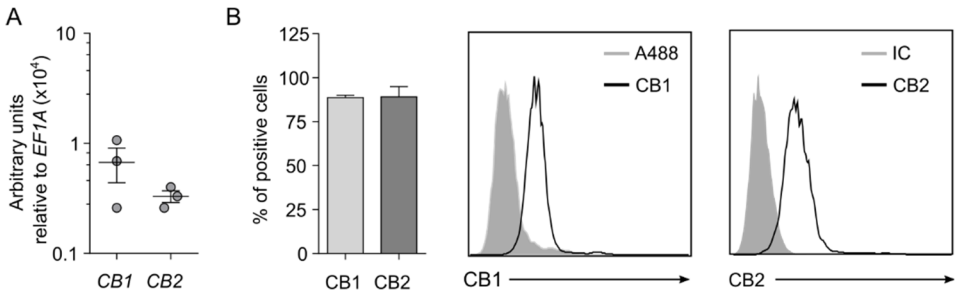

Figure R.9. Expression of CBRs in GM-MΦs. (**A**) Quantitative mRNA levels and (**B**) percentage of cells expressing protein levels of CB1 and CB2 (n=3). Values are shown as mean ± SEM.

Primary macrophages differentiated in the presence of GM-CSF (GM-MΦs) exert a proinflammatory prone profile (M1-like) and respond to TLR ligands with the production of large amounts of inflammatory mediators (219, 220). Therefore, we employed them as a suitable model to study the immunosuppressive potential of WIN55,212-2. For that, we stimulated GM-MΦs with LPS/IFNγ in the presence or absence of increasing doses of the cannabinoid and evaluated its capacity to dampen inflammatory responses. First, we assessed potential cytotoxicity and the expression of activation markers by flow cytometry. Interestingly, we observed that LPS/IFNγ promoted a dramatic drop in GM-MΦ viability, which was dose-dependently recovered by the coadministration with increasing doses of WIN55,212-2, suggesting that the cannabinoid prevents inflammatory cell death (**Figure R.10A**). Supporting this idea, viability changes were associated with the inhibition of the LPS/IFNγ-induced upregulation of the surface expression of MHC-II molecules and activation markers such as HLA-DR and CD83 in a dose-dependent manner (**Figure R.10B**). CD83 is usually considered as a DC maturation marker, however, upon inflammatory stimulation transient membrane expression of CD83 also takes place in macrophages (221). Similarly, the enhanced expression of HLA-DR is widely used as an activation marker of M1 polarized macrophages, associated to its upregulated antigen presenting functions (71). Taken together, our findings indicate that LPS/IFNγ activate potent inflammatory cell death pathways in GM-MΦs, which are prevented by the simultaneous administration of WIN55,212-2. Of note, we did not observe those differences in viability during our previous experiments in THP-1 MΦs. These differential observations between THP-1 MΦs and GM-MΦs after stimulation with LPS plus IFNγ might well be explained by the fact that GM-CSF has been described as driver of macrophage pyroptosis (222), which could act synergically with the reported effects of IFNγ to prime macrophage death (223).

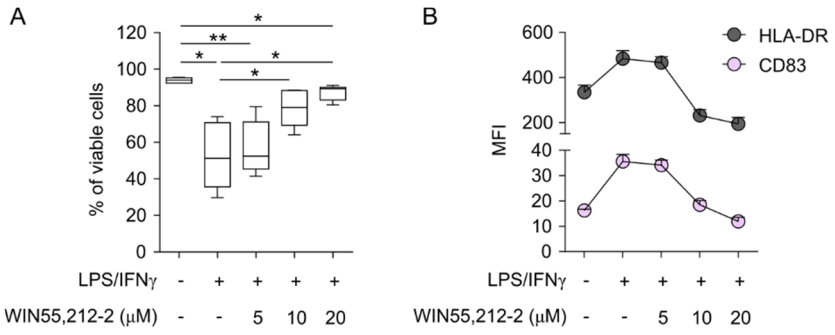

Figure R.10. WIN55,212-2 rescues viability and impairs surface activation marker expression in activated GM-MΦs. (**A**) Percentage of viable cells and (**B**) mean fluorescence intensity (MFI) of the indicated markers after GM-MFs stimulation with medium, LPS/IFNγ (100 ng/mL and 50 ng/mL) or LPS/IFNγ plus the indicated doses of WIN55,212-2 (n=6). Values are shown as mean ± SEM. Statistical significance was determined One-way ANOVA followed by Tukey's multiple comparisons correction: * $p < 0.05$, ** $p < 0.01$.

A further characterization of the immunosuppressive effects of WIN55,212-2 in GM-MΦs stimulated with LPS/IFNγ was performed by the analysis of their cytokine production. At the mRNA level, we observed a clear impairment of *TNF*, *IL1B* and *IL6* induction 4 h after the stimulation with LPS/IFNγ in the presence of WIN55,212-2 (**Figure R.11A**). Moreover, the treatment with the synthetic cannabinoid reduced proinflammatory TNFα, IL-1β and IL-6 production after 18 h of stimulation of LPS/IFNγ in a dose-dependent manner (**Figure R.11B**). Similar findings were also observed for IL-10 production,

indicating that WIN55,212-2 promotes the shutdown of inflammatory paths without shifting towards IL-10-producing M2 phenotypes, at least under these assayed conditions.

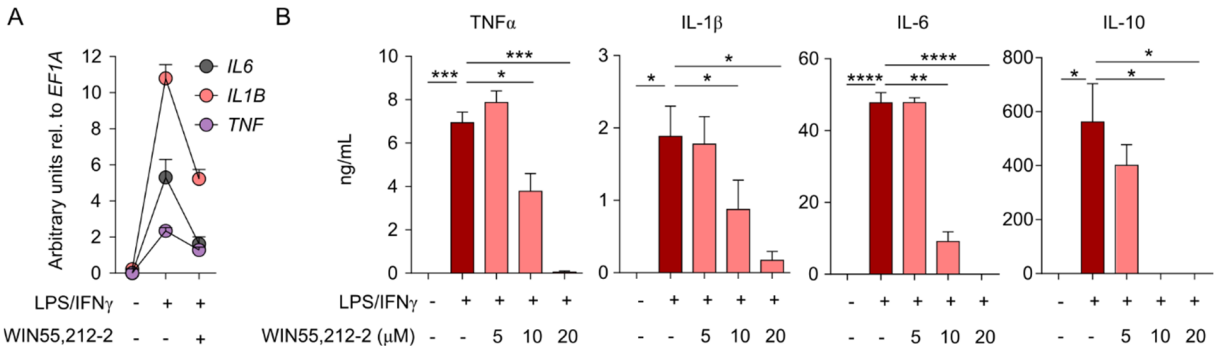

Figure R.11. WIN55,212-2 impairs cytokine production in activated GM-MΦs. (**A**) mRNA expression levels of the indicated cytokines after 4h stimulation of GM-MΦs with medium, LPS/IFNγ (100 ng/mL and 50 ng/mL) or LPS/IFNγ plus WIN55,212-2 (20 mM) (n=5). (**B**) Cytokine production after 18h stimulation with the indicated treatments (n=6). Values are shown as mean ± SEM. Statistical significance was determined One-way ANOVA followed by Dunnett's multiple comparisons correction: * $p < 0.05$, ** $p < 0.01$, *** $p < 0.001$, **** $p < 0.0001$.

Concomitant loss of cell viability and secretion of large amounts of IL-1β are hallmark features of inflammasome activation and macrophage pyroptotic cell death. As shown in **Figure R.12A**, we realized that our data displayed a significant inverse correlation between IL-1β production and macrophage viability in GM-MΦs stimulated under the different assayed conditions. This idea prompted us to investigate whether WIN55,212-2 could interfere with inflammasome signaling. With this purpose, we quantified the gene expression levels of inflammasome components such as nucleotide-binding domain leucine-rich–containing family pyrin domain–containing-3 (*NLRP3*) and caspase 1 (*CASP1*), and the pore-forming protein gasdermin D (*GSDMD*) in our model. Notably, the expression of the three assayed molecules was markedly upregulated by LPS/IFNγ stimulation, but significantly reduced when GM-MΦs were activated in the presence of WIN55,212-2. (**Figure R.12B**). Altogether, these findings indicate a potential involvement of WIN55,212-2 in the impairment of inflammasome signaling and pyroptotic cell death, which is congruent with studies using phytocannabinoids like THC or CBD (224).

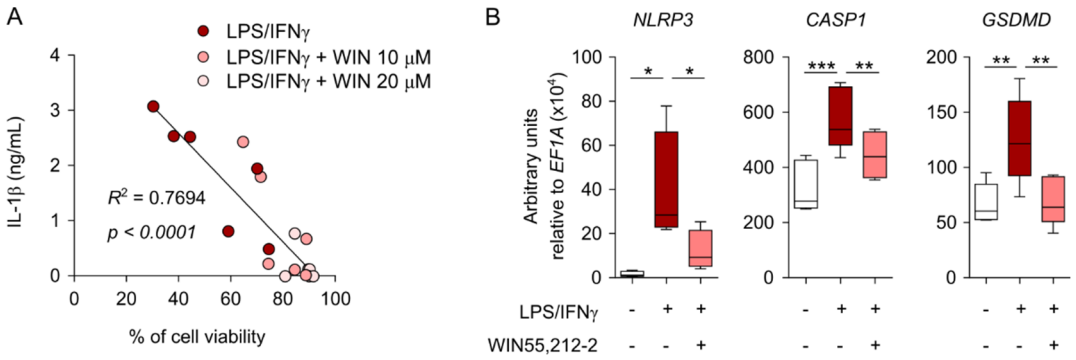

Figure R.12. WIN55,212-2 impairs inflammasome activation in classically activated GM-MΦs. (**A)** Correlation between IL-1β production and GM-MΦ viability after 18 h stimulation with LPS/IFNγ (100 ng/mL and 50 ng/mL) and LPS/IFNγ plus the indicated doses of WIN55,212-2 (n=6). (**B**) mRNA expression levels of the indicated genes after 4h stimulation of GM-MΦs with medium, LPS/IFNγ or LPS/IFNγ plus WIN55,212-2 (20 mM) (n=5). Values are shown as mean ± SEM. Statistical significance was determined by linear regression (A) or One-way ANOVA followed by Dunnett's multiple comparisons correction (B): * $p < 0.05$, ** $p < 0.01$, *** $p < 0.001$.

Collectively, our findings corroborate that WIN55,212-2 exerts immunosuppressive properties in M1-polarized human macrophages by impairing NF-κB/AP-1 activation and inflammasome-dependent pyroptosis, which were associated with a significant inhibition of macrophage potential antigen-presenting capabilities and proinflammatory cytokine secretion.

1.3. Elucidation of the molecular mechanisms by which WIN55,212-2 impairs inflammatory responses in human macrophages

In recent years, it has become clear that the metabolic pathways that immune cells commit to are crucial to the acquisition of specific functional features, in a novel concept defined as immunometabolism (75, 77). Accordingly, to identify the molecular mechanisms by which WIN55,212-2 exerts its above-described immunosuppressive effects, we sought to characterize the potential alterations induced by the cannabinoid on the major metabolic pathways linked to the acquisition of inflammatory phenotypes in human macrophages. Compelling experimental evidence associates macrophage commitment to Warburg metabolism and impairment of OXPHOS to an inflammatory M1 profile (77, 79). Our previous work demonstrated that WIN55,212-2 promotes tolerance in human DCs through mechanisms depending on the induction of autophagy and the inhibition of mammalian target of rapamycin complex 1 (mTORC1) signaling, which resulted in a metabolic shift from glycolysis and lactic acid fermentation towards a mitochondrial-based metabolism (49). Therefore, we sought to evaluate the potential involvement of these signaling and metabolic pathways in the effects observed for the synthetic cannabinoid in M1 activated human macrophages.

In this set of experiments, the activation of GM-MΦs was performed with LPS at a lower dose (10 ng/mL) in order to avoid the potential bias due to the activation of macrophage inflammatory cell death pathways described previously. Of note, we first confirmed that the stimulation of GM-MΦs with LPS (10 ng/mL) mimicked the previous LPS/IFNγ activation, by significantly inducing the production of pro-inflammatory cytokines without affecting cell viability, as well as corroborated the capacity of WIN55,212-2 to impair inflammatory cytokine production in this experimental setting (**Figure R.13**).

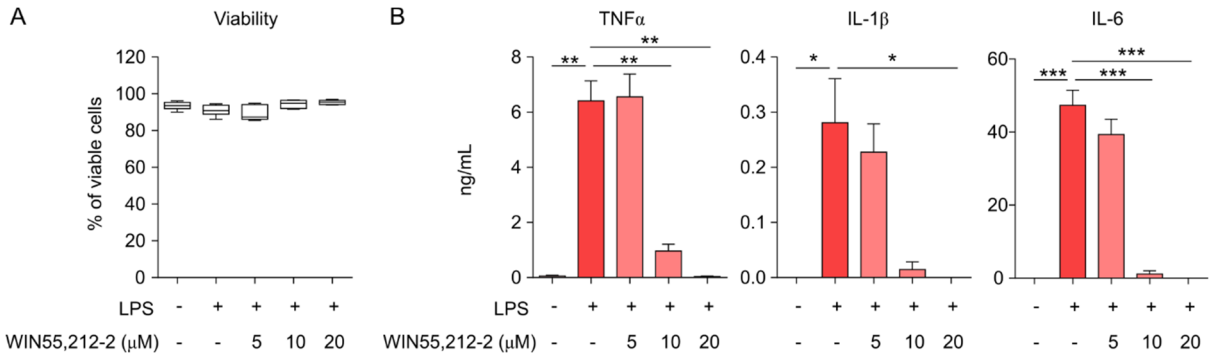

Figure R.13. Stimulation with low dose LPS induces inflammatory activation of GM-MΦs without affecting cell viability. Percentage of viable cells (**A**) and cytokine production (**B**) after stimulation of GM-MΦs with medium, LPS (10 ng/mL) or LPS plus the indicated doses of WIN55,212-2 (n=6). Values are shown as mean ± SEM. Statistical significance was determined by One-way ANOVA followed by Dunnett's multiple comparisons correction: * $p < 0.05$, ** $p < 0.01$, *** $p < 0.001$.

Once optimized the model, we analyzed the mTORC1 signaling pathway as key regulator of anabolic metabolism. The phosphorylation of mTORC1's upstream and downstream signaling molecules, Akt and p70S6K, were employed as proxies of the activation of the route.

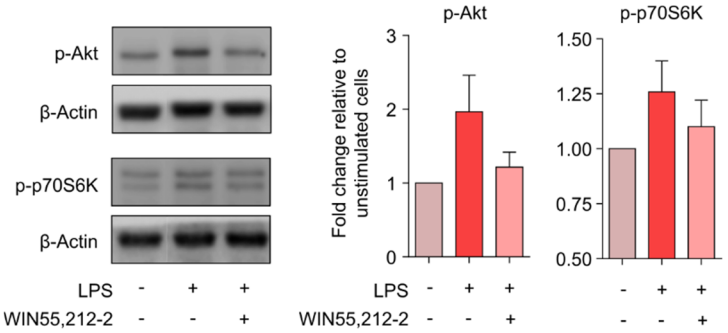

Figure R.14. Modulation of LPS-induced mTORC1 signaling by WIN55,212-2. Representative western blots (left) and quantification (right) of GM-MΦs stimulated with medium, LPS (10 ng/mL) or LPS plus WIN55,212-2 (10 μM). The graph shows combined results from 30 and 60 min of stimulation (n=6 independent experiments with 4 donors). Values are shown as mean ± SEM.

In line with our previous findings in hmoDCs (49), we observed that WIN55,212-2 impaired the LPS-induced phosphorylation of both Akt and p70S6K, suggesting the inhibition of mTORC1 signaling and the potential alteration of macrophage metabolic adaptations after TLR engagement (**Figure R.14**). A major hallmark feature of proinflammatory macrophage activation is the upregulation of glycolysis. M1 macrophages are characterized by an enhanced Warburg metabolism, meaning that they have strong commitment to the glycolytic and lactic acid fermentation paths as a source of energy, even in aerobic conditions (79, 80). Therefore, we investigated whether WIN55,212-2 interferes with the Warburg metabolism of proinflammatory macrophages. Our data showed that LPS stimulation significantly increased the consumption of glucose and the production of lactate, confirming a metabolic reprogramming towards aerobic glycolysis. Conversely, the stimulation of GM-MΦs in the presence of the WIN55,212-2 significantly impaired the LPS-induced increments in glucose consumption and lactate release, suggesting an inhibitory role on glycolytic metabolism (**Figure R.15**).

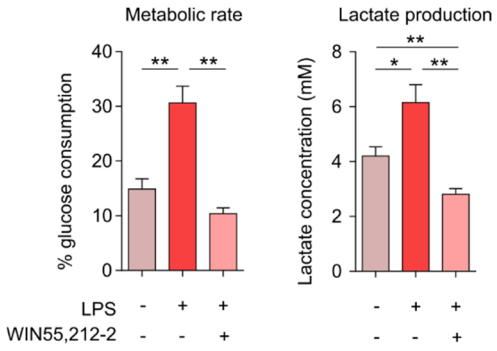

Figure R.15. WIN55,212-2 regulates glycolytic metabolism in proinflammatory macrophages. Metabolic rate (percentage of glucose consumed by the cells) and lactate concentration, measured from cell-free supernatants of GM-MΦs stimulated with medium, LPS (10 ng/mL) or LPS plus WIN55,212-2 (10 μM) (n=6).Values are shown as mean ± SEM. Statistical significance was determined by One-way ANOVA followed by Dunnett's multiple comparisons correction: * $p < 0.05$, ** $p < 0.01$.

To further verify these findings, we carried out real-time metabolic studies of GM-MΦs stimulated with LPS or LPS plus WIN55,212-2 using a Seahorse bioanalyzer. We monitored the glycolytic proton efflux rate (glycoPER) dynamics to measure glycolysis at basal conditions (basal glycolysis) and after the inhibition of the electron transport chain (compensatory glycolysis). Our results demonstrated that LPS-stimulated GM-MΦs had a significantly higher commitment to both basal and compensatory glycolysis compared to GM-MΦs activated with LPS+WIN55,212-2 (**Figure R.16**), confirming the capacity of WIN55,212-2 to reduce the LPS-induced glycolytic metabolism in human macrophages.

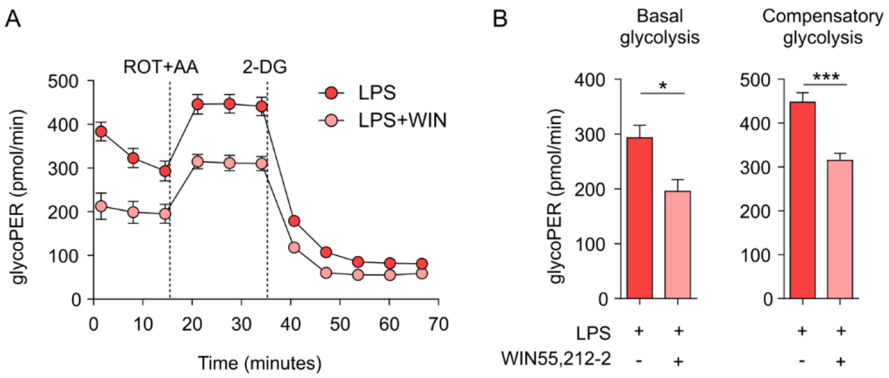

Figure R.16. Real time metabolic analysis of activated GM-MΦs. (**A**) Glycolytic Proton Efflux Rate (glycoPER) dynamics after 18h stimulation with LPS (10 ng/mL) or LPS plus WIN55,212-2 (10 μM) at basal conditions and after sequential addition of rotenone plus antimycin A (ROT+AA) and 2-deoxyglucose (2-DG). (**B**) Graphs representing basal and compensatory glycolysis of the indicated conditions (n=6 of two independent experiments). Values are shown as mean ± SEM. Statistical significance was determined by Unpaired t test: * $p < 0.05$ and *** $p < 0.001$.

Next, we investigated whether the effects of WIN55,212-2 on the modulation of aerobic glycolysis in TLR-activated GM-MΦs was associated with their functional features. We observed that the gene expression of the inflammatory mediators *TNF*, *IL1B*, *IL6* and *IL8* was simultaneously upregulated to the expression of key glycolysis-related enzymes such as hexokinase 2 (*HK2*), phosphofructokinase B 3 (*PFKB3*), lactate dehydrogenase A (*LDHA*) and hypoxia-inducible factor 1α (*HIF1A*) in LPS-stimulated GM-MΦs. Interestingly, all these genes were similarly downregulated by the coadministration of LPS with the synthetic cannabinoid, suggesting a potential link (**Figure R.17A**). Consistent with this idea, He Q. et al. reported that the inhibition of glycolysis using 2-DG mimicked the anti-inflammatory effects of WIN55,212-2 in M1-activated murine alveolar macrophages (225). In our data, the production of TNFα, IL-1β and IL-6 by GM-MΦs stimulated with LPS or LPS+WIN55,212-2, directly correlated with the amount of glucose consumed by those cells (**Figure R.17B**), indicating that the inhibition of glycolysis and glucose uptake might well be connected to the immunosuppressive effects of WIN55,212-2 in human macrophages as well.

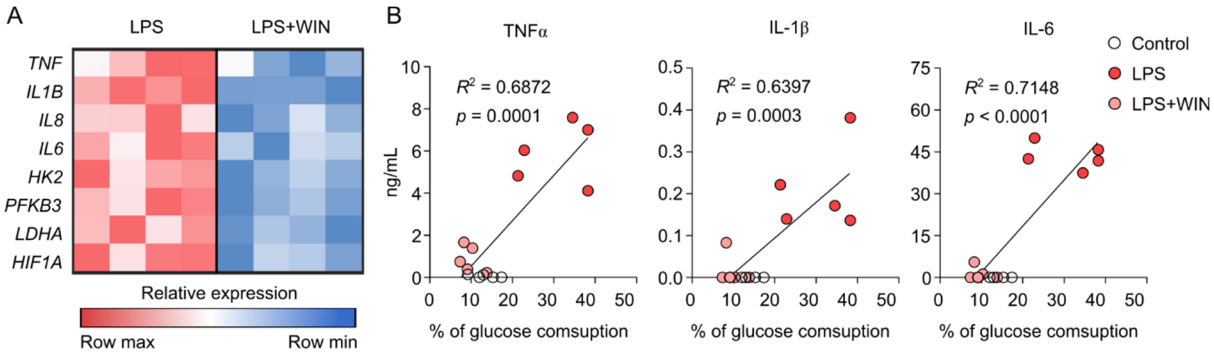

Figure R.17. Interplay between metabolic and inflammatory in GM-MΦs. (**A**) Heat map showing the expression of pro-inflammatory cytokine and glycolysis-related genes in GM-MΦs stimulated with LPS (10 ng/mL) or LPS+WIN55,212-2 (10 μM) (LPS+WIN) during 4 h (n=4). (**B**) Correlation between TNFα, IL-1β or IL-6 with the percentage of glucose consumed by GM-MΦs stimulated with medium (Control), LPS or LPS+WIN (n=5). Statistical significance was determined by linear regression analysis (B).

In recent years, some of the mechanisms by which the induction of aerobic glycolysis after TLR-engagement favor inflammatory functional features in macrophages have been revealed. The glycolytic path may serve as a source of metabolic substrates for the induction of inflammatory gene expression through epigenetic histone modifications (226, 227). For instance, Lauterbach et al. demonstrated that glycolysis supports early histone acetylation in distinct LPS-inducible gene sets through the generation of acetyl-CoA from glucose (227). In this context, we sought to investigate the involvement of chromatin modifications in the immunosuppressive potential of WIN55,212-2. With this purpose, we assessed the chromatin status near the gene promoters of the inflammatory mediators *TNF*, *IL1B* and *IL6*, in stimulated GM-MΦs by quantifying the presence of the activation histone mark, H3K27ac. We observed that LPS significantly enhanced the acetylation of H3K27 within *IL1B* and *IL6* gene promoters, while a similar non-significant tendency was reported in the *TNF* promoter region, confirming the contribution of the metabolic-epigenetic axis to the development of inflammatory features in activated GM-MΦs. Notably, these histone acetylation changes were significantly reduced when macrophages were stimulated with LPS in the presence of the cannabinoid (**Figure R.18**), demonstrating the capacity of WIN55,212-2 to interfere in the metabolic and epigenetic reprogramming induced by LPS in human macrophages.

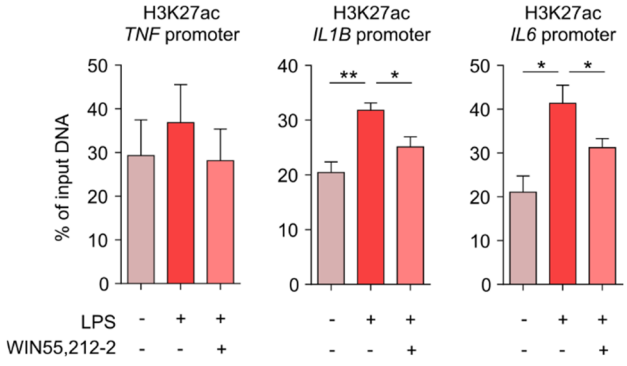

Figure R.18. WIN55,212-2 inhibits epigenetic modifications in inflammatory gene promotes of activated GM-MΦs. Analysis of H3K27ac histone modifications at the promoter sites of the indicated genes in GM-MΦs stimulated with LPS (10 ng/mL) or LPS+WIN55,212-2 (10 μM) (LPS+WIN) during 4h (n=5). All values are shown as ± SEM. Statistical significance was determined by One-way ANOVA followed by Holm-Sidak's multiple comparisons correction: * $p < 0.05$, ** $p < 0.01$.

Collectively, our data provide novel insights into the anti-inflammatory mechanisms of WIN55,212-2 in human macrophages. The treatment with the synthetic cannabinoid inhibits the LPS-induced mTORC1 signaling, Warburg metabolism and epigenetic modifications, substantially contributing to its functional immunosuppressive effects. In this sense, the reduced cytokine production of GM-MΦs stimulated with LPS in the presence of WIN55,212-2 may result from the combined capacity of the cannabinoid to impair NF-κB activation and the LPS-induced metabolic and epigenetic reprogramming. Similarly, the ability of WIN55,212-2 to recue macrophages from inflammatory cell death may be associated to the inhibition of mTORC1 signaling and glycolysis, as previous studies have linked them to inflammasome activation, gasdermin oligomerization and pyroptosis (228-230).

1.4. Assessment of the *ex vivo* and *in vivo* anti-inflammatory properties of WIN55,212-2

Systemic inflammatory diseases with unrestrained activation of immune responses and dysregulated release of proinflammatory mediators (cytokine storm), are life-threatening conditions that remain poorly

managed by current treatments (231). For instance, during endotoxin shock, the cooperative activation of inflammatory cytokine signaling and cell death pathways leads to severe tissue damage and multi-organ failure which may be eventually lethal (232).

Our previous work demonstrated that WIN55,212-2 protects mice during sepsis by increasing survival and promoting the generation of Tregs (49). However, the potential implications of the above-described effects on monocytes and macrophages remained unknown. Therefore, we proposed to investigate these novel immunomodulatory mechanisms of WIN55,212-2 in a preclinical model of LPS-induced sepsis. Mice were intraperitoneally injected with PBS, WIN55,212-2, or a lethal dose of LPS alone or in the presence of WIN55,212-2. After 12 h of treatment, we collected mice serum and quantified the levels of inflammatory and tissue injury markers (**Figure R.19A**). We observed that the serum levels of IL-1β were enhanced by the intraperitoneal administration of LPS, but significantly impaired when mice were administered with LPS in the presence of WIN55,212-2 (**Figure R.19B**). These findings indicate the potential capacity of WIN55,212-2 to inhibit inflammasome activation *in vivo*, which, during sepsis, is associated with the aggravation of the disease and worsening of prognosis. In fact, suppression of inflammasome induction and pyroptotic cell death protects mice from septic myocardial dysfunction (233). Moreover, the blockage of IL-1R was reported to play a protective role in clinical trials of septic patients, specifically in the ones developing macrophage activation syndrome (MAS) (234). A hallmark feature of MAS development during sepsis is hepatobiliary dysfunction, which is associated with significantly higher risk of death (235). To further confirm whether the protective properties of WIN55,212-2 depend on inflammasome activation and the prevention of tissue injury, we analyzed the expression of cardiac and hepatic damage markers in the serum of the mice. As shown in **Figure R.19C**, WIN55,212-2 reduced the LPS-increased expression of the myocardial and hepatic injury markers LDH and bilirubin, respectively. Our data corroborates the immunosuppressive efficacy of the cannabinoid in a model of acute uncontrolled inflammation, by mechanisms potentially associated with the inhibition of inflammasome activation.

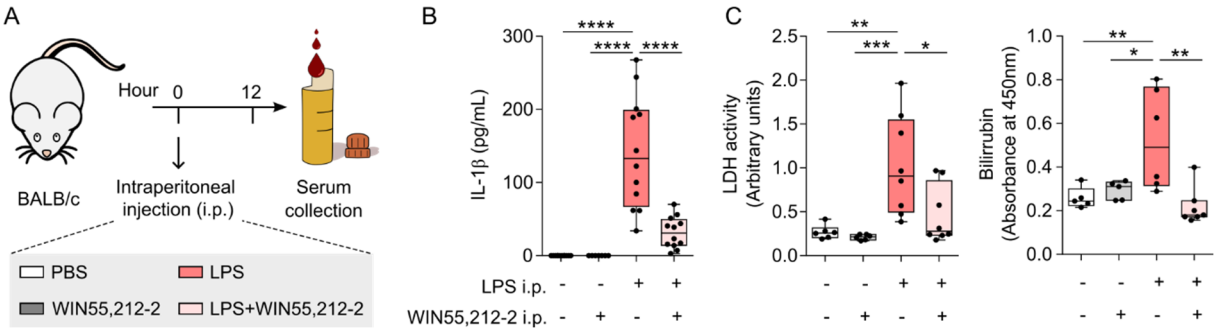

Figure R.19. WIN55,212-2 exerts i*n vivo* anti-inflammatory features and impairs inflammasome activation during sepsis. (**A**) Schematic representation of the *in vivo* model of LPS-induced sepsis. (**B**) Serum IL-1β levels after 12h of intraperitoneal (i.p.) administration of PBS (Control), WIN55,212-2 (5 mg/kg), LPS (20 mg/kg) or LPS plus WIN55,212-2 (n=7-12). (**C**) Assessment of the tissue injury parameters LDH and bilirubin in the serum of mice treated with the indicated conditions (n=5-8). All values are shown as ± SEM. Statistical significance was determined by One-way ANOVA followed by Holm-Sidak's multiple comparisons correction: * $p < 0.05$, ** $p < 0.01$, *** $p < 0.001$, **** $p < 0.0001$.

Peritoneal macrophages (PMΦs) constitute one of the main immune cell populations in the peritoneal cavity, providing a first line defense against severe pathologies such as abdominal sepsis. To evaluate the potential contribution of the effects of WIN55,212-2 in PMΦs to the therapeutic efficacy exerted in our septic shock model, we isolated PMΦs from naïve mice and stimulated them *ex vivo* with medium (control), LPS or LPS plus WIN55,212-2. We observed that WIN55,212-2 inhibited the production of the inflammatory mediators TNFα and IL-6 by LPS-stimulated PMΦs in a dose-dependent manner (**Figure R.20A**). Moreover, in line with our *in vitro* data, stimulation with LPS in the presence of WIN55,212-2 significantly impaired the LPS-induced glucose consumption and lactate production, suggesting that the cannabinoid inhibits the metabolic rewiring imprinted by LPS in *ex vivo* stimulated PMΦs (**Figure R.20B**).

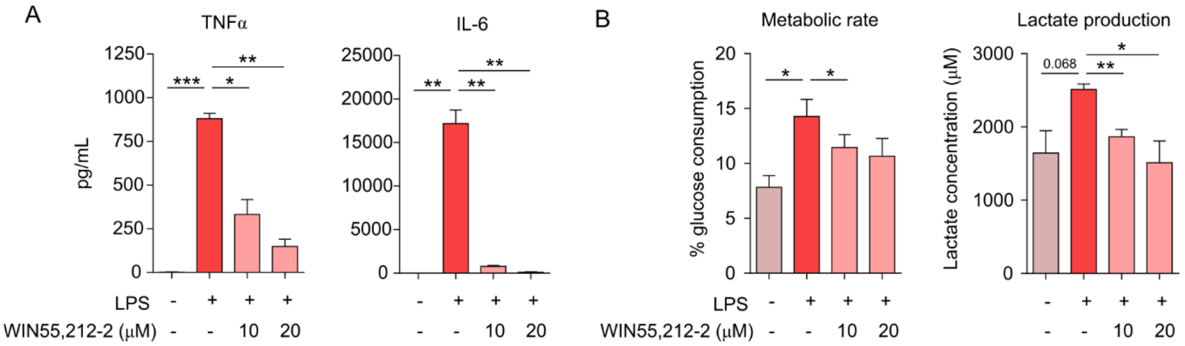

Figure R.20. WIN55,212-2 controls inflammatory and metabolic features of *ex vivo* stimulated PMΦs. (**A**) Cytokine production by ex vivo stimulated PMΦs with medium, LPS (10 ng/mL) or LPS plus the indicated doses of WIN55,212-2 (n=4). (**B**) Percentage of glucose consumption and lactate concentration measured from cell-free supernatants of PMΦs treated with the indicated stimuli (n=6). All values are shown as ± SEM. Statistical significance was determined by One-way ANOVA followed by Dunnett's multiple comparisons correction: * $p < 0.05$, ** $p < 0.01$, *** $p < 0.001$.

Real time metabolic experiments were conducted to thoroughly validate these findings. The analysis of glycoPER dynamics confirmed a significantly reduced commitment to both basal and compensatory glycolysis in LPS+WIN-stimulated PMΦs compared to LPS-stimulated PMΦs (**Figure R.21**).

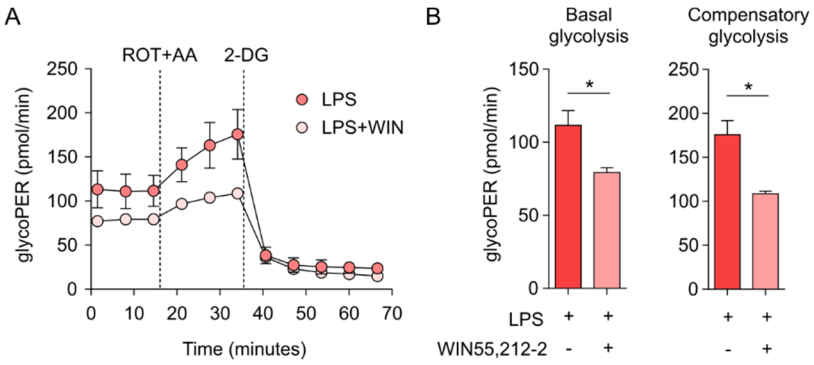

Figure R.21. WIN55,212-2 inhibits glycolysis in *ex vivo* activated PMΦs (**A**) Monitorization of glycolytic Proton Efflux Rate (glycoPER) of PMΦs after 18h stimulation with LPS (10 ng/mL) or LPS plus WIN55,212-2 (10 μM) at basal conditions and after sequential addition of rotenone plus antimycin A (ROT+AA) and 2-deoxyglucose (2-DG). (**B**) Graphs representing basal as well as compensatory glycolysis of the indicated conditions (n=3). All values are shown as ± SEM. Statistical significance was determined by Unpaired t-test: * $p < 0.05$.

The *in vivo* therapeutic potential of WIN55,212-2 has been addressed in many preclinical models of inflammatory diseases such as multiple sclerosis, neuroinflammation, colitis or atherosclerosis (236-239). However, little is known about the mechanisms that mediate those effects in specific immune cell populations. In recent reports, we have uncovered the immunoregulatory capacity of WIN55,212-2 on DCs, with potential implications during sepsis and food allergy (49, 203). Our current results provide novel evidence on the anti-inflammatory properties of WIN55,212-2 in a murine model of LPS-induced sepsis, by mechanisms related to the inhibition of inflammasome signaling and macrophage metabolic reprogramming. These data are consistent with the previous reported capacity of WIN55,212-2 to protect from acute lung injury through the modulation of macrophage activation in mice (225, 240). Together, our findings might well contribute to pave the way for the development of alternative cannabinoid-based therapies for inflammatory diseases.

Objective 2: Assessment of the capacity of WIN55,212-2 to regulate human bronchial epithelial integrity and function

Asthma is one of the most prevalent chronic inflammatory diseases of the airways with a high worldwide socioeconomic burden. Novel preventive and therapeutic strategies are needed to overcome challenges in asthma management involving the disease control of severe asthmatics, side-effects of conventional treatments, phenotyping difficulties and cost-efficient limitations of biological therapies (97, 139, 140). At this regard, the airway epithelium represents the first line defensive barrier against airborne insults and dysregulation of its homeostatic functions have been associated with the onset and progression of chronic airway diseases (83, 84, 88). Recurrent respiratory viral infections and type 2-mediated allergic sensitization significantly contribute to epithelial barrier alterations in asthma and constitute two major risk factors for disease development and worsening (94, 133). In this context, the therapeutic efficacy of cannabinoids as immunosuppressive or bronchodilator drugs has been addressed in many preclinical studies of asthma (144). However, our understanding of their potential capacity to modulate airway epithelial barrier function needs to be further investigated. In previous work from our research group, we uncovered that the synthetic cannabinoid WIN55,212-2 restored the airway epithelial barrier disruption induced by RV infection (177). Nonetheless, whether this synthetic cannabinoid may display prophylactic or therapeutic capacity to repair viral-induced epithelial barrier damage is still unknown. Likewise, the potential ability of WIN55,212-2 to interfere with type 2-induced airway epithelial barrier alterations remains elusive.

2.1. Study of the potential preventive and/or therapeutic capacity of WIN55,212-2 to restore epithelial barrier function in ALI cultures of human bronchial epithelial cells during RV-A16 infection

Current knowledge on the expression the ECS in the airways is scarce and controversial. Human bronchial epithelial cells (HBECs) have been reported to express CBRs (241, 242) and some authors indicate a higher expression of CB1 compared to CB2 in the airways (243). Conversely, others have exclusively assumed the expression of CBRs in the lungs to the nerves and immune cells that populate them (179). As displayed in **Figure R.22**, we performed flow cytometric analysis of *in vitro* expanded HBECs to analyze CBR protein levels, showing that around 70% of HBECs expressed CB1 while no CB2 expression was detected in our assayed conditions.

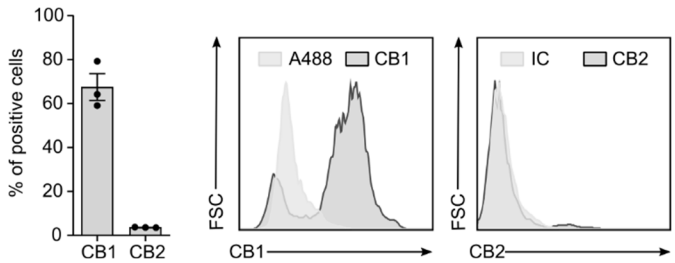

Figure R.22. Expression of CBRs in HBECs. Percentage of cells expressing protein levels of CB1 and CB2, the representative histograms are included on the right (n=3). Values are shown as mean ± SEM.

To study the protective potential of WIN55,212-2 in HBECs, we differentiated them under air-liquid interface (ALI) culture conditions to generate an airway pseudostratified epithelial architecture that properly resembles human physiological conditions (see **Figure M. 5** in materials and methods section). The use of transmission electron microscopy (TEM) confirmed the generation of a fully differentiated bronchial epithelium containing basal, ciliated and mucus secretory cell populations (**Figure R.23A, B).** Moreover, the expression of intercellular complexes including tight junctions and desmosomes in ALI cultures of HBECs was also confirmed using TEM and confocal microscopy (**Figure R.23C, D**).

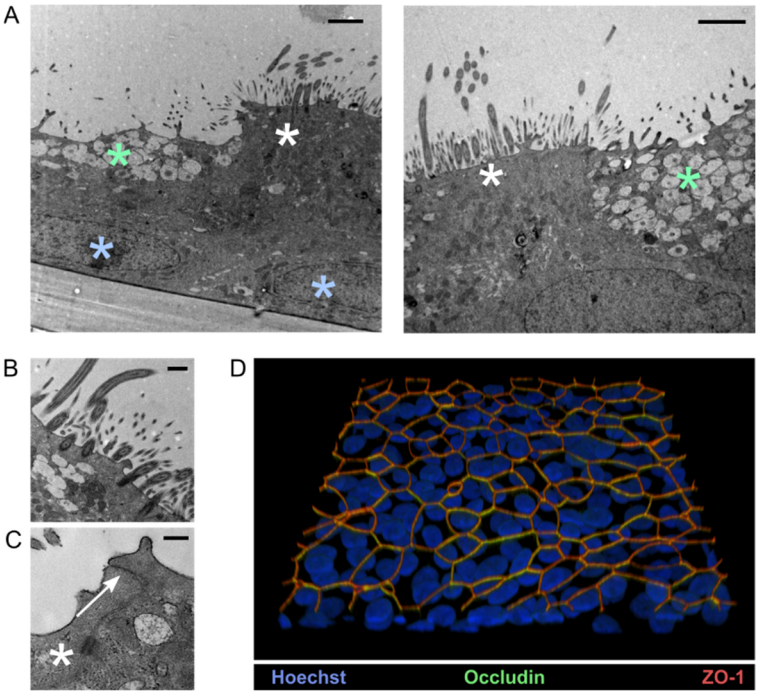

Figure R.23. Validation of the physiological features of the airway epithelium after ALI differentiation of HBECs. (**A**) Representative transmission electron microscopy images of the fully differentiated epithelium. Blue asterisks mark basal cells, green asterisks mark mucus secretory cells and white asterisks mark ciliated cells. Scale bars: 2 µm. (**B**) Details of a cilia rich area and (**C**) intercellular junctions in the apical surface of ALI cultures. Scale bars: 0.5 µm and 0.2 µm, respectively. White arrow points at tight junction complexes while the white asterisk marks a desmosome. (**D**) Confocal microscopy imaging of the tight junction proteins occludin and ZO-1 after immunostaining of ALI cultured HBECs.

In asthma, exacerbation episodes triggered by environmental stimuli, most frequently respiratory viruses, may be life-threatening and account for the main cause of morbidity and disease-related health care costs (94). As mentioned before, we have previously reported that the simultaneous administration of WIN55,212-2 during the onset of RV infection exerts a remarkable ability to restore RV-induced airway epithelial barrier dysfunction (177). In order to validate our previous studies, we performed a dose-response experiment in which ALI cultures of HBECs were infected with RV-A16 and simultaneously administered with increasing doses of WIN55,212-2 while monitoring their barrier integrity and permeability (**Figure R.24A**). Consistent with our previous findings, WIN55,212-2 did not affect the RV-A16-induced acute reduction of transepithelial electrical resistance (TER) values 24 h after the infection but dose-dependently favored the recovery of TER levels at 48 and 72 h after it (**Figure R.24B**). Accordingly, the treatment with the synthetic cannabinoid decreased the RV-A16-induced permeability of infected cultures in a dose-dependent manner, as determined by a reduced paracellular flux of FITC-dextran 72 h after the infection (**Figure R.24C**).

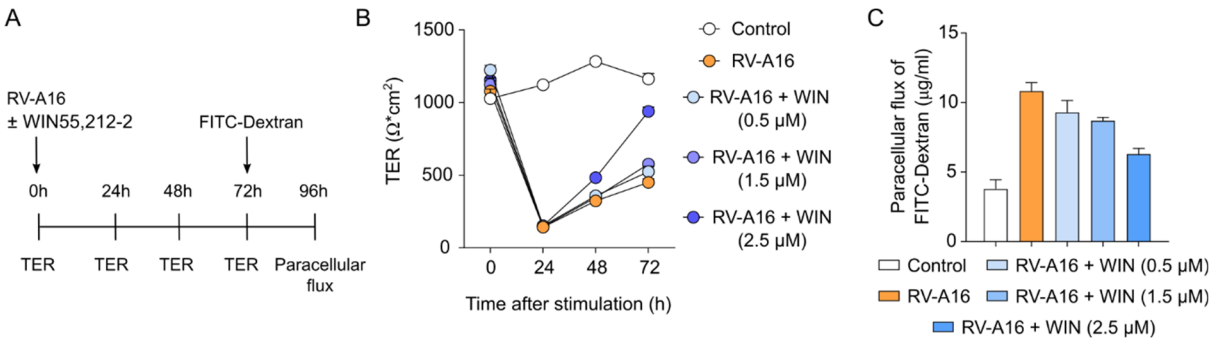

Figure R.24. Dose response analysis of WIN55,212-2 protective effects on RV-induced airway epithelial barrier dysfunction. (**A**) Schematic representation of the experimental protocol. (**B**) Dynamics of Transepithelial electrical resistance (TER) values in the different assayed conditions. (**C**) Paracellular permeability determined as the basolateral concentrations of FITC-Dextran after 24 h incubation with FITC-Dextran in the apical compartment (n = 1 donor in 2-3 technical replicates).

To explore the potential prophylactic and therapeutic capacity of WIN55,212-2 to protect the bronchial epithelium from RV-A16 infection, we employed two different experimental models using ALI cultures of HBECs. In the prophylactic model, WIN55,212-2 was administered 24 h prior to RV-A16 infection (**Figure R.25A**), whereas in the therapeutic protocol the cannabinoid was administered 24h after infection (**Figure R.25D**). In addition, controls including medium, WIN55,212-2-, UV-RV-A16- and RV-A16-stimulated cultures were included in all experiments.

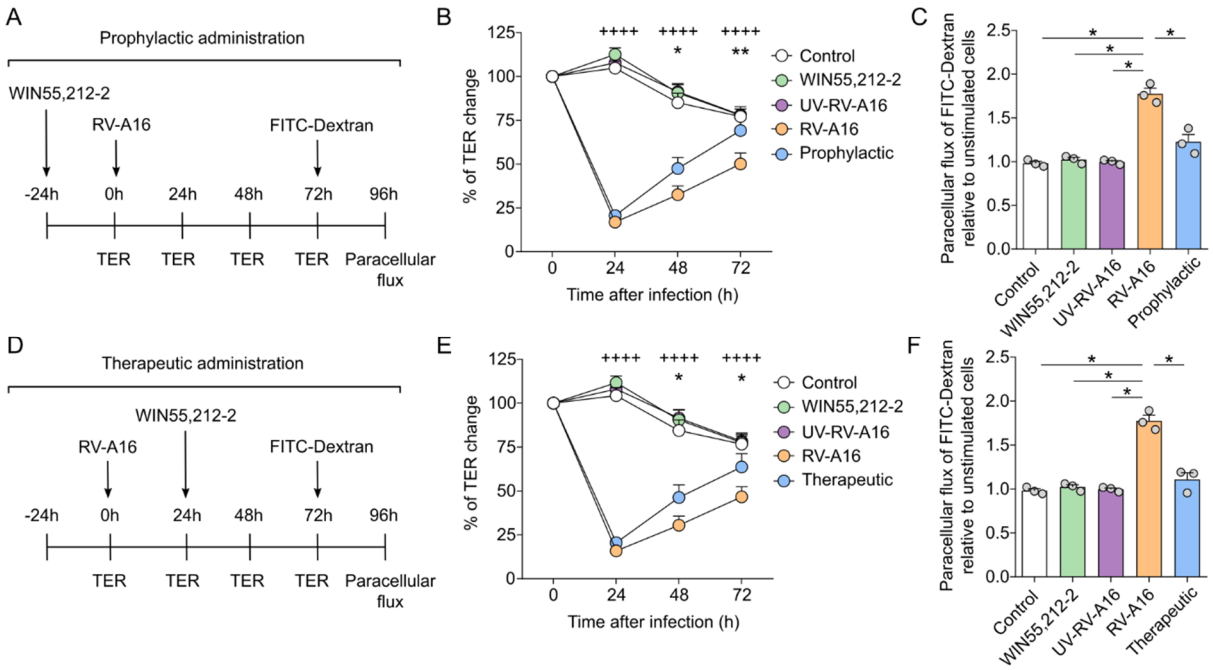

Figure R.25. Prophylactic and therapeutic capacity of WIN55,212-2 to restore barrier damage upon RV-A16 infection. Schematic representation of the prophylactic (**A**) or therapeutic (**D**) administration protocol of WIN55,212-2 (2.5 μM) before or after the infection with RV-A16, respectively. Percentage of TER change in the different assayed conditions including prophylactic (**B**) and therapeutic (**E**) treatments (n= 3 donors in triplicates). +, Unstimulated control vs. RV-A16 infection. *, RV-A16 infected cultures vs. prophylactic/therapeutic treatments. Fold change in the paracellular flux of apically administered FITC-dextran in the indicated assayed conditions including prophylactic (**C**) and therapeutic (**F**) treatments (n= 3 donors in triplicates, graph dots represent average values). All values are represented as mean ± SEM. Statistical significance was determined by Two-way ANOVA followed by Dunnett's multiple comparisons test (B, E) or One-way ANOVA followed by Holm-Sidak's multiple comparisons correction (C, F): * p <0.05, ** p <0.01 and **** p <0.0001.

We observed that all cultures infected with RV-A16 showed a drastic drop in TER values 24h after infection, suggesting that the prophylactic administration of WIN55,212-2 does not prevent infection of HBECs. Nonetheless, there was a significant enhancement of TER recovery 48 and 72 h after the infection in prophylactically treated HBECs compared to untreated cells (**Figure R.25B**). Supporting these data, the enhanced paracellular permeability observed in RV-A16-infected cultures was significantly reduced in HBECs pretreated with WIN55,212-2 before RV-A16 infection (**Figure R.25C**). Similarly, therapeutic administration of the synthetic cannabinoid resulted in a significant improvement in TER values 48 and 72 h after RV-A16 infection (**Figure R.25E**), which was also accompanied by a significant reduction in the RV-A16-induced increment in paracellular permeability (**Figure R.25F**). Medium, WIN55,212-2 alone or UV-RV-A16-stimulated cultures did not show significant differences in TER or FITC-dextran flux in any case.

Collectively, our findings demonstrate that the synthetic cannabinoid WIN55,212-2 boosts the recovery of RV-A16-induced bronchial epithelial barrier damage without preventing viral infection. Notably, similar patterns of accelerated recovery from either cytokine- or EDTA-induced intestinal permeability have been previously reported in epithelial cells exposed to the phytocannabinoids THC and CBD (168, 169), highlighting the potential of cannabinoid compounds to improve epithelial barrier function in diverse physiological systems.

2.2. Evaluation of the potential efficacy of WIN55,212-2 to improve epithelial barrier function in ALI cultures and epithelial spheroid cultures of human bronchial epithelial cells during type 2 inflammation

Multiple studies have demonstrated that respiratory viral infections promote type 2 responses in the airways (133, 137, 138). In turn, type 2 inflammation contributes to the impairment of epithelial barrier performance, immunomodulatory functions and antiviral immunity, creating a vicious cycle with deleterious consequences in asthma (105, 134). Therefore, we sought to investigate whether cannabinoids might also display protective effects on human bronchial epithelium exposed to effector cytokines involved in type 2 inflammation. ALI cultures of HBECs were stimulated with medium (control) or IL-13 in the absence or presence of WIN55,212-2, and the main pathophysiological asthma features were assessed.

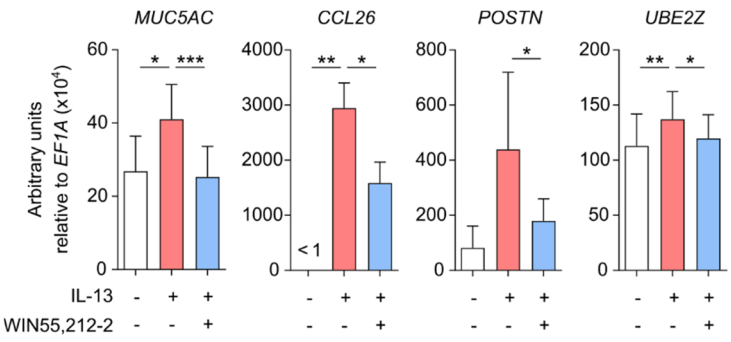

Figure R.26. WIN55,212-2 decreases the expression of type 2 biomarkers in HBECs. Analysis of the mRNA expression for the indicated genes after 24 h stimulation with medium (control), IL-13 (50 ng/mL) or IL-13 in the presence of WIN55,212-2 (2.5 μM) (n = 6-8). All values are represented as mean ± SEM. Statistical significance was determined by One-way ANOVA followed by Holm-Sidak multiple comparisons test, or Wilcoxon test: * p <0.05, ** p <0.01 and *** p <0.001.

As shown in **Figure R.26**, qPCR analysis showed that cultures stimulated with IL-13 in the presence of WIN55,212-2 significantly decreased the IL-13-induced expression of different well-known type 2 asthma biomarkers, such as the mucin component *MUC5AC*, the eosinophil chemoattractant *CCL26*, the early fibrosis and type 2 inflammation biomarker *POSTN*, and the tight junction degrading enzyme *UBE2Z*, suggesting that this synthetic cannabinoid displays potential immunomodulatory properties and capacity to impair mucus overproduction and barrier leakiness as key asthma features.

Defective airway epithelial barrier function, characterized by the degradation of junctional complexes between neighboring cells and a higher paracellular flux of molecules through the epithelium, is a hallmark feature of asthma pathophysiology (97, 101, 107). Compelling experimental evidence reports how type 2 effector cytokines reproduce these deleterious effects in barrier function *in vitro* (108-110, 121). Consistent with these data, we observed that stimulation of ALI cultures of HBECs with IL-13 resulted in a higher paracellular permeability and reduced protein expression of the tight junction molecules: occludin and ZO-1 (**Figure R.27**). Interestingly, stimulation in the presence of WIN55,212-2 significantly decreased the IL-13-induced permeability of the cultures (**Figure R.27A**), which was further associated with a significant restoration of the expression and integrity of both occludin and ZO-1 as determined by confocal microscopy (**Figure R.27B, C**). Together, our findings indicate that WIN55,212-2 inhibits the IL-13 induced airway epithelial barrier leakage.

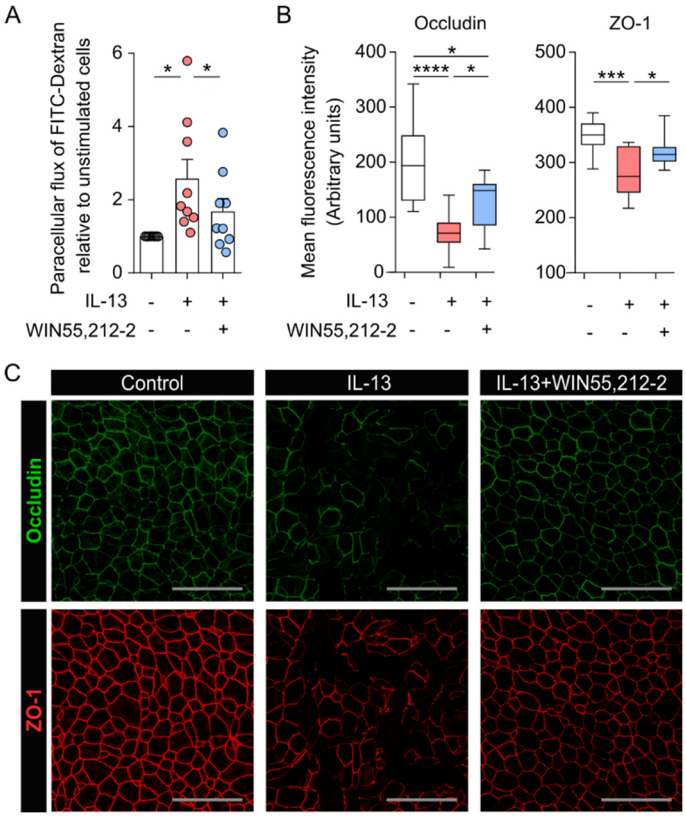

Figure R.27. WIN55,212-2 impairs IL-13-induced epithelial barrier leakage in ALI cultures of HBECs. (**A**) Fold change in the paracellular flux of apically administered FITC-dextran to the basolateral compartment after 72 h with medium (control), IL-13 (50 ng/mL) or IL-13 plus WIN55,212-2 (2.5 μM) (n = 9 in triplicates, graph dots represent average values). Quantification (**B**) and representative confocal microscopy images (**C**) of the tight junctions occludin and ZO-1 after 72 h stimulation with the indicated treatments (n = 10 random microscopy fields from 2 donors). Scale bars: 50 μm. All values are represented as mean ± SEM. Statistical significance was determined by One-way ANOVA followed by Holm-Sidak's multiple comparisons test: * p <0.05, *** p <0.001 and **** p <0.0001.

The airway epithelium constitutes a physical, chemical but also immunological barrier against airborne threats. Therefore, we investigated the capacity of WIN55,212-2 to interfere with the immunomodulatory properties of the bronchial epithelium in the context of type 2 inflammation. In line

with the previous gene expression results, we observed that WIN55,212-2 impairs the IL-13-induced production of the alarmin TSLP and the eotaxin CCL26 at the protein level in HBEC ALI cultures (**Figure R.28**)

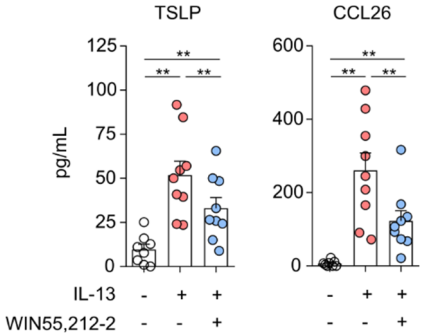

Figure R.28. Modulation of IL-13-induced HBEC cytokine production by WIN55,212-2. Quantification of the indicated cytokines in media samples from ALI cultures after 24 h treatment with medium (control), IL-13 (50 ng/mL) or IL-13 plus WIN55,212-2 (2.5 μM) (n = 9). All values are represented as mean ± SEM. Statistical significance was determined by One-way ANOVA followed by Holm-Sidak's multiple comparisons test: ** p <0.01.

Collectively, our data demonstrate that the synthetic cannabinoid WIN55,212-2 impairs the acquisition of the main IL-13-induced asthma features in HBECs by restoring barrier function and impairing epithelial-derived orchestration of type 2 immune responses. To verify our findings in a more physiologically relevant model, we developed three dimensional cultures of self-assembled airway epithelial structures, known as bronchial epithelial spheroids, which allow the *in vitro* study of changes in epithelial barrier function and cellular composition, closely resembling *in vivo* human physiology (110, 244). First, we analyzed potential changes in spheroid numbers and size after 72 h treatment of fully differentiated bronchial epithelial spheroids with medium (control), WIN55,212-2, IL-13 or IL-13+WIN55,212-2. None of the assayed conditions significantly altered spheroid count or size (**Figure R.29**).

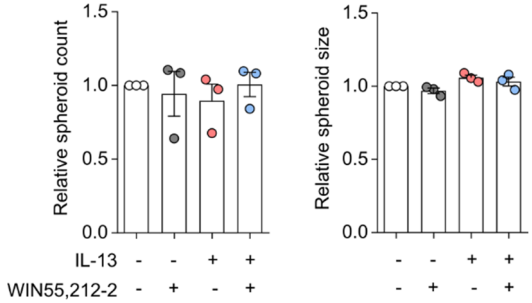

Figure R.29. Spheroid count and size after the different assayed conditions. Relative spheroid number and size after acute stimulation with medium (control), WIN55,212-2 (2.5 μM), IL-13 (50 ng/mL) or IL-13 plus WIN55,212-2 for 72 h (n = 3). All data are represented as mean ± SEM.

Next, we performed confocal microscopy imaging of spheroids treated with the previously indicated conditions to assess their luminal size and paracellular permeability to FITC-dextran. We observed that IL-13 significantly decreased luminal area while increased spheroid wall thickness and paracellular flux permeability, as determined by a lower lumen-to-total spheroid area and enhanced luminal FITC-dextran fluorescence intensity, respectively (**Figure R.30A-C**). WIN55,212-2 administration, either alone or in combination with IL-13, did not show any significant effect on bronchospheroid wall thickness compared to control cultures or IL-13-treated bronchospheroids, respectively (**Figure R.30A, B**). Nevertheless, the treatment with the synthetic cannabinoid significantly decreased the IL-13-induced increment in spheroid permeability (**Figure R.30A, C**), corroborating the barrier protective capacity of WIN55,212-2 previously observed in ALI cultures of HBECs. Our findings are consistent with the effects exerted by other reported strategies to protect epithelial barrier function

such as the inhibition of histone deacetylases (108), activation of GPR120/FFAR4 receptors (245), inhibition of JAK/STAT signaling (109, 246) or the neutralization of IL-13 (121), which have demonstrated the capacity to improve airway barrier performance.

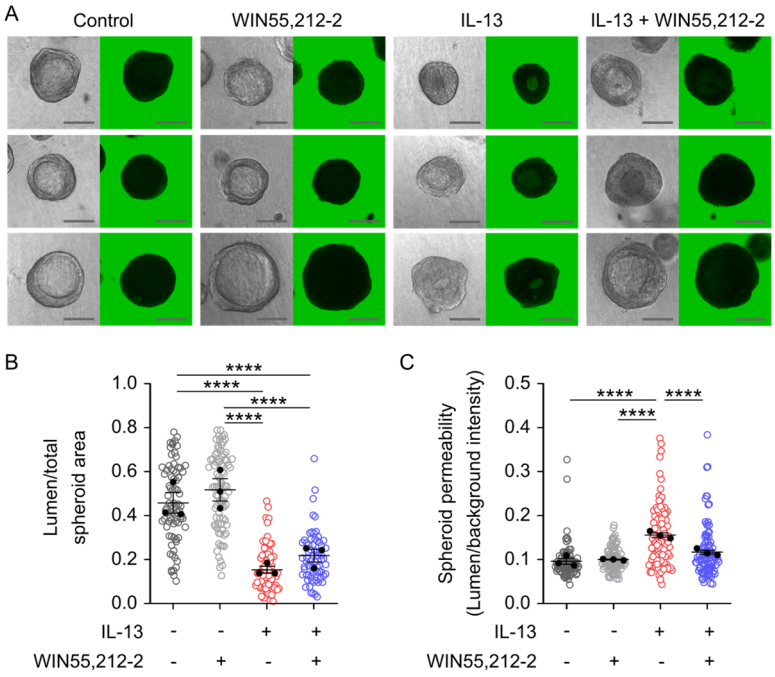

Figure R.30. WIN55,212-2 inhibits IL-13-induced epithelial permeability in human bronchospheroids (**A**) Representative transmitted light (left) and fluorescence (right) confocal microscopy images of spheroids after 48 h incubation with medium (control), WIN55,212-2 (2.5 μM), IL-13 (50 ng/mL) or IL-13 plus WIN55,212-2. (**B**) Quantification of spheroid thickness determined by the lumen to total bronchospheroid area ratios. (**C**) Analysis of spheroid permeability through the measurement of luminal to background fluorescence intensity. Hollow dots represent individual spheroids, and black dots display average value from each donor (n > 20 spheroids per donor, 3 donors). Scale bars: 100 μm. All values are shown as mean ± SEM. Statistical significance was determined by Kruskal-Wallis test followed by Dunn's correction for multiple comparisons: **** p <0.0001.

The exposure to type 2 effector cytokines, specially IL-13, also has consequences in the cellular composition of the airway epithelium. Stimulation with IL-13 promotes mucus overproduction and reshapes the epithelial landscape by reducing the amount of ciliated cells and enhancing the numbers of mucus-producing goblet cells, ultimately compromising proper mucociliary function. Therefore, to characterize the effects of WIN55,212-2 on the cellular composition of human bronchial epithelial spheroids, we compared the mRNA expression levels of several gene markers between IL-13- or IL-13+WIN55,212-2- treated spheroids. As expected by the above-described barrier protective capacity, we observed that the expression of the tight junction-degrading enzyme *UBE2Z* was reduced in IL-13+WIN55,212-2- compared to IL-13-stimulated bronchial epithelial spheroids, along with a concomitant increment in the expression of the tight junction proteins *OCLN* and *ZO-1*. Moreover, spheroids stimulated with IL-13 in the presence of WIN55,212-2 showed reduced expression of the basal cell marker *P63*, enhanced expression of ciliated cell markers *FOXJ1* and *DNAI2,* as well as decreased expression of mucus markers *MUC5AC* and *MUC5B* (**Figure R.31**). These results suggest that the

synthetic cannabinoid might impair the IL-13-induced reshaping of human bronchial epithelial spheroid composition.

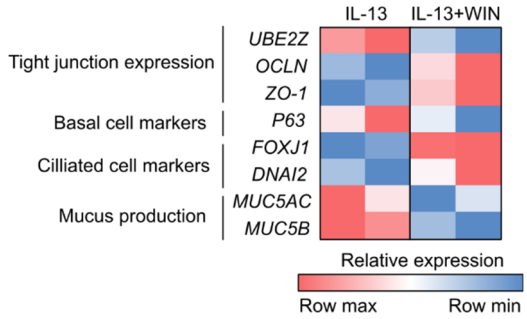

Figure R.31. WIN55,212-2 modulates the IL-13-dependent signature of genes associated to spheroid functionality and cellular composition. Heat map showing the relative mRNA expression of genes related to tight junctions, as well as gene markers for basal, ciliated and goblet cells in bronchial epithelial spheroids stimulated for 24 h with IL-13 alone (50 ng/mL) or in combination with WIN55,212-2 (2.5 μM) (n = 2).

To corroborate these data at the protein level, we performed immunostaining experiments for the glycoprotein MUC5AC and for acetylated α-tubulin as markers of mucus and cilia, respectively. As shown in **Figure R.32** we found that treatment with IL-13 significantly enhanced the protein levels of MUC5AC, which were decreased after stimulation with IL-13 in the presence of WIN55,212-2, confirming the capacity of the cannabinoid to impair IL-13-induced mucus overproduction in human bronchial epithelial spheroids.

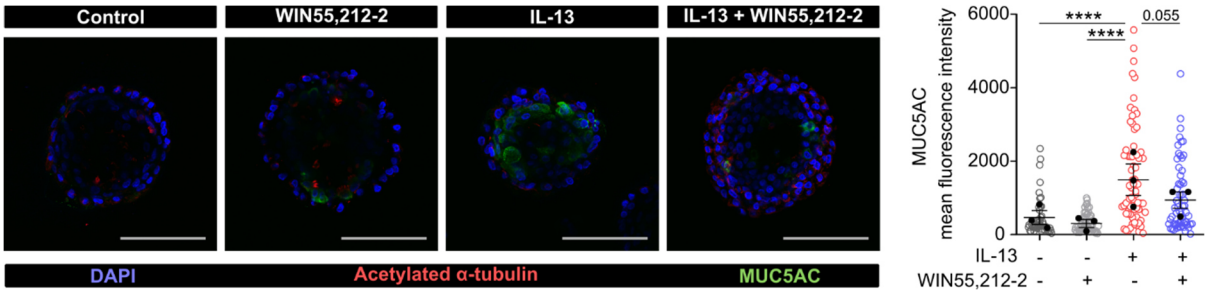

Figure R.32. WIN55,212-2 shapes the IL-13-induced changes on bronchospheroid cellular composition. (**A**) Representative confocal microscopy images of spheroids immunostained for the cilia marker, acetylated α-tubulin, or the mucus marker, MUC5AC, after 72 h treatment with medium (control), WIN55,212-2 (2.5 μM), IL-13 (50 ng/mL) or IL-13 plus WIN55,212-2. (**B**) Quantification of the mean fluorescence intensity of MUC5AC expression. Hollow dots represent individual spheroids, and black dots display average value from each donor (n > 15 spheroids per donor, 3 donors in total). Scale bars: 100 μm. All values are shown as mean ± SEM. Statistical significance was determined by Kruskal-Wallis test followed by Dunn's correction for multiple comparisons: **** p <0.0001.

Developing human bronchial epithelial spheroids acquire asthmatic features when exposed to IL-13 during their differentiation (110, 244). To gain insight into the relevance of our findings in a model of chronic exposure to IL-13, HBECs from healthy donors were differentiated into spheroids in the presence of medium (control), WIN55,212-2, IL-13 or IL-13 plus WIN55,212-2, which were administered every second day. Again, we evaluated the spheroid count after differentiation as well as the spheroid size, confirming that no differences were found between any of the assayed conditions (**Figure R.33**).

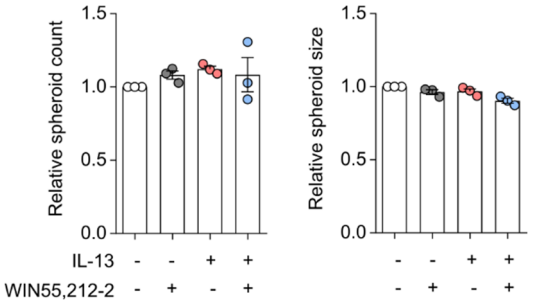

Figure R.33. Spheroid count and size after differentiation in the indicated assayed conditions. Relative spheroid number and size after incubation with medium (control), WIN55,212-2 (2.5 μM), IL-13 (2 ng/mL) or IL-13 plus WIN55,212-2 during their development (n = 3). All data are represented as mean ± SEM.

Next, we evaluated the morphology and functionality of the spheroids developed under the above-mentioned conditions by confocal microscopy. Differentiation in the presence of WIN55,212-2 alone promoted a higher lumen-to-total spheroid area compared to controls, without affecting permeability, suggesting that this synthetic cannabinoid might promote an earlier development of fully differentiated and functional spheroids. Consistent to previous reports (110), stimulation with IL-13 during the development gave raise to thick-walled spheroids with defective epithelial barrier function, defined by a drastic reduction in lumen-to-total area ratios and significantly enhanced paracellular flux of FITC-dextran inside the spheroid lumens. Notably, WIN55,212-2 significantly inhibited the IL-13-induced enhancement of bronchial epithelial spheroid wall thickness and permeability, highlighting its capacity to interfere with type 2 effector cytokines during the self-assembled development of bronchial epithelial spheroids (**Figure R.34**).

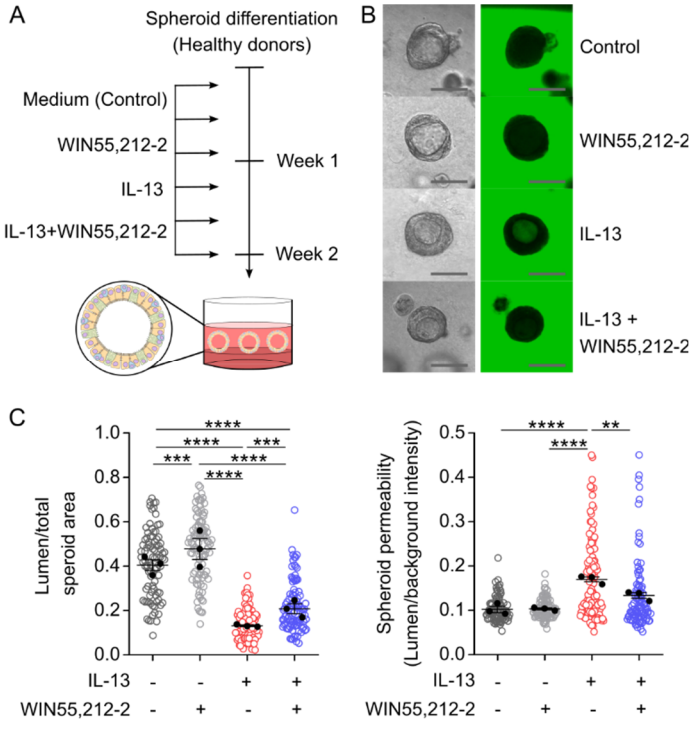

Figure R.34. WIN55,212-2 inhibits IL-13-induced asthma features in developing human bronchial epithelial spheroids (**A**) Schematic representation of the differentiation of bronchial epithelial spheroids in the presence of medium (control), WIN55,212-2 (2.5 μM), IL-13 (2 ng/mL) or IL-13 plus WIN55,212-2. (**B**) Representative transmitted light (left) and fluorescence microscopy (right) images of spheroids differentiated in the different assayed conditions, as well as (**C**) quantifications of spheroid thickness and permeability (n > 20 spheroids per donor, 3 donors). Scale bars: 100 μm. All values are expressed as mean ± SEM. Statistical significance was determined by Kruskal-Wallis test followed by Dunn's correction for multiple comparisons: ** p <0.01, *** p <0.001 and **** p <0.0001.

Finally, to validate the therapeutic potential of WIN55,212-2 in the airway epithelium of asthma patients, HBECs from asthmatic donors were differentiated into spheroids in the presence of medium (control) or WIN55,212-2 administered every second day. Interestingly, we observed a dose-dependent tendency towards a higher number of spheroids obtained after development in the presence of the

cannabinoids, with minor changes in spheroid size (**Figure R.35**), suggesting that WIN55,212-2 might favor the development of asthmatic spheroids.

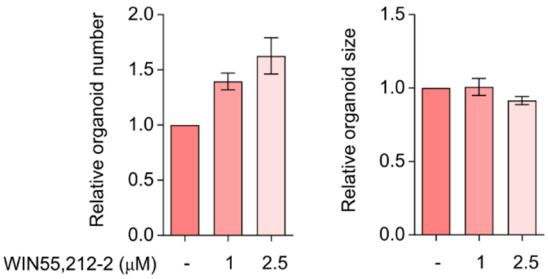

Figure R.35. Asthmatic spheroid count and size after differentiation in the presence of WIN55,212-2. Relative spheroid number and size after incubation with medium (control) or the indicated doses of WIN55,212-2 during their development (n = 1 in triplicate). All data are represented as mean ± SEM.

To further explore the effects of WIN55,212-2 in the bronchial epithelium of asthma patients, we assessed the changes in morphology and permeability after the differentiation of asthmatic spheroids in the presence or absence of the cannabinoid. Confocal microscopy imaging showed that developing asthmatic spheroids exposed to increasing doses of WIN55,212-2 displayed a dose-dependent reduction in bronchial epithelial spheroid wall thickness together with a decreased paracellular permeability (**Figure R.36**) . These findings highlight the therapeutic capacity of WIN55,212-2 to target defects in the airway epithelial barrier permeability of asthmatic patients.

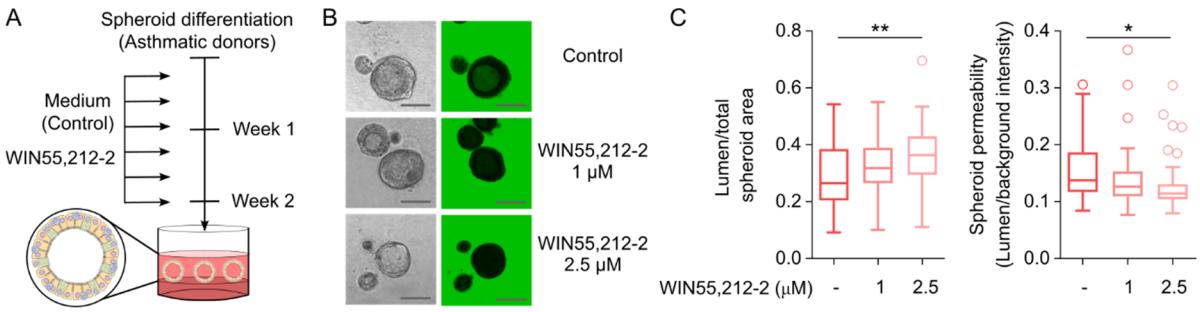

Figure R.36. WIN55,212-2 improves epithelial barrier performance in developing spheroids from asthma patients (**A**) Schematic representation of the differentiation of asthmatic bronchial epithelial spheroids in the presence of medium (control) or the indicated doses of WIN55,212-2. (**B**) Representative transmitted light (left) and fluorescence microscopy (right) images and (**C**) quantifications of spheroid wall thickness and permeability of spheroids developed in the indicated assayed conditions (n = 30-44 spheroids analyzed from one single donor). Scale bars: 100 μm. All values are expressed as mean ± SEM. Statistical significance was determined by Kruskal-Wallis test followed by Dunn's correction for multiple comparisons: * p <0.05 and ** p <0.01.

In summary, our data confirm that the synthetic cannabinoid WIN55,212-2 inhibits the IL-13-induced asthma features by restoring barrier function and inhibiting mucus overproduction in both ALI and self-assembled human bronchial epithelial spheroids. Of note, the protective effects of the cannabinoid were validated in three-dimensional cultures of asthmatic bronchial epithelial spheroids.

2.3. Investigation of the molecular mechanisms involved in the ability of WIN55,212-2 to regulate epithelial barrier integrity and function in human bronchial epithelial cells

To elucidate the mechanisms underlying the protective effects of WIN55,212-2 during type 2 inflammation, we first analyzed the major pathways upregulated by IL-13 in HBECs. We performed gene set enrichment analysis (GSEA) of a publicly available RNA sequencing dataset (GSE206510) of ALI cultures of HBECs from healthy and asthmatic individuals treated with or without IL-13 for 24 h (205). The analysis uncovered an enrichment in the O-glycan biosynthesis and Protein secretion gene sets in both healthy and asthmatics donors, which is congruent with our experimental data showing increased MUC5AC as well as TSLP and CCL26 production after IL-13 stimulation. Proteasome gene set was also enriched in IL-13-treated cells, suggesting potential degradation of proteins, including tight junctions (246). Of note, ALI cultures of HBECs from either control or asthmatic individuals stimulated with IL-13 showed a strong enrichment in the Oxidative phosphorylation and TCA cycle gene sets as well as the reactive oxygen species (ROS) pathway, suggesting a profound metabolic reprogramming towards a very oxidative profile (**Figure R.37**).

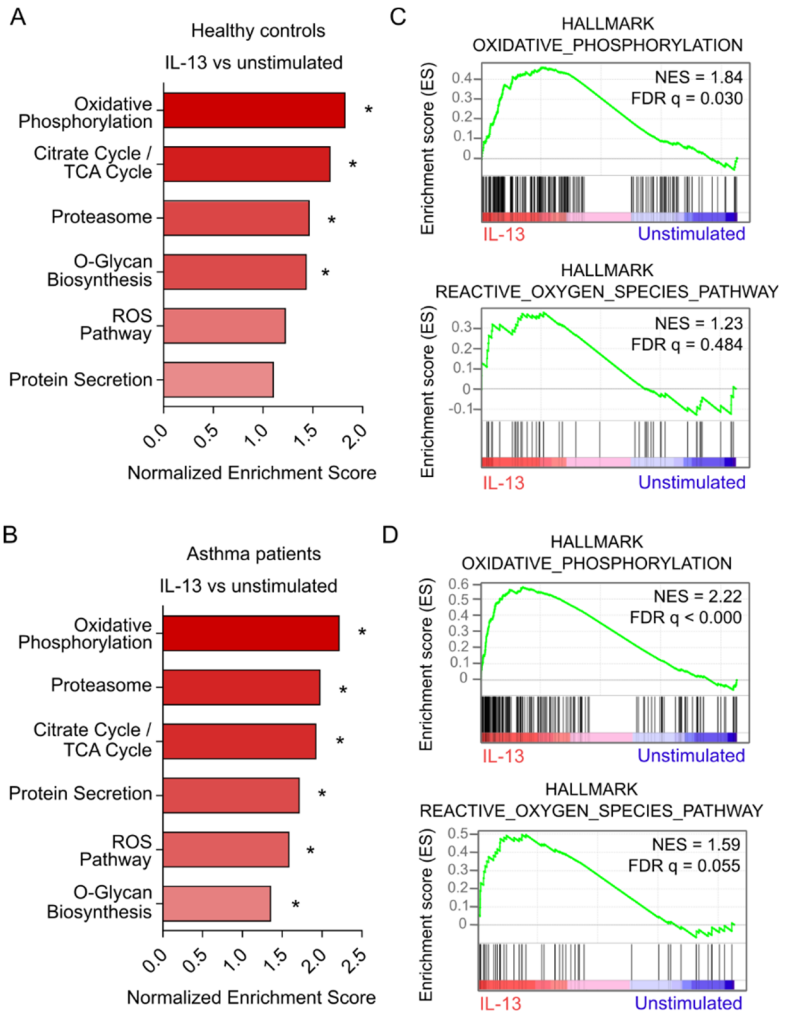

Figure R.37. Enriched gene paths in healthy and asthmatic HBECs after stimulation with IL-13. Bar graph showing gene set enrichment analysis (GSEA) of gene sets curated from HALLMARK and KEGG Legacy databases from next generation RNA sequencing of healthy (**A**) or asthmatic (**B**) ALI cultures of HBECs treated for 24 h with 50 ng/mL IL-13 vs unstimulated (n = 5). On the right, GSEA representation for HALLMARK_ OXIDATIVE_ PHOSPHORYLATION and HALLMARK_ REACTIVE_ OXIGEN_ SPECIES_ PATHWAY gene sets enriched in IL-13-treated HBECs compared to unstimulated cultures in both healthy (**C**) or asthma (**D**) donors. Statistical significance (*) was determined by FDR q values < 0.25.

Given the well-known role of cannabinoids as modulators of cellular metabolism and oxidative stress (247), we sought to study the capacity of WIN55,212-2 to interfere with the IL-13-induced changes

in metabolism by real-time metabolic experiments using a Seahorse bioanalyzer. A complete “Mito Stress Test” assay was performed to assess epithelial cell metabolism with a particular focus on mitochondrial activity. The results revealed that IL-13-stimulated HBECs enhanced their oxygen consumption rate (OCR) and extracellular acidification rate (ECAR) compared to controls, indicating the activation of mitochondrial respiration and glycolytic paths (**Figure R.38A, B**). Together with the GSEA, our experimental results agree with the previously observed augmented expression of mitochondrial respiratory complexes III and IV reported in HBECs from asthmatic patients (248), as well as the increased OCR and ECAR observed in HBECs from both lean and obese asthmatic donors (249). Interestingly, the bioenergetic profile of HBECs stimulated with IL-13 plus WIN55,212-2 resembled to that observed in control cells in terms of OCR and ECAR (**Figure R.38C**), suggesting that the cannabinoid might impair the IL-13-induced metabolic reprogramming of HBECs. A deeper evaluation of the metabolic effects of WIN55,212-2 on IL-13-stimulated HBECs showed that the cannabinoid significantly decreased basal, maximal and ATP-coupled mitochondrial respiration (**Figure R.38D-F**), indicating its capacity to modulate IL-13-induced OXPHOS. Moreover, HBECs stimulated with the combination of IL-13 plus WIN55,212-2 significantly increased mitochondrial coupling efficiency while decreased proton leak and non-mitochondrial oxygen consumption (**Figure R.38G-I**), suggesting a better efficacy in electron transport chain and a potentially reduced production of ROS.

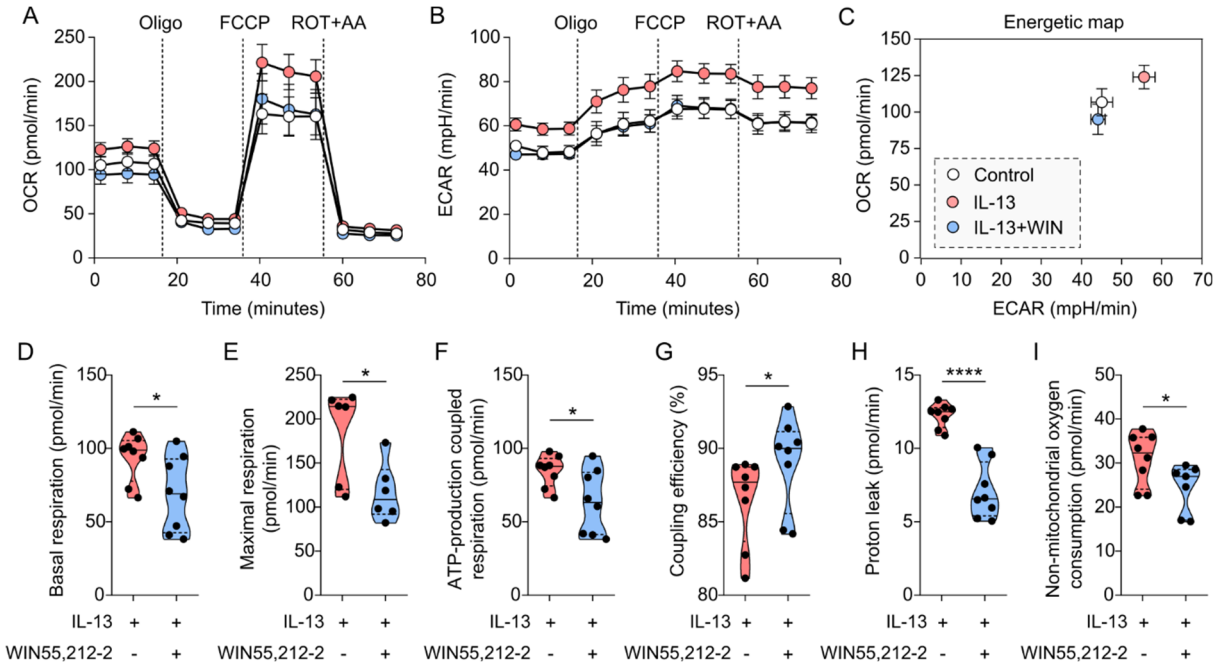

Figure R.38. WIN55,212-2 impairs metabolic reprogramming of HBECs exposed to IL-13. Real-time analysis of OCR (**A**) and ECAR (**B**) in HBECs stimulated 24 h with medium (control), IL-13 (50 ng/mL) or IL-13 in the presence of WIN55,212-2 (2.5 μM) (IL-13+WIN). Graph shows basal conditions and after sequential addition of 1.5 μM oligomycin (Oligo), 1 μM carbonyl cyanide 4-(trifluoromethoxy)phenylhydrazone (FCCP) and 0.5 μM rotenone plus 0.5 μM antimycin (ROT+AA). (**C**) Energetic map displaying basal OCR vs. ECAR of HBECs stimulated 24 h with the indicated conditions (n = 6-8). Parameters of mitochondrial function are represented in graphs for basal (**D**), maximal (**E**) and ATP-production coupled respiration (**F**) as well as mitochondrial coupling efficiency (**G**), proton leak (**H**) and non-mitochondrial oxygen consumption (**I**) after 24 h stimulation with IL-13 or IL-13 plus WIN55,212-2 (n = 6-8). All values are expressed as mean ± SEM. Statistical significance was determined by unpaired t-test (D, E, F, H, I) or Mann-Whitney test (G): * p <0.05 and **** p <0.0001.

Despite the above-mentioned studies suggesting a higher mitochondrial activity in HBECs of asthmatics (248, 249), the metabolic profile of airway epithelial cells in asthma remains controversial and our data may contrast with some authors reporting mitochondrial dysfunction in the epithelium of asthmatics (250). At this regard, *in vivo* data have shown that mitochondrial damage in airway epithelial cells may be caused by ROS in a model of allergen-induced airway inflammation (251). We hypothesize that after the acute stimulation with IL-13 a first peak of mitochondrial activity might be followed by subsequent dysfunction promoted by excessive ROS production. In fact, alterations in the redox balance and enhanced oxidative stress are well-documented in the airway epithelium in the context of type 2 inflammation (252-254). Moreover, elevated levels of inducible nitric oxide synthase (iNOS) are found in the epithelium of allergic asthmatics and can be upregulated *in vitro* with IL-13 stimulation, contributing to induction of the well-recognized type 2 biomarker FeNO (255, 256). To validate our hypothesis, we measured the levels of intracellular ROS and the expression of iNOS in HBECs stimulated with medium (control), WIN55,212-2, IL-13 and IL-13 plus WIN55,212-2. Treatment with the synthetic cannabinoid WIN55,212-2, either alone or in combination with IL-13 significantly reduced the intracellular ROS levels in HBECs (**Figure R.39A**). Likewise, WIN55,212-2 impaired the IL-13-dependent induction of the nitric oxide (NO)-producing enzyme iNOS in ALI cultures of HBECs (**Figure R.39B**), confirming that WIN55,212-2 impairs the IL-13-induced oxidative stress in the airway epithelium.

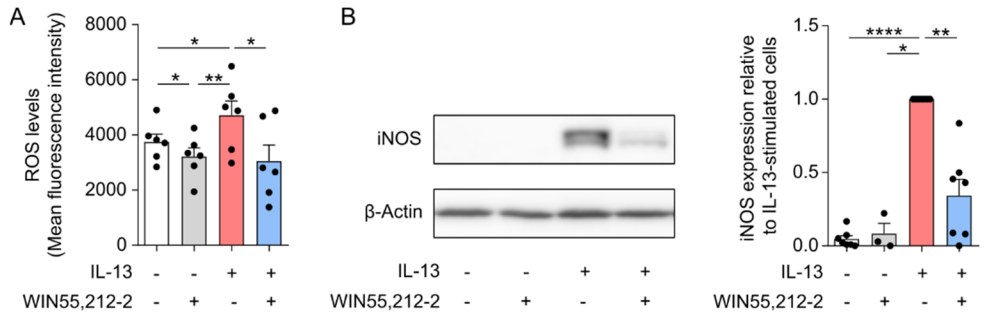

Figure R.39. WIN55,212-2 inhibits the oxidative stress induced by IL-13 in HBECs. (**A**) Measurement of intracellular levels of ROS in HBECs treated for 24 h with medium (control), WIN55,212-2, IL-13 (50 ng/mL) or IL-13 plus WIN55,212-2 (2.5 μM) (n = 6 in duplicates). (**B**) Representative western blot (left) and densitometric quantification (right) of iNOS expression in ALI cultures of HBECs after 24 h stimulation with the indicated treatments (n = 3-6). All data are represented as mean ± SEM. Statistical significance was determined by One-way ANOVA followed by Holm-Sidak's multiple comparisons correction: * p <0.05, ** p <0.01 and **** p <0.0001.

To further characterize the molecular mechanisms of WIN55,212-2 protective effects, we sought to investigate whether the cannabinoid-dependent regulation of oxidative balance could interfere with IL-13 signaling. As STAT6 is the major transduction pathway for Th2 cytokine signaling, we first performed time-course and dose-dependency experiments to evaluate its phosphorylation status after stimulation of ALI cultures of HBECs with IL-13 in the presence or absence of WIN55,212-2. As shown in **Figure R.40A**, we observed that among the assayed conditions, IL-13 induced the highest levels of STAT6 phosphorylation (pSTAT6) in ALI cultures of HBECs after 1 h of administration, which progressively fade after 4 h and 24 h. WIN55,212-2 inhibited IL-13-mediated pSTAT6 at all the assayed time points, with maximum inhibition values reached after 24 h and at a concentration of 2.5 μM (**Figure**

R40A-C). Our results suggest that WIN55,212-2 activity might be linked to the induction of an earlier dephosphorylation rather than the inhibition of STAT6 phosphorylation.

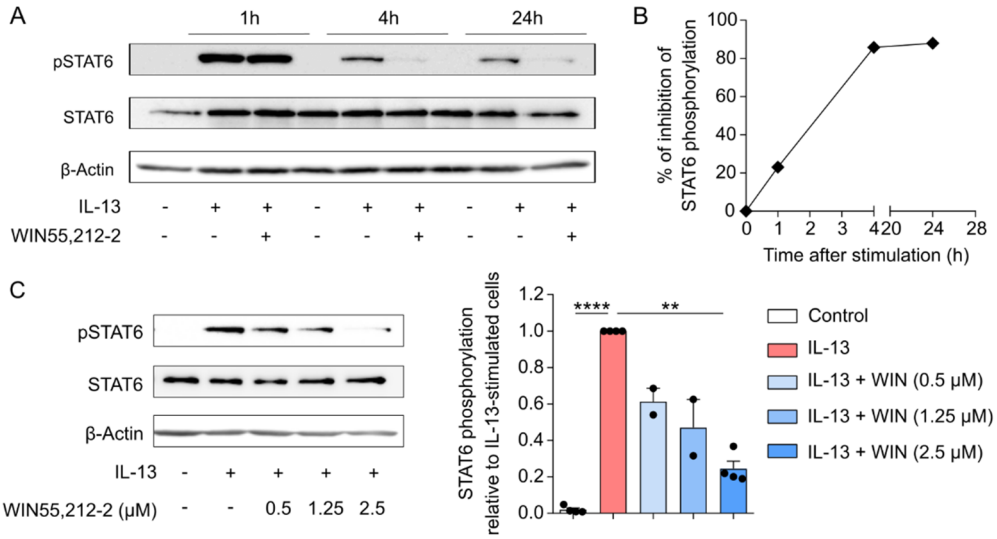

Figure R.40. WIN55,212-2 impairs IL-13 signaling in HBECs. (**A**) Representative western blot and quantification (**B**) of the inhibitory capacity of WIN55,212-2 (2.5 μM) on IL-13-induced STAT6 phosphorylation in HBECs at the indicated timepoints. (**C**) Representative western blot (left) and densitometric analysis (right) of STAT6 phosphorylation after 24 h incubation of ALI cultures of HBECs with medium (control), IL-13 (50 ng/mL) or IL-13 in the presence of the indicated doses of the cannabinoid. All values are shown as mean ± SEM. Statistical significance was determined by One-way ANOVA followed by Holm-Sidak's multiple comparisons correction: ** p <0.01 and **** p <0.0001.

pSTAT6 is a common target of protein tyrosine phosphatases (PTPs) and their oxidative inactivation by ROS has been described as a major keypoint to sustain type 2 cytokine signaling (257, 258). We hypothesized that WIN55,212-2-mediated inhibition of oxidative stress could alter phosphatase activity and favor an earlier dephosphorylation of STAT6. To validate our hypothesis, ALI cultures of HBECs were stimulated with IL-13 in the presence of the ROS scavenger N-acetyl-L-cysteine (NAC). Similar to the effects of the cannabinoid, NAC impaired IL-13-induced pSTAT6 (**Figure R.41A**), indicating that the inhibition of ROS may be involved in the capacity of the cannabinoid to interfere with type 2 cytokine signaling and IL-13-dependent asthmatic features in HBECs. Supporting these data, the production of the epithelial-derived mediators TSLP and CCL26, both under the control of STAT6 (259, 260), were equally decreased by either NAC or WIN55,212-2 treatments in ALI cultures of HBECs stimulated with IL-13 (**Figure R.41B, C**). To further confirm the potential involvement of ROS-dependent inactivation of PTPs in the protective effects of the cannabinoid, ALI cultures of HBECs were stimulated with IL-13+WIN55,212-2 in the presence or absence of the PTP pan-inhibitor, H_3VO_4. Our results showed that the inhibition of PTP activity in cultures treated with IL-13+WIN55,212-2 significantly restored pSTAT6 and rescued the IL-13-dependent production of TSLP and CCL26 mediators (**Figure R.41D-F**).

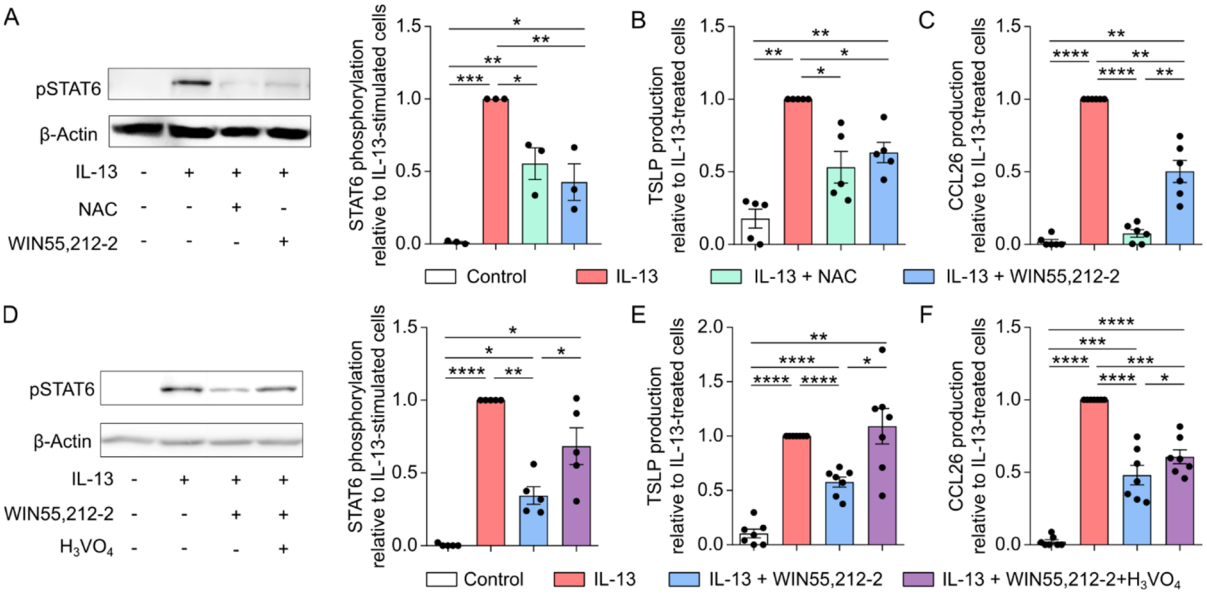

Figure R.41. WIN55,212-2 impairs IL-13 signaling in HBECs. (**A**) Illustrative western blot (left) and densitometric quantification (right) of STAT6 phosphorylation after 24 h incubation of ALI cultures of HBECs with medium (control), IL-13 (50 ng/mL), IL-13 plus WIN55,212-2 (2.5 μM) or IL-13 in the presence NAC (5 mM) (n = 3). Relative TSLP (**B**) or CCL26 (**C**) cytokine production of ALI cultures of HBECs stimulated with the assayed conditions (n = 5-6). (**D**) Western blot (left) and densitometric quantification (right) of STAT6 phosphorylation after 24 h stimulation of ALI cultures of HBECs with medium (control), IL-13 (50 ng/mL), IL-13 plus WIN55,212-2 (2.5 μM) or IL-13 plus WIN55,212-2 in the presence of H_3VO_4 (10 μM) (n = 5). Relative TSLP (**E**) or CCL26 (**F**) cytokine production of ALI cultures of HBECs stimulated with the assayed conditions (n = 7). All values are represented as mean ± SEM. Statistical significance was determined by One-way ANOVA followed by Holm-Sidak's multiple comparisons correction: * p <0.05, ** p <0.01, *** p <0.001 and **** p <0.0001.

Collectively, these findings indicate that the synthetic cannabinoid WIN55,212-2 confers its protective effects in HBECs by targeting STAT6 signaling via mechanisms associated with the preservation of phosphatase activity through inhibition of oxidative stress. *In vivo* studies highlight the relevance of STAT6 signaling in the pathogenic features of asthma, as mice lacking STAT6 were protected from all pulmonary deleterious effects of IL-13, while its reconstitution only in airway epithelial cells was sufficient to promote IL-13-induced airway hyperreactivity and mucus production (132). Moreover, our experimental data might well fit with the previously reported capacity of coal tar or benvitimod compounds to interfere with type 2 cytokine signaling, impair cytokine production and improve epithelial barrier function through upregulation of antioxidant pathways in other epithelial cells such as human keratinocytes (261, 262).

Objective 3: Evaluation of the potential therapeutic efficacy of the synthetic cannabinoid WIN55,212-2 in preclinical *in vivo* models of asthma

3.1. Study of the potential capacity of WIN55,212-2 to restore epithelial barrier function *in vivo* in murine models of IL-13-induced type 2 asthma

To gain insight into the *in vivo* relevance of our findings, we sought to investigate the barrier protective capacity of WIN55,212-2 in an asthma-like murine model of type 2 airway inflammation and epithelial barrier dysfunction. Mice were intranasally instilled with IL-13 for three consecutive days to generate acute type 2 airway inflammation. Three therapeutic groups involving different administration routes and doses were included in the study: i) intranasal WIN55,212-2 (0.2 mg/kg), ii) intranasal WIN55,212-2 (1 mg/kg), iii) intraperitoneal WIN55,212-2 (5 mg/kg). Alternatively, a group of mice receiving intranasal saline (PBS) was included as baseline control (**Figure R.42**).

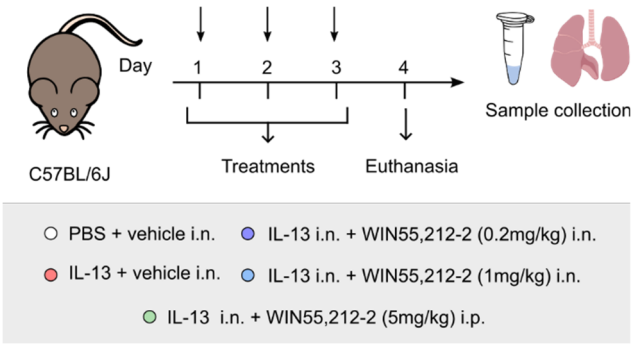

Figure R.42. Schematic illustration of the mice model protocol and therapeutic administration groups.

The analysis of bronchoalveolar lavage fluid (BALF) showed that IL-13-treated mice displayed significantly higher total protein and albumin concentrations than controls, indicating that IL-13 impairs epithelial barrier integrity and enhances the translocation of serum proteins into bronchoalveolar space (**Figure R.43**).

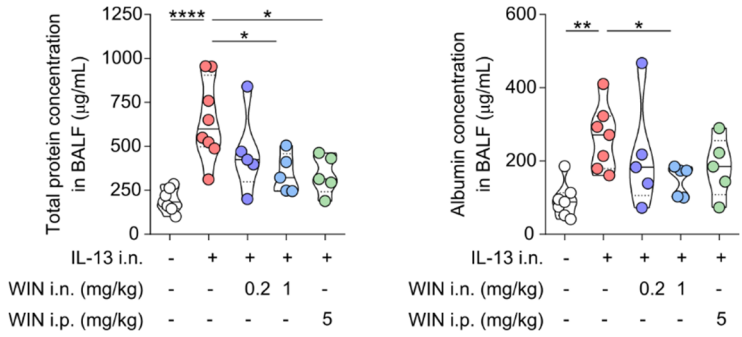

Figure R.43. WIN55,212-2 exerts *in vivo* protective epithelial barrier function of in the context of type 2 airway inflammation. Total protein content (left) and murine serum albumin concentration (right) in BALF 24 h after last intranasal administration of the indicated mice groups (n = 5-7). All data are expressed as mean ± SEM. Statistical significance was determined by One-way ANOVA followed by Holm-Sidak's multiple comparisons test: * p <0.05, ** p <0.01, and **** p <0.0001.

Supporting our *in vitro* findings, intraperitoneal or intranasal administration of WIN55,212-2 reduced these bronchial epithelial dysfunction markers, which displayed a dose-dependent effect in the case of the intranasal route (**Figure R.43**), confirming a barrier protective effect *in vivo*. Our results agree with the previously reported capacity of WIN55,212-2 to impair plasma extravasation in the airways of guinea pigs during an allergen-induced airway inflammation model. Nonetheless, the mechanisms of action of the cannabinoid were attributed to its capacity to activate lung C-fibers (188).

We also characterized the cellular subsets populating the airways of the different groups of mice by flow cytometric analysis of BALF. A significant reduction of alveolar macrophages (AM) along with an increase of inflammatory cells including eosinophils, neutrophils, T cells and DCs in BALF was found after intranasal administration of IL-13. Of note, intranasal or intraperitoneal treatments with WIN55,212-2 significantly inhibited the IL-13-dependent increase of eosinophils, DCs and T cells in BALF without affecting neutrophil infiltration or AM numbers (**Figure R.44**). Our data demonstrate the *in vivo* capacity of this cannabinoid to inhibit IL-13-induced type 2 inflammatory responses, which might well fit with our proposed mechanism of action, as STAT6-deficient mice display compromised asthmatic eosinophilia but unaltered allergen-induced neutrophilia (263).

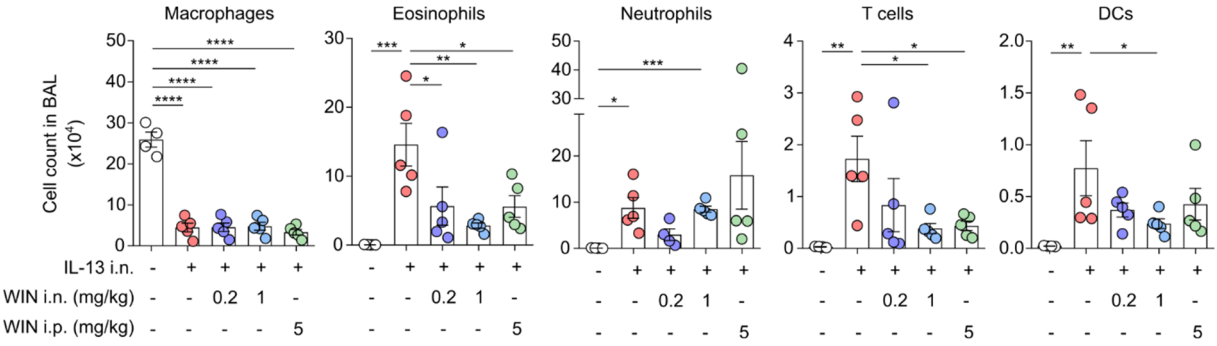

Figure R.44. WIN55,212-2 inhibits type 2 inflammatory cell recruitment in BALF of mice exposed to IL-13. Flow cytometric characterization of major BAL cell populations 24 h after last treatment of mice from the different groups (n = 4-5). All data are expressed as mean ± SEM. Statistical significance was determined by One-way ANOVA or Brown-Forsythe and Welch ANOVA followed by Holm-Sidak's multiple comparisons test: * p <0.05, ** p <0.01, *** p <0.001 and **** p <0.0001.

Next, we sought to identify potential modifications in the airway epithelial barrier composition and local inflammatory landscape of IL-13-treated mice in the absence or presence of intranasal WIN55,212-2 (1 mg/kg), as it showed most efficient therapeutic effects among the assayed groups. Murine models of IL-13-driven airway inflammation have reported that intranasal administration of IL-13 enhances the expression of mucus markers while decreasing lung tight junction mRNA and protein levels (121). As shown in **Figure R.45**, our experimental data demonstrates that WIN55,212-2 decreased the IL-13-induced lung mRNA expression levels of the goblet cell markers *Muc5ac* and *Gob5*, while restored to normal the levels of the club cell marker *Scgb1a1* and the tight junction protein *ZO-1*. Similarly, a reduced expression of the eosinophil-chemoattractant cytokine *Il5* was found in mice receiving IL-13 in the presence of the cannabinoid (**Figure R.45**), supporting the inhibition of type 2 inflammation in the mice lungs. Together, our findings indicate that WIN55,212-2 inhibits the IL-13-driven

pathogenic mucus overproduction and eosinophilia while confirming the preservation of homeostatic club cell populations and epithelial barrier integrity.

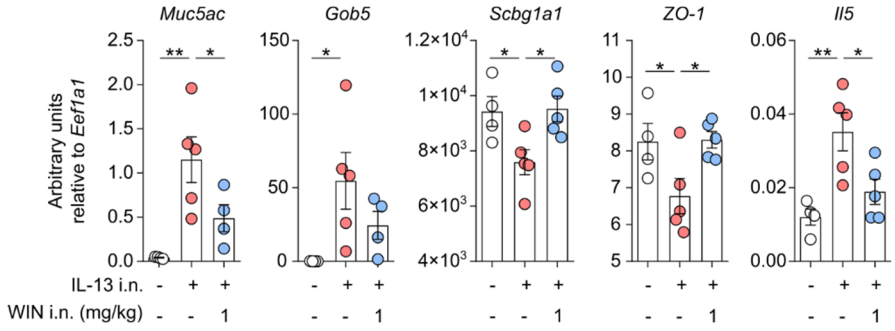

Figure R.45. WIN55,212-2 impairs the IL-13-mediated inflammatory reshaping of the lung cellular landscape. qPCR determination of mRNA expression levels of the indicated genes in the different assayed mice groups (n = 4-5). All data are shown as mean ± SEM. Statistical significance was determined by One-way ANOVA followed by Holm-Sidak's multiple comparisons test: * p <0.05, and ** p <0.01.

To further corroborate our data, we carried out hematoxylin and eosin (H&E) and periodic acid Schiff (PAS) stainings of the lungs from the different groups of mice. H&E staining revealed that intranasal administration of IL-13 significantly increased the recruitment of inflammatory cells into the perivascular and peribronchial areas of mice, which were decreased when administered in combination with the synthetic cannabinoid (**Figure R.46**).

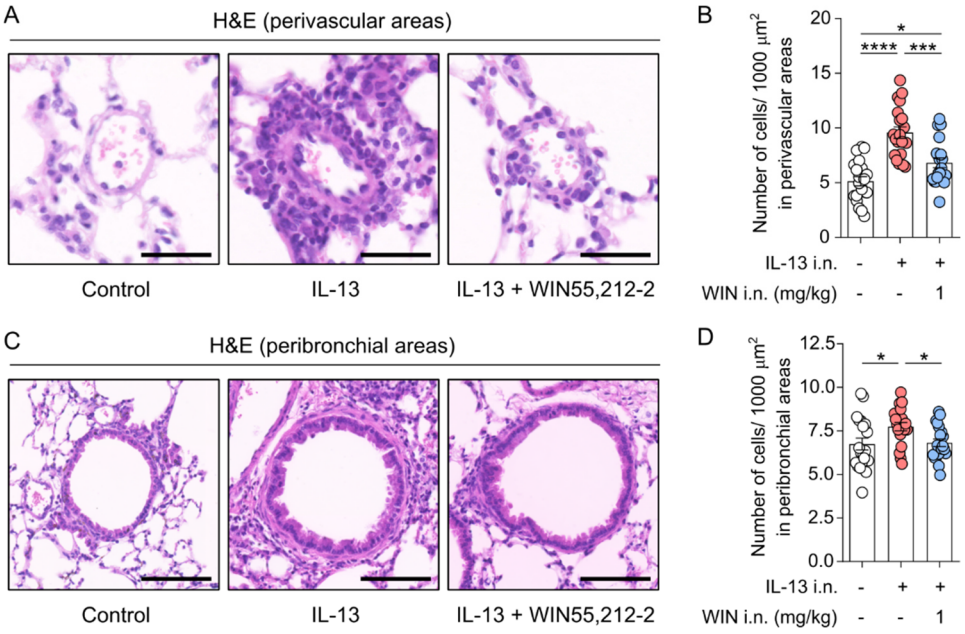

Figure R.46. WIN55,212-2 inhibits the IL-13-dependent inflammatory cell recruitment in mice lungs. Representative images of vascular (**A**) or bronchial (**C**) areas from mouse lung tissue sections stained with H&E. Quantification of inflammatory cell recruitment in perivascular (**B**) and peribronchial (**D**) areas of H&E-stained lung tissue sections. Scale bars: 40 µm (perivascular images) or 100 µm (peribronchial images), (n = 20 microscopy fields from 2 random mice per group). All data are shown as mean ± SEM. Statistical significance was determined by One-way ANOVA followed by Holm-Sidak's multiple comparisons test (B and D): * p <0.05, *** p <0.001, and **** p <0.0001.

As previously reported, intranasal administration of IL-13 increases lung mucus production by mechanisms dependent on STAT6 activation in airway epithelial cells (132). Accordingly, our analysis from PAS-stained lung tissue sections showed an enhancement of mucus secretion in the airways of mice intranasally administered with IL-13. Notably, mice that were treated with WIN55,212-2 displayed a significant reduction of the IL-13-induced mucus overproduction (**Figure R.47**).

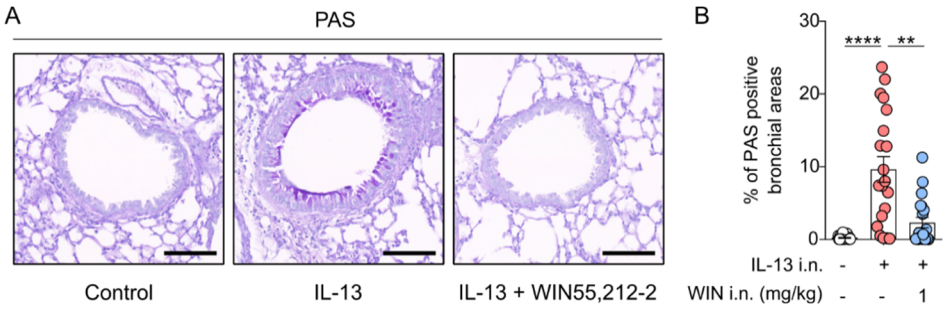

Figure R.47. WIN55,212-2 impairs the IL-13-induced mucus overproduction in the lungs of mice. Representative images (**A**) and quantification of mucus production (**B**) in bronchial areas from mouse lung tissue sections stained with PAS. Scale bars: 100 µm, (n = 20 microscopy fields from 2 random mice per group). All data are shown as mean ± SEM. Statistical significance was determined by Kruskal-Wallis test followed by Dunn's correction for multiple comparisons: ** p <0.01 and **** p <0.0001.

In summary, our findings validate our *in vitro* data and confirm the capacity of WIN55,212-2 to impair the development of type 2-dependent asthma features *in vivo.*

3.2. Investigate the potential immunomodulatory properties of WIN55,212-2 in *in vitro* and *in vivo* models of HDM-induced asthma.

Murine models of cytokine-induced airway inflammation are quite relevant for the study of specific cellular targets in asthma. However, aeroallergen-induced eosinophilic asthma models provide a more physiologically relevant perspective (264). Therefore, we sought to corroborate the therapeutic potential of WIN55,212-2 in an allergic asthma model induced by the airborne perennial allergen, HDM.

The latest research on type 2 chronic inflammatory diseases like asthma points out that the better understanding of the upstream disease-driving pathways as well as the identification of novel strategies that target them is crucial for the development of new therapies (97). In this context, recent evidence indicates that the airway epithelium is a major orchestrator of inflammation in asthma, playing an essential role in disease onset and severity (103). Additionally, antigen presenting cells, specially DCs, play key roles in asthma pathogenesis as bridging point between innate and adaptive immunity (93). We have previously demonstrated that WIN55,212-2 exerts immunomodulatory properties on DCs in the context of Th2-diseases such peanut allergy. Therefore, we hypothesized that WIN55,212-2 might protect from HDM-induced allergic asthma by synergic mechanisms combining its immunomodulatory properties on DCs and barrier protective functions in the context of type 2 inflammation.

To evaluate whether WIN55,212-2 confers tolerogenic properties to DCs encountering HDM in the airways, we differentiated hmoDCs and treated them with medium (control) or HDM in the absence

or presence of the cannabinoid. Afterwards, we analyzed the functional and phenotypical characteristics of the cells by measuring their cytokine signature and activation marker expression. As shown in **Figure R.48**, stimulation with HDM enhanced the expression of the maturation marker CD83 and the costimulatory molecule OX40L, which were significantly inhibited by stimulation in the presence of WIN55,212-2. OX40L has been described to play a crucial role in allergic lung inflammation, as the blockage of its receptor OX40 prevents *in vitro* allergic responses in humans and HDM-induced airway inflammation *in vivo* (265). Moreover, the expression of OX40L by DCs is involved in the induction of Th2 cell responses and is upregulated by epithelial-derived TSLP (266). Considering these facts, our results suggest that WIN55,212-2 inhibits the HDM-induced maturation of DCs and impairs the expression of the type 2 polarizing factor OX40L. Together with our findings on the inhibition of IL-13-dependent TSLP production by WIN55,2122 in HBECs, the TSLP/OX40L axis might well represent a potential key target of WIN55,212-2 in the context asthma.

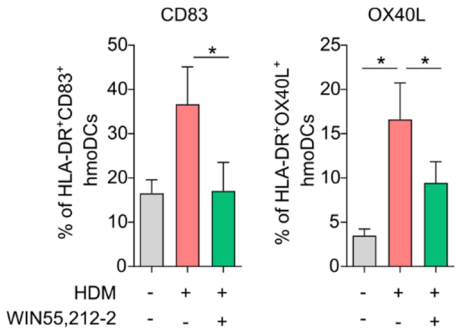

Figure R.48. WIN55,212-2 inhibits the HDM-induced maturation of DCs. Percentage of HLA$^+$ CD83$^+$ or HLA$^+$ OX40L$^+$ hmoDCs after 18 h stimulation with medium (control), HDM (100 µg/mL) or HDM plus WIN55,212-2 (10 µM) (n = 7-8). All values are shown as mean ± SEM. Statistical significance was determined by One-way ANOVA followed by Dunnett's multiple comparisons correction: * $p < 0.05$.

The analysis of the cytokine signature of stimulated hmoDCs showed that HDM enhanced the production of proinflammatory mediators TNFα, IL-1β and IL-6 as well as significant amounts of the anti-inflammatory IL-10. Of note, stimulation in the presence of WIN55,212-2 significantly inhibited the production of IL-1β, IL-6 and IL-10, with a non-significant downwards tendency in the production of TNFα as well (**Figure R.49**). Our data resemble to the previous reported effects of WIN55,212-2 in hmoDCs stimulated with LPS or a crude peanut extract, in which the cannabinoid shut down cytokine production. However, this immature phenotype and compromised cytokine production did not affect the capacity of WIN55,212-2 treated DCs to polarize Treg responses (49, 203).

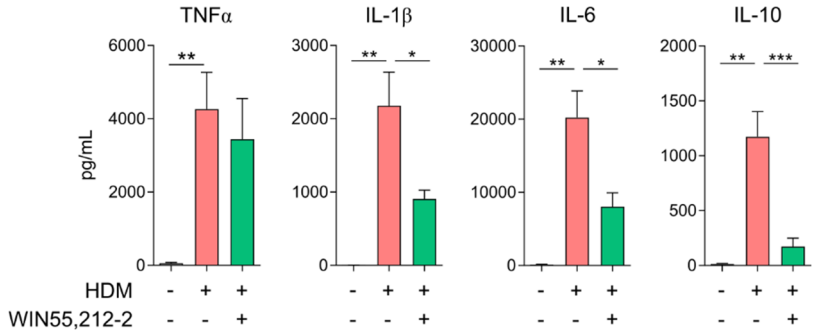

Figure R.49. WIN55,212-2 impairs cytokine production induced by HDM in hmoDCs. Concentrations of the indicated cytokines in cell-free supernatants after 18 h stimulation of hmoDCs with medium (control), HDM (100 µg/mL) or HDM plus WIN55,212-2 (10 µM) (n = 8-10). All values are shown as mean ± SEM. Statistical significance was determined by One-way ANOVA followed by Dunnett's multiple comparisons correction: * $p < 0.05$, ** $p < 0.01$ and *** $p < 0.001$.

To assess the capacity of WIN55212-2 to modulate the polarization of T cell responses by HDM-activated DCs, we performed coculture experiments with naïve T cells as described previously (see **Figure M.2** in Materials and Methods section). HDM-stimulated hmoDCs generated T cells producing high levels of IFNγ and IL-5, which were significantly reduced when T cells were primed by hmoDCs stimulated with the combination of HDM and WIN55,212-2. Interestingly, no changes were observed regarding IL-10 production in any of the assayed conditions (**Figure R.50A**), suggesting that WIN55,212-2 suppresses effector T cell responses without altering the levels of anti-inflammatory IL-10. Flow cytometric analysis was performed to evaluate the potential induction of FOXP3⁺ Tregs in our experimental protocol. However, no differences in the proportions of Tregs were found in any of the assayed conditions (**Figure R.50B**).

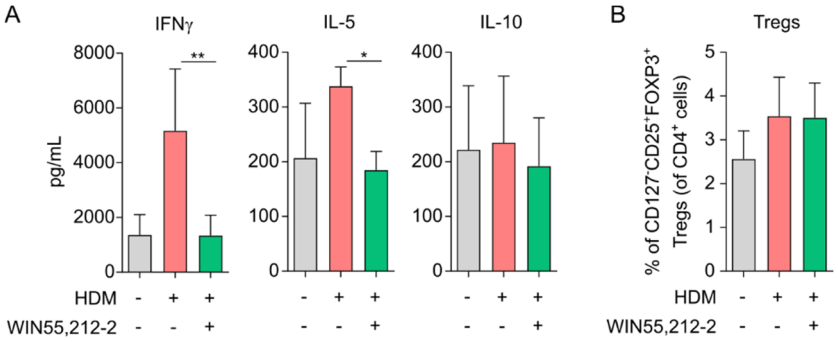

Figure R.50. WIN55,212-2 shapes the polarization of T cell responses by HDM-activated hmoDCs. (**A**) Cytokines produced by T cells primed by hmoDCs with medium (control), HDM (100 µg/mL) or HDM plus WIN55,212-2 (10 µM) for 5 days (n = 5-7). (**B**) Percentage of $CD4^{+}CD25^{high}CD127^{-}FOXP3^{high}$ Tregs induced by allogeneic hmoDCs treated with the indicated conditions (n=8). All values are shown as mean ± SEM. Statistical significance was determined by ratio paired t test (IFNγ) or paired t test (IL-5) : * $p < 0.05$ and ** $p < 0.01$.

Collectively, our findings indicate that WIN55,212-2 impairs the HDM-induced maturation of hmoDCs and suppresses their capacity to promote effector T cell responses without affecting regulatory responses. In the context of HDM-driven asthma, WIN55,212-2 effects on DCs might target type 2 inflammation by downregulating the expression of OX40L and compromising the induction and expansion of Th2 cells.

To further validate whether the combined effects of WIN55,212-2 on DCs and the airway epithelium may have any impact on key events of allergic asthma pathogenesis, we sought to investigate its potential therapeutic efficacy in an acute model of HDM-induced allergic eosinophilic asthma.

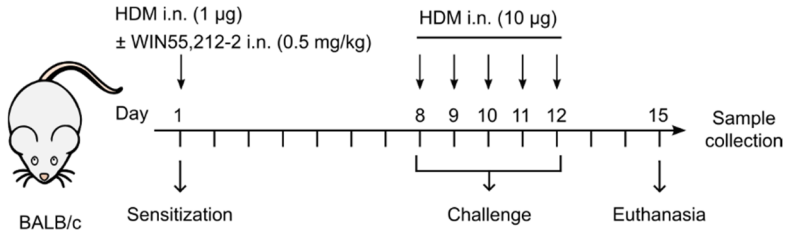

Figure R.51. Schematic illustration of the HDM-induced allergic eosinophilic asthma model and therapeutic administration protocol.

As displayed in **Figure R.51**, mice were intranasally sensitized on day 1 and afterwards challenged during 5 consecutive days (days 8-12) with HDM extracts. To evaluate the capacity of WIN55,212-2 to interfere with allergen sensitization and subsequent type 2 eosinophilic airway inflammation, a group of mice was sensitized with HDM in the presence of WIN55,212-2 at day 1 and challenged normally at days 8 to 12. In addition, a group of animals receiving intranasal PBS during sensitization and challenge was used as baseline control. After 72 h since the last challenge mice were sacrificed and BALF, spleen, and serum samples were collected to evaluate parameters of the major asthmatic features.

First, we analyzed the cellular infiltration in the airways of mice. The quantification of the cellular recruitment into BALF of mice demonstrated that administration of WIN55,212-2 during sensitization prevented the infiltration of immune cells into the BALF of HDM-challenged mice (**Figure R.52**), suggesting a potent capacity to impair the initiation of immune responses in the airways.

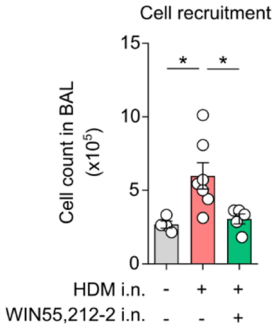

Figure R.52. WIN55,212-2 regulates cellular infiltration into the airways of asthmatic mice. Determination of the number of cells in BALF of mice from the indicated groups (n= 4-7). All values are shown as mean ± SEM. Statistical significance was determined by One-way ANOVA followed by Holm-Sidak's multiple comparisons correction: * p <0.05.

Next, we performed flow cytometric analysis to characterize the inflammatory cell populations recruited into the airways of the animals. Mice sensitized and challenged with HDM showed a significant infiltration of eosinophils, neutrophils, T cells, Th2 cells, B cells and DCs. Of note, the administration of WIN55,212-2 during sensitization to HDM significantly decreased the amount of eosinophils and Th2 cells, confirming a strong inhibition of type 2 responses in the airways. Additionally, solid downwards tendencies were found in the neutrophil, T cell, B cell and DC compartments (**Figure R.53**). Together, our data agree with the previous *in vivo* studies reporting a reduced cellular recruitment in the airways of rodents treated with phytocannabinoids such as THC, CBD or CP55,940 (198, 199, 267).

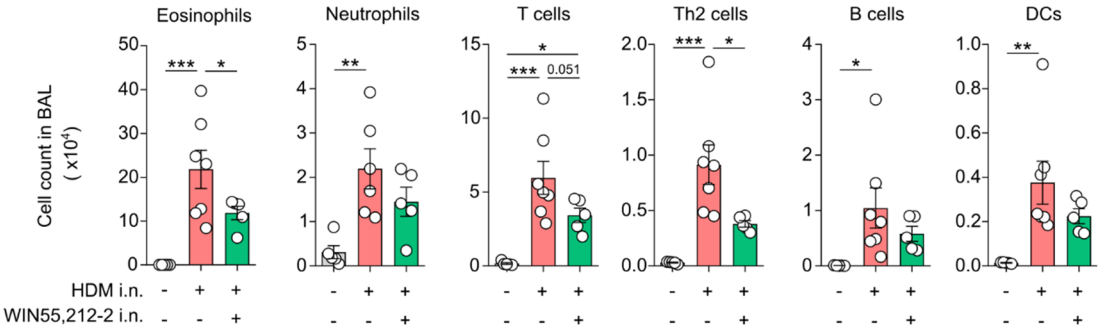

Figure R.53. WIN55,212-2 inhibits the inflammatory cell recruitment into the airways of asthmatic mice. Flow cytometric characterization of BALF cell populations 72 h after last challenge of mice from the indicated groups (n= 4-7). All values are shown as mean ± SEM. Statistical significance was determined by One-way ANOVA followed by Holm-Sidak's multiple comparisons correction: * p < 0.05, ** p < 0.01 and *** p < 0.001.

To assess the potential involvement of the barrier protective effects of WIN55,212-2 in the model, we analyzed the expression of epithelial markers of barrier status and damage in BALF. We observed that the translocation of serum proteins into bronchoalveolar space was increased in HDM asthmatic mice and associated with a significant enhancement of the injury marker LDH in BALF. Although no significant changes were observed in the group of mice receiving WIN55,212-2 during sensitization, a trend towards a reduction in epithelial dysfunction and damage markers was shown (**Figure R.54**). Our findings suggest that the protective effects of the cannabinoid on barrier impairment are moderate under these assayed conditions. Such relatively poor response might well be explained by the protease activity of HDM extracts which could directly impact the airway epithelial barrier during challenge with the allergen (268, 269), when no cannabinoid administration was conducted. Future experiments should explore the potential preventive or therapeutic ability of WIN55,212-2 to protect from HDM-induced barrier alterations by employing different doses and administration protocols.

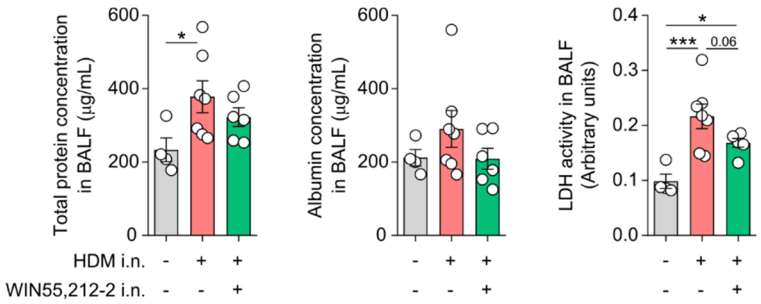

Figure R.54. Modulation of airway epithelial barrier function in HDM-asthmatic mice treated with WIN55,212-2. Total protein content, murine serum albumin concentration and LDH activity in BALF 72 h after last challenge of the indicated mice groups (n = 4-7). All data are represented as mean ± SEM. Statistical significance was determined by One-way ANOVA followed by Holm-Sidak's multiple comparisons test: * p <0.05 and *** p <0.001.

The coordinated interplay between the airway epithelium and lung DCs is crucial for the orchestration of type 2 responses to allergens (93). Therefore, we wondered whether the administration of WIN55,212-2 during the intranasal sensitization of mice to HDM, may prevent the generation of systemic adaptive responses to the allergen. We collected the spleens of mice 72 h after the last challenge, isolated splenocytes and re-stimulated them *ex vivo* with HDM to assess allergen-specific responses. Splenocytes from HDM-asthmatic mice produced high levels of IFNγ, IL-5 and IL-10 compared to controls, confirming allergen-sensitization and the development of HDM-specific T cell responses in the spleen. Remarkably, we observed that mice sensitized with HDM plus WIN55,212-2 produced significantly lower amounts of IFNγ and IL-5 than the group sensitized with HDM alone, without significant changes in IL-10 production (**Figure R.55A**). Accordingly, mice receiving WIN55,212-2 during sensitization displayed higher IL-10/IFNγ and IL-10/IL-5 ratios (**Figure R.55B**). These findings are consistent with our previous *in vitro* coculture experiments in humans and corroborate the capacity of WIN55,212-2 to suppress the generation of HDM-specific effector T cells while preserving IL-10-dependent tolerogenic responses.

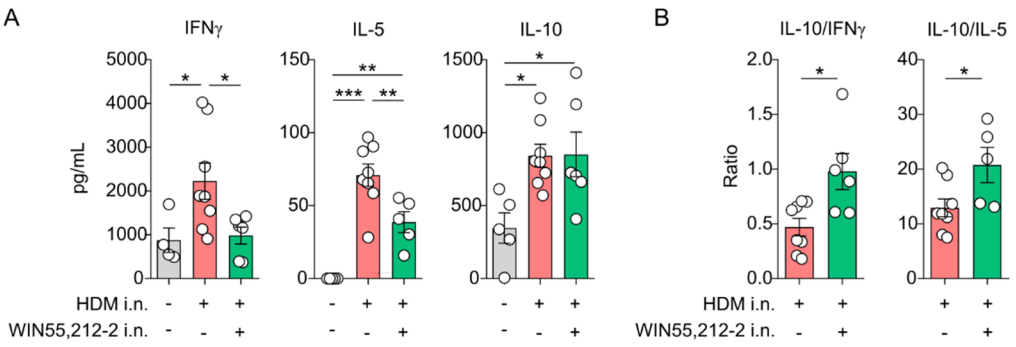

Figure R.55. WIN55,212-2 suppresses the induction of systemic HDM-specific effector responses *in vivo*. (**A**) Cytokines and (**B**) ratios produced by splenocytes from the indicated groups *ex vivo* stimulated with HDM (50 µg/mL) for 3 days (n= 5-8). All values are shown as mean ± SEM. Statistical significance was determined by One-way ANOVA followed by Holm-Sidak's multiple comparisons correction (A) or unpaired t test (B): * $p < 0.05$, ** $p < 0.01$ and *** $p < 0.001$.

To verify the impairment of HDM sensitization by the synthetic cannabinoid, we quantified the total IgE levels in the different groups of mice. As shown in **Figure R.56**, mice sensitized with HDM displayed significantly enhanced levels of total IgE in serum, which were decreased in mice sensitized to HDM in the presence of WIN55,212-2, confirming its efficacy to interfere with HDM allergic sensitization *in vivo*.

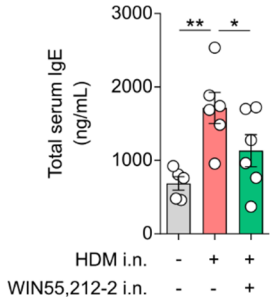

Figure R.56. WIN55,212-2 impairs HDM allergic sensitization *in vivo*. Total IgE levels in serum of the indicated mice groups (n= 5-6). All values are shown as mean ± SEM. Statistical significance was determined by One-way ANOVA followed by Holm-Sidak's multiple comparisons correction: * $p < 0.05$ and ** $p < 0.01$.

In summary, we uncovered the unprecedented capacity of the synthetic cannabinoid WIN55,212-2 to inhibit local airway inflammation as well as systemic immune responses and IgE generation in a murine model of HDM-induced allergic eosinophilic asthma. Our data confirm in a new experimental setting, our previous published data demonstrating the ability of WIN55,212-2 to impair epicutaneous sensitization to peanut extracts, as well as its efficacy to promote allergen-specific tolerance and inhibit effector T cell responses *in vivo* (49, 203). Nonetheless, further studies are guaranteed to better explore and understand the potential synergistic effects of the synthetic cannabinoid WIN55,212-2 as immunomodulator but also as regulator of epithelial barrier function in the context of airway inflammatory diseases.

Objective 4: Identification of new potentially harmful agents for the airway epithelium and lung function

Over the last decades, lifestyle changes associated with urbanization and technological advances in modern societies have been accompanied by an alarming rise in the prevalence of chronic non-communicable diseases. The epithelial barrier theory attributes these events to the exposure to newly introduced substances capable of compromising the homeostatic functions of epithelial barriers. Epithelial-damaging compounds include pollutants such as particulate matter, ozone, diesel exhaust particles, nano-and/or micro-plastics, detergents and surfactants used in cleaning products, or certain additives, emulsifiers and flavor enhancers employed in the food industry (83, 84, 87).

According to the epithelial barrier theory, the exposome, meaning the sum of all the environmental exposures during the lifetime of an individual, together with genetic factors determine the risk for epithelial barrier disruption and potential development or exacerbation of chronic non-communicable pathologies (87). Certain groups of people are more susceptible due to higher exposition to toxic substances. Compelling epidemiological evidence demonstrates that cleaning workers highly exposed to detergents, disinfectants and irritants are more susceptible to the development of asthma and other respiratory diseases (270, 271). High performance athletes exposed to airborne pollutants and toxic substances are prone to infections as well as lung and gut inflammatory diseases (272). Likewise, populations living in geographic locations more frequently hit by sandstorms, wildfires or other sources of particulate matter are at higher risk of developing inflammatory disorders (273, 274). Therefore, the identification of new epithelial-damaging agents as well as susceptible population groups at risk of a deleterious exposome are required.

Similar to how urbanization and modernization have dramatically reshaped the exposome of populations worldwide since the 1960s, new advances in the space race could impact astronauts' exposome in the short term and potentially humanity in the long-term future. In this context, in collaboration with Dr. Jorge Domínguez-Andrés and Dr. Mihai Netea from Radboud University Medical Centre, Netherlands, we sought to explore the potential deleterious effects of new substances which may be encountered during the exploration of outer space. Particularly, we focused on the potential consequences in the human respiratory tract of the exposition to the particulate materials found in the surface of celestial bodies, known as regoliths.

4.1. Study the potential deleterious effects of Lunar and Martian regolith exposure on the integrity and function of the human bronchial epithelium

To study the potential harmful effects of regoliths in the airway epithelial barrier, ALI cultures of HBECs were exposed to simulants of Lunar and Martian regoliths in a model of daily repetitive exposure for three consecutive days (**Figure R.57**). A Lunar mare simulant, LMS-1, and two Mars global simulants, MGS-1 and MGS-1S, kindly provided by our collaborators Dr. Jorge Domínguez-Andrés and Dr. Mihai

Netea, were employed in this protocol. Alternatively, cultures stimulated with PBS or ground silica quartz (SiO_2) were used as baseline controls or Earth particulate matter controls, respectively.

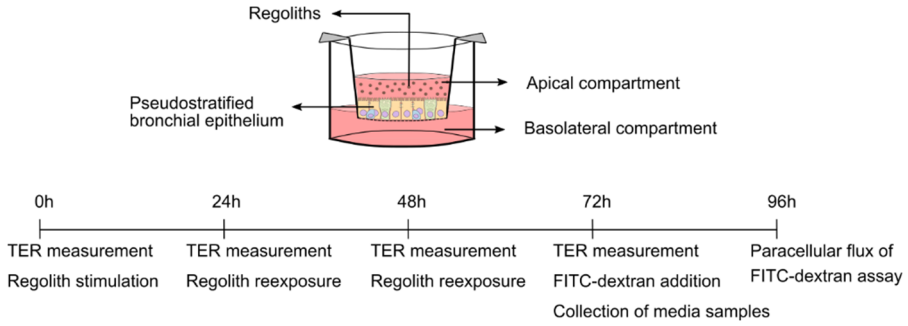

Figure R.57. Schematic representation of the regolith exposure protocol to ALI cultures of HBECs.

Briefly, once cultures reached complete differentiation they were apically exposed to the regolith simulants. After 24 h, the apical compartment was emptied and re-filled with fresh regolith-containing medium. The next day, this same process was repeated to complete the three-day protocol. To assess epithelial barrier integrity, TER values were followed up every day and the paracellular flux to apically administered FITC-dextran was evaluated 24 h after the last stimulation. In addition, medium samples from apical and basolateral compartments were collected 24 h after the last stimulation (**Figure R.57**).

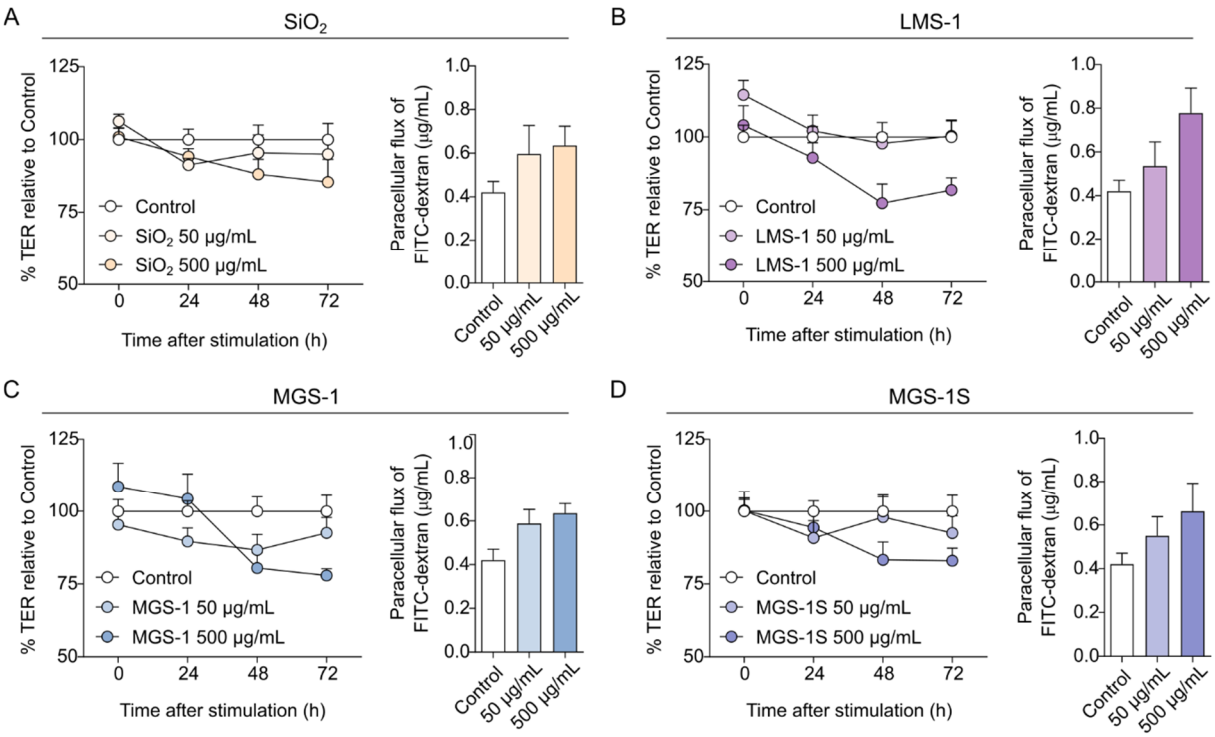

Figure R.58. Dose-response study of the effect of regolith simulants on airway epithelial barrier. Left panels show TER values relative to control unstimulated cells and right panels display paracelular permeability to apically administered FITC-dextran after stimulation of cultures with the indicated doses of SiO_2 (**A**), LMS-1 (**B**), MGS-1 (**C**) or MGS-1S (**D**) (n = 5-9 using 3 donors). All data are shown as mean ± SEM.

First, we assayed several doses of the regoliths to identify their potential deleterious effects on the bronchial epithelial barrier integrity. Since Earth silica is known to alter the barrier function of the airway epithelium (275), we included cultures exposed to doses of 50 or 500 µg/mL of Earth silica particles (SiO_2) as positive controls. As reported in **Figure R.58**, the analysis of TER values showed that the dose of 50 µg/mL did not induce major changes in any of the culture conditions exposed to Earth silica or to any of the regoliths assayed. However, at the highest stimulation dose of 500 µg/mL, we found that Earth silica reduced TER values compared to unstimulated controls indicating a loss in the integrity of the epithelial barrier of the cultures. Interestingly, all Lunar and Martian regoliths including LMS-1, MGS-1 or MGS-1S also decreased TER levels compared to controls, at the dose of 500 µg/mL. These effects were evidenced as soon as 48 h after the first stimulation and maintained until the last measurement at 72 h after the first exposure. Supporting these data, the paracellular permeability to FITC-dextran of cultures exposed to either LMS-1, MGS-1 or MGS-1S was increased in both of the doses used in the experiments and displayed a clear dose-response tendency, confirming the capacity of regoliths to disrupt airway epithelial barrier function. Again, Earth silica promoted an enhanced airway permeability in a similar dose-dependent pattern to the regoliths, suggesting that the capacity of regolith simulants to induce barrier dysfunction might well resemble the harmful exposure to silica dusts in Earth.

Next, we exclusively compared the effects of the different exposure conditions used at 500 µg/mL, as this dose exerted the most harmful potential.

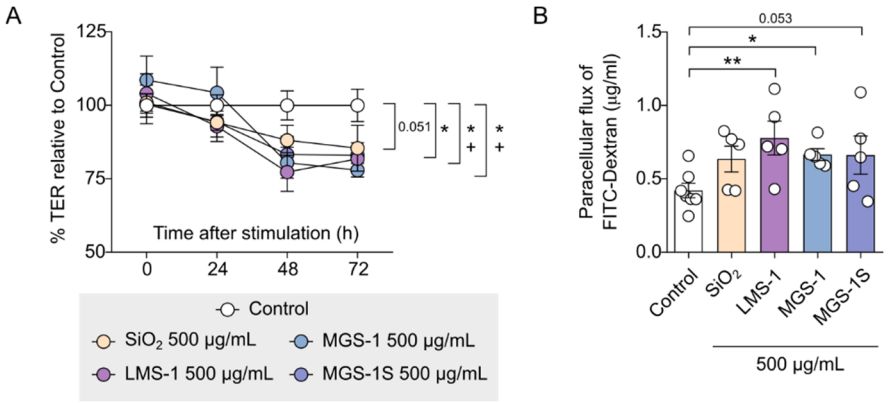

Figure R.59. Lunar and Martian regolith simulants impair airway epithelial barriers. (**A**) TER values relative to unstimulated cells at the indicated assayed timepoints and stimulations (n = 6-9 using 3 donors). + Control vs. indicated treatment 48h after stimulation, * Control vs. indicated treatment 72h after stimulation. (**B**) Paracellular permeability to apically administered FITC-dextran after stimulation of cultures with the indicated treatments (n = 5-7 using 3 donors). All data are shown as mean ± SEM. Statistical significance was determined by Two-way ANOVA followed by Fisher's LSD test (A) or One-way ANOVA followed by Fisher's LSD test (B): *,+ $p < 0.05$ and ** $p < 0.01$.

Compared to unstimulated controls, we found that LMS-1 and MGS-1 promoted the earliest significant drop in TER values 48 h after the first exposure of the cells, which remained significantly below control levels also at 72 h timepoint. Meanwhile, the Martian regolith, MGS-1S, induced a significant decrease in TER values only after 72 h since the first stimulation. The exposure of ALI cultures to Earth silica did not significantly reduce TER at any of the timepoints assayed, but displayed a solid downward tendency compared to control cultures after 72 h of the first stimulation (**Figure R.59A**). In

line with these findings, the analysis of the paracellular flux showed that LMS-1 and MGS-1 displayed significant increments in airway permeability to FITC-dextran compared to control cultures, whereas Earth silica and MGS-1S only displayed a non-significant trend towards a higher permeability (**Figure R.59B**). Our data suggest that LMS-1 and MGS-1 could be potentially more harmful to the airway epithelium than silica or MGS-1S.

The exposure of airway epithelial cells to particulate matter has been reported to affect cell viability at high doses (275, 276). The analysis of the LDH release of ALI cultures exposed to the highest dose of regoliths or silica demonstrated that none of the assayed conditions induced significant cytotoxicity in the cultures (**Figure R.60**), indicating that the epithelial barrier damaging effects of regoliths are not directly related to epithelial cell death at these assayed conditions.

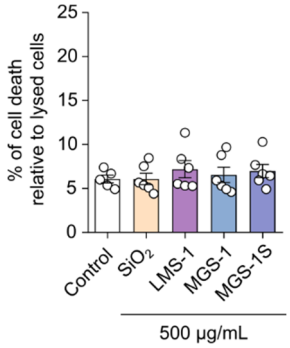

Figure R.60. Regolith simulants do not compromise viability of ALI cultures of HBECs. Percentage of cell death calculated as the relative LDH activity in culture media compared to a positive control of lysed cells. Data are shown as mean ± SEM.

A major feature observed after exposure of the airway epithelium to particulate matter is the orchestration of inflammatory responses (275, 276). To explore the potential initiation of immune responses by lung epithelial cells exposed to regolith simulants, we analyzed the inflammatory cytokines produced into the apical and basolateral compartments of ALI cultures after stimulation.

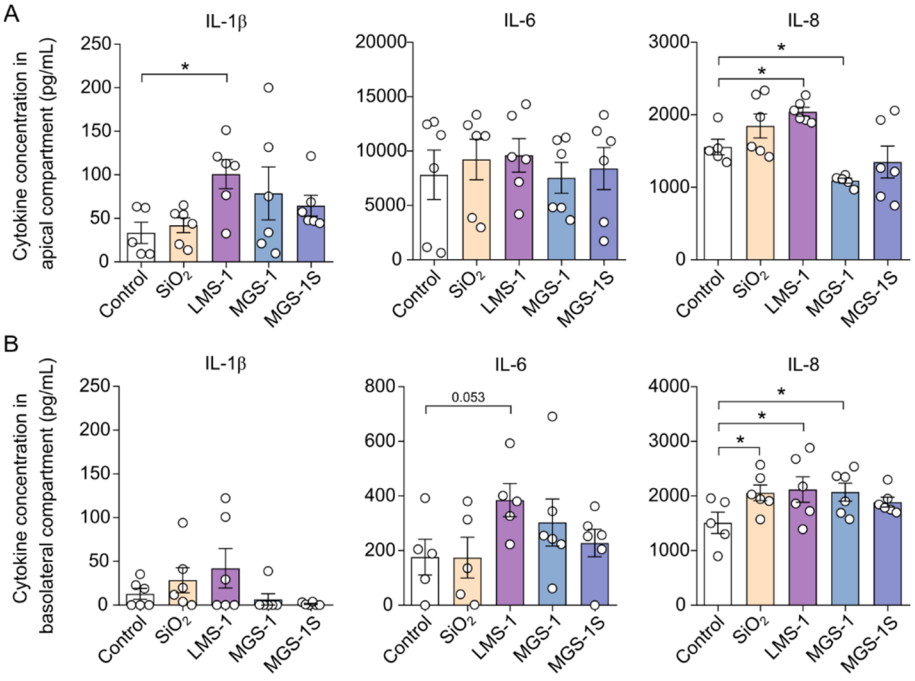

Figure R.61. Lunar and Martian regolith simulants can initiate inflammatory responses in airway epithelial cell cultures. Cytokine measurements from (**A**) the apical compartment and (**B**) the basolateral compartment (n=5-6 using 3 donors). All data are represented as mean ± SEM. Statistical significance was determined by Kruskal-Wallis test followed by uncorrected Dunn's test or One-way ANOVA followed by Fisher's LSD test: * $p < 0.05$.

At the apical compartment, LMS-1 triggered significantly higher levels of IL-1β and IL-8 compared to PBS-stimulated (Control) cultures, but neither LMS-1 nor any of the other stimuli promoted significant changes in apical IL-6 concentration. Silica and MGS-1S did not significantly modify the production of any of the cytokines assayed, while MGS-1 lowered apical IL-8 levels (**Figure R.61A**). Differential secretion of cytokines and chemokines towards the apical or basolateral compartment has been reported in *in vitro* stimulated cultures of HBECs (277). Accordingly, we also observed differences in the cytokine abundance between the apical and basolateral compartment of our cultures. In the basolateral compartment, we found that SiO_2, LMS-1 and MGS-1 significantly upregulate IL-8 production as well as a solid upwards tendency in cultures exposed to MGS-1S. LMS-1 also tended to increase IL-6 and IL-1β levels, but no significant changes were observed regarding the production of those cytokines by any of the other stimuli (**Figure R61B**). Collectively, our data indicates that regolith simulants and silica are capable of inducing polarized secretion of inflammatory mediators such as IL-8 in the airway epithelium. In particular, LMS-1 displayed the most potent inflammatory profile as it induced the release of IL-1β into the apical compartment, suggesting the activation of inflammasome signaling.

In summary, we report that regolith simulants, especially LMS-1 and MGS-1, compromise the epithelial barrier integrity and trigger inflammation in an ALI culture *in vitro* model of repetitive exposure to HBECs.

4.2. Assessment of the potential capacity of Lunar and Martian regoliths to induce in vivo acute lung inflammation in mice

To validate our *in vitro* results suggesting that Lunar and Martian regoliths could be detrimental to the airways, C57BL/6J mice were intranasally instilled with PBS (control), silica (SiO_2), LMS-1 or MGS-1 for three consecutive days and the *in vivo* epithelial barrier status and inflammatory features were evaluated (**Figure R.62**). Based on the 3Rs rule for animal research, we selected LMS-1 and MGS-1 and omitted MGS-1S from the *in vivo* experiment as the first two regolith simulants showed most disruptive potential on airway epithelial cell cultures while MGS-1S effects were comparatively moderate.

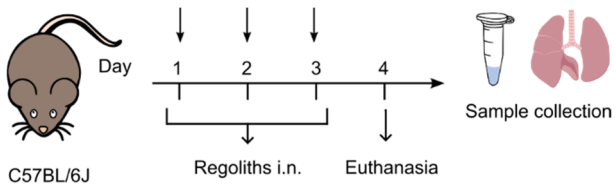

Figure R.62. Schematic representation of the *in vivo* murine model of intranasal regolith exposure.

Analysis of epithelial barrier integrity markers showed that LMS-1 caused the highest translocation of serum proteins into BALF, determined by increased levels of total protein and serum albumin contents (**Figure R.63A, B**), indicating that this regolith simulant displayed a potent barrier disruptive capacity *in vivo*, which is consistent with our previous *in vitro* findings. Moreover, mice receiving intranasal LMS-1 displayed significantly upregulated LDH activity in BALF (**Figure R.63C**), suggesting that barrier permeability was associated with epithelial cell damage. Similar tendencies were

found in mice treated with the Martian regolith simulant, MGS-1, but only significant in terms of the serum albumin content in BALF (**Figure R.63B**), suggesting that this regolith is potentially less harmful for the airway epithelial barrier than LMS-1. Of note, mice intranasally administered with silica, the used Earth control, which may well represent a murine model of silicosis (278), also displayed increased markers of epithelial barrier dysfunction (**Figure R.63A-C**).

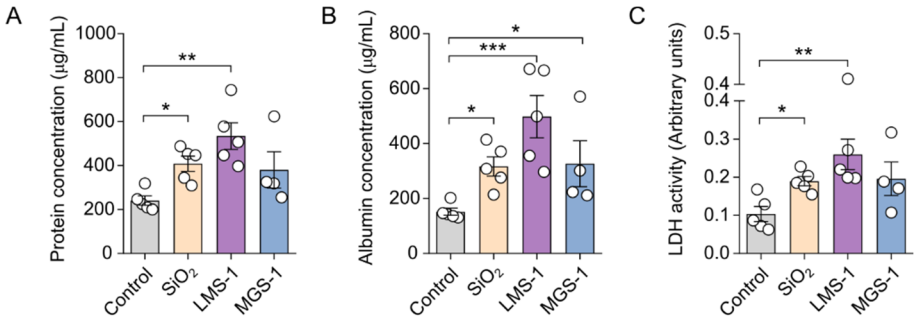

Figure R.63. Assessment of the *in vivo* barrier function of mice exposed to regolith simulants. Total protein content (**A**), murine serum albumin concentration (**B**) and LDH presence (**C**) in BALF 24 h after last treatment of the indicated groups of mice (n = 4-5). All data are expressed as mean ± SEM. Statistical significance was determined by Kruskal-Wallis test followed by uncorrected Dunn's test: * p <0.05, ** p <0.01, and *** p <0.001.

To further evaluate whether the exposition to regoliths shapes the architecture and cellular composition of the airways of mice, we performed lung mRNA expression analysis of gene markers for different airway epithelial cell subsets and functional properties.

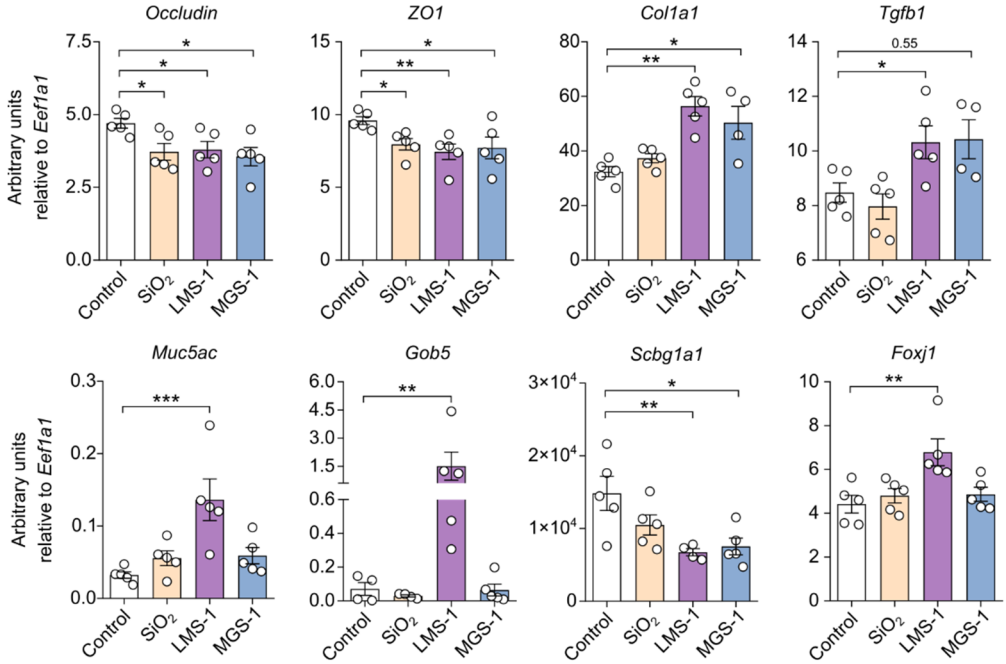

Figure R.64. Modulation of the lung epithelial landscape and function by regolith simulants *in vivo*. (n = 4-5). Quantification of the mRNA expression levels of the indicated gene markers after 24 h since the last administration of mice with the indicated stimuli. All data are expressed as mean ± SEM. Statistical significance was determined by Kruskal-Wallis test followed by uncorrected Dunn's test: * p <0.05, ** p <0.01, and *** p <0.001.

Intranasal instillation with silica significantly reduced the expression of the tight junction proteins *Occludin* and *ZO-1*, confirming the barrier disruptive capabilities, but did not have major consequences in the expression of other gene markers. In contrast, LMS-1 decreased the mRNA levels of tight junctions but also upregulated the expression of fibrosis markers such as *Col1a1* and *Tgfb*; goblet cell markers including *Muc5ac* and *Gob5*; and the cilliogenesis master transcription factor *Foxj1*, while reduced *Scgb1a1*, which identifies club cells. Similarly, MGS-1 reduced *Occludin*, *ZO-1* and *Scgb1a1* expression, while enhancing fibrosis-related genes (**Figure R.64**).

Together, our findings indicate that regolith simulants reshape the cellular landscape and composition of the murine airways by reducing the epithelial tight junction complexes, decreasing the homeostatic populations of club cells and inducing airway fibrosis. Interestingly, the Lunar regolith simulant LMS-1 significantly enhanced the gene markers related to mucus secretion suggesting goblet cell hyperplasia. The fact that we did not observe the upregulation of fibrosis markers after intranasal instillation of mice with silica particles contrast with compelling experimental evidence reporting fibrosis as a major feature of silicosis. Nonetheless, this might be explained by the short duration of the animal model, since fibrosis takes weeks to develop in mouse models of silicosis (278, 279). Beyond, it underlines the potential fibrotic capacity of regolith simulants, which did upregulate fibrosis markers at this early stage of exposition. Defective epithelial barrier function, fibrosis and mucus plugs are hallmark features of chronic airway inflammatory diseases such as asthma or COPD (280). Accordingly, we could extrapolate that regolith exposure in the respiratory tract could induce similar pathologies *in vivo*, highlighting their harmful potential to human health.

To assess the potential involvement of inflammatory pathways to the pathologic features observed after exposure to regolith simulants, we analyzed the expression of inflammatory genes by qPCR.

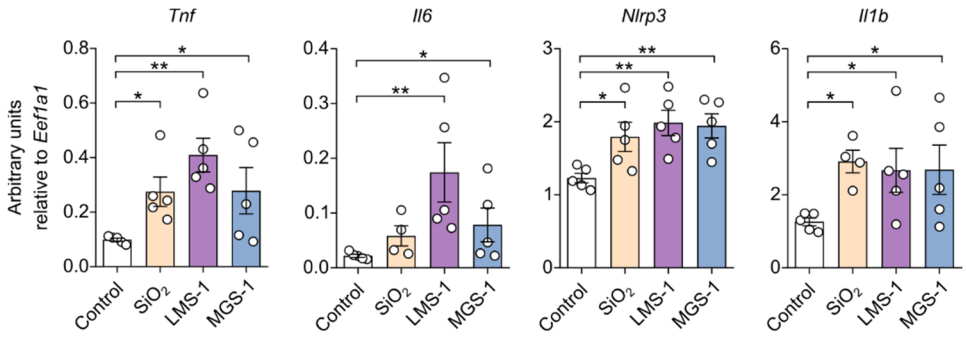

Figure R.65. Regolith simulants activate inflammatory signaling pathways *in vivo*. Quantification of the mRNA expression levels of the indicated gene markers after 24 h since the last administration of mice with the indicated conditions. All data are expressed as mean ± SEM. Statistical significance was determined by Kruskal-Wallis test followed by uncorrected Dunn's test: * p <0.05 and ** p <0.01.

Compared to controls, the lungs of mice treated with Lunar and Mars regolith simulants showed a significant upregulation of inflammatory mediators *Tnf* and *Il6*, which was accompanied by the induction of genes such as *Nlrp3* and *Il1b*, indicating an ongoing lung inflammation as well as the induction of inflammasome activation, respectively. Earth silica particles also induced a significant

increase in the expression of inflammatory genes *Tnf*, *Nlrp3* and *Il1b* (**Figure R.65**), similar to previous reports of mice models of silicosis (278, 279). Of note, the activation of inflammasome signaling is one of the major contributors to lung fibrosis in murine models of airway disease (279, 281), which agrees with the previously reported upregulation of *Col1a1* and *Tgfb* fibrosis markers in the lungs of mice treated with regolith simulants.

Next, to further investigate the recruitment of inflammatory cells into the airways of the different groups of mice, we analyzed lung tissue and BALF samples by H&E staining and flow cytometry. As displayed in **Figure R.66A**, H&E staining of lung tissue sections showed an increase in the number of immune cells surrounding the bronchial areas of mice exposed to either silica, LMS-1 or MGS-1. These results were supported by a significant enhanced cell recruitment into the BALF of mice intranasally instilled with silica or regolith simulants (**Figure R.66B**), confirming an ongoing inflammatory process in the airways of those mice. The most abundant cellular subset in the BALF of mice were alveolar macrophages, which were not significantly impacted by any of the assayed exposures. Nevertheless, silica and regolith treatments induced a significant recruitment of predominantly neutrophils but also eosinophils and, to a lesser extent, T cells and DCs in BALF (**Figure R.66C**). Our findings are consistent with the increased recruitment of inflammatory cells, especially neutrophils, in models of acute airway inflammation induced by silica particles (279).

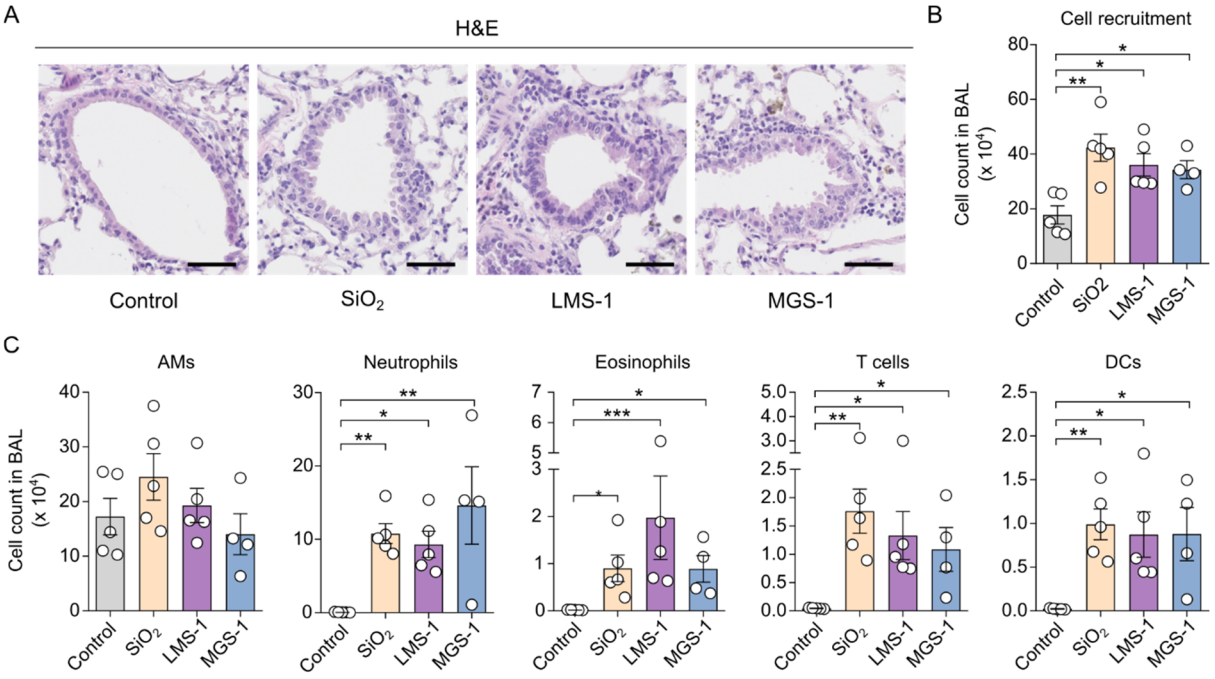

Figure R.66. Regolith simulants activate inflammatory immune responses in the airways of mice. (**A**) Representative H&E staining of lung tissue sections of mice treated with the indicated conditions. (**B**) Cell counts and (**C**) flow cytometric characterization of the cellular populations infiltrated into the BALF of the indicated mice (n = 4-5). All data are expressed as mean ± SEM. Statistical significance was determined by Kruskal-Wallis test followed by uncorrected Dunn's test: * p <0.05, ** p <0.01 and *** p <0.001.

Together with their deleterious impact on epithelial barrier integrity, our findings demonstrate that the potential exposure to regoliths during space missions, future human settlements and mineral

resource exploitations in outer space may be detrimental to human health. Future studies are warranted to better understand the underlying mechanisms of these harmful effects of regoliths in the airways and how specific particle properties (composition, size, etc.) affect the differential outcomes observed in our experimental data.

GLOBAL DISCUSSION

Asthma is the most prevalent chronic inflammatory disease of the airways, affecting both children and adults, and representing a high socio-economic burden worldwide. It is a complex syndrome encompassing different pheno-endotypes characterized by airway inflammation, BHR, mucus overproduction and airway remodeling, which ultimately lead to recurring respiratory symptoms and variable airflow limitation (91, 122).

Current mainstay therapies for asthma management consist of the use of bronchodilators and anti-inflammatory drugs targeting bronchoconstriction and airway inflammation to improve airflow obstruction. Nonetheless, conventional treatments display limitations in terms of disease control of severe patients or side effects associated with the use of high doses of corticosteroids. The use of biologic-based therapies provided a tailored treatment opportunity that has significantly improved the quality of life of many severe patients. However, they still face challenges regarding adequate patient phenotyping, high treatment costs, or their limited capacity to modify the course of the disease (97, 100, 139). Therefore, novel treatments are needed to overcome such inconveniences and improve current strategies in asthma. At this regard, compelling evidence has demonstrated the involvement of epithelial barrier defects in the development of chronic inflammatory diseases (83, 84, 87, 88). Therefore, novel safe and cost-efficient drugs not only targeting the inflammatory process but also directly improving the airway epithelial barrier function might well represent promising strategies for the prevention and treatment of the disease.

The endocannabinoid system (ECS) is a complex signaling network whose therapeutic exploitation is being explored for several immune-related pathologies, including asthma (144, 145, 178). Most preclinical studies of the potential therapeutic capacity of cannabinoids for asthma treatment focus on their role as bronchodilators or anti-inflammatory drugs (144, 179). For instance, the endocannabinoid AEA exerts airway relaxant effects both *in vitro* and *in vivo* (201), and the phytocannabinoids THC and CBD display anti-inflammatory effects in the airways of rodents (196-198). However, our understanding of the effects of these and other cannabinoids in the airway epithelium and its protective epithelial barrier functions is still scarce. Previous research from our group demonstrated the anti-inflammatory and tolerogenic capabilities of the synthetic cannabinoid WIN55,212-2 on different immune cell types including DCs and tonsil mononuclear cells, particularly highlighting its capacity to promote the generation of Tregs both *in vitro* and *in vivo* (49, 202-204). Additionally, the simultaneous administration of WIN55,212-2 during the onset of RV infection exerted a remarkable ability to restore RV-induced airway epithelial barrier disruption (177). In this Doctoral Thesis, we have further explored the therapeutic potential of WIN55,212-2 in the context of asthma. Particularly, we have characterized the anti-inflammatory properties of WIN55,212-2 during monocyte differentiation and macrophage activation, as well as its capacity to regulate epithelial barrier alterations induced by RVs and type 2 inflammation and the underlying mechanisms involved in such effects. Beyond, we have assessed the tolerogenic effects of WIN55,212-2 in the context of exposure to a common perennial allergen such as HDM and evaluated its therapeutic efficacy in murine models of airway inflammation and allergen-induced eosinophilic asthma.

Monocytes are versatile immune cells characterized for their capacity to differentiate into DCs and macrophages, especially during inflammatory conditions (209). In asthma, the accumulation of monocytes has been reported in the airways of children who faced fatal exacerbation episodes (282). Monocyte-derived DCs are sufficient to initiate allergic Th2 responses in the lungs of mice, and their major contribution to pathophysiology is the production of proinflammatory mediators and the presentation of antigens during re-exposition to allergens (283). Herein, we have reported that WIN55,212-2 reprograms monocyte to DC differentiation by conferring anti-inflammatory features to the resulting cells. HmoDCs differentiated in the presence of the synthetic cannabinoid displayed a tolerogenic profile in response to LPS, which was characterized by a reduced proinflammatory cytokine production, sustained IL-10 secretion and enhanced ability to suppress effector T cell responses and polarize Tregs (**Figure D.1**). Our data provides new insights into the anti-inflammatory features of the synthetic cannabinoid WIN55,212-2 and how these mechanisms could substantially contribute to suppress airway inflammation in asthma patients. In fact, opposing effects might be involved in asthma development and progression, as particulate matter from air pollution trains monocytes of asthmatic patients towards a proinflammatory profile with high secretion of mediators against non-related stimuli like allergens (284). The synergic capacity of WIN55,212-2 to impair inflammatory cytokine secretion while generating Tregs might well contribute to restore tolerance to allergens, which is a hallmark of successful treatments with potential disease-modifying capacity such as allergen-specific immunotherapy (61, 285).

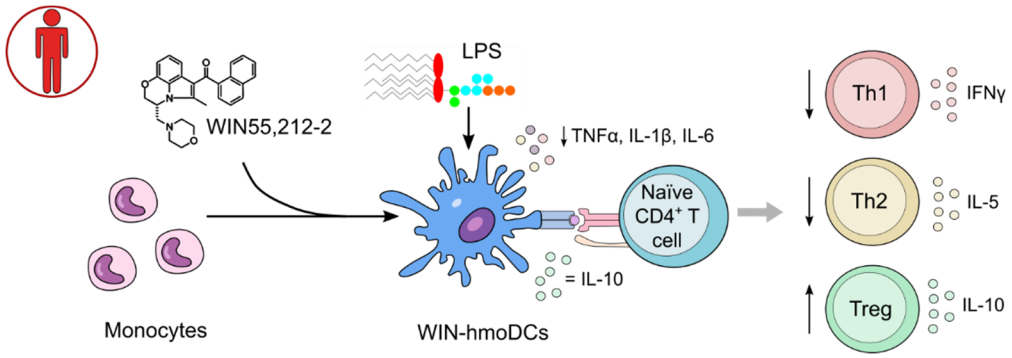

Figure D.1. Monocytes differentiated into DCs in the presence of WIN55,212-2 acquire tolerogenic properties and promote de generation of Tregs upon LPS exposure.

The contribution of macrophages to the pathophysiology of asthma is complex due to the differential functions of tissue-resident vs. recruited monocyte-derived subsets as well as the diverse activation profiles depending on asthma endotypes (286, 287). In murine models of asthma, allergic lung inflammation is mainly driven by monocyte-derived macrophages whereas tissue-resident subsets display immunoregulatory functions (288). In fact, monocyte-derived macrophages from HDM-allergic mice or asthma patients show inflammatory transcriptional reprogramming and excessive secretion of cytokines upon stimulation (289). In this work, we have demonstrated that WIN55,212-2 impairs classical activation of THP-1 MΦs and primary cultures of human monocyte-derived MΦs. The presence of WIN55,212-2 during stimulation inhibited NF-kB activation and inflammasome signaling, impairing

the production of mediators such as TNFα, IL-1β and IL-6, reducing the expression of MHC-II molecules and activation makers, and inhibiting pyroptotic cell death (**Figure D.2**). The collective inhibition of all these inflammatory pathways agrees with the well-known reported efficacy of cannabinoids as anti-inflammatory drugs but also underlines the potential protective effects of WIN55,212-2 in airway diseases. Several studies have described the induction of inflammasome signaling in asthma, and deficiency of Nlrp3 or the pyroptotic effector protein, gasdermin D, alleviates allergic asthmatic features in mice (290, 291). Similarly, PGE_2 suppresses pyroptosis in murine and human macrophages and protects mice from allergic airway inflammation (292). Supporting our *in vitro* data, we confirmed the capacity of WIN55212-2 to impair inflammasome signaling in an *in vivo* model of LPS-induced sepsis. Furthermore, comprehensive mechanistic studies involving *in vitro* and *ex vivo* cultures of macrophages demonstrated that the anti-inflammatory properties of WIN55,212-2 were associated with the inhibition of LPS-induced mTORC1 signaling, Warburg metabolism, and the modifications of the metabolic-epigenetic axis that sustain cellular inflammatory adaptations (**Figure D.2**). A metabolic switch towards aerobic glycolysis has been described in lung macrophages during experimental models of OVA-induced asthma (293, 294). Furthermore, the induction of glycolysis by environmental toxic substances like formaldehyde has been reported to aggravate airway inflammation (295). In this context, our data are consistent with the reported capacity of WIN55,212-2 to protect from acute lung injury through the modulation of macrophage metabolism in mice (225) and highlight its therapeutic potential for the treatment of airway inflammatory diseases like asthma.

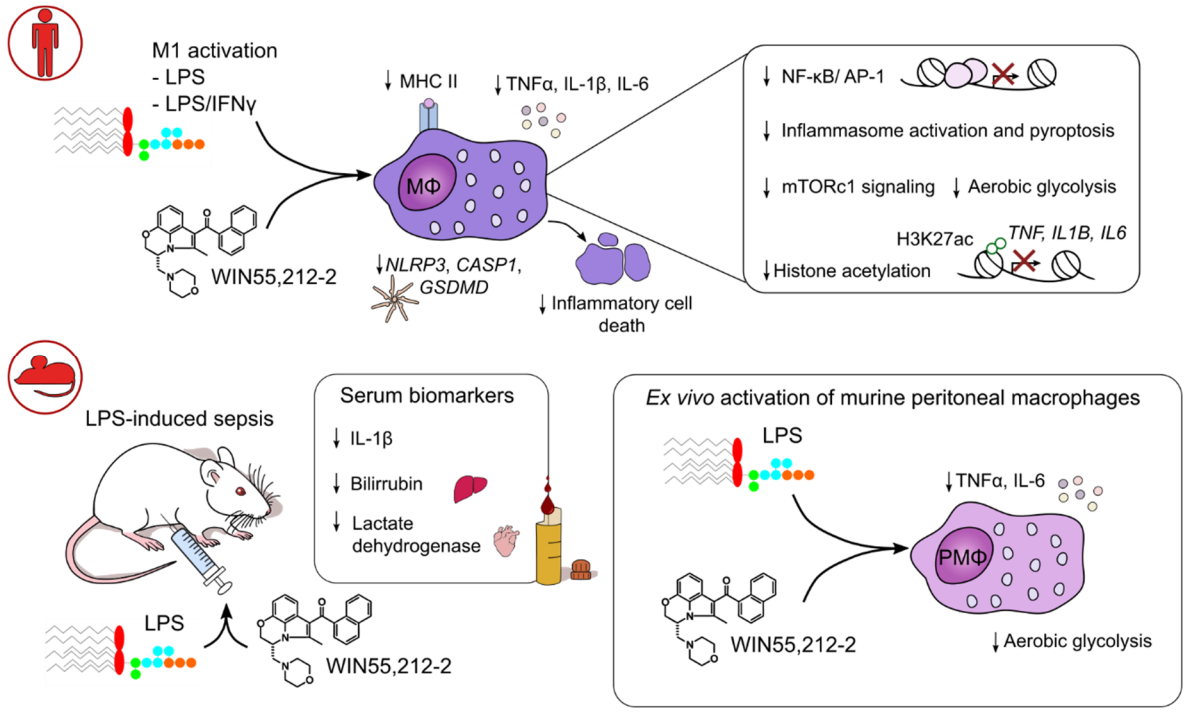

Figure D.2. The synthetic cannabinoid WIN55,212-2 inhibits classical M1 activation of macrophages and exerts anti-inflammatory properties in preclinical *in vitro* and *in vivo* models of LPS-induced sepsis.

Of note, we are aware that the macrophage polarization in asthma is not exclusively governed by a classical M1 activation profile but rather a spectrum of activation states depending on the inflammatory phase and pheno-endotype of the patient (286). In type 2 asthma presence of high amounts epithelial alarmins, IL-4 and IL-13 drives M2-like polarization profiles in the airways, which contribute to pathogenesis (73, 286). In this thesis we did not focus on M2 polarization states, which will be the aim of future work. Nonetheless, the induction of glycolysis to sustain TCA cycle has been related to the acquisition of M2 profiles in macrophages (80). Therefore, we cannot rule out that the mechanisms by which WIN55,212-2 impair classical activation of macrophages may also interfere with the induction of M2 polarization states. Moreover, our findings on HBECs suggest that the cannabinoid interferes with type 2 cytokine signaling. Future studies are warranted to cover this knowledge gap.

In the front line of airway mucosal defense, bronchial epithelial cells form a physical, chemical and immunological barrier that confers protection against airborne threats (103). Respiratory viruses and type 2- mediated allergic sensitization constitute two major risk factors for asthma development and progression as they cooperate to create a vicious cycle that compromises barrier function and perpetuates airway inflammation. Viral infections increase subepithelial antigen sampling and the release of epithelial-derived alarmins, which result in higher risk for allergen-sensitization and development of type 2 inflammatory responses in the airways (133, 137, 138). In turn, type 2 cytokines produced by alarmin-activated ILC2s or allergen-specific Th2 cells promote airway epithelial barrier dysfunction, impair antiviral immunity and facilitate exposure to same or other allergens as well as other environmental insults (109, 134). At this regard, our previous work demonstrated that the synthetic cannabinoid WIN55,212-2 restored bronchial epithelial barrier alterations induced by RV-A16 in ALI cultures of HBECs (144). Here, we have further characterized the preventive or therapeutic properties of the cannabinoid, showing that WIN55,212-2 does not prevent RV-A16 infection but accelerates the recovery of airway epithelial integrity and permeability after it. Our findings resemble the patterns of enhanced recovery from either cytokine- or EDTA-induced intestinal permeability previously described in epithelial cell cultures exposed to the phytocannabinoids THC and CBD (168, 169). In addition, we assayed the barrier protective functions of the cannabinoid in the context of airway type 2 inflammation. IL-13 stimulation recapitulates major asthmatic features in the airways both *in vitro* and *in vivo* (108, 110, 121, 246). Here, we demonstrate that WIN55,212-2 impairs the IL-13-induced mucus glycoprotein expression, barrier leakage and the production of type 2-polarizing mediators in ALI cultures of HBECs and self-assembled bronchial epithelial spheroids, confirming a potent inhibitory role on type 2 inflammatory conditions (**Figure D.3**). Mechanistically, GSEA of a publicly available RNA sequencing data of ALI cultures of HBECs exposed to IL-13 (205) identified enriched pathways associated with oxidative metabolism and redox imbalance. In fact, single-cell RNA sequencing data have showed that airway epithelial cells from allergic asthmatics fail to upregulate antioxidant pathways after allergen challenge (296). Additionally, the bronchial epithelium is well-recognized as one of the major sources of oxidative stress in response to type 2 cytokines, including NO production by iNOS, which contributes to the type 2 asthma biomarker FeNO (252, 254-256). In this context, we report that WIN55,212-2 blunts intracellular levels of ROS and reduces the IL-13-induced expression of iNOS, indicating that the

synthetic cannabinoid mitigates the oxidative stress triggered by type 2 cytokine stimulation in epithelial cells. The oxidative inactivation of PTPs has been described as a major mechanism to amplify type 2 cytokine signaling in human pulmonary epithelial cells and keratinocytes (257, 258). Accordingly, our studies on IL-13 signaling determined that WIN55,212-2 impaired IL-13-dependent phosphorylation of STAT6 by mechanisms dependent on the inhibition of ROS and restoration of PTPs activity (**Figure D.3**). These findings might well fit with the previously reported capacity of coal tar or benvitimod compounds to interfere with type 2 cytokine signaling, impair cytokine production and improve epithelial barrier function through upregulation of antioxidant pathways in human keratinocytes (261, 262).

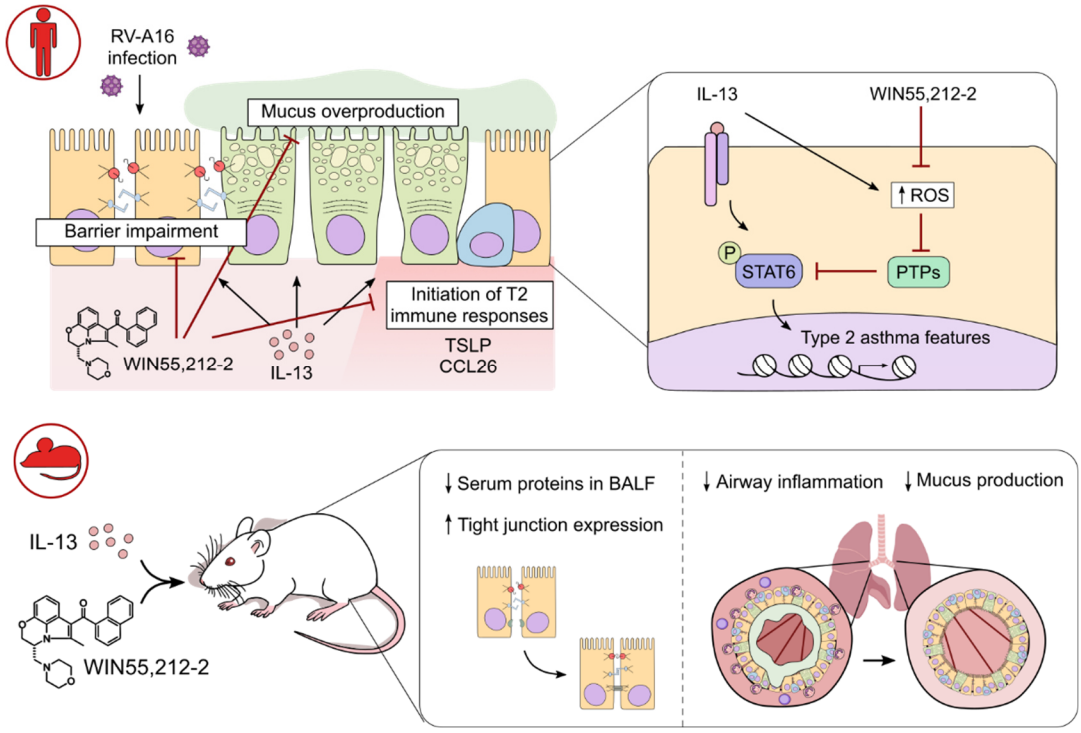

Figure D.3. The synthetic cannabinoid WIN55,212-2 impairs the acquisition of asthmatic features in the bronchial epithelium during rhinoviral infections and type 2 inflammation.

The potential *in vivo* relevance of our findings was evaluated in a murine asthma-like model of IL-13-driven airway inflammation, which is characterized by defective epithelial barrier function (121). We demonstrated that intranasal or intraperitoneal administration of WIN55,212-2 reduced the IL-13-induced translocation of serum proteins into BALF, indicating a protective function on bronchial epithelial permeability. Previous reports attributed the ability of WIN55,212-2 to impair plasma extravasation in guinea pig airways to its capacity to activate C-fibers in a murine model of allergen-induced airway inflammation (195). Nonetheless, our *in vitro* results together with the *in vivo* BALF data and the increased *ZO1* expression in the lungs of mice receiving IL-13 and WIN55,212-2, highlight that this protective barrier function may be mainly driven by the capacity of the cannabinoid to directly impact on the functional properties of the bronchial epithelium. Supporting this idea, compelling experimental evidence underlines the involvement of the ECS in the regulation of epithelial barrier integrity. For instance, CB1 KO animals show greater intestinal permeability and decreased skin epithelial barrier

recovery after damage (166, 172). Remarkably, intranasal administration of WIN55,212-2 also inhibited the IL-13-dependent mucus overproduction in the airways of mice and decreased inflammatory cell numbers in the lung and BALF (**Figure D.3**). Our results are consistent with the proposed mechanism of action of the cannabinoid, as mice lacking STAT6 were protected from all pulmonary deleterious effects of IL-13, while its reconstitution only in epithelial cells was sufficient to promote IL-13-induced airway hyperreactivity and mucus production (132).

Recently, we reported that WIN55,212-2 exerts immunomodulatory properties in type 2 mediated diseases such as food allergy. Particularly, we demonstrated the capacity of the synthetic cannabinoid to impair epicutaneous peanut allergic sensitization and inhibit anaphylactic shock by mechanisms associated to the induction of tolerogenic DCs and Tregs (49, 203). HDMs are the source of the most important indoor allergens associated with asthma worldwide (297). Therefore, we sought to validate the therapeutic potential of WIN55,212-2 in preclinical *in vitro* and *in vivo* models of HDM-induced allergic eosinophilic asthma. Consistent with our findings in peanut allergy models, WIN55,212-2 impaired the HDM-induced maturation of hmoDCs as well as reduced their capacity to promote effector T cell responses *in vitro*. In addition, WIN55,212-2 inhibited local airway inflammation, systemic immune responses and the generation IgE in a murine model of HDM-driven acute eosinophilic asthma, confirming its capacity to impair HDM-allergic sensitization and the development of type 2 inflammation *in vivo* (**Figure D.4**).

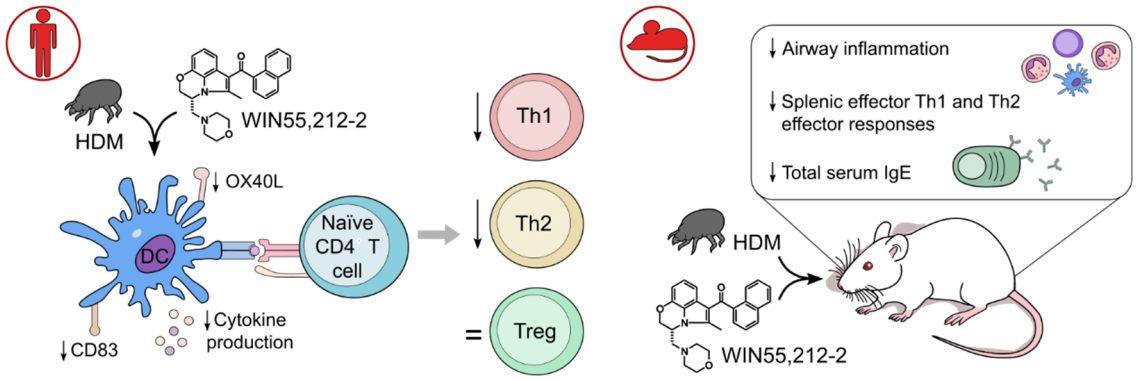

Figure D.4. The synthetic cannabinoid WIN55,212-2 exerts immunomodulatory properties on human DC exposed to HDM and impairs allergic sensitization and the development of type 2 inflammation in a model of HDM-driven acute eosinophilic asthma.

The prevalence of chronic non-communicable diseases like asthma has reached pandemic proportions in recent years. This phenomenon has been attributed to defects in the defensive and homeostatic functions of epithelial barriers caused by environmental agents introduced into our daily lives during industrialization and urbanization. Leaky barriers lead to microbial dysbiosis, bacterial translocation, and perpetuation of local and systemic inflammation, which ultimately results in the development and/or progression of allergies, autoimmunity and other chronic inflammatory disorders (84, 85, 87-89). Airway diseases associated with these events include asthma, allergic rhinitis, chronic rhinosinusitis, idiopathic pulmonary fibrosis and COPD (83). Some population groups are at higher risk of experiencing alterations in epithelial barriers due to a deleterious exposome. A paradigmatic example

is occupational asthma and the exacerbation of respiratory diseases in cleaning workers exposed to disinfectants, irritants, detergents and other toxic substances (270, 271). In this context, identifying harmful agents that constitute a deleterious exposome is key to developing proper prevention and avoidance recommendations for individuals at risk. New advances in aerospace industry and perspectives on the plausible colonization of outer space will be associated with the potential exposure to novel epithelial-damaging substances, especially for astronauts, but also during plausible exploitation of mineral sources from celestial bodies. Herein, we have evaluated the potential harmful effects of regolith simulants mimicking the particles found in the surface of the Moon or Mars. We demonstrate that Lunar and Mars regolith simulants compromise the epithelial barrier integrity and initiate inflammatory responses *in vitro.* Furthermore, we validated those findings in a murine model of repetitive intranasal regolith exposure where mice treated with regolith simulants displayed impaired bronchial epithelial integrity, airway damage, inflammatory cell infiltration and induction of early fibrosis markers in the lungs (**Figure D.5**). Our results resemble to the pathologic changes observed in murine models of lung disease induced by Earth particles such as silicosis (278, 279), but also share many pathophysiological characteristics with some of the above-listed diseases associated with airway barrier defects. Accordingly, regoliths found in celestial bodies might represent environmental harmful agents during space missions. Further research is needed to determine the underlying mechanisms of their deleterious effects as well as their potential differences with similar particulate exposures on Earth.

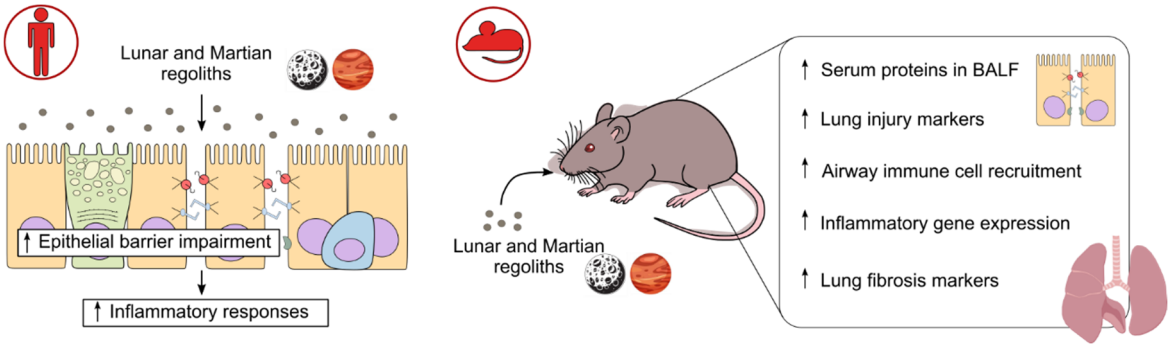

Figure D.5. The exposure to Lunar and Martian regoliths exerts detrimental effects on the airways both *in vitro* and *in vivo*.

In summary, we have uncovered the anti-inflammatory and tolerogenic capabilities of the synthetic cannabinoid WIN55,212-2 on different immune cell types including DCs, monocytes, and macrophages. Moreover, we have characterized the airway epithelial barrier protective functions of this synthetic cannabinoid in the context of viral infections and type 2 inflammation, identifying mechanisms dependent on the inhibition of type 2 cytokine signaling and modulation of oxidative stress. The potential clinical relevance of such effects was validated in several preclinical *in vivo* models of systemic and local airway inflammation. Our findings might well contribute to the development of novel cannabinoid-based strategies for the prevention and treatment of asthma and other airway inflammatory diseases. In addition, we have identified Lunar and Martian regoliths as novel epithelial-damaging compounds to the respiratory tract. Collectively, the herein reported findings might open future research paths for the development of preventive and therapeutic interventions for airway inflammatory disorders.

CONCLUSIONS

The main conclusions of this Doctoral Thesis are:

1. Human DCs differentiated from monocytes in the presence of the synthetic cannabinoid WIN55,212-2 acquire tolerogenic features characterized by a reduced inflammatory cytokine production in response to LPS, sustained anti-inflammatory IL-10 release and enhanced capacity to induce Tregs.

2. The synthetic cannabinoid WIN55,212-2 exerts anti-inflammatory features in classically activated human macrophages through the impairment of NF-κB/ AP-1 activation, inflammasome signaling and pyroptotic cell death.

3. The immunosuppressive effects of WIN55,212-2 in macrophages are associated with the inhibition of LPS-induced mTORC1 signaling pathway, aerobic glycolysis and epigenetic reprogramming.

4. The synthetic cannabinoid WIN55,212-2 inhibits inflammatory features in *ex vivo* stimulated peritoneal macrophages and impairs inflammasome activation in a murine model of LPS-induced sepsis.

5. Prophylactic and therapeutic administration of WIN55,212-2 improve airway epithelial barrier recovery during RV-A16 infections.

6. Administration of synthetic cannabinoid WIN55,212-2 impairs the IL-13-mediated acquisition of type 2 asthmatic features in ALI cultures of HBECs and three-dimensional cultures of self-assembled bronchial epithelial spheroids.

7. The synthetic cannabinoid WIN55,212-2 inhibits IL-13-induced oxidative stress in HBECs and impairs type 2 cytokine signaling by restoring PTP activity.

8. Intranasal or intraperitoneal administration of WIN55,212-2 protects mice from IL-13-driven epithelial barrier dysfunction, mucus overproduction and airway inflammation *in vivo*.

9. The synthetic cannabinoid WIN55,212-2 exerts immunomodulatory properties in hmoDCs exposed to HDM allergen extracts. Administration of WIN55,212-2 during HDM allergen sensitization reduces inflammatory cell recruitment into the airways, suppresses systemic effector immune responses and decreases total levels of IgE in a murine model of HDM-driven allergic asthma.

10. Lunar and Martian regolith simulants compromise epithelial barrier integrity and trigger airway inflammation in ALI cultures of HBECs and *in vivo* models of acute exposure to particulate materials.

BIBLIOGRAPHY

1. Medzhitov R, Iwasaki A. Exploring new perspectives in immunology. Cell. 2024;187(9):2079-94.

2. Wang R, Lan C, Benlagha K, Camara NOS, Miller H, Kubo M, et al. The interaction of innate immune and adaptive immune system. MedComm (2020). 2024;5(10):e714.

3. Chaplin DD. Overview of the immune response. J Allergy Clin Immunol. 2010;125(2 Suppl 2):S3-23.

4. Paludan SR, Pradeu T, Masters SL, Mogensen TH. Constitutive immune mechanisms: mediators of host defence and immune regulation. Nat Rev Immunol. 2021;21(3):137-50.

5. Netea MG, Quintin J, van der Meer JW. Trained immunity: a memory for innate host defense. Cell Host Microbe. 2011;9(5):355-61.

6. Dominguez-Andres J, Joosten LA, Netea MG. Induction of innate immune memory: the role of cellular metabolism. Curr Opin Immunol. 2019;56:10-6.

7. Bekkering S, Dominguez-Andres J, Joosten LAB, Riksen NP, Netea MG. Trained Immunity: Reprogramming Innate Immunity in Health and Disease. Annu Rev Immunol. 2021;39:667-93.

8. Martin-Cruz L, Benito-Villalvilla C, Angelina A, Subiza JL, Palomares O. Trained immunity-based vaccines for infections and allergic diseases. J Allergy Clin Immunol. 2024.

9. Steinman RM, Cohn ZA. Identification of a novel cell type in peripheral lymphoid organs of mice. I. Morphology, quantitation, tissue distribution. J Exp Med. 1973;137(5):1142-62.

10. Steinman RM, Gutchinov B, Witmer MD, Nussenzweig MC. Dendritic cells are the principal stimulators of the primary mixed leukocyte reaction in mice. J Exp Med. 1983;157(2):613-27.

11. Steinman RM, Witmer MD. Lymphoid dendritic cells are potent stimulators of the primary mixed leukocyte reaction in mice. Proc Natl Acad Sci U S A. 1978;75(10):5132-6.

12. Steinman RM, Banchereau J. Taking dendritic cells into medicine. Nature. 2007;449(7161):419-26.

13. Cabeza-Cabrerizo M, Cardoso A, Minutti CM, Pereira da Costa M, Reis e Sousa C. Dendritic Cells Revisited. Annu Rev Immunol. 2021;39:131-66.

14. Collin M, Bigley V. Human dendritic cell subsets: an update. Immunology. 2018;154(1):3-20.

15. Li D, Wu M. Pattern recognition receptors in health and diseases. Signal Transduct Target Ther. 2021;6(1):291.

16. Xiao Q, Xia Y. Insights into dendritic cell maturation during infection with application of advanced imaging techniques. Front Cell Infect Microbiol. 2023;13:1140765.

17. Carroll SL, Pasare C, Barton GM. Control of adaptive immunity by pattern recognition receptors. Immunity. 2024;57(4):632-48.

18. Walsh KP, Mills KH. Dendritic cells and other innate determinants of T helper cell polarisation. Trends Immunol. 2013;34(11):521-30.

19. Dalod M, Chelbi R, Malissen B, Lawrence T. Dendritic cell maturation: functional specialization through signaling specificity and transcriptional programming. EMBO J. 2014;33(10):1104-16.

20. Reis e Sousa C. Dendritic cells in a mature age. Nat Rev Immunol. 2006;6(6):476-83.

21. Alloatti A, Kotsias F, Magalhaes JG, Amigorena S. Dendritic cell maturation and cross-presentation: timing matters! Immunol Rev. 2016;272(1):97-108.

22. Bosteels V, Janssens S. Striking a balance: new perspectives on homeostatic dendritic cell maturation. Nat Rev Immunol. 2024.

23. Martin-Cruz L, Vinuela M, Kalograiaki I, Angelina A, Oquist-Phillips P, Real-Arevalo I, et al. A tumor-associated heparan sulfate-related glycosaminoglycan promotes the generation of functional regulatory T cells. Cell Mol Immunol. 2023;20(12):1499-512.

24. Bosteels V, Marechal S, De Nolf C, Rennen S, Maelfait J, Tavernier SJ, et al. LXR signaling controls homeostatic dendritic cell maturation. Sci Immunol. 2023;8(83):eadd3955.

25. Benito-Villalvilla C, Perez-Diego M, Angelina A, Kisand K, Rebane A, Subiza JL, et al. Allergoid-mannan conjugates reprogram monocytes into tolerogenic dendritic cells via epigenetic and metabolic rewiring. J Allergy Clin Immunol. 2022;149(1):212-22 e9.

26. Fucikova J, Palova-Jelinkova L, Bartunkova J, Spisek R. Induction of Tolerance and Immunity by Dendritic Cells: Mechanisms and Clinical Applications. Front Immunol. 2019;10:2393.

27. Morante-Palacios O, Fondelli F, Ballestar E, Martinez-Caceres EM. Tolerogenic Dendritic Cells in Autoimmunity and Inflammatory Diseases. Trends Immunol. 2021;42(1):59-75.

28. Morelli AE, Thomson AW. Tolerogenic dendritic cells and the quest for transplant tolerance. Nat Rev Immunol. 2007;7(8):610-21.

29. Cytlak U, Resteu A, Pagan S, Green K, Milne P, Maisuria S, et al. Differential IRF8 Transcription Factor Requirement Defines Two Pathways of Dendritic Cell Development in Humans. Immunity. 2020;53(2):353-70 e8.

30. Nutt SL, Chopin M. Transcriptional Networks Driving Dendritic Cell Differentiation and Function. Immunity. 2020;52(6):942-56.

31. Zhang S, Audiger C, Chopin M, Nutt SL. Transcriptional regulation of dendritic cell development and function. Front Immunol. 2023;14:1182553.

32. Segura E. Human dendritic cell subsets: An updated view of their ontogeny and functional specialization. Eur J Immunol. 2022;52(11):1759-67.

33. Wculek SK, Cueto FJ, Mujal AM, Melero I, Krummel MF, Sancho D. Dendritic cells in cancer immunology and immunotherapy. Nat Rev Immunol. 2020;20(1):7-24.

34. Dutertre CA, Becht E, Irac SE, Khalilnezhad A, Narang V, Khalilnezhad S, et al. Single-Cell Analysis of Human Mononuclear Phagocytes Reveals Subset-Defining Markers and Identifies Circulating Inflammatory Dendritic Cells. Immunity. 2019;51(3):573-89 e8.

35. Villani AC, Satija R, Reynolds G, Sarkizova S, Shekhar K, Fletcher J, et al. Single-cell RNA-seq reveals new types of human blood dendritic cells, monocytes, and progenitors. Science. 2017;356(6335).

36. Macri C, Pang ES, Patton T, O'Keeffe M. Dendritic cell subsets. Semin Cell Dev Biol. 2018;84:11-21.

37. Yin X, Chen S, Eisenbarth SC. Dendritic Cell Regulation of T Helper Cells. Annu Rev Immunol. 2021;39:759-90.

38. Sulczewski FB, Maqueda-Alfaro RA, Alcantara-Hernandez M, Perez OA, Saravanan S, Yun TJ, et al. Transitional dendritic cells are distinct from conventional DC2 precursors and mediate proinflammatory antiviral responses. Nat Immunol. 2023;24(8):1265-80.

39. Ziegler-Heitbrock L, Ohteki T, Ginhoux F, Shortman K, Spits H. Reclassifying plasmacytoid dendritic cells as innate lymphocytes. Nat Rev Immunol. 2023;23(1):1-2.

40. Reizis B, Idoyaga J, Dalod M, Barrat F, Naik S, Trinchieri G, et al. Reclassification of plasmacytoid dendritic cells as innate lymphocytes is premature. Nat Rev Immunol. 2023;23(5):336-7.

41. Adams NM, Das A, Yun TJ, Reizis B. Ontogeny and Function of Plasmacytoid Dendritic Cells. Annu Rev Immunol. 2024;42(1):347-73.

42. Arroyo Hornero R, Idoyaga J. Plasmacytoid dendritic cells: A dendritic cell in disguise. Mol Immunol. 2023;159:38-45.

43. Liu Z, Wang H, Li Z, Dress RJ, Zhu Y, Zhang S, et al. Dendritic cell type 3 arises from Ly6C(+) monocyte-dendritic cell progenitors. Immunity. 2023;56(8):1761-77 e6.

44. Bourdely P, Anselmi G, Vaivode K, Ramos RN, Missolo-Koussou Y, Hidalgo S, et al. Transcriptional and Functional Analysis of CD1c(+) Human Dendritic Cells Identifies a CD163(+) Subset Priming CD8(+)CD103(+) T Cells. Immunity. 2020;53(2):335-52 e8.

45. Yanez A, Coetzee SG, Olsson A, Muench DE, Berman BP, Hazelett DJ, et al. Granulocyte-Monocyte Progenitors and Monocyte-Dendritic Cell Progenitors Independently Produce Functionally Distinct Monocytes. Immunity. 2017;47(5):890-902 e4.

46. Coillard A, Segura E. In vivo Differentiation of Human Monocytes. Front Immunol. 2019;10:1907.

47. Sallusto F, Lanzavecchia A. Efficient presentation of soluble antigen by cultured human dendritic cells is maintained by granulocyte/macrophage colony-stimulating factor plus interleukin 4 and downregulated by tumor necrosis factor alpha. J Exp Med. 1994;179(4):1109-18.

48. Martin-Cruz L, Angelina A, Baydemir I, Bulut O, Subiza JL, Netea MG, et al. Candida albicans V132 induces trained immunity and enhances the responses triggered by the polybacterial vaccine MV140 for genitourinary tract infections. Front Immunol. 2022;13:1066383.

49. Angelina A, Perez-Diego M, Lopez-Abente J, Ruckert B, Nombela I, Akdis M, et al. Cannabinoids induce functional Tregs by promoting tolerogenic DCs via autophagy and metabolic reprograming. Mucosal Immunol. 2022;15(1):96-108.

50. Heras-Murillo I, Adan-Barrientos I, Galan M, Wculek SK, Sancho D. Dendritic cells as orchestrators of anticancer immunity and immunotherapy. Nat Rev Clin Oncol. 2024;21(4):257-77.

51. Hume DA. Macrophages as APC and the dendritic cell myth. J Immunol. 2008;181(9):5829-35.

52. Cassell DJ, Schwartz RH. A quantitative analysis of antigen-presenting cell function: activated B cells stimulate naive CD4 T cells but are inferior to dendritic cells in providing costimulation. J Exp Med. 1994;180(5):1829-40.

53. Liu W, Almo SC, Zang X. Co-stimulate or Co-inhibit Regulatory T Cells, Which Side to Go? Immunol Invest. 2016;45(8):813-31.

54. Hilligan KL, Ronchese F. Antigen presentation by dendritic cells and their instruction of CD4+ T helper cell responses. Cell Mol Immunol. 2020;17(6):587-99.

55. Sun L, Su Y, Jiao A, Wang X, Zhang B. T cells in health and disease. Signal Transduct Target Ther. 2023;8(1):235.

56. Angkasekwinai P, Dong C. IL-9-producing T cells: potential players in allergy and cancer. Nat Rev Immunol. 2021;21(1):37-48.

57. Zhang K, Chen L, Zhu C, Zhang M, Liang C. Current Knowledge of Th22 Cell and IL-22 Functions in Infectious Diseases. Pathogens. 2023;12(2).

58. Chen J, Yao J. Th22 cells and the intestinal mucosal barrier. Front Immunol. 2023;14:1221068.

59. Song W, Craft J. T Follicular Helper Cell Heterogeneity. Annu Rev Immunol. 2024;42(1):127-52.

60. Palomares O, Elewaut D, Irving PM, Jaumont X, Tassinari P. Regulatory T cells and immunoglobulin E: A new therapeutic link for autoimmunity? Allergy. 2022;77(11):3293-308.

61. Martin-Cruz L, Benito-Villalvilla C, Sirvent S, Angelina A, Palomares O. The Role of Regulatory T Cells in Allergic Diseases: Collegium Internationale Allergologicum (CIA) Update 2024. Int Arch Allergy Immunol. 2024;185(5):503-18.

62. Hodge AL, Baxter AA, Poon IKH. Gift bags from the sentinel cells of the immune system: The diverse role of dendritic cell-derived extracellular vesicles. J Leukoc Biol. 2022;111(4):903-20.

63. Lucca LE, Dominguez-Villar M. Modulation of regulatory T cell function and stability by co-inhibitory receptors. Nat Rev Immunol. 2020;20(11):680-93.

64. Santosh Nirmala S, Kayani K, Gliwinski M, Hu Y, Iwaszkiewicz-Grzes D, Piotrowska-Mieczkowska M, et al. Beyond FOXP3: a 20-year journey unravelling human regulatory T-cell heterogeneity. Front Immunol. 2023;14:1321228.

65. Metschnikoff E. Lecture on Phagocytosis and Immunity. Br Med J. 1891;1(1570):213-7.

66. Lazarov T, Juarez-Carreno S, Cox N, Geissmann F. Physiology and diseases of tissue-resident macrophages. Nature. 2023;618(7966):698-707.

67. Mosser DM, Hamidzadeh K, Goncalves R. Macrophages and the maintenance of homeostasis. Cell Mol Immunol. 2021;18(3):579-87.

68. Bleriot C, Chakarov S, Ginhoux F. Determinants of Resident Tissue Macrophage Identity and Function. Immunity. 2020;52(6):957-70.

69. Park MD, Silvin A, Ginhoux F, Merad M. Macrophages in health and disease. Cell. 2022;185(23):4259-79.

70. Mass E, Nimmerjahn F, Kierdorf K, Schlitzer A. Tissue-specific macrophages: how they develop and choreograph tissue biology. Nat Rev Immunol. 2023;23(9):563-79.

71. Martinez FO, Gordon S. The M1 and M2 paradigm of macrophage activation: time for reassessment. F1000Prime Rep. 2014;6:13.

72. Ginhoux F, Schultze JL, Murray PJ, Ochando J, Biswas SK. New insights into the multidimensional concept of macrophage ontogeny, activation and function. Nat Immunol. 2016;17(1):34-40.

73. Luo M, Zhao F, Cheng H, Su M, Wang Y. Macrophage polarization: an important role in inflammatory diseases. Front Immunol. 2024;15:1352946.

74. Murray PJ, Allen JE, Biswas SK, Fisher EA, Gilroy DW, Goerdt S, et al. Macrophage activation and polarization: nomenclature and experimental guidelines. Immunity. 2014;41(1):14-20.

75. O'Neill LA, Kishton RJ, Rathmell J. A guide to immunometabolism for immunologists. Nat Rev Immunol. 2016;16(9):553-65.

76. Al-Khami AA, Rodriguez PC, Ochoa AC. Energy metabolic pathways control the fate and function of myeloid immune cells. J Leukoc Biol. 2017;102(2):369-80.

77. O'Neill LA, Pearce EJ. Immunometabolism governs dendritic cell and macrophage function. J Exp Med. 2016;213(1):15-23.

78. Bekkering S, Arts RJW, Novakovic B, Kourtzelis I, van der Heijden C, Li Y, et al. Metabolic Induction of Trained Immunity through the Mevalonate Pathway. Cell. 2018;172(1-2):135-46 e9.

79. Van den Bossche J, O'Neill LA, Menon D. Macrophage Immunometabolism: Where Are We (Going)? Trends Immunol. 2017;38(6):395-406.

80. Natoli G, Pileri F, Gualdrini F, Ghisletti S. Integration of transcriptional and metabolic control in macrophage activation. EMBO Rep. 2021;22(9):e53251.

81. van Teijlingen Bakker N, Pearce EJ. Cell-intrinsic metabolic regulation of mononuclear phagocyte activation: Findings from the tip of the iceberg. Immunol Rev. 2020;295(1):54-67.

82. Ryan DG, O'Neill LAJ. Krebs Cycle Reborn in Macrophage Immunometabolism. Annu Rev Immunol. 2020;38:289-313.

83. Sun N, Ogulur I, Mitamura Y, Yazici D, Pat Y, Bu X, et al. The epithelial barrier theory and its associated diseases. Allergy. 2024.

84. Akdis CA. Does the epithelial barrier hypothesis explain the increase in allergy, autoimmunity and other chronic conditions? Nat Rev Immunol. 2021;21(11):739-51.

85. Akdis CA. The epithelial barrier hypothesis proposes a comprehensive understanding of the origins of allergic and other chronic noncommunicable diseases. J Allergy Clin Immunol. 2022;149(1):41-4.

86. Celebi Sozener Z, Cevhertas L, Nadeau K, Akdis M, Akdis CA. Environmental factors in epithelial barrier dysfunction. J Allergy Clin Immunol. 2020;145(6):1517-28.

87. Pat Y, Yazici D, D'Avino P, Li M, Ardicli S, Ardicli O, et al. Recent advances in the epithelial barrier theory. Int Immunol. 2024;36(5):211-22.

88. Yazici D, Ogulur I, Pat Y, Babayev H, Barletta E, Ardicli S, et al. The epithelial barrier: The gateway to allergic, autoimmune, and metabolic diseases and chronic neuropsychiatric conditions. Semin Immunol. 2023;70:101846.

89. Kucuksezer UC, Ozdemir C, Yazici D, Pat Y, Mitamura Y, Li M, et al. The epithelial barrier theory: Development and exacerbation of allergic and other chronic inflammatory diseases. Asia Pac Allergy. 2023;13(1):28-39.

90. Global Initiative for Asthma (GINA). Global Strategy for Asthma Management and Prevention, 2024. Updated May 2024. Available from: www.ginasthma.org.

91. Porsbjerg C, Melen E, Lehtimaki L, Shaw D. Asthma. Lancet. 2023;401(10379):858-73.

92. Holgate ST, Wenzel S, Postma DS, Weiss ST, Renz H, Sly PD. Asthma. Nat Rev Dis Primers. 2015;1(1):15025.

93. Hammad H, Lambrecht BN. The basic immunology of asthma. Cell. 2021;184(6):1469-85.

94. Castillo JR, Peters SP, Busse WW. Asthma Exacerbations: Pathogenesis, Prevention, and Treatment. J Allergy Clin Immunol Pract. 2017;5(4):918-27.

95. Wenzel SE. Asthma phenotypes: the evolution from clinical to molecular approaches. Nat Med. 2012;18(5):716-25.

96. Papi A, Brightling C, Pedersen SE, Reddel HK. Asthma. Lancet. 2018;391(10122):783-800.

97. Kolkhir P, Akdis CA, Akdis M, Bachert C, Bieber T, Canonica GW, et al. Type 2 chronic inflammatory diseases: targets, therapies and unmet needs. Nat Rev Drug Discov. 2023;22(9):743-67.

98. Kyriakopoulos C, Gogali A, Bartziokas K, Kostikas K. Identification and treatment of T2-low asthma in the era of biologics. ERJ Open Res. 2021;7(2).

99. Gonzalez-Uribe V, Romero-Tapia SJ, Castro-Rodriguez JA. Asthma Phenotypes in the Era of Personalized Medicine. J Clin Med. 2023;12(19).

100. Bourdin A, Brusselle G, Couillard S, Fajt ML, Heaney LG, Israel E, et al. Phenotyping of Severe Asthma in the Era of Broad-Acting Anti-Asthma Biologics. J Allergy Clin Immunol Pract. 2024;12(4):809-23.

101. Hellings PW, Steelant B. Epithelial barriers in allergy and asthma. J Allergy Clin Immunol. 2020;145(6):1499-509.

102. Davis JD, Wypych TP. Cellular and functional heterogeneity of the airway epithelium. Mucosal Immunol. 2021;14(5):978-90.

103. Russell RJ, Boulet LP, Brightling CE, Pavord ID, Porsbjerg C, Dorscheid D, et al. The airway epithelium: an orchestrator of inflammation, a key structural barrier and a therapeutic target in severe asthma. Eur Respir J. 2024;63(4).

104. Heijink IH, Kuchibhotla VNS, Roffel MP, Maes T, Knight DA, Sayers I, et al. Epithelial cell dysfunction, a major driver of asthma development. Allergy. 2020;75(8):1902-17.

105. Georas SN, Rezaee F. Epithelial barrier function: at the front line of asthma immunology and allergic airway inflammation. J Allergy Clin Immunol. 2014;134(3):509-20.

106. Frey A, Lunding LP, Ehlers JC, Weckmann M, Zissler UM, Wegmann M. More Than Just a Barrier: The Immune Functions of the Airway Epithelium in Asthma Pathogenesis. Front Immunol. 2020;11:761.

107. Xiao C, Puddicombe SM, Field S, Haywood J, Broughton-Head V, Puxeddu I, et al. Defective epithelial barrier function in asthma. J Allergy Clin Immunol. 2011;128(3):549-56 e1-12.

108. Wawrzyniak P, Wawrzyniak M, Wanke K, Sokolowska M, Bendelja K, Ruckert B, et al. Regulation of bronchial epithelial barrier integrity by type 2 cytokines and histone deacetylases in asthmatic patients. J Allergy Clin Immunol. 2017;139(1):93-103.

109. Saatian B, Rezaee F, Desando S, Emo J, Chapman T, Knowlden S, et al. Interleukin-4 and interleukin-13 cause barrier dysfunction in human airway epithelial cells. Tissue Barriers. 2013;1(2):e24333.

110. Pat Y, Ruckert B, Ogulur I, Yazici D, Perez-Diego M, Kucukkase OC, et al. Differentiation of bronchial epithelial spheroids in the presence of IL-13 recapitulates characteristic features of asthmatic airway epithelia. Allergy. 2022;77(7):2229-33.

111. Jackson ND, Everman JL, Chioccioli M, Feriani L, Goldfarbmuren KC, Sajuthi SP, et al. Single-Cell and Population Transcriptomics Reveal Pan-epithelial Remodeling in Type 2-High Asthma. Cell Rep. 2020;32(1):107872.

112. Hackett TL. Epithelial-mesenchymal transition in the pathophysiology of airway remodelling in asthma. Curr Opin Allergy Clin Immunol. 2012;12(1):53-9.

113. Gauvreau GM, Bergeron C, Boulet LP, Cockcroft DW, Cote A, Davis BE, et al. Sounding the alarmins-The role of alarmin cytokines in asthma. Allergy. 2023;78(2):402-17.

114. Hong H, Liao S, Chen F, Yang Q, Wang DY. Role of IL-25, IL-33, and TSLP in triggering united airway diseases toward type 2 inflammation. Allergy. 2020;75(11):2794-804.

115. Whitcutt MJ, Adler KB, Wu R. A biphasic chamber system for maintaining polarity of differentiation of cultured respiratory tract epithelial cells. In Vitro Cell Dev Biol. 1988;24(5):420-8.

116. Baldassi D, Gabold B, Merkel O. Air-liquid interface cultures of the healthy and diseased human respiratory tract: promises, challenges and future directions. Adv Nanobiomed Res. 2021;1(6).

117. Pezzulo AA, Starner TD, Scheetz TE, Traver GL, Tilley AE, Harvey BG, et al. The air-liquid interface and use of primary cell cultures are important to recapitulate the transcriptional profile of in vivo airway epithelia. Am J Physiol Lung Cell Mol Physiol. 2011;300(1):L25-31.

118. Si L, Bai H, Rodas M, Cao W, Oh CY, Jiang A, et al. A human-airway-on-a-chip for the rapid identification of candidate antiviral therapeutics and prophylactics. Nat Biomed Eng. 2021;5(8):815-29.

119. Mori A, Vermeer M, van den Broek LJ, Heijmans J, Nicolas A, Bouwhuis J, et al. High-throughput Bronchus-on-a-Chip system for modeling the human bronchus. Sci Rep. 2024;14(1):26248.

120. Steelant B, Seys SF, Van Gerven L, Van Woensel M, Farre R, Wawrzyniak P, et al. Histamine and T helper cytokine-driven epithelial barrier dysfunction in allergic rhinitis. J Allergy Clin Immunol. 2018;141(3):951-63 e8.

121. Sugita K, Steer CA, Martinez-Gonzalez I, Altunbulakli C, Morita H, Castro-Giner F, et al. Type 2 innate lymphoid cells disrupt bronchial epithelial barrier integrity by targeting tight junctions through IL-13 in asthmatic patients. J Allergy Clin Immunol. 2018;141(1):300-10 e11.

122. Akdis CA, Arkwright PD, Bruggen MC, Busse W, Gadina M, Guttman-Yassky E, et al. Type 2 immunity in the skin and lungs. Allergy. 2020;75(7):1582-605.

123. Lambrecht BN, Hammad H, Fahy JV. The Cytokines of Asthma. Immunity. 2019;50(4):975-91.

124. Maspero J, Adir Y, Al-Ahmad M, Celis-Preciado CA, Colodenco FD, Giavina-Bianchi P, et al. Type 2 inflammation in asthma and other airway diseases. ERJ Open Res. 2022;8(3).

125. Hammad H, Lambrecht BN. Barrier Epithelial Cells and the Control of Type 2 Immunity. Immunity. 2015;43(1):29-40.

126. Palomares O, Sanchez-Ramon S, Davila I, Prieto L, Perez de Llano L, Lleonart M, et al. dIvergEnt: How IgE Axis Contributes to the Continuum of Allergic Asthma and Anti-IgE Therapies. Int J Mol Sci. 2017;18(6).

127. Sallmann E, Reininger B, Brandt S, Duschek N, Hoflehner E, Garner-Spitzer E, et al. High-affinity IgE receptors on dendritic cells exacerbate Th2-dependent inflammation. J Immunol. 2011;187(1):164-71.

128. Weng CM, Lee MJ, Chao W, Lin YR, Chou CJ, Chen MC, et al. Airway epithelium IgE-FcepsilonRI cross-link induces epithelial barrier disruption in severe T2-high asthma. Mucosal Immunol. 2023;16(5):685-98.

129. Palaniyandi S, Tomei E, Li Z, Conrad DH, Zhu X. CD23-dependent transcytosis of IgE and immune complex across the polarized human respiratory epithelial cells. J Immunol. 2011;186(6):3484-96.

130. Scott G, Asrat S, Allinne J, Keat Lim W, Nagashima K, Birchard D, et al. IL-4 and IL-13, not eosinophils, drive type 2 airway inflammation, remodeling and lung function decline. Cytokine. 2023;162:156091.

131. Grunig G, Warnock M, Wakil AE, Venkayya R, Brombacher F, Rennick DM, et al. Requirement for IL-13 independently of IL-4 in experimental asthma. Science. 1998;282(5397):2261-3.

132. Kuperman DA, Huang X, Koth LL, Chang GH, Dolganov GM, Zhu Z, et al. Direct effects of interleukin-13 on epithelial cells cause airway hyperreactivity and mucus overproduction in asthma. Nat Med. 2002;8(8):885-9.

133. Jackson DJ, Gern JE. Rhinovirus Infections and Their Roles in Asthma: Etiology and Exacerbations. J Allergy Clin Immunol Pract. 2022;10(3):673-81.

134. Contoli M, Ito K, Padovani A, Poletti D, Marku B, Edwards MR, et al. Th2 cytokines impair innate immune responses to rhinovirus in respiratory epithelial cells. Allergy. 2015;70(8):910-20.

135. Lopez-Abente J, Benito-Villalvilla C, Jaumont X, Pfister P, Tassinari P, Palomares O. Omalizumab restores the ability of human plasmacytoid dendritic cells to induce Foxp3(+)Tregs. Eur Respir J. 2021;57(1).

136. Comstock AT, Ganesan S, Chattoraj A, Faris AN, Margolis BL, Hershenson MB, et al. Rhinovirus-induced barrier dysfunction in polarized airway epithelial cells is mediated by NADPH oxidase 1. J Virol. 2011;85(13):6795-808.

137. Jackson DJ, Makrinioti H, Rana BM, Shamji BW, Trujillo-Torralbo MB, Footitt J, et al. IL-33-dependent type 2 inflammation during rhinovirus-induced asthma exacerbations in vivo. Am J Respir Crit Care Med. 2014;190(12):1373-82.

138. Beale J, Jayaraman A, Jackson DJ, Macintyre JDR, Edwards MR, Walton RP, et al. Rhinovirus-induced IL-25 in asthma exacerbation drives type 2 immunity and allergic pulmonary inflammation. Sci Transl Med. 2014;6(256):256ra134.

139. Shah PA, Brightling C. Biologics for severe asthma-Which, when and why? Respirology. 2023;28(8):709-21.

140. Sardon-Prado O, Diaz-Garcia C, Corcuera-Elosegui P, Korta-Murua J, Valverde-Molina J, Sanchez-Solis M. Severe Asthma and Biological Therapies: Now and the Future. J Clin Med. 2023;12(18).

141. Chen ML, Nopsopon T, Akenroye A. Incidence of Anti-Drug Antibodies to Monoclonal Antibodies in Asthma: A Systematic Review and Meta-Analysis. J Allergy Clin Immunol Pract. 2023;11(5):1475-84 e20.

142. Howell I, Howell A, Pavord ID. Type 2 inflammation and biological therapies in asthma: Targeted medicine taking flight. J Exp Med. 2023;220(7).

143. Velasco G, Sanchez C, Guzman M. Towards the use of cannabinoids as antitumour agents. Nat Rev Cancer. 2012;12(6):436-44.

144. Angelina A, Perez-Diego M, Lopez-Abente J, Palomares O. The Role of Cannabinoids in Allergic Diseases: Collegium Internationale Allergologicum (CIA) Update 2020. Int Arch Allergy Immunol. 2020;181(8):565-84.

145. Klein TW. Cannabinoid-based drugs as anti-inflammatory therapeutics. Nat Rev Immunol. 2005;5(5):400-11.

146. Lowe H, Toyang N, Steele B, Bryant J, Ngwa W. The Endocannabinoid System: A Potential Target for the Treatment of Various Diseases. Int J Mol Sci. 2021;22(17).

147. Toczek M, Malinowska B. Enhanced endocannabinoid tone as a potential target of pharmacotherapy. Life Sci. 2018;204:20-45.

148. Bourke SL, Schlag AK, O'Sullivan SE, Nutt DJ, Finn DP. Cannabinoids and the endocannabinoid system in fibromyalgia: A review of preclinical and clinical research. Pharmacol Ther. 2022;240:108216.

149. Maccarrone M, Di Marzo V, Gertsch J, Grether U, Howlett AC, Hua T, et al. Goods and Bads of the Endocannabinoid System as a Therapeutic Target: Lessons Learned after 30 Years. Pharmacol Rev. 2023;75(5):885-958.

150. Pacher P, Kogan NM, Mechoulam R. Beyond THC and Endocannabinoids. Annu Rev Pharmacol Toxicol. 2020;60:637-59.

151. Di Marzo V. New approaches and challenges to targeting the endocannabinoid system. Nat Rev Drug Discov. 2018;17(9):623-39.

152. Ye L, Cao Z, Wang W, Zhou N. New Insights in Cannabinoid Receptor Structure and Signaling. Curr Mol Pharmacol. 2019;12(3):239-48.

153. Diaz-Laviada I, Ruiz-Llorente L. Signal transduction activated by cannabinoid receptors. Mini Rev Med Chem. 2005;5(7):619-30.

154. Maia J, Fonseca BM, Teixeira N, Correia-da-Silva G. The fundamental role of the endocannabinoid system in endometrium and placenta: implications in pathophysiological aspects of uterine and pregnancy disorders. Hum Reprod Update. 2020;26(4):586-602.

155. Ibsen MS, Connor M, Glass M. Cannabinoid CB(1) and CB(2) Receptor Signaling and Bias. Cannabis Cannabinoid Res. 2017;2(1):48-60.

156. O'Sullivan SE. Cannabinoids go nuclear: evidence for activation of peroxisome proliferator-activated receptors. Br J Pharmacol. 2007;152(5):576-82.

157. Chiurchiu V, Battistini L, Maccarrone M. Endocannabinoid signalling in innate and adaptive immunity. Immunology. 2015;144(3):352-64.

158. Rahaman O, Ganguly D. Endocannabinoids in immune regulation and immunopathologies. Immunology. 2021;164(2):242-52.

159. Cui Sun M, Otalora-Alcaraz A, Prenderville JA, Downer EJ. Toll-like receptor signalling as a cannabinoid target. Biochem Pharmacol. 2024;222:116082.

160. McCoy KL. Interaction between Cannabinoid System and Toll-Like Receptors Controls Inflammation. Mediators Inflamm. 2016;2016:5831315.

161. Dai Y, Zhou J, Shi C. Inflammasome: structure, biological functions, and therapeutic targets. MedComm (2020). 2023;4(5):e391.

162. Suryavanshi SV, Kovalchuk I, Kovalchuk O. Cannabinoids as Key Regulators of Inflammasome Signaling: A Current Perspective. Front Immunol. 2020;11:613613.

163. van Niekerk G, Mabin T, Engelbrecht AM. Anti-inflammatory mechanisms of cannabinoids: an immunometabolic perspective. Inflammopharmacology. 2019;27(1):39-46.

164. Henshaw FR, Dewsbury LS, Lim CK, Steiner GZ. The Effects of Cannabinoids on Pro- and Anti-Inflammatory Cytokines: A Systematic Review of In Vivo Studies. Cannabis Cannabinoid Res. 2021;6(3):177-95.

165. Wiley MB, DiPatrizio NV. Diet-Induced Gut Barrier Dysfunction Is Exacerbated in Mice Lacking Cannabinoid 1 Receptors in the Intestinal Epithelium. Int J Mol Sci. 2022;23(18).

166. Zoppi S, Madrigal JL, Perez-Nievas BG, Marin-Jimenez I, Caso JR, Alou L, et al. Endogenous cannabinoid system regulates intestinal barrier function in vivo through cannabinoid type 1 receptor activation. Am J Physiol Gastrointest Liver Physiol. 2012;302(5):G565-71.

167. Tajik N, Frech M, Schulz O, Schalter F, Lucas S, Azizov V, et al. Targeting zonulin and intestinal epithelial barrier function to prevent onset of arthritis. Nat Commun. 2020;11(1):1995.

168. Alhamoruni A, Wright KL, Larvin M, O'Sullivan SE. Cannabinoids mediate opposing effects on inflammation-induced intestinal permeability. Br J Pharmacol. 2012;165(8):2598-610.

169. Alhamoruni A, Lee AC, Wright KL, Larvin M, O'Sullivan SE. Pharmacological effects of cannabinoids on the Caco-2 cell culture model of intestinal permeability. J Pharmacol Exp Ther. 2010;335(1):92-102.

170. Kim HJ, Kim B, Park BM, Jeon JE, Lee SH, Mann S, et al. Topical cannabinoid receptor 1 agonist attenuates the cutaneous inflammatory responses in oxazolone-induced atopic dermatitis model. Int J Dermatol. 2015;54(10):e401-8.

171. Gaffal E, Glodde N, Jakobs M, Bald T, Tuting T. Cannabinoid 1 receptors in keratinocytes attenuate fluorescein isothiocyanate-induced mouse atopic-like dermatitis. Exp Dermatol. 2014;23(6):401-6.

172. Roelandt T, Heughebaert C, Bredif S, Giddelo C, Baudouin C, Msika P, et al. Cannabinoid receptors 1 and 2 oppositely regulate epidermal permeability barrier status and differentiation. Exp Dermatol. 2012;21(9):688-93.

173. Shin KO, Kim S, Park BD, Uchida Y, Park K. N-Palmitoyl Serinol Stimulates Ceramide Production through a CB1-Dependent Mechanism in In Vitro Model of Skin Inflammation. Int J Mol Sci. 2021;22(15).

174. Jang YS, Jeong S, Kim AR, Mok BR, Son SJ, Ryu JS, et al. Cannabidiol mediates epidermal terminal differentiation and redox homeostasis through aryl hydrocarbon receptor (AhR)-dependent signaling. J Dermatol Sci. 2023;109(2):61-70.

175. Shang VC, O'Sullivan SE, Kendall DA, Roberts RE. The endogenous cannabinoid anandamide increases human airway epithelial cell permeability through an arachidonic acid metabolite. Pharmacol Res. 2016;105:152-63.

176. Shang VC, Kendall DA, Roberts RE. Delta(9)-Tetrahydrocannabinol reverses TNFalpha-induced increase in airway epithelial cell permeability through CB(2) receptors. Biochem Pharmacol. 2016;120:63-71.

177. Angelina A, Martin-Fontecha M, Ruckert B, Wawrzyniak P, Perez-Diego M, Lopez-Abente J, et al. The cannabinoid WIN55212-2 restores rhinovirus-induced epithelial barrier disruption. Allergy. 2021;76(6):1900-2.

178. Palomares O. Could we co-opt the cannabinoid system for asthma therapy? Expert Rev Clin Immunol. 2023;19(10):1183-6.

179. Bozkurt TE. Endocannabinoid System in the Airways. Molecules. 2019;24(24).

180. Tashkin DP, Shapiro BJ, Frank IM. Acute effects of smoked marijuana and oral delta9-tetrahydrocannabinol on specific airway conductance in asthmatic subjects. Am Rev Respir Dis. 1974;109(4):420-8.

181. Tashkin DP, Reiss S, Shapiro BJ, Calvarese B, Olsen JL, Lodge JW. Bronchial effects of aerosolized delta 9-tetrahydrocannabinol in healthy and asthmatic subjects. Am Rev Respir Dis. 1977;115(1):57-65.

182. Abboud RT, Sanders HD. Effect of oral administration of delta-tetrahydrocannabinol on airway mechanics in normal and asthmatic subjects. Chest. 1976;70(4):480-5.

183. Roviezzo F, Rossi A, Caiazzo E, Orlando P, Riemma MA, Iacono VM, et al. Palmitoylethanolamide Supplementation during Sensitization Prevents Airway Allergic Symptoms in the Mouse. Front Pharmacol. 2017;8:857.

184. Zoerner AA, Stichtenoth DO, Engeli S, Batkai S, Winkler C, Schaumann F, et al. Allergen challenge increases anandamide in bronchoalveolar fluid of patients with allergic asthma. Clin Pharmacol Ther. 2011;90(3):388-91.

185. Martin-Fontecha M, Eiwegger T, Jartti T, Rueda-Zubiaurre A, Tiringer K, Stepanow J, et al. The expression of cannabinoid receptor 1 is significantly increased in atopic patients. J Allergy Clin Immunol. 2014;133(3):926-9 e2.

186. Frei RB, Luschnig P, Parzmair GP, Peinhaupt M, Schranz S, Fauland A, et al. Cannabinoid receptor 2 augments eosinophil responsiveness and aggravates allergen-induced pulmonary inflammation in mice. Allergy. 2016;71(7):944-56.

187. Sugawara K, Zakany N, Hundt T, Emelianov V, Tsuruta D, Schafer C, et al. Cannabinoid receptor 1 controls human mucosal-type mast cell degranulation and maturation in situ. J Allergy Clin Immunol. 2013;132(1):182-93.

188. Grassin-Delyle S, Naline E, Buenestado A, Faisy C, Alvarez JC, Salvator H, et al. Cannabinoids inhibit cholinergic contraction in human airways through prejunctional CB1 receptors. Br J Pharmacol. 2014;171(11):2767-77.

189. Bozkurt TE, Kaya Y, Durlu-Kandilci NT, Onder S, Sahin-Erdemli I. The effect of cannabinoids on dinitrofluorobenzene-induced experimental asthma in mice. Respir Physiol Neurobiol. 2016;231:7-13.

190. Wiley MB, Bobardt SD, Nordgren TM, Nair MG, DiPatrizio NV. Cannabinoid Receptor Subtype-1 Regulates Allergic Airway Eosinophilia During Lung Helminth Infection. Cannabis Cannabinoid Res. 2021;6(3):242-52.

191. Kwon EK, Choi Y, Sim S, Ye YM, Shin YS, Park HS, et al. Cannabinoid receptor 2 as a regulator of inflammation induced oleoylethanolamide in eosinophilic asthma. J Allergy Clin Immunol. 2024;153(4):998-1009 e9.

192. Ferrini ME, Hong S, Stierle A, Stierle D, Stella N, Roberts K, et al. CB2 receptors regulate natural killer cells that limit allergic airway inflammation in a murine model of asthma. Allergy. 2017;72(6):937-47.

193. Hurrell BP, Helou DG, Shafiei-Jahani P, Howard E, Painter JD, Quach C, et al. Cannabinoid receptor 2 engagement promotes group 2 innate lymphoid cell expansion and enhances airway hyperreactivity. J Allergy Clin Immunol. 2022;149(5):1628-42 e10.

194. Yoshihara S, Morimoto H, Ohori M, Yamada Y, Abe T, Arisaka O. Endogenous cannabinoid receptor agonists inhibit neurogenic inflammations in guinea pig airways. Int Arch Allergy Immunol. 2005;138(1):80-7.

195. Fukuda H, Abe T, Yoshihara S. The cannabinoid receptor agonist WIN 55,212-2 inhibits antigen-induced plasma extravasation in guinea pig airways. Int Arch Allergy Immunol. 2010;152(3):295-300.

196. Vuolo F, Abreu SC, Michels M, Xisto DG, Blanco NG, Hallak JE, et al. Cannabidiol reduces airway inflammation and fibrosis in experimental allergic asthma. Eur J Pharmacol. 2019;843:251-9.

197. Jan TR, Farraj AK, Harkema JR, Kaminski NE. Attenuation of the ovalbumin-induced allergic airway response by cannabinoid treatment in A/J mice. Toxicol Appl Pharmacol. 2003;188(1):24-35.

198. Braun A, Engel T, Aguilar-Pimentel JA, Zimmer A, Jakob T, Behrendt H, et al. Beneficial effects of cannabinoids (CB) in a murine model of allergen-induced airway inflammation: role of CB1/CB2 receptors. Immunobiology. 2011;216(4):466-76.

199. Giannini L, Nistri S, Mastroianni R, Cinci L, Vannacci A, Mariottini C, et al. Activation of cannabinoid receptors prevents antigen-induced asthma-like reaction in guinea pigs. J Cell Mol Med. 2008;12(6A):2381-94.

200. Abohalaka R, Karaman Y, Recber T, Onder SC, Nemutlu E, Bozkurt TE. Endocannabinoid metabolism inhibition ameliorates ovalbumin-induced allergic airway inflammation and hyperreactivity in Guinea pigs. Life Sci. 2022;306:120808.

201. Simon A, von Einem T, Seidinger A, Matthey M, Bindila L, Wenzel D. The endocannabinoid anandamide is an airway relaxant in health and disease. Nat Commun. 2022;13(1):6941.

202. Angelina A, Perez-Diego M, Maldonado A, Ruckert B, Akdis M, Martin-Fontecha M, et al. The cannabinoid WIN55212-2 suppresses effector T-cell responses and promotes regulatory T cells in human tonsils. Allergy. 2022;77(3):1029-32.

203. Angelina A, Jimenez-Saiz R, Perez-Diego M, Maldonado A, Ruckert B, Akdis M, et al. Cannabinoid WIN55212-2 impairs peanut-allergic sensitization and promotes the generation of allergen-specific regulatory T cells. Clin Exp Allergy. 2022;52(4):540-9.

204. Martin-Fontecha M, Angelina A, Ruckert B, Rueda-Zubiaurre A, Martin-Cruz L, van de Veen W, et al. A Fluorescent Probe to Unravel Functional Features of Cannabinoid Receptor CB(1) in Human Blood and Tonsil Immune System Cells. Bioconjug Chem. 2018;29(2):382-9.

205. Stocker N, Radzikowska U, Wawrzyniak P, Tan G, Huang M, Ding M, et al. Regulation of angiotensin-converting enzyme 2 isoforms by type 2 inflammation and viral infection in human airway epithelium. Mucosal Immunol. 2023;16(1):5-16.

206. Netea MG, Balkwill F, Chonchol M, Cominelli F, Donath MY, Giamarellos-Bourboulis EJ, et al. A guiding map for inflammation. Nat Immunol. 2017;18(8):826-31.

207. Nathan C, Ding A. Nonresolving inflammation. Cell. 2010;140(6):871-82.

208. Greene JT, Brian BFt, Senevirathne SE, Freedman TS. Regulation of myeloid-cell activation. Curr Opin Immunol. 2021;73:34-42.

209. Geissmann F, Manz MG, Jung S, Sieweke MH, Merad M, Ley K. Development of monocytes, macrophages, and dendritic cells. Science. 2010;327(5966):656-61.

210. Jakubzick CV, Randolph GJ, Henson PM. Monocyte differentiation and antigen-presenting functions. Nat Rev Immunol. 2017;17(6):349-62.

211. Unger WW, Laban S, Kleijwegt FS, van der Slik AR, Roep BO. Induction of Treg by monocyte-derived DC modulated by vitamin D3 or dexamethasone: differential role for PD-L1. Eur J Immunol. 2009;39(11):3147-59.

212. Hackstein H, Taner T, Zahorchak AF, Morelli AE, Logar AJ, Gessner A, et al. Rapamycin inhibits IL-4--induced dendritic cell maturation in vitro and dendritic cell mobilization and function in vivo. Blood. 2003;101(11):4457-63.

213. Benito-Villalvilla C, Perez-Diego M, Subiza JL, Palomares O. Allergoid-mannan conjugates imprint tolerogenic features in human macrophages. Allergy. 2022;77(1):320-3.

214. Saeed S, Quintin J, Kerstens HH, Rao NA, Aghajanirefah A, Matarese F, et al. Epigenetic programming of monocyte-to-macrophage differentiation and trained innate immunity. Science. 2014;345(6204):1251086.

215. Roth MD, Castaneda JT, Kiertscher SM. Exposure to Delta9-Tetrahydrocannabinol Impairs the Differentiation of Human Monocyte-derived Dendritic Cells and their Capacity for T cell Activation. J Neuroimmune Pharmacol. 2015;10(2):333-43.

216. Hao MX, Jiang LS, Fang NY, Pu J, Hu LH, Shen LH, et al. The cannabinoid WIN55,212-2 protects against oxidized LDL-induced inflammatory response in murine macrophages. J Lipid Res. 2010;51(8):2181-90.

217. Downer EJ, Clifford E, Gran B, Nel HJ, Fallon PG, Moynagh PN. Identification of the synthetic cannabinoid R(+)WIN55,212-2 as a novel regulator of IFN regulatory factor 3 activation and IFN-beta expression: relevance to therapeutic effects in models of multiple sclerosis. J Biol Chem. 2011;286(12):10316-28.

218. Staiano RI, Loffredo S, Borriello F, Iannotti FA, Piscitelli F, Orlando P, et al. Human lung-resident macrophages express CB1 and CB2 receptors whose activation inhibits the release of angiogenic and lymphangiogenic factors. J Leukoc Biol. 2016;99(4):531-40.

219. Fleetwood AJ, Lawrence T, Hamilton JA, Cook AD. Granulocyte-macrophage colony-stimulating factor (CSF) and macrophage CSF-dependent macrophage phenotypes display differences in cytokine profiles and transcription factor activities: implications for CSF blockade in inflammation. J Immunol. 2007;178(8):5245-52.

220. Cuevas VD, Simon-Fuentes M, Orta-Zavalza E, Samaniego R, Sanchez-Mateos P, Escribese M, et al. The Gene Signature of Activated M-CSF-Primed Human Monocyte-Derived Macrophages Is IL-10-Dependent. J Innate Immun. 2022;14(3):243-56.

221. Cao W, Lee SH, Lu J. CD83 is preformed inside monocytes, macrophages and dendritic cells, but it is only stably expressed on activated dendritic cells. Biochem J. 2005;385(Pt 1):85-93.

222. Di Carlo S, Hacker G, Gentle IE. GM-CSF suppresses antioxidant signaling and drives IL-1beta secretion through NRF2 downregulation. EMBO Rep. 2022;23(8):e54226.

223. Simpson DS, Pang J, Weir A, Kong IY, Fritsch M, Rashidi M, et al. Interferon-gamma primes macrophages for pathogen ligand-induced killing via a caspase-8 and mitochondrial cell death pathway. Immunity. 2022;55(3):423-41 e9.

224. Suryavanshi SV, Zaiachuk M, Pryimak N, Kovalchuk I, Kovalchuk O. Cannabinoids Alleviate the LPS-Induced Cytokine Storm via Attenuating NLRP3 Inflammasome Signaling and TYK2-Mediated STAT3 Signaling Pathways In Vitro. Cells. 2022;11(9).

225. He Q, Yin J, Zou B, Guo H. WIN55212-2 alleviates acute lung injury by inhibiting macrophage glycolysis through the miR-29b-3p/FOXO3/PFKFB3 axis. Mol Immunol. 2022;149:119-28.

226. Yu W, Wang Z, Zhang K, Chi Z, Xu T, Jiang D, et al. One-Carbon Metabolism Supports S-Adenosylmethionine and Histone Methylation to Drive Inflammatory Macrophages. Mol Cell. 2019;75(6):1147-60 e5.

227. Lauterbach MA, Hanke JE, Serefidou M, Mangan MSJ, Kolbe CC, Hess T, et al. Toll-like Receptor Signaling Rewires Macrophage Metabolism and Promotes Histone Acetylation via ATP-Citrate Lyase. Immunity. 2019;51(6):997-1011 e7.

228. Evavold CL, Hafner-Bratkovic I, Devant P, D'Andrea JM, Ngwa EM, Borsic E, et al. Control of gasdermin D oligomerization and pyroptosis by the Ragulator-Rag-mTORC1 pathway. Cell. 2021;184(17):4495-511 e19.

229. Moon JS, Hisata S, Park MA, DeNicola GM, Ryter SW, Nakahira K, et al. mTORC1-Induced HK1-Dependent Glycolysis Regulates NLRP3 Inflammasome Activation. Cell Rep. 2015;12(1):102-15.

230. Xie M, Yu Y, Kang R, Zhu S, Yang L, Zeng L, et al. PKM2-dependent glycolysis promotes NLRP3 and AIM2 inflammasome activation. Nat Commun. 2016;7:13280.

231. Karki R, Kanneganti TD. The 'cytokine storm': molecular mechanisms and therapeutic prospects. Trends Immunol. 2021;42(8):681-705.

232. van der Poll T, Shankar-Hari M, Wiersinga WJ. The immunology of sepsis. Immunity. 2021;54(11):2450-64.

233. Dai S, Ye B, Zhong L, Chen Y, Hong G, Zhao G, et al. GSDMD Mediates LPS-Induced Septic Myocardial Dysfunction by Regulating ROS-dependent NLRP3 Inflammasome Activation. Front Cell Dev Biol. 2021;9:779432.

234. Shakoory B, Carcillo JA, Chatham WW, Amdur RL, Zhao H, Dinarello CA, et al. Interleukin-1 Receptor Blockade Is Associated With Reduced Mortality in Sepsis Patients With Features of

Macrophage Activation Syndrome: Reanalysis of a Prior Phase III Trial. Crit Care Med. 2016;44(2):275-81.

235. Anderko RR, Gomez H, Canna SW, Shakoory B, Angus DC, Yealy DM, et al. Sepsis with liver dysfunction and coagulopathy predicts an inflammatory pattern of macrophage activation. Intensive Care Med Exp. 2022;10(1):6.

236. Arevalo-Martin A, Molina-Holgado E, Guaza C. A CB(1)/CB(2) receptor agonist, WIN 55,212-2, exerts its therapeutic effect in a viral autoimmune model of multiple sclerosis by restoring self-tolerance to myelin. Neuropharmacology. 2012;63(3):385-93.

237. Marchalant Y, Rosi S, Wenk GL. Anti-inflammatory property of the cannabinoid agonist WIN-55212-2 in a rodent model of chronic brain inflammation. Neuroscience. 2007;144(4):1516-22.

238. Zhao Y, Liu Y, Zhang W, Xue J, Wu YZ, Xu W, et al. WIN55212-2 ameliorates atherosclerosis associated with suppression of pro-inflammatory responses in ApoE-knockout mice. Eur J Pharmacol. 2010;649(1-3):285-92.

239. Feng YJ, Li YY, Lin XH, Li K, Cao MH. Anti-inflammatory effect of cannabinoid agonist WIN55, 212 on mouse experimental colitis is related to inhibition of p38MAPK. World J Gastroenterol. 2016;22(43):9515-24.

240. He Q, Zhang W, Zhang J, Deng Y. Cannabinoid Analogue WIN 55212-2 Protects Paraquat-Induced Lung Injury and Enhances Macrophage M2 Polarization. Inflammation. 2022;45(6):2256-67.

241. Fantauzzi MF, Aguiar JA, Tremblay BJ, Mansfield MJ, Yanagihara T, Chandiramohan A, et al. Expression of endocannabinoid system components in human airway epithelial cells: impact of sex and chronic respiratory disease status. ERJ Open Res. 2020;6(4).

242. Gkoumassi E, Dekkers BG, Droge MJ, Elzinga CR, Schmidt M, Meurs H, et al. Virodhamine and CP55,940 modulate cAMP production and IL-8 release in human bronchial epithelial cells. Br J Pharmacol. 2007;151(7):1041-8.

243. Kicman A, Pedzinska-Betiuk A, Kozlowska H. The potential of cannabinoids and inhibitors of endocannabinoid degradation in respiratory diseases. Eur J Pharmacol. 2021;911:174560.

244. Danahay H, Pessotti AD, Coote J, Montgomery BE, Xia D, Wilson A, et al. Notch2 is required for inflammatory cytokine-driven goblet cell metaplasia in the lung. Cell Rep. 2015;10(2):239-52.

245. Moonwiriyakit A, Yimnual C, Noitem R, Dinsuwannakol S, Sontikun J, Kaewin S, et al. GPR120/FFAR4 stimulation attenuates airway remodeling and suppresses IL-4- and IL-13-induced airway epithelial injury via inhibition of STAT6 and Akt. Biomed Pharmacother. 2023;168:115774.

246. Schmidt H, Braubach P, Schilpp C, Lochbaum R, Neuland K, Thompson K, et al. IL-13 Impairs Tight Junctions in Airway Epithelia. Int J Mol Sci. 2019;20(13).

247. Pagano C, Savarese B, Coppola L, Navarra G, Avilia G, Laezza C, et al. Cannabinoids in the Modulation of Oxidative Signaling. Int J Mol Sci. 2023;24(3).

248. Xu W, Ghosh S, Comhair SA, Asosingh K, Janocha AJ, Mavrakis DA, et al. Increased mitochondrial arginine metabolism supports bioenergetics in asthma. J Clin Invest. 2016;126(7):2465-81.

249. Winnica D, Corey C, Mullett S, Reynolds M, Hill G, Wendell S, et al. Bioenergetic Differences in the Airway Epithelium of Lean Versus Obese Asthmatics Are Driven by Nitric Oxide and Reflected in Circulating Platelets. Antioxid Redox Signal. 2019;31(10):673-86.

250. Ravi A, Goorsenberg AWM, Dijkhuis A, Dierdorp BS, Dekker T, van Weeghel M, et al. Metabolic differences between bronchial epithelium from healthy individuals and patients with asthma and the effect of bronchial thermoplasty. J Allergy Clin Immunol. 2021;148(5):1236-48.

251. Aguilera-Aguirre L, Bacsi A, Saavedra-Molina A, Kurosky A, Sur S, Boldogh I. Mitochondrial dysfunction increases allergic airway inflammation. J Immunol. 2009;183(8):5379-87.

252. Nagasaki T, Schuyler AJ, Zhao J, Samovich SN, Yamada K, Deng Y, et al. 15LO1 dictates glutathione redox changes in asthmatic airway epithelium to worsen type 2 inflammation. J Clin Invest. 2022;132(1).

253. Queener AM, Chiarella SE, Cuervo-Pardo L, Coden ME, Abdala-Valencia H, Berdnikovs S. Metabolism of Epithelial Cells in Health and Allergic Disease: Collegium Internationale Allergologicum Update 2021. Int Arch Allergy Immunol. 2021;182(8):663-78.

254. Harper RW, Xu C, Eiserich JP, Chen Y, Kao CY, Thai P, et al. Differential regulation of dual NADPH oxidases/peroxidases, Duox1 and Duox2, by Th1 and Th2 cytokines in respiratory tract epithelium. FEBS Lett. 2005;579(21):4911-7.

255. Chibana K, Trudeau JB, Mustovich AT, Hu H, Zhao J, Balzar S, et al. IL-13 induced increases in nitrite levels are primarily driven by increases in inducible nitric oxide synthase as compared with effects on arginases in human primary bronchial epithelial cells. Clin Exp Allergy. 2008;38(6):936-46.

256. Roos AB, Mori M, Gronneberg R, Osterlund C, Claesson HE, Wahlstrom J, et al. Elevated exhaled nitric oxide in allergen-provoked asthma is associated with airway epithelial iNOS. PLoS One. 2014;9(2):e90018.

257. Sharma P, Chakraborty R, Wang L, Min B, Tremblay ML, Kawahara T, et al. Redox regulation of interleukin-4 signaling. Immunity. 2008;29(4):551-64.

258. Hirakawa S, Saito R, Ohara H, Okuyama R, Aiba S. Dual oxidase 1 induced by Th2 cytokines promotes STAT6 phosphorylation via oxidative inactivation of protein tyrosine phosphatase 1B in human epidermal keratinocytes. J Immunol. 2011;186(8):4762-70.

259. Miyata M, Nakamura Y, Shimokawa N, Ohnuma Y, Katoh R, Matsuoka S, et al. Thymic stromal lymphopoietin is a critical mediator of IL-13-driven allergic inflammation. Eur J Immunol. 2009;39(11):3078-83.

260. Mandal PK, Morlacchi P, Knight JM, Link TM, Lee GRt, Nurieva R, et al. Targeting the Src Homology 2 (SH2) Domain of Signal Transducer and Activator of Transcription 6 (STAT6) with Cell-Permeable, Phosphatase-Stable Phosphopeptide Mimics Potently Inhibits Tyr641 Phosphorylation and Transcriptional Activity. J Med Chem. 2015;58(22):8970-84.

261. Wang X, Mao D, Jia J, Zhang J. Benvitimod Inhibits IL-4- and IL-13-Induced Tight Junction Impairment by Activating AHR/ARNT Pathway and Inhibiting STAT6 Phosphorylation in Human Keratinocytes. J Invest Dermatol. 2024;144(3):509-19 e7.

262. van den Bogaard EH, Bergboer JG, Vonk-Bergers M, van Vlijmen-Willems IM, Hato SV, van der Valk PG, et al. Coal tar induces AHR-dependent skin barrier repair in atopic dermatitis. J Clin Invest. 2013;123(2):917-27.

263. Valladao AC, Frevert CW, Koch LK, Campbell DJ, Ziegler SF. STAT6 Regulates the Development of Eosinophilic versus Neutrophilic Asthma in Response to Alternaria alternata. J Immunol. 2016;197(12):4541-51.

264. Alessandrini F, Musiol S, Schneider E, Blanco-Perez F, Albrecht M. Mimicking Antigen-Driven Asthma in Rodent Models-How Close Can We Get? Front Immunol. 2020;11:575936.

265. Burrows KE, Dumont C, Thompson CL, Catley MC, Dixon KL, Marshall D. OX40 blockade inhibits house dust mite driven allergic lung inflammation in mice and in vitro allergic responses in humans. Eur J Immunol. 2015;45(4):1116-28.

266. Liu YJ. Thymic stromal lymphopoietin and OX40 ligand pathway in the initiation of dendritic cell-mediated allergic inflammation. J Allergy Clin Immunol. 2007;120(2):238-44; quiz 45-6.

267. Ribeiro A, Almeida VI, Costola-de-Souza C, Ferraz-de-Paula V, Pinheiro ML, Vitoretti LB, et al. Cannabidiol improves lung function and inflammation in mice submitted to LPS-induced acute lung injury. Immunopharmacol Immunotoxicol. 2015;37(1):35-41.

268. Wan H, Winton HL, Soeller C, Tovey ER, Gruenert DC, Thompson PJ, et al. Der p 1 facilitates transepithelial allergen delivery by disruption of tight junctions. J Clin Invest. 1999;104(1):123-33.

269. Wan H, Winton HL, Soeller C, Taylor GW, Gruenert DC, Thompson PJ, et al. The transmembrane protein occludin of epithelial tight junctions is a functional target for serine peptidases from faecal pellets of Dermatophagoides pteronyssinus. Clin Exp Allergy. 2001;31(2):279-94.

270. Folletti I, Zock JP, Moscato G, Siracusa A. Asthma and rhinitis in cleaning workers: a systematic review of epidemiological studies. J Asthma. 2014;51(1):18-28.

271. Medina-Ramon M, Zock JP, Kogevinas M, Sunyer J, Torralba Y, Borrell A, et al. Asthma, chronic bronchitis, and exposure to irritant agents in occupational domestic cleaning: a nested case-control study. Occup Environ Med. 2005;62(9):598-606.

272. Angelina A, Perez-Diego M, Palomares O. Nutritional and environmental exposures in athletes: Implications on the epithelial barrier function. Allergy. 2024;79(11):2909-11.

273. D'Amato G, Akdis CA. Desert dust and respiratory diseases: Further insights into the epithelial barrier hypothesis. Allergy. 2022;77(12):3490-2.

274. Celebi Sozener Z, Treffeisen ER, Ozdel Ozturk B, Schneider LC. Global warming and implications for epithelial barrier disruption and respiratory and dermatologic allergic diseases. J Allergy Clin Immunol. 2023;152(5):1033-46.

275. Goksel O, Sipahi MI, Yanasik S, Saglam-Metiner P, Benzer S, Sabour-Takanlou L, et al. Comprehensive analysis of resilience of human airway epithelial barrier against short-term PM2.5 inorganic dust exposure using in vitro microfluidic chip and ex vivo human airway models. Allergy. 2024;79(11):2953-65.

276. Janbazacyabar H, van Bergenhenegouwen J, Varasteh S, Garssen J, Folkerts G, Braber S. Repeated exposure of bronchial epithelial cells to particular matter increases allergen-induced cytokine release and permeability. Cytokine. 2022;154:155878.

277. Blume C, Swindle EJ, Dennison P, Jayasekera NP, Dudley S, Monk P, et al. Barrier responses of human bronchial epithelial cells to grass pollen exposure. Eur Respir J. 2013;42(1):87-97.

278. Li B, Mu M, Sun Q, Cao H, Liu Q, Liu J, et al. A suitable silicosis mouse model was constructed by repeated inhalation of silica dust via nose. Toxicol Lett. 2021;353:1-12.

279. Guo J, Gu N, Chen J, Shi T, Zhou Y, Rong Y, et al. Neutralization of interleukin-1 beta attenuates silica-induced lung inflammation and fibrosis in C57BL/6 mice. Arch Toxicol. 2013;87(11):1963-73.

280. Aegerter H, Lambrecht BN. The Pathology of Asthma: What Is Obstructing Our View? Annu Rev Pathol. 2023;18:387-409.

281. Gasse P, Mary C, Guenon I, Noulin N, Charron S, Schnyder-Candrian S, et al. IL-1R1/MyD88 signaling and the inflammasome are essential in pulmonary inflammation and fibrosis in mice. J Clin Invest. 2007;117(12):3786-99.

282. Eguiluz-Gracia I, Malmstrom K, Dheyauldeen SA, Lohi J, Sajantila A, Aalokken R, et al. Monocytes accumulate in the airways of children with fatal asthma. Clin Exp Allergy. 2018;48(12):1631-9.

283. Plantinga M, Guilliams M, Vanheerswynghels M, Deswarte K, Branco-Madeira F, Toussaint W, et al. Conventional and monocyte-derived CD11b(+) dendritic cells initiate and maintain T helper 2 cell-mediated immunity to house dust mite allergen. Immunity. 2013;38(2):322-35.

284. Movassagh H, Prunicki M, Kaushik A, Zhou X, Dunham D, Smith EM, et al. Proinflammatory polarization of monocytes by particulate air pollutants is mediated by induction of trained immunity in pediatric asthma. Allergy. 2023;78(7):1922-33.

285. Palomares O, Akdis M, Martin-Fontecha M, Akdis CA. Mechanisms of immune regulation in allergic diseases: the role of regulatory T and B cells. Immunol Rev. 2017;278(1):219-36.

286. Miller RL, Grayson MH, Strothman K. Advances in asthma: New understandings of asthma's natural history, risk factors, underlying mechanisms, and clinical management. J Allergy Clin Immunol. 2021;148(6):1430-41.

287. Britt RD, Jr., Ruwanpathirana A, Ford ML, Lewis BW. Macrophages Orchestrate Airway Inflammation, Remodeling, and Resolution in Asthma. Int J Mol Sci. 2023;24(13).

288. Zaslona Z, Przybranowski S, Wilke C, van Rooijen N, Teitz-Tennenbaum S, Osterholzer JJ, et al. Resident alveolar macrophages suppress, whereas recruited monocytes promote, allergic lung inflammation in murine models of asthma. J Immunol. 2014;193(8):4245-53.

289. Lechner A, Henkel FDR, Hartung F, Bohnacker S, Alessandrini F, Gubernatorova EO, et al. Macrophages acquire a TNF-dependent inflammatory memory in allergic asthma. J Allergy Clin Immunol. 2022;149(6):2078-90.

290. Wu J, Wang P, Xie X, Yang X, Tang S, Zhao J, et al. Gasdermin D silencing alleviates airway inflammation and remodeling in an ovalbumin-induced asthmatic mouse model. Cell Death Dis. 2024;15(6):400.

291. Ma M, Li G, Qi M, Jiang W, Zhou R. Inhibition of the Inflammasome Activity of NLRP3 Attenuates HDM-Induced Allergic Asthma. Front Immunol. 2021;12:718779.

292. Zaslona Z, Flis E, Wilk MM, Carroll RG, Palsson-McDermott EM, Hughes MM, et al. Caspase-11 promotes allergic airway inflammation. Nat Commun. 2020;11(1):1055.

293. Chen N, Xie QM, Song SM, Guo SN, Fang Y, Fei GH, et al. Dexamethasone protects against asthma via regulating Hif-1alpha-glycolysis-lactate axis and protein lactylation. Int Immunopharmacol. 2024;131:111791.

294. Ji X, Nie C, Yao Y, Ma Y, Huang H, Hao C. S100A8/9 modulates perturbation and glycolysis of macrophages in allergic asthma mice. PeerJ. 2024;12:e17106.

295. Xuan L, Ren L, Zhang W, Du P, Li B, An Z. Formaldehyde aggravates airway inflammation through induction of glycolysis in an experimental model of asthma exacerbated by lipopolysaccharide. Sci Total Environ. 2024;912:168947.

296. Alladina J, Smith NP, Kooistra T, Slowikowski K, Kernin IJ, Deguine J, et al. A human model of asthma exacerbation reveals transcriptional programs and cell circuits specific to allergic asthma. Sci Immunol. 2023;8(83):eabq6352.

297. Miller JD. The Role of Dust Mites in Allergy. Clin Rev Allergy Immunol. 2019;57(3):312-29.

APPENDIX

List of publications:

- **Pérez-Diego, M**., Angelina, A., Martín-Cruz, L., de la Rocha-Muñoz, A., Maldonado, A., Sevilla-Ortega, C., & Palomares, O. (2023). Cannabinoid WIN55,212-2 reprograms monocytes and macrophages to inhibit LPS-induced inflammation. *Frontiers in immunology*, 14, 1147520. https://doi.org/10.3389/fimmu.2023.1147520.
- Angelina, A.*, **Pérez-Diego, M**.*, & Palomares, O. (2024). Nutritional and environmental exposures in athletes: Implications on the epithelial barrier function. *Allergy*, 79(11), 2909–2911. https://doi.org/10.1111/all.16280. * The authors equally contributed to this work.

frontiers | Frontiers in Immunology

TYPE Original Research
PUBLISHED 16 March 2023
DOI 10.3389/fimmu.2023.1147520

OPEN ACCESS

EDITED BY
Samer Ihsan Bazzi,
University of Balamand, Lebanon

REVIEWED BY
Anjie Zhen,
UCLA Department of Medicine,
United States
Divya Ramnath,
The University of Queensland, Australia

*CORRESPONDENCE
Oscar Palomares
oscar.palomares@quim.ucm.es

SPECIALTY SECTION
This article was submitted to Molecular Innate Immunity, a section of the journal Frontiers in Immunology

RECEIVED 18 January 2023
ACCEPTED 06 March 2023
PUBLISHED 16 March 2023

CITATION
Pérez-Diego M, Angelina A, Martín-Cruz L, de la Rocha-Muñoz A, Maldonado A, Sevilla-Ortega C and Palomares O (2023) Cannabinoid WIN55,212-2 reprograms monocytes and macrophages to inhibit LPS-induced inflammation. *Front. Immunol.* 14:1147520. doi: 10.3389/fimmu.2023.1147520

Cannabinoid WIN55,212-2 reprograms monocytes and macrophages to inhibit LPS-induced inflammation

Mario Pérez-Diego[1], Alba Angelina[1], Leticia Martín-Cruz[1], Andrés de la Rocha-Muñoz[1,2], Angel Maldonado[1], Carmen Sevilla-Ortega[1] and Oscar Palomares[1]*

[1]Department of Biochemistry and Molecular Biology, School of Chemistry, Complutense University of Madrid, Madrid, Spain, [2]Autonomous University of Madrid, Madrid, Spain

Introduction: Chronic or uncontrolled activation of myeloid cells including monocytes, macrophages and dendritic cells (DCs) is a hallmark of immune-mediated inflammatory disorders. There is an urgent need for the development of novel drugs with the capacity to impair innate immune cell overactivation under inflammatory conditions. Compelling evidence pointed out cannabinoids as potential therapeutic tools with anti-inflammatory and immunomodulatory capacity. WIN55,212-2, a non-selective synthetic cannabinoid agonist, displays protective effects in several inflammatory conditions by mechanisms partially depending on the generation of tolerogenic DCs able to induce functional regulatory T cells (Tregs). However, its immunomodulatory capacity on other myeloid cells such as monocytes and macrophages remains incompletely understood.

Methods: Human monocyte-derived DCs (hmoDCs) were differentiated in the absence (conventional hmoDCs) or presence of WIN55,212-2 (WIN-hmoDCs). Cells were stimulated with LPS, cocultured with naive T lymphocytes and their cytokine production and ability to induce T cell responses were analysed by ELISA or flow cytometry. To evaluate the effect of WIN55,212-2 in macrophage polarization, human and murine macrophages were activated with LPS or LPS/IFNγ, in the presence or absence of the cannabinoid. Cytokine, costimulatory molecules and inflammasome markers were assayed. Metabolic and chromatin immunoprecipitation assays were also performed. Finally, the protective capacity of WIN55,212-2 was studied in vivo in BALB/c mice after intraperitoneal injection with LPS.

Results: We show for the first time that the differentiation of hmoDCs in the presence of WIN55,212-2 generates tolerogenic WIN-hmoDCs that are less responsive to LPS stimulation and able to prime Tregs. WIN55,212-2 also impairs the pro-inflammatory polarization of human macrophages by inhibiting cytokine production, inflammasome activation and rescuing macrophages from pyroptotic cell death. Mechanistically, WIN55,212-2 induced a metabolic and epigenetic shift in macrophages by decreasing LPS-induced mTORC1 signaling, commitment to glycolysis and active histone marks in pro-inflammatory cytokine promoters. We confirmed these data in *ex vivo* LPS-stimulated peritoneal macrophages (PMΦs), which were also supported by

the *in vivo* anti-inflammatory capacity of WIN55,212-2 in a LPS-induced sepsis mouse model.

Conclusion: Overall, we shed light into the molecular mechanisms by which cannabinoids exert anti-inflammatory properties in myeloid cells, which might well contribute to the future rational design of novel therapeutic strategies for inflammatory disorders.

KEYWORDS

cannabinoids, WIN55,212-2, monocyte differentiation, macrophage polarization, immunomodulation, anti-inflammatory, metabolic and epigenetic reprogramming

Introduction

Inflammation is a vital defense mechanism that can be initiated by the immune system after detecting invading pathogens and/or cellular damage. Inflammatory responses are orchestrated to eliminate the cause of injury and to initiate healing upon tissue damage. Alterations of these tightly regulated processes are associated with different immune-mediated diseases and inflammatory disorders such as autoimmune and allergic diseases, autoinflammatory syndromes or sepsis (1, 2). Myeloid cells such as conventional dendritic cells (DCs), monocytes and macrophages are specialized in the initiation and amplification of inflammatory responses. These cells are equipped with a large battery of pattern-recognition receptors (PRRs) to sense a plethora of harmful pathogens and damage-associated stimuli, which allows their activation, initiation of inflammatory responses and spreading of the alarm throughout the body (1, 3, 4). Compelling experimental evidence shows that inflammatory responses orchestrated by myeloid cells are closely linked to their metabolic profile (5, 6). For example, the activation of mammalian target of rapamycin complex 1 (mTORC1) on myeloid cells promotes anabolic metabolism and shift from glycolysis towards lactic fermentation as a faster energetic source to induce and sustain the functional adaptations required under a pro-inflammatory scenario (6). Under certain pathological conditions, the chronic or uncontrolled activation of myeloid cells significantly contributes to perpetuate inflammation and tissue damage, which leads to the main clinical manifestations associated to such diseases (2, 7). Although current immunosuppressive therapies represent the mainstay of treatment for many inflammatory conditions, their clinical efficacy is still limited for many patients and their overuse is associated with significant adverse effects (8). Therefore, the discovery of novel molecules able to target myeloid cells and dampen inflammation as well as the better understanding of their mode of action at the molecular level might well contribute to the development of alternative therapeutic interventions for many immune-mediated and inflammatory diseases.

The endocannabinoid system (ECS) is a complex signaling network encompassing the cannabinoid receptors (CBRs), the endogenous cannabinoids (anandamide, AEA) and 2-arachidonoylglycerol, 2-AG) and the enzymes involved in their synthesis and degradation (9, 10). In addition, phytocannabinoids from *Cannabis sativa L.*, marijuana, (Δ^9-tetrahydrocannabinol, THC) and synthetic cannabinoids (WIN55,212-2, HU210, or HU308) also activate CBRs regulating proliferation, differentiation, cell survival, metabolism or immunity (9, 10). The therapeutic exploitation of the ECS is an emerging field of research, and different pre-clinical and clinical studies point out cannabinoids as potential therapeutic tools for inflammatory diseases (9–12). At this regard, we have previously demonstrated that human DCs express functional CBRs and that the synthetic cannabinoid WIN55,212-2 induces anti-inflammatory immune responses by promoting metabolic reprogramming in fully differentiated DCs, which eventually led to the generation of functional regulatory T cells (Tregs) with suppressive capacity both *in vitro* and *in vivo* (13). We have also shown that WIN55,212-2 is able to restore rhinovirus-induced bronchial epithelial barrier disruption (14). However, the potential capacity of WIN55,212-2 to regulate the generation of human monocyte-derived DCs (hmoDCs) and its anti-inflammatory properties on other myeloid cells such as macrophages remains elusive. Herein, we show for the first time that the differentiation of hmoDCs in the presence of WIN55,212-2 generates tolerogenic DCs (WIN-hmoDCs) that are less responsive to

Abbreviations: 2-AG, 2-arachidonoylglycerol; 2-DG, 2-deoxy-D-glucose; A488, Alexa Fluor 488; AA, antimycin A; AEA, anandamide; APC, allophycocyanin; BSA, bovine serum albumin; CBD, cannabidiol; CBRs, cannabinoid receptors; ChIP, chromatin immunoprecipitation; DCs dendritic cells; ECS, endocannabinoid system; FBS, fetal bovine serum; FITC, fluorescein-5-isothiocyanate; glycoPER, glycolytic proton efflux rate; GM-CSF, granulocyte-macrophage colony-stimulating factor; H3K27ac, histone 3 acetylation of lysine 27; hmoDCs, human monocyte-derived dendritic cells; HRP, horseradish peroxidase; LDH, lactate dehydrogenase; LPS, lipopolysaccharide; MAS, macrophage activation syndrome; mTORC1, mammalian target of rapamycin complex 1; PBMCs, peripheral blood mononuclear cells; PE, phycoerythrin; PerCP, peridinin chlorophyll protein complex; PI, propidium iodide; PMA, phorbol 12-myristate 13-acetate; PMΦs, peritoneal macrophages; PPARα, peroxisome proliferator-activated receptor α; PRRs, pattern-recognition receptors; qPCR, quantitative PCR; ROI, region of interest; Rot, rotenone; SDS-PAGE, SDS-polyacrylamide gel electrophoresis; SEAP, secreted embryonic alkaline phosphatase; THC, Δ9-tetrahydrocannabinol; THP-1 MΦs, THP-1 Macrophages; Tregs, regulatory T cells; WIN, WIN55,212-2.

lipopolysaccharide (LPS) stimulation and able to prime functional Tregs. We also uncover that WIN55,212-2 inhibits the pro-inflammatory M1 activation in THP-1 Macrophages (THP-1 MΦs) and primary cultures of human monocyte-derived macrophages by mechanisms depending on metabolic and epigenetic rewiring. WIN55,212-2 protects from LPS-induced sepsis *in vivo* and limits LPS-induced metabolic reprogramming of *ex vivo* stimulated peritoneal macrophages (PMΦs). Our data enhance the knowledge about the molecular mechanisms by which cannabinoids exert anti-inflammatory properties in myeloid cells, which might help to the development of novel therapeutic interventions for inflammatory diseases.

Materials and methods

Material, media and reagents

Cell cultures were growth in RPMI 1640 medium (Lonza) supplemented with 10% heat-inactivated fetal bovine serum (FBS, Hyclone), 100 µg/mL normocin (*Invivo*Gen), 50 µg/mL penicillin-streptomycin, 1% nonessential amino acids, 1% MEM vitamins and 1 mmol/L sodium pyruvate (all from Life Technologies).

In vitro cell activation was performed with LPS from *Escherichia coli* (O127:B8, Sigma-Aldrich) and/or IFNγ (PeproTech). In *ex vivo* and *in vivo* experiments, LPS from *E. coli* (O155:B5, Sigma-Aldrich) was employed. The cannabinoid agonist WIN55,212-2 (Sigma-Aldrich) was used. The specific doses and time points are specifically detailed for each corresponding experiment.

Generation of human monocyte-derived dendritic cells and WIN-hmoDCs

Peripheral blood mononuclear cells (PBMCs) were isolated from buffy coats of healthy anonymous donors (Transfusion Centre of Madrid, under the approved code "PODIS09") by Ficoll Paque density-gradient. Then, monocytes were purified by positive magnetic isolation using anti-human CD14 microbeads and AutoMACS technology (Miltenyi Biotec). To generate hmoDCs, monocytes were seeded at $1x10^6$ cells/mL concentration and differentiated in the presence of 100 ng/mL of granulocyte-macrophage colony-stimulating factor (GM-CSF) and 100 ng/mL IL-4 (Preprotech) for 6 days. To generate WIN-hmoDCs, WIN55,212-2 (Sigma-Aldrich) at a final concentration of 50 nM was added at days 0 and 4 of the hmoDCs differentiation.

Coculture experiments

Peripheral blood naïve $CD4^+$ T cells were purified from PBMCs obtained from buffy coats of healthy donors using the "Naïve $CD4^+$ T Cell Isolation Kit" (Miltenyi Biotec). LPS-stimulated hmoDCs and WIN-hmoDCs were cocultured with allogeneic naïve $CD4^+$ T cells (hmoDC:T cell ratio of 1:5) during 5 days. Then, cell-free supernatants were collected for cytokine quantification and cells were stained for flow cytometry analysis.

Differentiation of THP-1 MΦs and primary human monocyte-derived macrophages

THP-1 and THP-1 XBlue cell lines (*Invivo*Gen) were seeded at $0,25x10^6$ cells/mL and stimulated with 10 ng/mL phorbol 12-myristate 13-acetate (PMA, Sigma-Aldrich) for 24 h. Then, culture media was removed and fresh media was added. After resting for 24 h, cells were stimulated with medium or 100 ng/mL LPS from *E. coli* (O127:B8, Sigma-Aldrich) + 50 ng/mL IFNγ (Preprotech) (LPS/IFNγ) during 24h to generate M0 and M1 polarized THP-1 MΦs, respectively. To generate primary human macrophages, monocytes were purified from PBMCs as previously described (15, 16), seeded at $0,5x10^6$ cells/mL and cultured in the presence of 100 ng/mL of GM-CSF (Preprotech) for 7 days. Cultures were supplemented with GM-CSF every second day.

NF-κB/AP-1 activation assay

The evaluation of NF-κB/AP-1 activation in human macrophages was performed using the THP-1 XBlue™ monocytic cell line (*Invivo*Gen), which is stably integrated with a NF-κB/AP-1 inducible secreted embryonic alkaline phosphatase (SEAP) reporter construct. Briefly, THP-1 XBlue monocytes were differentiated into human THP-1 MΦs as described above. Then, after incubation with the indicated stimuli, the activation of NF-κB/AP-1 was determined in cell-free supernatants using a SEAP colorimetric detection reagent called QUANTIBlue™.

Cytokine quantification

Concentrations of human TNFα, IL-1β, IL-6, IL-10, IL-5, IFNγ and murine IL-6 in cell-free supernatants were quantified using sandwich ELISA cytokine kits from BD Biosciences. Murine TNFα and IL-1β levels were assessed by sandwich ELISA using specific kits from Invitrogen. In all cases, the manufacturer protocols were followed with minor modifications.

Flow cytometry

For flow cytometry determinations, monoclonal antibodies were purchased from BioLegend: human anti-FOXP3-Alexa Fluor 488 (A488), anti-CD127-phycoerythrin (PE), anti-CD25-allophycocyanin (APC), anti-CD4-peridinin chlorophyll protein complex (PerCP), anti-HLA-DR-Fluorescein-5-isothiocyanate (FITC) anti-CD86-PE and anti-CD83-APC. Staining for CB1 was performed using the HU210-A488 fluorescent probe as previously described (15), A488 alone was use as control. For the detection of CB2 receptor, a first incubation with the primary CB2 polyclonal antibody (PA1744, Invitrogen) was followed by the incubation with an A488-conjugated goat anti-rabbit secondary antibody (Invitrogen). Cell viability was analyzed by propidium iodide (PI, Life technologies) or eFluor660 (Invitrogen) staining. For surface staining, cells were harvested, washed in 2 mM PBS/EDTA with

0.5% bovine serum albumin (BSA) and stained in the darkness for 15 min at room temperature with the corresponding fluorescence-labelled or isotype control antibodies. For the analysis of FOXP3 expression in human T cells cocultured with hmoDCs, a first surface staining with anti-human CD4-PerCP, CD127-PE, and CD25-APC antibodies was followed by subsequent fixation and permeabilization. Then, cells were stained with anti-human FOXP3–A488 according to the manufacturer's recommendations. The corresponding isotype controls were included in every staining step. Flow cytometry analysis was performed with a FACSCalibur cytometer (Becton Dickinson) in the cytometry and fluorescence microscopy unit at the Complutense University of Madrid.

Western Blot

After the corresponding treatments, cells were washed and lysed with RIPA buffer (Thermo Fisher Scientific) supplemented with Protease/Phosphatase Inhibitor Cocktail (Cell Signaling) and 1 mM PMSF (Sigma-Aldrich) for 30 min at 4°C. Protein was quantified with Micro BCA Kit (Pierce) following the manufacturer's protocols. 10 µg of total protein from cell lysates were separated in 10% SDS-polyacrylamide gel electrophoresis (SDS-PAGE) and transferred onto a nitrocellulose membrane (Bio-Rad Laboratories). The membrane was blocked with 5% BSA, 0.1% Tween-20 in Tris buffered saline for 1 h and incubated with the indicated primary antibodies: phospho-Akt (Ser473) (1:1000, Cell Signaling), phospho-p70 S6 Kinase (Thr389) (1:750, Cell Signaling), and β-actin (1:15000, Sigma-Aldrich). Then, the membrane was washed and incubated with goat anti-rabbit (1:4000; Bio-Rad Laboratories) or goat anti-mouse (1:2500, Pierce) conjugated with horseradish peroxidase (HRP) as a secondary antibody. The signal was developed with Clarity Western ECL Substrate, detected in a Chemidoc XRS System and analyzed with Image Lab Software (all from Bio-Rad). Briefly, for the quantification of the images obtained, same-size regions of interest (ROIs) were displayed over the different bands and the intensity/mm^2 of each ROI was quantified. After removal of the background value, the quantification of each band was then relativized to the one of its corresponding loading control (β-actin).

Metabolic studies

The determination of glucose concentration in cell-free culture supernatants was assessed by using the Glucose (GO) Assay Kit (Sigma-Aldrich). The metabolic rate was derived mathematically as the percentage of glucose consumed relative to its concentration in medium without cells (2 mg/mL). Lactate concentration was measured in perchloric acid deproteinized culture supernatants by means of a two-step coupled lactate oxidase (Sigma-Aldrich) and HRP (Fisher Scientific) enzymatic reactions. Briefly, lactate was oxidized producing H_2O_2 which was coupled to the conversion of Amplex Red reagent (Fisher Scientific) to fluorescent resorufin by HRP. The fluorescence intensity of resorufin was analyzed using FLUOstar OPTIMA fluorescence reader (BMG LabTech).

Real-time metabolic profiling of macrophages was performed using a Seahorse XF HS Mini Analyzer (Agilent) following conventional protocols for adherent cells. Briefly, human macrophages were harvested at day 5 of differentiation and seeded ($50x10^3$ cells/well) in XFp Cell Culture Miniplates with cRPMI supplemented with 100 ng/mL GM-CSF. Cells were incubated 24 h and then activated for 18 h with LPS or LPS+WIN55,212-2 (LPS +WIN), 10 ng/mL and 10 µM respectively. For peritoneal macrophage experiments, mice peritoneal cells were seeded ($400x10^3$ cells/well) in XFp Cell Culture Miniplates with cRPMI supplemented with 20 ng/mL M-CSF and incubated for 3h. Peritoneal macrophages were purified by adherence through three consecutive washing steps and stimulated for 18 h with LPS or LPS+WIN55,212-2 (LPS+WIN), 10 ng/mL and 10 µM respectively. After stimulation, cRPMI medium was removed, cells were washed and cultured with XF DMEM medium supplemented with 10 mM glucose, 1 mM pyruvate and 2 mM glutamine in a CO_2-free incubator for at least 1 h at 37°C before the assay. To accurately monitor glycolysis, we analysed the glycolytic proton efflux rate (glycoPER) at three consecutive stages: basal conditions (no drugs administrated), inhibition of the electron transport chain (0,5 µM Rotenone, ROT) and (0,5 µM Antimycin A, AA) and inhibition of glycolysis (50 mM 2-deoxy-D-glucose, 2-DG) (Sigma-Aldrich).

Quantitative PCR

The RNA from collected samples was isolated with RNeasy Mini Kit (Qiagen) according to the manufacturer's protocol. Next, complementary DNA was generated with a PrimeScript RT Reagent Kit (Takara Bio). Finally, quantitative PCR (qPCR) was performed by using FastStart Universal SYBR Green Master (Roche). The sequences of the primer pairs used are listed in Supplementary Table 1.

Chromatin Immunoprecipitation

For chromatin immunoprecipitation (ChIP), cells were harvested and fixed after stimulation. Samples were lysed and sonicated using a Branson 1200 Ultrasonic Cleaner to obtain chromatin fragments of optimal size (300-800 bp). Sheared chromatin was incubated using 2 µL of anti-H3K27ac antibody (Abcam, ab4729) or 2 µL of anti-IgG antibody (Millipore, 12-370), and immunoprecipitated with Dynabeads A (Invitrogen, 10001D) and Dynabeads G (Invitrogen, 10003D) magnetic beads. ChIP samples were de-cross-linked with proteinase K (Thermo Fisher Scientific) at 65°C for 4 h. Then, DNA was purified with the DNA Clean Kit & Concentrator TM-5 (Zymo Research). Quantitative analysis of the purified ChIP and Input DNAs was performed by using FastStart Universal SYBR Green Master (Roche) by real time qPCR.

Ex vivo culture of PMΦs

Female BALB/c mice were anesthetized using isoflurane and subjected to intraperitoneal lavage with 3 mL of 20 mM PBS/EDTA.

10.3389/fimmu.2023.1147520

The peritoneal cells were then washed, seeded in medium at $0,5x10^6$ cells/mL and allowed to rest for 3h. Then, PMΦs were isolated by adherence after three consecutive washing steps and treated with the indicated stimuli.

In vivo LPS-induced sepsis model

All mice procedures included in this study were reviewed and ethically approved by Universidad Complutense de Madrid (UCM) and Comunidad Autónoma de Madrid (CAM) within the context of project SAF-2017-84978-R and PID2020-114396RB-I00 (*CAM:ref.10/250312.9/18 and CAM:ref.10/465020.9/21*). 6-week-old female BALB/c mice (Charles River) were randomly assigned into 4 groups. Then, mice were intraperitoneally injected with vehicle (PBS+DMSO), WIN55,212-2 (5 mg/kg), LPS (20 mg/kg), or LPS plus WIN55,212-2, respectively. Blood samples were collected 12 h after LPS administration *via* retro-orbital bleeding using lime grass Pasteur pipettes and microtainer tubes (Beckton Dickinson). To collect serum, samples were centrifuged at 10,000 rpm for 10 min at room temperature. Then, the presence of bilirubin in mice serum was determined by its absorbance at 450 nm, lactate dehydrogenase (LDH) activity was analyzed using CyQUANT LDH Cytotoxicity Assay Kit (Fisher) and the concentration of TNFα, IL-1β and IL-6 was measured by ELISA.

Statistical analysis

Statistical analyses were performed with GraphPad Prism software (version 6.0) by using Paired t test, Unpaired t test, Wilcoxon test, One-way ANOVA or Spearman test. Significance was defined as: * $P < 0.05$, ** $P < 0.01$, *** $P < 0.001$ and **** $P < 0.0001$.

Results

Monocyte-derived dendritic cells differentiated in the presence of WIN55,212-2 display anti-inflammatory and tolerogenic features

To determine the capacity of WIN55,212-2 to modulate the phenotype and function of human monocyte-derived DCs (hmoDCs), monocytes were differentiated into DCs under conventional protocols in the absence or presence of this synthetic cannabinoid (Figure 1A). First, the expression of CBRs in monocytes was confirmed at both mRNA and protein level (Supplementary Figure 1). Then, we used 50 nM of WIN55,212-2 during the differentiation process to generate WIN-hmoDCs, as this concentration showed the most effective results without affecting cell viability during dose-response optimization experiments (Supplementary Figure 2). After 18 h of LPS stimulation, conventional hmoDCs produced higher amounts of the pro-inflammatory cytokines TNFα, IL-1β and IL-6 than WIN-hmoDCs (Figure 1B). No significant differences were observed in the production of the anti-inflammatory cytokine IL-10. The IL-10/TNFα, IL-10/IL-1β and IL-10/IL-6 cytokine ratios were significantly higher in LPS-stimulated WIN-hmoDCs than conventional hmoDCs (Figure 1C), indicating that WIN55,212-2 reprograms the differentiation of monocytes towards DCs displaying anti-inflammatory features upon LPS stimulation. Interestingly, no differences in the expression of HLA-DR or the costimulatory molecules CD83 or CD86 were observed between conventional hmoDCs and WIN-hmoDCs (Supplementary Figure 3),

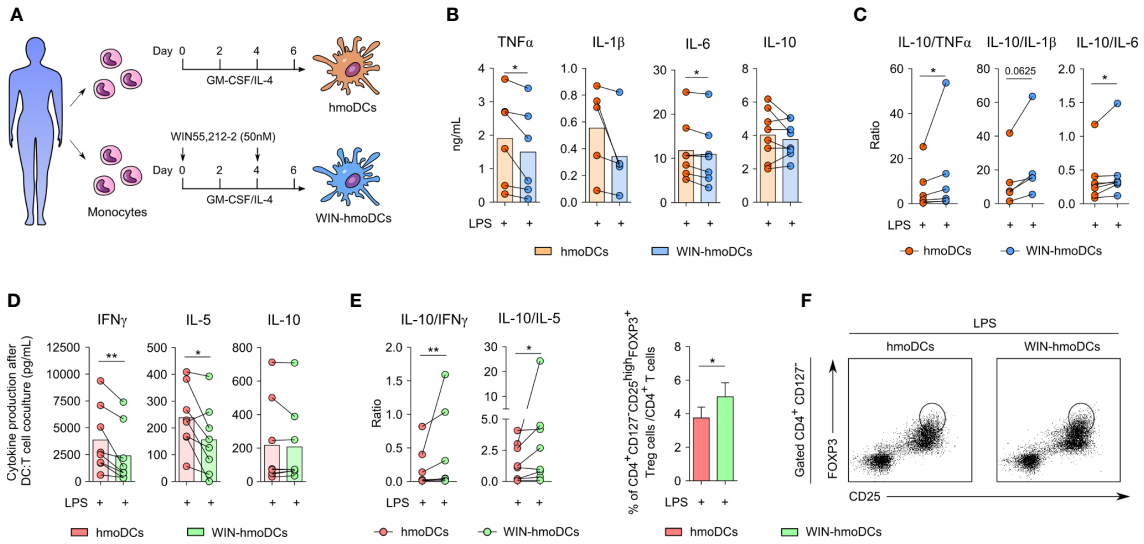

FIGURE 1
WIN-hmoDCs display anti-inflammatory and tolerogenic properties upon LPS stimulation. **(A)** Differentiation protocol of hmoDCs and WIN-hmoDCs from monocytes. **(B, C)** cytokine production **(B)** and ratios **(C)** of conventional hmoDCs and WIN-hmoDCs after LPS stimulation (100 ng/mL) (n=5-8). **(D E)** cytokines **(D)** and ratios **(E)** produced by allogeneic naive $CD4^+$ T cells primed by LPS-stimulated hmoDCs or WIN-hmoDCs after 5 days of coculture (n=8). **(F)** Percentage (left), and representative dot plots (right) of induced $CD4^+CD25^{high}CD127^-FOXP3^{high}$ Tregs by allogeneic LPS-stimulated hmoDCs or WIN-hmoDCs (n=7). Values are shown as mean ± SEM. Statistical significance was determined by Paired t test **(B, D, F)** or Wilcoxon test **(C, E)**. *P<0.05, **P<0.01.

10.3389/fimmu.2023.1147520

suggesting that WIN-hmoDCs might well preserve their capacity to antigen presentation and T cell activation. To further assay the capacity of the generated WIN-hmoDCs to polarize T cell responses upon LPS stimulation, we performed allogeneic coculture experiments with naïve $CD4^+$ T cells. LPS-stimulated WIN-hmoDCs generated T cells that produced significantly lower amounts of IFNγ and IL-5 than LPS-activated hmoDCs, without significant differences observed in the production of IL-10 (Figure 1D). The IL-10/IL-5 and IL-10/IFNγ ratios were significantly higher in T cells generated by WIN-hmoDCs than conventional hmoDCs (Figure 1E), suggesting the generation of Tregs by WIN-hmoDCs. Supporting these data, the frequency of $CD4^+$ $CD127^-$ $CD25^{high}$ $FOXP3^{high}$ Tregs generated by LPS-activated WIN-hmoDCs was significantly higher than by LPS-stimulated conventional hmoDCs (Figure 1F). Collectively, these data indicate that the presence of WIN55,212-2 during monocyte differentiation promotes the generation of DCs with anti-inflammatory properties upon LPS stimulation and with increased capacity to polarize Tregs.

WIN55,212-2 inhibits the activation of pro-inflammatory M1 human macrophages

To investigate the effects of WIN55,212-2 in human macrophages under inflammatory conditions, we first generated human macrophages from the THP-1 monocytic cell line (THP-1 MΦs) and stimulated them with medium (control), LPS/IFNγ alone (M1) or in the presence of WIN55,212-2 (M1+WIN) (Figure 2A). WIN55,212-2 inhibited LPS/IFNγ-induced NF-κB/AP-1 activation in THP-1 MΦs in a dose dependent manner (Figure 2B). Supporting these data, WIN55,212-2 impaired the mRNA expression of the classical M1 markers *CCR7*, *TNF* or *CD80* induced by LPS/IFNγ stimulation in THP-1 MΦs (Figure 2C) and inhibited the production of the pro-inflammatory cytokines TNFα and IL-6 in a dose-dependent manner (Figure 2D).

To further verify these results, we generated primary human monocyte-derived macrophages as shown in Figure 2E, which we termed as GM-MΦs according to Murray et al. (17). The expression levels of CBRs in GM-MΦs was confirmed at both mRNA and

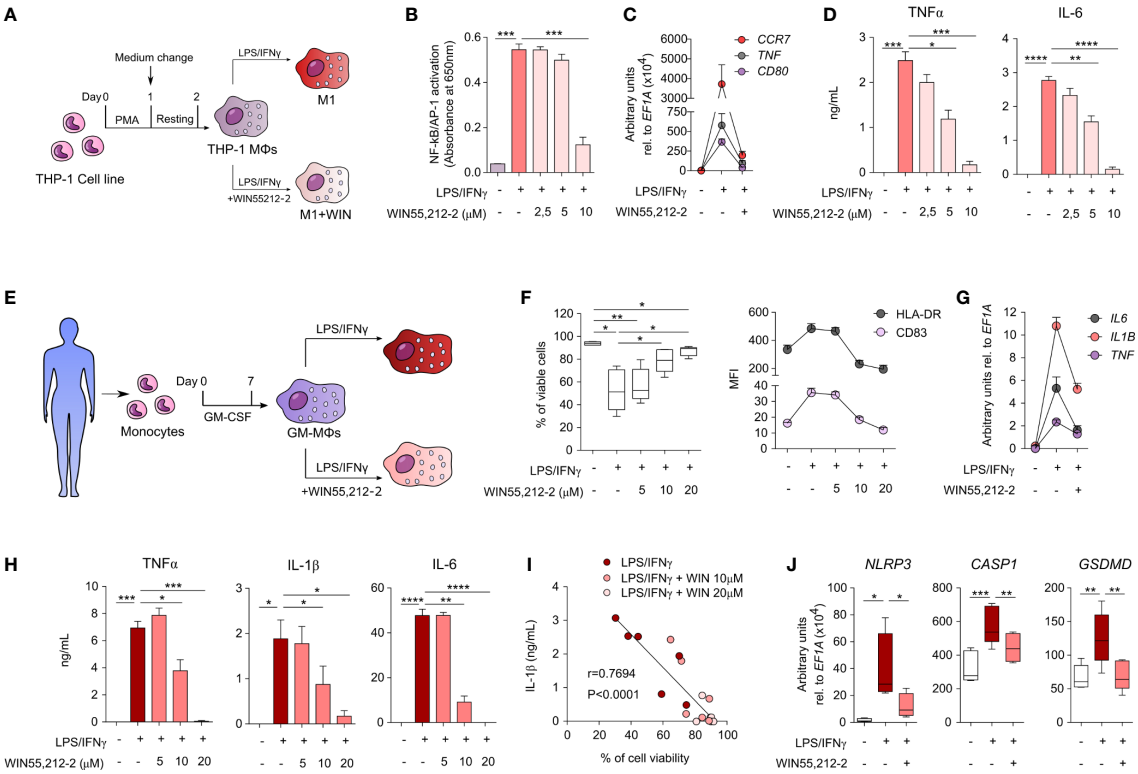

FIGURE 2
WIN55,212-2 inhibits pro-inflammatory activation of human macrophages. **(A)** THP-1 MΦs generation and activation protocol. **(B)** NF-κB/AP-1 activation in THP-1 XBlue MΦs after 18h of stimulation with medium, LPS/IFNγ (100 ng/mL and 50 ng/mL, respectively) or LPS/IFNγ plus the indicated doses of WIN55,212-2 (n=6). **(C)** mRNA expression levels of the indicated genes after 18h of stimulation of THP-1 MΦs with medium, LPS/IFNγ or LPS/IFNγ plus WIN55,212-2 (10 μM) (n=5). **(D)** Cytokine production by THP-1 MΦs stimulated with medium, LPS/IFNγ or LPS/IFNγ plus the indicated doses of WIN55,212-2 (n=6). **(E)** Protocol of human GM-MΦs differentiation and activation. **(F)** Percentage of viable cells (left) and mean fluorescence intensity (MFI) of the indicated markers (right) after GM-MΦs stimulation with medium, LPS/IFNγ (100 ng/mL and 50 ng/mL) or LPS/IFNγ plus the indicated doses of WIN55,212-2 (n=6). **(G)** mRNA expression levels of the indicated cytokines after 4h stimulation of GM-MΦs with medium, LPS/IFNγ or LPS/IFNγ plus WIN55,212-2 (20 μM) (n=5). **(H)** Cytokine production after 18h stimulation of GM-MΦs with medium, LPS/IFNγ or LPS/IFNγ plus the indicated doses of WIN55,212-2 (n=6). **(I)** Correlation between IL-1β production and GM-MØ viability after stimulation with LPS/IFNγ and LPS/IFNγ plus the indicated doses of WIN55,212-2 (n=6). **(J)** mRNA expression levels of the indicated genes after 4h stimulation of GM-MΦs with medium, LPS/IFNγ or LPS/IFNγ plus WIN55,212-2 (20 μM) (n=5). Values are shown as mean ± SEM. Statistical significance was determined by One-way ANOVA **(B, D, F, H, J)** or Spearman test **(I)**. *P<0.05, **P<0.01, ***P<0.001 and ****P<0.0001.

protein level (Supplementary Figure 4). Next, GM-MΦs were stimulated with medium (control), LPS/IFNγ alone or in the presence of WIN55,212-2 at different doses during 18 h to monitor cell viability and activation status. The viability of GM-MΦs stimulated with LPS/IFNγ alone was significantly compromised compared to unstimulated cells. Interestingly, WIN55,212-2 dose-dependently enhanced cell viability of LPS/IFNγ-stimulated GM-MΦs (Figure 2F), suggesting the inhibition of LPS/IFNγ-induced inflammatory cell death pathways in human GM-MΦs. The cannabinoid also downregulated the LPS/IFNγ-induced expression of HLA-DR and the costimulatory molecule CD83 in a dose dependent manner (Figure 2F). Likewise, LPS/IFNγ-activated GM-MΦs treated with WIN55,212-2 reduced the production of the pro-inflammatory cytokines TNFα, IL-1β and IL-6 both at the mRNA (Figure 2G) and protein level (Figure 2H), thus confirming the potent anti-inflammatory profile. In all cases, LPS/IFNγ-induced IL-10 levels were also inhibited by WIN55,212-2 in a dose-dependent manner (Supplementary Figure 5), suggesting that IL-10-producing M2 phenotypes in human macrophages are not generated under the assayed conditions. Remarkably, we uncovered a significant inverse correlation between IL-1β production and cell viability in GM-MΦs stimulated under the different assayed conditions (Figure 2I), which prompted us to investigate whether WIN55,212-2 could interfere with inflammasome activation and pyroptotic-mediated cell death. For that, we quantified the mRNA expression levels of the inflammasome components *NLRP3* and *CASP1*, and the pore-forming protein *GSDMD* after macrophage activation under different conditions. LPS/IFNγ stimulation significantly enhanced the mRNA expression levels of all the assayed molecules, which were in all the cases significantly impaired by WIN55,212-2 (Figure 2J), confirming its potential capacity to rescue human macrophages from this inflammatory cell death pathway.

WIN55,212-2 impairs the LPS-induced metabolic and epigenetic reprogramming in human macrophages

To shed light into the molecular mechanisms underlying the anti-inflammatory capacity of WIN55,212-2 in human macrophages, we sought to investigate the potential effects of this cannabinoid on the metabolic pathways linked to the acquisition of inflammatory phenotypes in innate immune cells. For this set of experiments, we chose a lower dose of LPS for macrophage stimulation to avoid bias due to overactivation-induced cell death. Stimulation of GM-MΦs with LPS (10 ng/mL) mimics the previous LPS/IFNγ activation by significantly inducing the production of pro-inflammatory cytokines without affecting cell viability (Supplementary Figure 6). We initially analysed the mTORC1 signalling pathway as the key regulator of anabolic metabolism linked to inflammatory features in macrophages. WIN55,212-2 inhibited the LPS-induced phosphorylation of Akt and p70S6K (Figure 3A), indicating a reduced activation of the mTORC1 pathway and suggesting the potential regulation of LPS-induced metabolic reprogramming. The administration of WIN55,212-2 alone showed minimal changes in glucose uptake and lactate production (Supplementary Figure 7). Nonetheless, WIN55212,2 significantly reduced the high glucose consumption and the increased lactate production observed in LPS-stimulated GM-MΦs (Figure 3B), demonstrating the capacity of this cannabinoid to interfere with the glycolytic metabolism. Supporting these data, WIN55,212-2 significantly reduced the mRNA expression levels of the glycolysis-related genes *HK2*, *PFKB3*, *LDHA1* and *HIF1A* in LPS-stimulated macrophages, which was accompanied by significantly lower mRNA levels of the pro-inflammatory cytokines *TNF*, *IL1B*, *IL8* and *IL6* (Figure 3C). To further confirm these results, we performed functional metabolic experiments using a Seahorse bioanalyzer to monitor real-time glycolytic proton efflux rate (glycoPER) in LPS- or LPS + WIN55,212-2-stimulated GM-MΦs. Our data showed that commitment to glycolysis was significantly higher in LPS-stimulated than LPS+WIN55,212-2-stimulated GM-MΦs both at basal conditions (basal glycolysis) and after the inhibition of the electron transport chain (compensatory glycolysis) (Figure 3D). Remarkably, the production of TNFα, IL-1β and IL-6 by GM-MΦs stimulated with LPS or LPS+WIN55,212-2, directly correlated with the amount of glucose consumed by those cells (Figure 3E), indicating that the inhibition of the glucose uptake by human macrophages might well be connected to WIN55,212-2 anti-inflammatory effects. As recent evidence links LPS-induced glycolysis with epigenetic changes that govern pro-inflammatory cytokine production in macrophages (18, 19), we studied chromatin status near the *TNF*, *IL1B* and *IL6* gene promoters by quantifying the activation histone mark H3K27ac by ChIP analysis. LPS significantly enhanced the acetylation of H3K27 within the pro-inflammatory *IL1B* and *IL6* genes, which was significantly reduced by WIN55,212-2 (Figure 3F). A similar non-significant tendency was also observed within the *TNF* gene promoter. Collectively, these findings indicate that WIN55,212-2 inhibits the metabolic and epigenetic inflammatory reprogramming induced by LPS in human macrophages.

WIN55,212-2 protects from LPS-induced sepsis *in vivo* and limits LPS-induced metabolic reprogramming of *ex vivo* stimulated peritoneal macrophages

To assess the potential *in vivo* anti-inflammatory properties of WIN55,212-2, we employed a mice model of LPS-induced sepsis. Mice were intraperitoneally injected with PBS, WIN55,212-2 or a lethal dose of LPS alone or in the presence of WIN55,212-2 (Figure 4A). After 12h, we collected mice serum and quantified the levels of IL-1β, lactate dehydrogenase (LDH) activity and bilirubin levels as hallmarks of the inflammatory response/inflammasome activation, cell death or organ injury, respectively. Intraperitoneal administration of LPS significantly enhanced the levels of serum IL-1β, which was significantly impaired by WIN55,212-2 (Figure 4B). Remarkably, not only inflammasome-dependent IL-1β release but the levels of other inflammatory mediators such as TNFα and IL-6 were also reduced by the

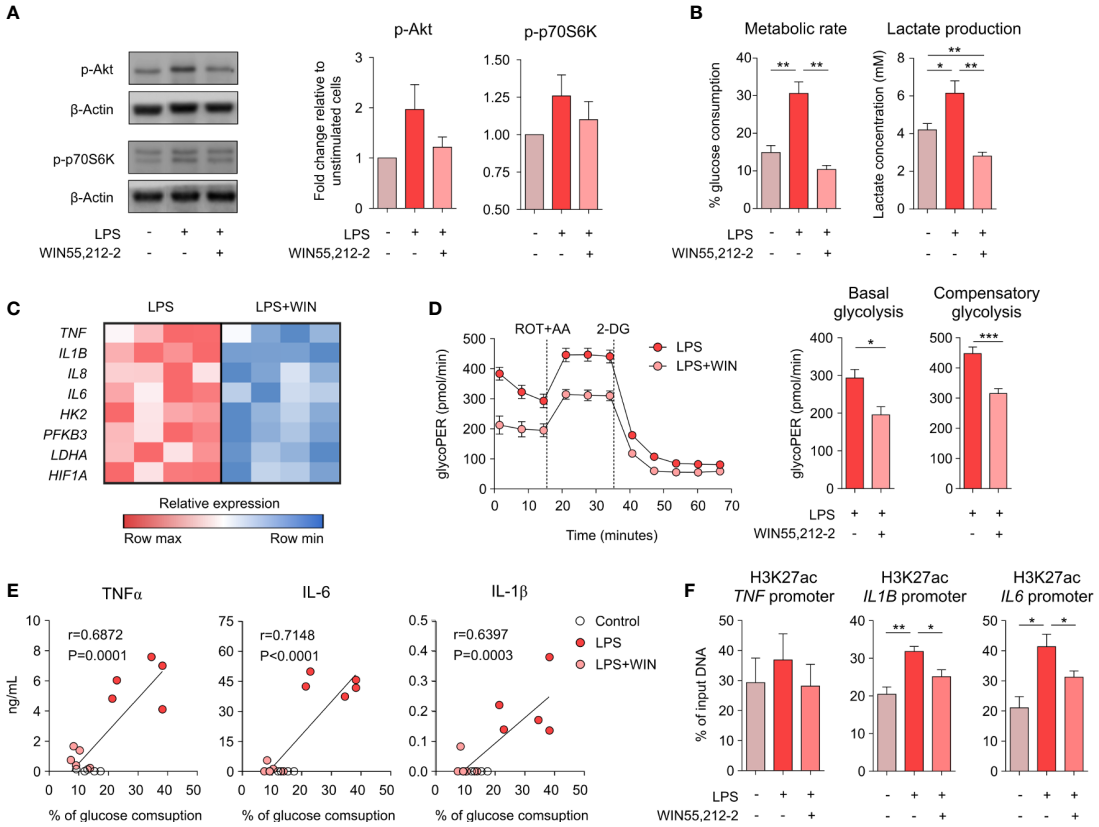

FIGURE 3
WIN55,212-2 impairs the metabolic and epigenetic reprogramming induced by LPS in human macrophages. **(A)** Representative western blot (left) and densitometric quantification (right) of GM-MΦs stimulated with medium, LPS (10 ng/mL) or LPS plus WIN55,212-2 (10 μM). The graph shows combined results from 30 and 60 min of stimulation (n=6 independent experiments with 4 different donors). **(B)** Percentage of glucose consumption and lactate concentration measured from cell-free supernatants of GM-MΦs stimulated with medium, LPS (10 ng/mL) or LPS plus WIN55,212-2 (10μM) (n=6). **(C)** Heat map showing the expression of pro-inflammatory cytokine and glycolysis-related genes in GM-MΦs stimulated with LPS or LPS+WIN55,212-2 during 4h (n=4). **(D)** Real-time analysis of glycolytic Proton Efflux Rate (glycoPER) of GM-MΦs after 18h stimulation with LPS or LPS plus WIN55,212-2 (LPS+WIN) at basal conditions and after sequential addition of rotenone plus antimycin A (ROT+AA) and 2-deoxyglucose (2-DG). Graphs representing basal and compensatory glycolysis are displayed (right) (n=6 of two independent experiments). **(E)** Correlation between TNFα, IL-1β or IL-6 with the % of glucose consumption of GM-MΦs stimulated with medium (Control), LPS or LPS+WIN (n=5). **(F)** Analysis of H3K27ac histone modifications at the promoter sites of the indicated genes in GM-MΦs stimulated with medium, LPS or LPS plus WIN55,212-2 for 4h (n=5). Values are shown as mean ± SEM. Statistical significance was determined by One-way ANOVA **(B, F)** Unpaired t test **(D)** or Spearman test **(E)**. *P<0.05, **P<0.01 and ***P<0.001.

treatment with the cannabinoid (Supplementary Figure 8). Similarly, increased levels of serum LDH and bilirubin were found in LPS-treated mice while mice receiving LPS+WIN55,212-2 showed significantly lower levels of both parameters (Figure 4C). These data confirmed the *in vivo* anti-inflammatory properties of WIN55,212-2 in the context of LPS-induce sepsis. As macrophages depict one of the main immune cell populations of the peritoneal cavity (20), we next sought to investigate their potential contribution into such protective anti-inflammatory effects. For that, we isolated peritoneal macrophages (PMΦs) and stimulated them *ex vivo* with medium (control), LPS or LPS+WIN55,212-2 (Figure 4D). WIN55,212-2 inhibited the production of TNFα and IL-6 by LPS-stimulated PMΦs in a dose-dependent manner (Figure 4E). Likewise, LPS-induced glucose consumption and lactate production was significantly impaired by WIN55,212-2, suggesting that this synthetic cannabinoid also inhibits LPS-induced metabolic rewiring in *ex vivo* stimulated PMΦs (Figure 4F). Supporting these data, real-time metabolic experiments showed a significantly reduced basal and compensatory glycolysis in LPS+WIN-stimulated PMΦs compared LPS-stimulated PMΦs, thus confirming our findings (Figure 4G). Collectively, these data show the *in vivo* anti-inflammatory capacity of WIN55,212-2 and its potential to immunomodulate tissue-specific macrophage populations during LPS-induced inflammatory conditions.

Discussion

In this study, we uncover unpreceded mechanisms about how the synthetic cannabinoid WIN55,212-2 displays immunomodulatory and anti-inflammatory properties by regulating the differentiation of human monocytes into DCs and the activation of pro-inflammatory macrophages. We showed that tolerogenic WIN-hmoDCs are less responsive to LPS and prime functional Tregs. In addition, WIN55,212-2 impaired the pro-inflammatory polarization of human

10.3389/fimmu.2023.1147520

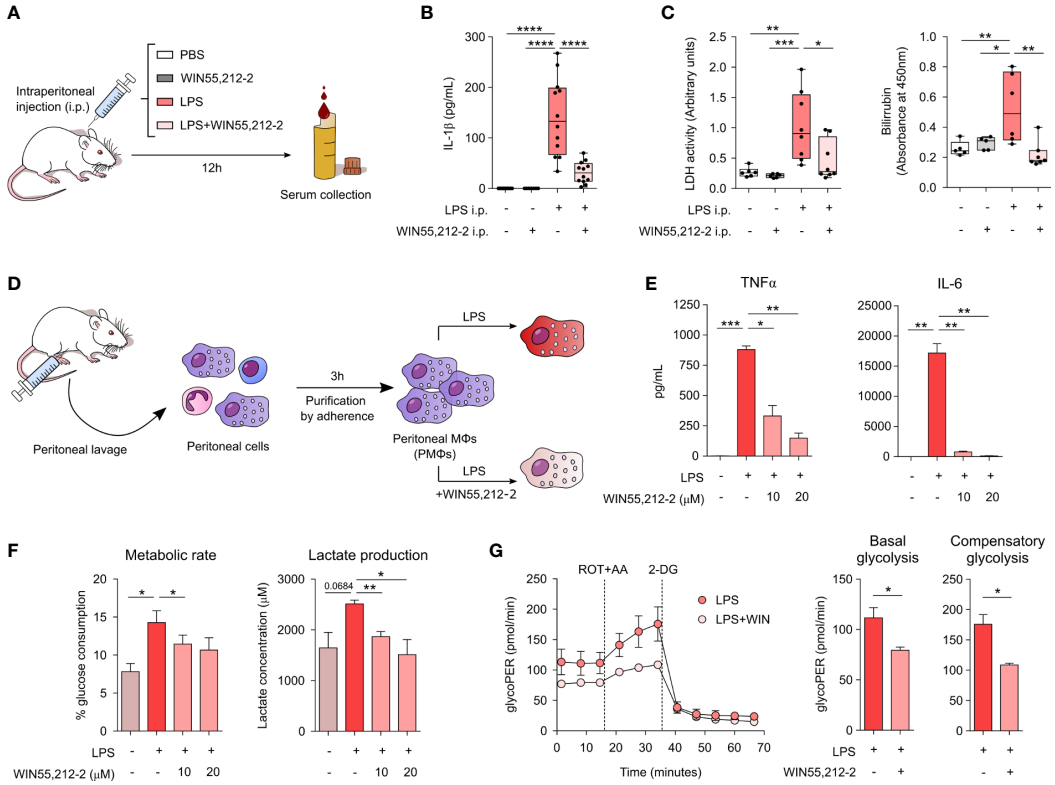

FIGURE 4
In vivo and *ex vivo* protective and anti-inflammatory potential of WIN55,212-2. **(A)** Schematic representation of the LPS-induced sepsis model. **(B)** Serum IL-1β levels after 12h of intraperitoneal (i.p.) administration of PBS (Control), WIN55,212-2 (5mg/kg), LPS (20mg/kg) or LPS plus WIN55,212-2 (n=7-12). **(C)** Assessment of the clinical parameters LDH and bilirubin in the serum of mice treated with the indicated conditions (n=5-8). **(D)** Protocol for peritoneal macrophages (PMΦs) isolation and activation. **(E)** Cytokine production by *ex vivo* stimulated PMΦs with medium, LPS (10 ng/mL) or LPS plus the indicated doses of WIN55,212-2 (n=4). **(F)** Percentage of glucose consumption and lactate concentration measured from cell-free supernatants of PMΦs treated with medium, LPS or LPS plus the indicated doses of WIN55,212-2 (n=6). **(G)** Real-time analysis of glycolytic Proton Efflux Rate (glycoPER) of PMΦs after 18h stimulation with LPS or LPS plus WIN55,212-2 at basal conditions and after sequential addition of rotenone plus antimycin A (ROT+AA) and 2-deoxyglucose (2-DG). Graphs representing basal as well as compensatory glycolysis are included on the right (n=3). Statistical significance was determined by One-way ANOVA or Unpaired t test. *P<0.05, **P<0.01, ***P<0.001 and ****P<0.0001.

macrophages by inhibiting cytokine production, inflammasome activation and rescuing macrophages from pyroptotic cell death. Mechanistically, WIN55,212-2 induced a metabolic and epigenetic shift in macrophages by decreasing LPS-induced mTORC1 signaling, commitment to glycolysis and active histone marks in pro-inflammatory cytokine promoters. These data were confirmed in *ex vivo* stimulated PMΦs and supported by the anti-inflammatory capacity of WIN55,212-2 in a LPS-induced sepsis mouse model. Overall, we report novel insights into the anti-inflammatory capacity of WIN55,212-2 in myeloid cells, enhancing the knowledge on cell targets and mechanisms driving its potential beneficial effects in inflammatory conditions. Our findings might well contribute to open new avenues for the rational design of alternative cannabinoid-based therapeutic agents that are not able to cross the blood-brain barrier but retain anti-inflammatory/immunomodulatory properties on peripheral immune cells.

Monocytes are myeloid cells whose immune versatility relies on their capacity to differentiate into DCs or macrophages (4, 21). The environmental milieu to what monocytes are exposed is linked to the immunogenicity of the resulting differentiated cells. For example, the presence of stimuli such as dexamethasone (Dex), vitamin D3 (VitD3), rapamycin, or allergoid-mannan conjugates promotes the differentiation of monocytes into tolerogenic DCs or immunosuppressive macrophages (22–26). Conversely, monocytes exposed with whole heat-inactivated *Candida albicans* or β-glucans from its cell wall give raise to trained monocyte-derived macrophages (27–29). Here, we show that LPS-stimulated WIN-hmoDCs displayed reduced production of the pro-inflammatory cytokines TNFα, IL-1β and IL-6 without changes in IL-10. Supporting these data, previous studies demonstrated that hmoDCs generated in the presence of THC produced less IL-12 after activation. THC also reduced the phagocytic activity, maturation state and the capacity of the differentiated hmoDCs to activate T cells (30). Likewise, WIN-hmoDCs primed FOXP3$^+$ Tregs and displayed reduced capacity to polarize both Th1 and Th2 responses. The induction and/or expansion of Tregs is essential to keep homeostasis in the context of immune-mediated and inflammatory diseases (31–33), which might be regulated by exogenous signals including cannabinoids like cannabidiol (CBD), JTE907 or O-1966 (34–36). We previously showed that fully

differentiated conventional hmoDCs and blood DCs subsets stimulated *in vitro* with toll-like receptor ligands in the presence of WIN55,212-2 promote functional Tregs (13, 37, 38), which was further corroborated *in vivo* in LPS-induced sepsis, peanut-allergic sensitization and anaphylaxis models (13, 37). Our current data enhance the knowledge on how WIN55,212-2 could promote Tregs not only by directly acting on fully differentiated DCs, but also by imprinting tolerogenicity during monocyte differentiation into DC.

Macrophages are major producers of cytokines and chemokines that are essential for innate immune responses (3, 4). In this work, we focused on the capacity of WIN55,212-2 to impair pro-inflammatory macrophage polarization. Previous studies reported that AEA, 2-AG, THC or CBD inhibit the production of inflammatory mediators in macrophages (39–41). WIN55,212-2 impaired NF-κB activation and cytokine release in LPS-stimulated TLR3/TLR4-transfected HEK293 cells, hmoDCs and murine macrophages activated with oxidized-LDL (13, 42, 43). Consistent with these reports, we showed that WIN55,212-2 impaired NF-κB/AP-1-activation, decreased the expression of activation markers and the production of inflammatory cytokines in classically M1 activated THP-1 MΦs, which was comprehensively validated in primary human macrophages (GM-MΦs) and murine tissue-resident macrophages (PMΦs). WIN55,212-2 also restored GM-MΦs viability after LPS/IFNγ-induced inflammatory cell death, which correlated with a reduced release of IL-1β and impaired expression of *NLRP3*, *CASP1* and *GSDMD*. These findings suggest that WIN55,212-2 interferes with inflammasome activation and protects from pyroptotic macrophage death, which is congruent with the previous reported capacity of CBD or THC to prevent inflammasome-mediated signalling (41, 44). Nonetheless, we cannot rule out the potential contribution of WIN55,212-2 to interfere with other cell death pathways, since the recently coined term PANoptosis recognizes the complexity of programmed cell death signalling and the potential interplay between its molecular executors (45, 46). In fact, it was recently described that caspase 8 and other apoptotic proteins were involved in the IFNγ priming of macrophage TLR-induced death (47). The combination of IFNγ with pro-inflammatory cytokines, mainly TNFα, also induces macrophage death and perpetuates inflammation during cytokine shock syndrome (48). Herein, the cannabinoid WIN55,212-2 dose-dependently reduced the production of TNFα in LPS/IFNγ-treated GM-MΦs, suggesting its potential to prevent both cytokine storm and inflammatory cell death.

The anti-inflammatory capacity of cannabinoids has been linked with their ability to interfere with TLR-signalling and to induce metabolic reprogramming in immune cells (9, 49, 50). Our previous findings in human DCs indicate that the WIN55,212-2-mediated activation of CB1 as well as of the non-canonical cannabinoid receptor, peroxisome proliferator-activated receptor α (PPARα), leads to a tolerogenic profile characterized by AMPK-mediated induction of autophagy and promotion of oxidative phosphorylation over glycolysis (13). Herein, we show that WIN55,212-2 impaired LPS-induced phosphorylation of mTORc1's upstream and downstream signalling molecules, Akt and p70S6K, in human macrophages. Aerobic glycolysis is the main supply for the energetic demands of pro-inflammatory activated macrophages after TLR-engagement (51, 52). Our real time metabolic experiments in LPS or LPS+WIN55,212-2-stimulated GM-MΦs showed reduced basal and compensatory glycolysis in the latter ones, indicating inhibition of TLR-induced metabolic rewiring. In this context, Lauterbach and others demonstrated that glucose uptake and glycolysis provide metabolic substrates that support LPS-induced inflammatory gene expression through epigenetic histone modifications (18, 19). LPS augments H3K27ac at *IL1B* and *IL6* gene promoters in GM-MΦs, which was impaired by WIN55,212-2, supporting that WIN55,212-2 may alter the LPS-induced metabolic-epigenetic axis in human macrophages. Beyond the potentiation of inflammatory cytokine expression, the induction of aerobic glycolysis also sustains inflammasome induction and its inhibition compromises IL-1β production (53–55). In addition, activation of mTORc1 pathway is linked to inflammasome activation, gasdermin D oligomerization and pyroptosis (56, 57). Altogether these data might well support our findings on the capacity of WIN55,212-2 to prevent inflammatory cell death.

Systemic inflammatory diseases with uncontrolled release of pro-inflammatory mediators (cytokine storm), are life-threatening conditions that remain poorly managed by current treatments (58–60). For instance, during endotoxin shock, the cooperative activation of inflammatory cytokine and cell death signalling drives severe tissue injury and multi-organ failure that may be eventually lethal (61, 62). Here, WIN55,212-2 abolished the LPS-induced increase of serum IL-1β in mice, confirming its previously reported *in vivo* anti-inflammatory capacity (13, 37, 42, 63–66). Inflammasome activation during sepsis aggravates organ injury and worsens prognosis. Suppression of inflammasome and pyroptosis protects mice from septic myocardial dysfunction, and clinical trial data shows reduced mortality after blockage of IL-1R in septic patients developing macrophage activation syndrome (MAS) (67, 68). Patients that develop MAS were characterized by hepatobiliary dysfunction and had significantly higher risk of death (69). We showed that WIN55,212-2-mediated decrease of serum IL-1β was associated with reduced levels of the myocardial and hepatic injury markers LDH and bilirubin. Remarkably, we showed that cytokine production of *ex vivo* stimulated PMΦs was dose-dependently modulated by WIN55,212-2 and associated with a markedly reduced glucose consumption and commitment to glycolysis. Our findings are congruent with the fact that inhibition of glycolysis with 2-DG mimicked WIN55,212-2 immunomodulatory effects in M1-activated murine alveolar macrophages and the capacity of WIN55,212-2 to protect mice from acute lung injury (63, 64).

Collectively, we uncover novel findings on the immunosuppressive capacity of WIN55,212-2 by acting on monocytes and macrophages and provide novel insights into the molecular mechanisms underlying such effects. Our *in vivo* data confirms WIN55,212-2 anti-inflammatory properties and highlights the important involvement of myeloid lineage cells in its potential therapeutic benefits. Our data might well contribute to pave the way for the development of alternative cannabinoid-based therapies for immune-mediated and inflammatory diseases.

Data availability statement

The raw data supporting the conclusions of this article will be made available by the authors, without undue reservation.

Ethics statement

All mice procedures included in this study were reviewed and ethically approved by Universidad Complutense de Madrid (UCM) and Comunidad Autoínoma de Madrid (CAM) within the context of project SAF-2017-84978-R and PID2020-114396RB-I00 (CAM:ref.10/250312.9/18 and CAM:ref.10/465020.9/21).

Author contributions

Conceived and designed the study: OP. Performed the experiments: MP-D (human and mice experiments), AA (mice experiments and technical support for human experiments), LM-C, AR-M, AM, and CS-O (technical support for human experiments). Analyzed and discussed the data: MP-D, AA, LM-C, AR-M, AM, CS-O, and OP. Wrote the paper: MP-D and OP. All authors contributed to the article and approved the submitted version.

Funding

The authors' laboratory is supported by grant PID2020-114396RB-I00 to OP from MINECO, Spain. MP-D and LM-C are recipients of FPI (SAF-2017-84978-R) and FPU predoctoral fellowships from MINECO, respectively. AR-M is a recipient of a Margarita Salas contract (Reference: CA1/RSUE/2021-00843) cofinanced by the Ministerio de Universidades, the "Plan de Recuperación, Transformación y Resiliencia" and the Autonomous University of Madrid. CS-O is recipient of a predoctoral fellowship from "Doctorado Industrial between UCM-Inmunotek # IND2019/BMD-17182 by CAM.

Conflict of interest

OP has received fees for lectures or participation in Advisory Boards from AstraZeneca, GSK, Pfizer, Inmunotek SL, Novartis, Sanofi Genzyme, and Regeneron. OP has received research grants from Inmunotek SL, Novartis SL, Amgen-AstraZeneca, MINECO, MICINNIN and CAM.

The remaining authors declare that the research was conducted in the absence of any commercial or financial relationships that could be construed as a potential conflict of interest.

Publisher's note

Supplementary material

The Supplementary Material for this article can be found online at: https://www.frontiersin.org/articles/10.3389/fimmu.2023.1147520/full#supplementary-material

SUPPLEMENTARY FIGURE 1
Expression of CBRs in human monocytes. mRNA **(A)** and protein levels **(B)** of CB1 and CB2 in human monocytes was assayed by qPCR and flow cytometry (n=3). Values are shown as mean ± SEM.

SUPPLEMENTARY FIGURE 2
Viability **(A)** and relative cytokine production **(B)** of LPS-activated conventional hmoDCs or hmoDCs differentiated from monocytes in the presence of the indicated doses of WIN55,212-2 (n=2-5). Values are shown as mean ± SEM.

SUPPLEMENTARY FIGURE 3
Expression of costimulatory molecules in conventional hmoDCs and WIN-hmoDCs. Mean fluorescence intensity (MFI) of the indicated surface molecules expressed by LPS-activated conventional hmoDCs or WIN-hmoDCs (n=7). Values are shown as mean ± SEM.

SUPPLEMENTARY FIGURE 4
Expression of CBRs in human macrophages. mRNA **(A)** and protein levels **(B)** of CB1 and CB2 in human macrophages was assayed by qPCR and flow cytometry (n=3). Values are shown as mean ± SEM.

SUPPLEMENTARY FIGURE 5
WIN55,212-2 effect on IL-10 production. Graph shows IL-10 levels after stimulation of GM-MΦs with medium, LPS/IFNγ (100 ng/mL and 50 ng/mL) or LPS/IFNγ plus the indicated doses of WIN55,212-2 (n=6). Values are shown as mean ± SEM. Statistical significance was determined by One-way ANOVA. * P<0.05.

SUPPLEMENTARY FIGURE 6
Lower doses of LPS induces inflammatory activation of GM-MΦs without affecting cell viability. Percentage of viable cells **(A)** and cytokine production **(B)** after stimulation of GM-MΦs with medium, LPS (10 ng/mL) or LPS plus the indicated doses of WIN55,212-2 (n=6). Values are shown as mean ± SEM. Statistical significance was determined by One-way ANOVA. * P<0.05, ** P<0.01 and *** P<0.001.

SUPPLEMENTARY FIGURE 7
Metabolic changes induced by WIN55,212-2 administration in human macrophages. Percentage of glucose consumed **(A)** and lactate produced **(B)** by unstimulated or WIN55,212-2 activated GM-MOs (n=2). Values are shown as mean ± SEM.

SUPPLEMENTARY FIGURE 8
WIN55,212-2 inhibits cytokine production in LPS-induced septic mice. Serum levels of TNFα **(A)** and IL-6 **(B)** after 12h of intraperitoneal (i.p.) administration of PBS (Control), WIN55,212-2 (5mg/kg), LPS (20mg/kg) or LPS plus WIN55,212-2 (n=4-5). Values are shown as mean ± SEM. Statistical significance was determined by One-way ANOVA. * P<0.05, ** P<0.01, *** P<0.001 and **** P<0.0001.

References

1. Netea MG, Balkwill F, Chonchol M, Cominelli F, Donath MY, Giamarellos-Bourboulis EJ, et al. A guiding map for inflammation. *Nat Immunol* (2017) 18(8):826–31. doi: 10.1038/ni.3790

2. Nathan C, Ding A. Nonresolving inflammation. *Cell.* (2010) 140(6):871–82. doi: 10.1016/j.cell.2010.02.029

3. Hamidzadeh K, Christensen SM, Dalby E, Chandrasekaran P, Mosser DM. Macrophages and the recovery from acute and chronic inflammation. *Annu Rev Physiol* (2017) 79:567–92. doi: 10.1146/annurev-physiol-022516-034348

4. Geissmann F, Manz MG, Jung S, Sieweke MH, Merad M, Ley K. Development of monocytes, macrophages, and dendritic cells. *Science.* (2010) 327(5966):656–61. doi: 10.1126/science.1178331

5. O'Neill LA, Pearce EJ. Immunometabolism governs dendritic cell and macrophage function. *J Exp Med* (2016) 213(1):15–23. doi: 10.1084/jem.20151570

6. Stienstra R, Netea-Maier RT, Riksen NP, Joosten LAB, Netea MG. Specific and complex reprogramming of cellular metabolism in myeloid cells during innate immune responses. *Cell Metab* (2017) 26(1):142–56. doi: 10.1016/j.cmet.2017.06.001

7. Greene JT, Brian B, Senevirathne SE, Freedman TS. Regulation of myeloid-cell activation. *Curr Opin Immunol* (2021) 73:34–42. doi: 10.1016/j.coi.2021.09.004

8. Strehl C, Buttgereit F. Optimized glucocorticoid therapy: teaching old drugs new tricks. *Mol Cell Endocrinol* (2013) 380(1-2):32–40. doi: 10.1016/j.mce.2013.01.026

9. Angelina A, Perez-Diego M, Lopez-Abente J, Palomares O. The role of cannabinoids in allergic diseases: Collegium internationale allergologicum (CIA) update 2020. *Int Arch Allergy Immunol* (2020) 181(8):565–84. doi: 10.1159/000508989

10. Di Marzo V. New approaches and challenges to targeting the endocannabinoid system. *Nat Rev Drug Discovery* (2018) 17(9):623–39. doi: 10.1038/nrd.2018.115

11. Klein TW. Cannabinoid-based drugs as anti-inflammatory therapeutics. *Nat Rev Immunol* (2005) 5(5):400–11. doi: 10.1038/nri1602

12. Graczyk M, Lewandowska AA, Dzierzanowski T. The therapeutic potential of cannabis in counteracting oxidative stress and inflammation. *Molecules.* (2021) 26 (15):4551. doi: 10.3390/molecules26154551

13. Angelina A, Perez-Diego M, Lopez-Abente J, Ruckert B, Nombela I, Akdis M, et al. Cannabinoids induce functional tregs by promoting tolerogenic DCs *via* autophagy and metabolic reprograming. *Mucosal Immunol* (2022) 15(1):96–108. doi: 10.1038/s41385-021-00455-x

14. Angelina A, Martin-Fontecha M, Ruckert B, Wawrzyniak P, Perez-Diego M, Lopez-Abente J, et al. The cannabinoid WIN55212-2 restores rhinovirus-induced epithelial barrier disruption. *Allergy.* (2021) 76(6):1900–2. doi: 10.1111/all.14707

15. Martin-Fontecha M, Angelina A, Ruckert B, Rueda-Zubiaurre A, Martin-Cruz L, van de Veen W, et al. A fluorescent probe to unravel functional features of cannabinoid receptor CB(1) in human blood and tonsil immune system cells. *Bioconjug Chem* (2018) 29(2):382–9. doi: 10.1021/acs.bioconjchem.7b00680

16. Martin-Cruz L, Sevilla-Ortega C, Benito-Villalvilla C, Diez-Rivero CM, Sanchez-Ramon S , Subiza JL, et al. A combination of polybacterial MV140 and candida albicans V132 as a potential novel trained immunity-based vaccine for genitourinary tract infections. *Front Immunol* (2020) 11:612269. doi: 10.3389/fimmu.2020.612269

17. Murray PJ, Allen JE, Biswas SK, Fisher EA, Gilroy DW, Goerdt S, et al. Macrophage activation and polarization: nomenclature and experimental guidelines. *Immunity.* (2014) 41(1):14–20. doi: 10.1016/j.immuni.2014.06.008

18. Yu W, Wang Z, Zhang K, Chi Z, Xu T, Jiang D, et al. One-carbon metabolism supports s-adenosylmethionine and histone methylation to drive inflammatory macrophages. *Mol Cell* (2019) 75(6):1147–60 e5. doi: 10.1016/j.molcel.2019.06.039

19. Lauterbach MA, Hanke JE, Serefidou M, Mangan MSJ, Kolbe CC, Hess T, et al. Toll-like receptor signaling rewires macrophage metabolism and promotes histone acetylation *via* ATP-citrate lyase. *Immunity.* (2019) 51(6):997–1011 e7. doi: 10.1016/j.immuni.2019.11.009

20. Bain CC, Jenkins SJ. Isolation and identification of murine serous cavity macrophages. *Methods Mol Biol* (2018) 1784:51–67. doi: 10.1007/978-1-4939-7837-3_5

21. Jakubzick CV, Randolph GJ, Henson PM. Monocyte differentiation and antigen-presenting functions. *Nat Rev Immunol* (2017) 17(6):349–62. doi: 10.1038/nri.2017.28

22. Benito-Villalvilla C, Perez-Diego M, Angelina A, Kisand K, Rebane A, Subiza JL, et al. Allergoid-mannan conjugates reprogram monocytes into tolerogenic dendritic cells *via* epigenetic and metabolic rewiring. *J Allergy Clin Immunol* (2022) 149(1):212–22 e9. doi: 10.1016/j.jaci.2021.06.012

23. Benito-Villalvilla C, Perez-Diego M, Subiza JL, Palomares O. Allergoid-mannan conjugates imprint tolerogenic features in human macrophages. *Allergy.* (2022) 77 (1):320–3. doi: 10.1111/all.15118

24. Svajger U, Rozman PJ. Recent discoveries in dendritic cell tolerance-inducing pharmacological molecules. *Int Immunopharmacol.* (2020) 81:106275. doi: 10.1016/j.intimp.2020.106275

25. Hackstein H, Taner T, Zahorchak AF, Morelli AE, Logar AJ, Gessner A, et al. Rapamycin inhibits IL-4–induced dendritic cell maturation *in vitro* and dendritic cell mobilization and function in vivo. *Blood* (2003) 101(11):4457–63. doi: 10.1182/blood-2002-11-3370

26. Unger WW, Laban S, Kleijwegt FS, van der Slik AR, Roep BO. Induction of treg by monocyte-derived DC modulated by vitamin D3 or dexamethasone: differential role for PD-L1. *Eur J Immunol* (2009) 39(11):3147–59. doi: 10.1002/eji.200839103

27. Martin-Cruz L, Angelina A, Baydemir I, Bulut O, Subiza JL , Netea MG, et al. Candida albicans V132 induces trained immunity and enhances the responses triggered by the polybacterial vaccine MV140 for genitourinary tract infections. *Front Immunol* (2022) 13:1066383. doi: 10.3389/fimmu.2022.1066383

28. Saeed S, Quintin J, Kerstens HH, Rao NA, Aghajanirefah A, Matarese F, et al. Epigenetic programming of monocyte-to-macrophage differentiation and trained innate immunity. *Science.* (2014) 345(6204):1251086. doi: 10.1126/science.1251086

29. Martin-Cruz L, Sevilla-Ortega C, Angelina A, Dominguez-Andres J, Netea MG, Subiza JL, et al. From trained immunity in allergy to trained immunity-based allergen vaccines. *Clin Exp Allergy* (2022) 53(2):145–55. doi: 10.1111/cea.14261

30. Roth MD, Castaneda JT, Kiertscher SM. Exposure to Delta9-tetrahydrocannabinol impairs the differentiation of human monocyte-derived dendritic cells and their capacity for T cell activation. *J Neuroimmune Pharmacol* (2015) 10(2):333–43. doi: 10.1007/s11481-015-9587-z

31. Sakaguchi S, Mikami N, Wing JB, Tanaka A, Ichiyama K, Ohkura N. Regulatory T cells and human disease. *Annu Rev Immunol* (2020) 38:541–66. doi: 10.1146/annurev-immunol-042718-041717

32. Palomares O, Elewaut D, Irving PM, Jaumont X, Tassinari P. Regulatory T cells and immunoglobulin e: A new therapeutic link for autoimmunity? *Allergy* (2022) 77 (11):3293–308. doi: 10.1111/all.15449

33. Palomares O, Akdis M, Martin-Fontecha M, Akdis CA. Mechanisms of immune regulation in allergic diseases: the role of regulatory T and b cells. *Immunol Rev* (2017) 278(1):219–36. doi: 10.1111/imr.12555

34. Dhital S, Stokes JV, Park N, Seo KS, Kaplan BL. Cannabidiol (CBD) induces functional tregs in response to low-level T cell activation. *Cell Immunol* (2017) 312:25–34. doi: 10.1016/j.cellimm.2016.11.006

35. Jayarajan S, Meissler JJ, Adler MW , Eisenstein TK. A cannabinoid 2-selective agonist inhibits allogeneic skin graft rejection *In vivo*. *Front Pharmacol* (2021) 12:804950. doi: 10.3389/fphar.2021.804950

36. Gentili M, Ronchetti S, Ricci E, Di Paola R, Gugliandolo E, Cuzzocrea S, et al. Selective CB2 inverse agonist JTE907 drives T cell differentiation towards a treg cell phenotype and ameliorates inflammation in a mouse model of inflammatory bowel disease. *Pharmacol Res* (2019) 141:21–31. doi: 10.1016/j.phrs.2018.12.005

37. Angelina A, Jimenez-Saiz R, Perez-Diego M, Maldonado A, Ruckert B, Akdis M, et al. Cannabinoid WIN55212-2 impairs peanut-allergic sensitization and promotes the generation of allergen-specific regulatory T cells. *Clin Exp Allergy* (2022) 52(4):540–9. doi: 10.1111/cea.14092

38. Angelina A, Perez-Diego M, Maldonado A, Ruckert B, Akdis M, Martin-Fontecha M, et al. The cannabinoid WIN55212-2 suppresses effector T-cell responses and promotes regulatory T cells in human tonsils. *Allergy.* (2022) 77 (3):1029–32. doi: 10.1111/all.15160

39. Gallily R, Breuer A, Mechoulam R. 2-arachidonylglycerol, an endogenous cannabinoid, inhibits tumor necrosis factor-alpha production in murine macrophages, and in mice. *Eur J Pharmacol* (2000) 406(1):R5–7. doi: 10.1016/S0014-2999(00)00653-1

40. Chang YH, Lee ST, Lin WW. Effects of cannabinoids on LPS-stimulated inflammatory mediator release from macrophages: involvement of eicosanoids. *J Cell Biochem* (2001) 81(4):715–23. doi: 10.1002/jcb.1103

41. Suryavanshi SV, Zaiachuk M, Pryimak N, Kovalchuk I, Kovalchuk O. Cannabinoids alleviate the LPS-induced cytokine storm via attenuating NLRP3 inflammasome signaling and TYK2-mediated STAT3 signaling pathways *In vitro*. *Cells* (2022) 11(9):1391. doi: 10.3390/cells11091391

42. Downer EJ, Clifford E, Gran B, Nel HJ, Fallon PG, Moynagh PN. Identification of the synthetic cannabinoid R(+)WIN55,212-2 as a novel regulator of IFN regulatory factor 3 activation and IFN-beta expression: relevance to therapeutic effects in models of multiple sclerosis. *J Biol Chem* (2011) 286(12):10316–28. doi: 10.1074/jbc.M110.188599

43. Hao MX, Jiang LS, Fang NY, Pu J, Hu LH, Shen LH, et al. The cannabinoid WIN55,212-2 protects against oxidized LDL-induced inflammatory response in murine macrophages. *J Lipid Res* (2010) 51(8):2181–90. doi: 10.1194/jlr.M001511

44. Dopkins N, Miranda K, Wilson K, Holloman BL, Nagarkatti P, Nagarkatti M. Effects of orally administered cannabidiol on neuroinflammation and intestinal inflammation in the attenuation of experimental autoimmune encephalomyelitis. *J Neuroimmune Pharmacol* (2021) 17(1-2):15–32. doi: 10.1007/s11481-021-10023-6

45. Wang Y, Kanneganti TD. From pyroptosis, apoptosis and necroptosis to PANoptosis: A mechanistic compendium of programmed cell death pathways. *Comput Struct Biotechnol J* (2021) 19:4641–57. doi: 10.1016/j.csbj.2021.07.038

46. Malireddi RKS, Kesavardhana S , Kanneganti TD. ZBP1 and TAK1: Master regulators of NLRP3 Inflammasome/Pyroptosis, apoptosis, and necroptosis (PAN-optosis). *Front Cell Infect Microbiol* (2019) 9:406. doi: 10.3389/fcimb.2019.00406

47. Simpson DS, Pang J, Weir A, Kong IY, Fritsch M, Rashidi M, et al. Interferon-gamma primes macrophages for pathogen ligand-induced killing *via* a caspase-8 and mitochondrial cell death pathway. *Immunity.* (2022) 55(3):423–41 e9. doi: 10.1016/j.immuni.2022.01.003

48. Karki R, Sharma BR, Tuladhar S, Williams EP, Zalduondo L, Samir P, et al. Synergism of TNF-alpha and IFN-gamma triggers inflammatory cell death, tissue damage, and mortality in SARS-CoV-2 infection and cytokine shock syndromes. *Cell.* (2021) 184(1):149–68 e17. doi: 10.1016/j.cell.2020.11.025

49. McCoy KL. Interaction between cannabinoid system and toll-like receptors controls inflammation. *Mediators Inflamm* (2016) 2016:5831315. doi: 10.1155/2016/5831315

50. van Niekerk G, Mabin T, Engelbrecht AM. Anti-inflammatory mechanisms of cannabinoids: an immunometabolic perspective. *Inflammopharmacology.* (2019) 27 (1):39–46. doi: 10.1007/s10787-018-00560-7

51. Rodriguez-Prados JC, Traves PG, Cuenca J, Rico D, Aragones J, Martin-Sanz P, et al. Substrate fate in activated macrophages: a comparison between innate, classic, and alternative activation. *J Immunol* (2010) 185(1):605–14. doi: 10.4049/jimmunol.0901698

52. Kelly B, O'Neill LA. Metabolic reprogramming in macrophages and dendritic cells in innate immunity. *Cell Res* (2015) 25(7):771–84. doi: 10.1038/cr.2015.68

53. Liao ST, Han C, Xu DQ, Fu XW, Wang JS, Kong LY. 4-octyl itaconate inhibits aerobic glycolysis by targeting GAPDH to exert anti-inflammatory effects. *Nat Commun* (2019) 10(1):5091. doi: 10.1038/s41467-019-13078-5

54. Xie M, Yu Y, Kang R, Zhu S, Yang L, Zeng L, et al. PKM2-dependent glycolysis promotes NLRP3 and AIM2 inflammasome activation. *Nat Commun* (2016) 7:13280. doi: 10.1038/ncomms13280

55. Tannahill GM, Curtis AM, Adamik J, Palsson-McDermott EM, McGettrick AF, Goel G, et al. Succinate is an inflammatory signal that induces IL-1beta through HIF-1alpha. *Nature.* (2013) 496(7444):238–42. doi: 10.1038/nature11986

56. Evavold CL, Hafner-Bratkovic I, Devant P, D'Andrea JM, Ngwa EM, Borsic E, et al. Control of gasdermin d oligomerization and pyroptosis by the ragulator-Rag-mTORC1 pathway. *Cell.* (2021) 184(17):4495–511 e19. doi: 10.1016/j.cell.2021.06.028

57. Moon JS, Hisata S, Park MA, DeNicola GM, Ryter SW, Nakahira K, et al. mTORC1-induced HK1-dependent glycolysis regulates NLRP3 inflammasome activation. *Cell Rep* (2015) 12(1):102–15. doi: 10.1016/j.celrep.2015.05.046

58. Knoll R, Schultze JL , Schulte-Schrepping J. Monocytes and macrophages in COVID-19. *Front Immunol* (2021) 12:720109. doi: 10.3389/fimmu.2021.720109

59. Merad M, Martin JC. Pathological inflammation in patients with COVID-19: a key role for monocytes and macrophages. *Nat Rev Immunol* (2020) 20(6):355–62. doi: 10.1038/s41577-020-0331-4

60. Karki R, Kanneganti TD. The 'cytokine storm': molecular mechanisms and therapeutic prospects. *Trends Immunol* (2021) 42(8):681–705. doi: 10.1016/j.it.2021.06.001

61. Chen H, Li Y, Wu J, Li G, Tao X, Lai K, et al. RIPK3 collaborates with GSDMD to drive tissue injury in lethal polymicrobial sepsis. *Cell Death Differ* (2020) 27(9):2568–85. doi: 10.1038/s41418-020-0524-1

62. van der Poll T, Shankar-Hari M, Wiersinga WJ. The immunology of sepsis. *Immunity.* (2021) 54(11):2450–64. doi: 10.1016/j.immuni.2021.10.012

63. He Q, Yin J, Zou B, Guo H. WIN55212-2 alleviates acute lung injury by inhibiting macrophage glycolysis through the miR-29b-3p/FOXO3/PFKFB3 axis. *Mol Immunol* (2022) 149:119–28. doi: 10.1016/j.molimm.2022.06.005

64. He Q, Zhang W, Zhang J, Deng Y. Cannabinoid analogue WIN 55212-2 protects paraquat-induced lung injury and enhances macrophage M2 polarization. *Inflammation.* (2022) 45(6):2256–67. doi: 10.1007/s10753-022-01688-z

65. de Lago E, Moreno-Martet M, Cabranes A, Ramos JA, Fernandez-Ruiz J. Cannabinoids ameliorate disease progression in a model of multiple sclerosis in mice, acting preferentially through CB1 receptor-mediated anti-inflammatory effects. *Neuropharmacology.* (2012) 62(7):2299–308. doi: 10.1016/j.neuropharm.2012.01.030

66. Arevalo-Martin A, Molina-Holgado E, Guaza C. A CB(1)/CB(2) receptor agonist, WIN 55,212-2, exerts its therapeutic effect in a viral autoimmune model of multiple sclerosis by restoring self-tolerance to myelin. *Neuropharmacology.* (2012) 63 (3):385–93. doi: 10.1016/j.neuropharm.2012.04.012

67. Shakoory B, Carcillo JA, Chatham WW, Amdur RL, Zhao H, Dinarello CA, et al. Interleukin-1 receptor blockade is associated with reduced mortality in sepsis patients with features of macrophage activation syndrome: Reanalysis of a prior phase III trial. *Crit Care Med* (2016) 44(2):275–81. doi: 10.1097/CCM.0000000000001402

68. Dai S, Ye B, Zhong L, Chen Y, Hong G , Zhao G, et al. GSDMD mediates LPS-induced septic myocardial dysfunction by regulating ROS-dependent NLRP3 inflammasome activation. *Front Cell Dev Biol* (2021) 9:779432. doi: 10.3389/fcell.2021.779432

69. Anderko RR, Gomez H, Canna SW, Shakoory B, Angus DC, Yealy DM, et al. Sepsis with liver dysfunction and coagulopathy predicts an inflammatory pattern of macrophage activation. *Intensive Care Med Exp* (2022) 10(1):6. doi: 10.1186/s40635-022-00433-y

Received: 30 July 2024 | Revised: 8 August 2024 | Accepted: 10 August 2024

DOI: 10.1111/all.16280

Allergy EUROPEAN JOURNAL OF ALLERGY AND CLINICAL IMMUNOLOGY EAACI WILEY

EDITORIAL

Nutritional and environmental exposures in athletes: Implications on the epithelial barrier function

Over the last decades, industrialization, and technological advances associated with a modern lifestyle have been accompanied by an alarming rise in the prevalence of chronic noncommunicable diseases.[1] The epithelial barrier theory attributes this phenomenon to exposure to newly introduced toxic substances that are capable of disrupting the protective epithelial barriers since the 1960s.[1] Pollutants such as particulate matter, ozone, diesel exhaust particles, nano- and/or micro-plastics, surfactants, and detergents included in cleaning products, or several additives, emulsifiers and flavor enhancers used in the food industry can compromise the epithelial barriers in the skin, airways, and the gut.[1,2] Genetic factors and exposure to epithelial barrier-damaging agents promote leaky barriers, leading to microbial dysbiosis, bacterial translocation, and perpetuation of local and systemic inflammation.[1,2] In this elegant review article, Kistler W. et al. discuss the impact of a hazardous exposome and physical exertion typically endured by elite athletes. These factors may counteract the health benefits of regular physical activity by disrupting the epithelial barrier function. In this context, experimental evidence supporting the epithelial barrier theory can be applied to sports medicine.[3]

There is a social and scientific consensus on the health benefits of regular, mild to moderate physical activity. However, epidemiological studies indicate that athletes undergoing excessive training are not in optimal overall health, which can negatively impact their sport performance. For instance, gastrointestinal disorders are very common among elite athletes.[4] Likewise, they show a higher risk of infections and noninfectious respiratory diseases, such as exercise-induced asthma, rhinitis, and laryngeal disorders.[5] In the context of the epithelial barrier, the benefits of exercise may display a J-shaped relationship. Moderate exercise improves the integrity of the intestinal barrier and in turn, promotes the growth of healthy microbiota populations and ameliorates a proinflammatory immune state.[6] On the other hand, compelling evidence shows that prolonged intense physical activity impairs the intestinal epithelial tight junctions, compromising its barrier integrity and allowing the entry of microbes and pollutants that can trigger an inflammatory cascade.[7] In some cases, it may also aggravate an existing pathology; for example, a leaky gut facilitates the passage of food allergens and reduces the threshold for food-dependent anaphylaxis.[8] Similarly, excessive training has been closely associated with airway epithelial barrier damage and local inflammation, especially in endurance sports, as epithelial injury is a key factor in the development of exercise-induced bronchoconstriction.[9]

Another facet highlighted by the authors is that athletes are at higher risk of exposure to toxic substances. During intense exercise, hyperpnea and an increase in respiratory rate occur to satisfy oxygen demands, resulting in increased inhalation of toxic airborne substances that may damage the airway epithelial barrier and promote airway inflammation.[10] Endurance runners and swimmers are some of the most susceptible athletes due to their high exposure to pollution in urban areas and chlorine-based disinfectants present in swimming pools, respectively.[9,10] The nutrition of athletes should be carefully monitored. Athletes requiring a high-calorie diet may have a higher consumption of processed food products marketed for athletes. Sports drinks and dietary supplements may contain emulsifiers, preservatives, flavor enhancers, and other artificial additives that can disrupt the intestinal epithelial barrier and imbalance microbiota populations, eventually aggravating the well-known gastrointestinal symptoms associated with high-impact exercise such as vomiting and diarrhea. Moreover, it is important to point out that the good hygienic conditions required during elite sports practice can increase the athletes' exposure to chemical disinfectants and detergents, such as those used to clean the changing rooms, towels, and training gear. Altogether, these routines and activities associated with vigorous exercise make athletes more susceptible to potentially harmful substances compared to less active individuals. Considering all of the above-mentioned aspects, the authors conclude that a call for action is necessary to implement strategies that mitigate the environmental burden continuously faced by athletes, including the identification and avoidance of epithelial barrier-damaging agents, the development of safer products, the discovery of novel biomarkers of epithelial barrier disruption, the implementation of therapeutic approaches based on improving barrier function, and further research[3] (Figure 1).

In summary, the article by Kistler W. et al. provides a comprehensive review of the potential mechanisms underlying the harmful effects of intense physical training in the context of the epithelial barrier theory. The physical exertion reached during intense exercise and the elevated risk of exposure to airborne pollutants and toxic substances might contribute to an impaired epithelial barrier in athletes and physically active individuals. Consequently, athletes

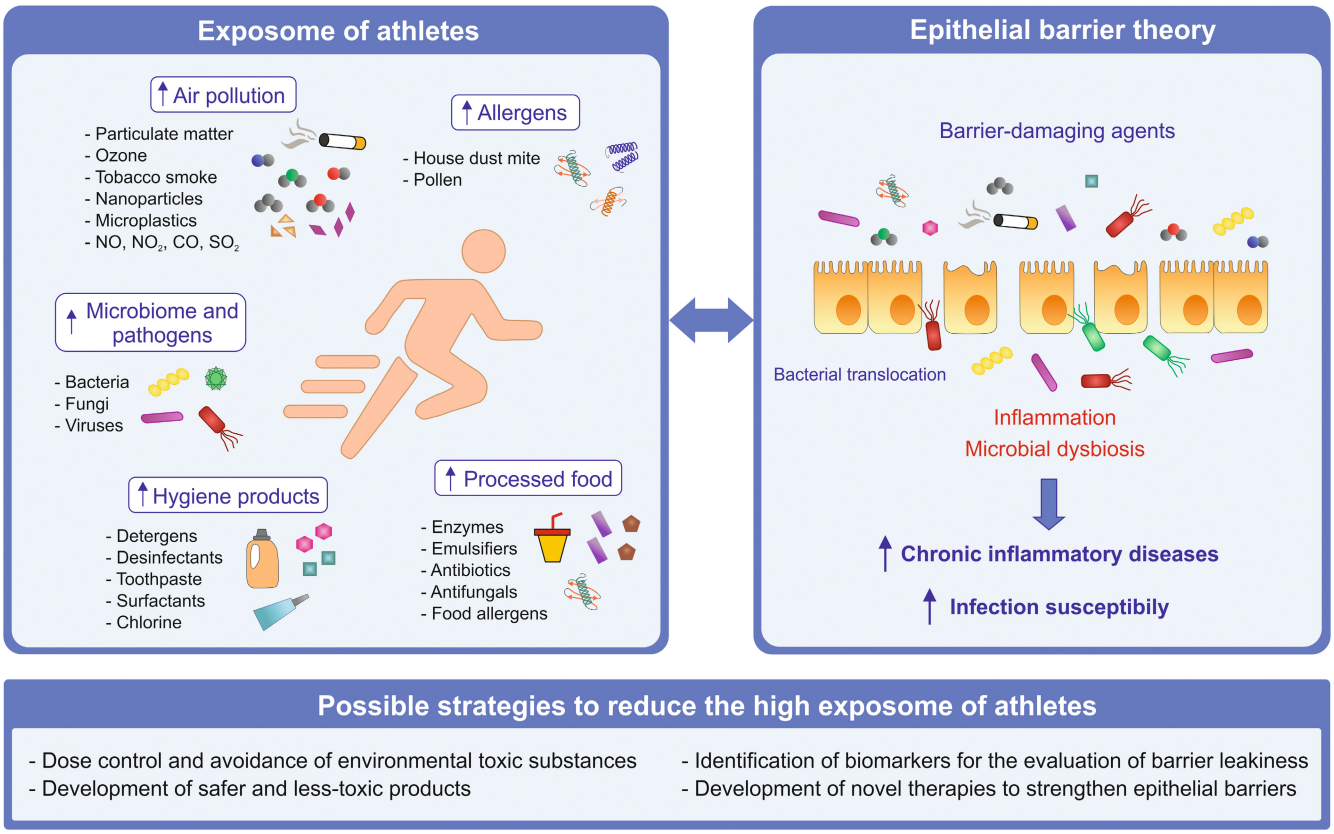

FIGURE 1 The hazardous exposome encountered by athletes and its association to the epithelial barrier theory: Connections, consequences, and potential management. Elite athletes have an elevated exposure to environmental toxic substances, including particulate matter, toxic gases, allergens, pathogens, cleaning products, and processed foods. All these substances can disturb the function of epithelial barriers and compromise the health of athletes by increasing their risk of infections and the development of chronic non-communicable diseases. Future approaches to mitigate the deleterious exposome faced by athletes may involve the avoidance of toxic substances, development of safer products, identification of biomarkers of epithelial barrier integrity and the design of novel strategies to repair barrier function.

are more prone to infections and chronic inflammatory diseases, thereby compromising their sports performance. Future research in sports medicine should include novel strategies to mitigate the deleterious exposome faced by athletes as well as the repair of the epithelial barrier tight junctions.

FUNDING INFORMATION

This work was supported by grant PID2020-114396RB-I00 to O.P. from MICINN, Spain. MP-D is a recipient of an FPI (SAF-20217-84978-R) predoctoral fellowship from Ministerio de Economía y Competitividad. A.A. is recipient of a Margarita Salas contract (Reference: UCM-CT18/22) cofinanced by the Ministerio de Universidades, the "Plan de Recuperación, Transformación y Resilencia" and the Complutense University of Madrid.

KEYWORDS

athletes, epithelial barrier theory, exercise, exposome, nutrition

CONFLICT OF INTEREST STATEMENT

Dr. Oscar Palomares declares research grants from MINECO, Ministerio de Ciencia e Innovación, CAM, Inmunotek S.L., Novartis, and AstraZeneca and receiving fees for presenting scientific lectures or participation in advisory boards from AstraZeneca, Pfizer, GlaxoSmithKline, Inmunotek S.L, Novartis and Sanofi-Genzyme.

DATA AVAILABILITY STATEMENT

Data sharing not applicable to this article as no datasets were generated or analysed during the current study.

Alba Angelina
Mario Pérez-Diego
Oscar Palomares

Department of Biochemistry and Molecular Biology, School of Chemistry, Complutense University, Madrid, Spain

Correspondence
Oscar Palomares, Department of Biochemistry and Molecular Biology, School of Chemistry, Complutense University of Madrid, Avenida Complutense s/n, Madrid 28040, Spain.
Email: oscar.palomares@quim.ucm.es

Alba Angelina and Mario Pérez-Diego contributed equally and share first authorship.

ORCID

Oscar Palomares https://orcid.org/0000-0003-4516-0369

REFERENCES

1. Akdis CA. Does the epithelial barrier hypothesis explain the increase in allergy, autoimmunity and other chronic conditions? *Nat Rev Immunol*. 2021;21(11):739-751.
2. Celebi Sozener Z, Ozdel Ozturk B, Cerci P, et al. Epithelial barrier hypothesis: effect of the external exposome on the microbiome and epithelial barriers in allergic disease. *Allergy*. 2022;77(5):1418-1449.
3. Kistler W, Villiger M, Villiger B, et al. Epithelial barrier theory in the context of nutrition and environmental exposure in athletes. *Allergy*. 2024;79(11):2912-2923. doi:10.1111/all.16221
4. Pugh JN, Fearn R, Morton JP, Close GL. Gastrointestinal symptoms in elite athletes: time to recognise the problem? *Br J Sports Med*. 2018;52(8):487-488.
5. Gleeson M, Pyne DB. Respiratory inflammation and infections in high-performance athletes. *Immunol Cell Biol*. 2016;94(2):124-131.
6. O'Brien MT, O'Sullivan O, Claesson MJ, Cotter PD. The athlete gut microbiome and its relevance to health and performance: a review. *Sports Med*. 2022;52(Suppl 1):119-128.
7. Zuhl M, Schneider S, Lanphere K, Conn C, Dokladny K, Moseley P. Exercise regulation of intestinal tight junction proteins. *Br J Sports Med*. 2014;48(12):980-986.
8. JanssenDuijghuijsen LM, van Norren K, Grefte S, et al. Endurance exercise increases intestinal uptake of the Peanut allergen Ara h 6 after Peanut consumption in humans. *Nutrients*. 2017;9(1):84. doi:10.3390/nu9010084
9. Couto M, Kurowski M, Moreira A, et al. Mechanisms of exercise-induced bronchoconstriction in athletes: current perspectives and future challenges. *Allergy*. 2018;73(1):8-16.
10. Goossens J, Jonckheere AC, Seys SF, et al. Activation of epithelial and inflammatory pathways in adolescent elite athletes exposed to intense exercise and air pollution. *Thorax*. 2023;78(8):775-783.